

DISSERTATION

MEMBRANE BEHAVIOR OF CLAY LINER MATERIALS

Submitted by

Jong Beom Kang

Department of Civil and Environmental Engineering

In partial fulfillment of the requirements

For the Degree of Doctor of Philosophy

Colorado State University

Fort Collins, Colorado

Fall 2008

UMI Number: 3346460

INFORMATION TO USERS

The quality of this reproduction is dependent upon the quality of the copy submitted. Broken or indistinct print, colored or poor quality illustrations and photographs, print bleed-through, substandard margins, and improper alignment can adversely affect reproduction.

In the unlikely event that the author did not send a complete manuscript and there are missing pages, these will be noted. Also, if unauthorized copyright material had to be removed, a note will indicate the deletion.

UMI[®]

UMI Microform 3346460

Copyright 2009 by ProQuest LLC.

All rights reserved. This microform edition is protected against unauthorized copying under Title 17, United States Code.

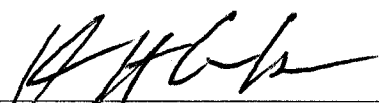
ProQuest LLC
789 E. Eisenhower Parkway
PO Box 1346
Ann Arbor, MI 48106-1346

COLORADO STATE UNIVERSITY

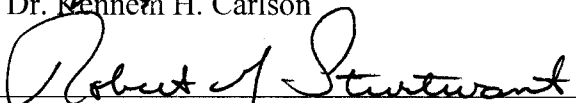
September 25, 2008

WE HEREBY RECOMMEND THAT THE DISSERTATION PREPARED UNDER OUR SUPERVISION BY JONG BEOM KANG ENTITLED "MEMBRANE BEHAVIOR OF CLAY LINER MATERIALS" BE ACCEPTED AS FULFILLING, IN PART, THE REQUIREMENTS FOR THE DEGREE OF DOCTOR OF PHILOSOPHY.

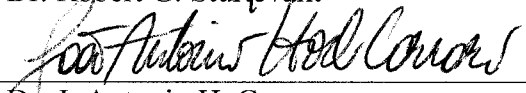
COMMITTEE ON GRADUATE WORK



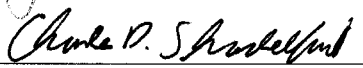
Dr. Kenneth H. Carlson



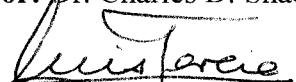
Dr. Robert G. Sturtevant



Dr. J. Antonio H. Carraro



Advisor: Dr. Charles D. Shackelford



Department Head: Dr. Luis A. Garcia

ABSTRACT OF DISSERTATION

MEMBRANE BEHAVIOR OF CLAY LINER MATERIALS

Membrane behavior represents the ability of porous media to restrict the migration of solutes, leading to the existence of chemico-osmosis, or the flow of liquid in response to a chemical concentration gradient. Membrane behavior is an important consideration with respect to clay soils with small pores and interactive electric diffuse double layers associated with individual particles, such as bentonite. The results of recent studies indicate the existence of membrane behavior in bentonite-based hydraulic barriers used in waste containment applications. Thus, measurement of the existence and magnitude of membrane behavior in such clay soils is becoming increasingly important. Accordingly, this research focused on evaluating the existence and magnitude of membrane behavior for three clay-based materials that typically are considered for use as liners for waste containment applications, such as landfills. The three clay-based liner materials included a commercially available geosynthetic clay liner (GCL) consisting of sodium bentonite sandwiched between two geotextiles, a compacted natural clay known locally as Nelson Farm Clay, and compacted NFC amended with 5 % (dry wt.) of a sodium bentonite. The study also included the development and evaluation of a new flexible-wall cell for clay membrane testing that was used subsequently to measure the membrane behaviors of the three clay liner materials. The consolidation behavior of the GCL under isotropic states of stress also was evaluated as a preliminary step in the

determination of the membrane behavior of the GCL under different effective consolidation stresses.

The consolidation behavior of the GCL was evaluated by consolidating duplicate specimens of the GCL under isotropic states of stress in a flexible-wall cell to a final effective consolidation stress, σ' , of 241 kPa (35.0 psi). The hydraulic conductivity, k , also was measured at the end of each loading increment. The results indicated that the GCL was normally consolidated for values of σ' greater than 34.5 kPa (5.0 psi), which correlates well with limited consolidation data reported in the literature based on one-dimensional consolidation. Values of the measured k , k_{measured} , for the GCL were low ($\leq 5.0 \times 10^{-9}$ cm/s) due to the sodium bentonite content of the GCL, and were within a factor of about two of the values of k based on consolidation theory, k_{theory} (i.e., $0.5 \leq k_{\text{theory}}/k_{\text{measured}} \leq 2.0$), suggesting that k_{theory} provided a good estimate of k_{measured} . Overall, the low k of the GCL dominated the consolidation behavior of the GCL. For example, values of the coefficient of consolidation, c_v , for the GCL ranged from 5.2×10^{-10} m²/s to 1.8×10^{-9} m²/s, which is among the lowest range of c_v values reported in the literature for clays. In addition, c_v for a given GCL specimen decreased with increasing σ' , albeit only slightly, primarily due to the decrease in k with increasing σ' . Finally, an estimate of the measured compression index, C_c , for the GCL based solely on empirical correlation with the liquid limit, LL , of the bentonite in the GCL ($LL = 478\%$) was found to be not only inaccurate but also high (conservative) by about 300 %.

Since semi-permeable membrane behavior in clay soils is a function of the stress-strain behavior and the state of stress in the clay soil, a flexible-wall cell was developed for use in measuring the membrane behavior of the clay liner materials under closed-

system boundary conditions. The advantages of the flexible-wall cell include complete control over the state of stress existing within the test specimen and the ability to back-pressure saturate and consolidate the specimen prior to membrane testing. The developed cell was evaluated by comparing the membrane efficiencies of the GCL measured using the developed cell with those previously measured on specimens of the same GCL and the same closed-system boundary conditions but using a rigid-wall cell that does not allow for control of the specimen stress conditions. The results indicated that the membrane efficiencies of duplicate specimens of the GCL measured using the flexible-wall cell were both reproducible and similar to, but somewhat lower than, those previously reported for the same GCL using a rigid-wall cell under the same closed-system boundary conditions. As a result, the developed flexible-wall cell was considered appropriate for measuring the membrane efficiencies of both the GCL and the compacted clay liner materials.

In this regard, the potential effect of effective consolidation stress, σ' , on the membrane efficiency coefficient, ω , of the GCL was evaluated using the developed flexible-wall cell. The membrane behavior was evaluated by establishing steady KCl concentration differences of 3.9 mM, 6.0 mM, 8.7 mM, 20 mM, and 47 mM across specimens of the GCL. The results indicated that an increase in σ' from 34.5 kPa (5.0 psi) to 241 kPa (35.0 psi) resulted in a decrease in void ratio, e , from 1.896 to 4.049 and a corresponding increase in ω from 0.015 (1.5 %) to 0.784 (78.4 %), respectively. These trends among σ' , e , and ω are consistent with expected behavior in that lower void ratios correlate with smaller pores and greater restriction in solute migration. The measured membrane efficiencies at the relatively high values for σ' of 172 kPa (25.0 psi) and 241

kPa (35.0 psi) also were similar to those previously reported for the same GCL using a rigid-wall cell at unknown states of stress

Finally, values of ω for compacted specimens of both the natural and the bentonite amended NFC were measured by establishing steady KCl concentration differences of 3.9, 8.7, 20 and/or 47 mM across the specimens in the flexible-wall cell under closed-system boundary conditions. The results indicate that the compacted natural NFC exhibited essentially no membrane behavior (i.e., $\omega \approx 0$), even though the specimen was compacted at conditions that should have resulted in a suitably low value of hydraulic conductivity, k (i.e., $k < 10^{-7}$ cm/s). In contrast, compacted specimens of the bentonite amended NFC exhibited both lower k than those of the natural NFC as well as significant membrane behavior, with ω ranging from 0.762 (76.2 %) to 0.027 (2.7 %) as the KCl concentration ranged from 3.9 to 20 mM, respectively. The results suggest that natural clays typically suitable for use as compacted clay liners on the basis of low k in waste containment applications may not behave as semi-permeable membranes unless bentonite is added to the clay.

Jong Beom Kang
Civil and Environmental Engineering Department
Colorado State University
Fort Collins, CO 80523
Fall 2008

ACKNOWLEDGMENTS

I would like to express my sincere gratitude to my advisor, Professor Charles D. Shackelford, for insightful guidance, patience, and continuous encouragement throughout this study. I would never have accomplished the study without his unfailing instruction and incessant support. I am also indebted to Professor J. Antonio H. Carraro for his fruitful advice and suggestion. I would like to extend my thanks to other committee members, Professors Kenneth H. Carlson and Robert G. Sturtevant, for reviewing the dissertation and suggesting improvements to the text.

Also, I would like to thank my parents, Ho-Yeol Kang and You-Cha Young, my parents-in-law, Byung-Ho Lee and Kwang-Ja Yuk, and my kids, Seong-Min Kang and Seong-Gil kang for their endless love and support. Thanks are extended to my brother, Jong-Myun, and sisters Myung-Suk, Kyeong-Suk, and Jeong-Suk, for their continued love, support, and encouragement. Especially, my wife, Jeong-Mi Lee, deserves special acknowledgement for her sacrifice, patience, support, love, and everything I can imagine. I would be always grateful to my family for their great support and sacrifice.

Also, I would like to thank all staffs in Engineering Analytics, Inc. including Dr. John D. Nelson, Daniel D. Overton, Erik J. Nelson, Jason Andrews, Andrea Bennett, Denise, Debbie, Ron, and attorneys, Nicole Murad Rothstein and Yvan E. Murad. Especially, my mentors, Dr. Geoff Chao in EA, Inc. and Eileen in Tetra Tech, Inc., deserves special acknowledgement for their advice, support, and everything I can

appreciate. I would be always grateful to EA Inc.'s staffs for their great support and encouragement.

I also need to thank many other people, including Professors Wayne A. Charlie, Thomas J. Siller, Deanna S. Durnford, James W. Warner, and former or current fellow students, Dr. Jae-Myung Lee, Dr. Michael A. Malusis, Dr. Jin-Chul Joo, Dr. Sang-Sik Yeo, Catherine Soo-Jung Hong, and Joon-Cheol Lee, and staffs or others, Linda L. Hinshaw, Laurie Alburn (Student Advisor), Joe Wilmetti (Civil Engineering Laboratory Manager), Shelby Sack (International Student Advisor), Deb Carter (Graduate School). Especially, my English mentor, Theron Felmlee and Patricia Carpenter including Judith Barrientos and Steve Allen, deserves special acknowledgement for their kind advices, teaching, and everything I can thank. I would be always grateful to my mentors and Toastmaster members including Jane Rothfeld and Bob, who were a great mentor in CSU Toastmaster Club and Case Ferguson and Rachel's family of Bible Study Club.

Finally, the financial support of this study by the U. S. National Science Foundation (NSF) is gratefully acknowledged. Once again, without the contribution and support from all the people that I have known during this study, this dissertation would not have been fulfilled.

DEDICATION

I would like to dedicate this dissertation to my father, Ho-Yeol Kang (August 1934 – July 2008), from whom I learned honesty, integrity, patience, and commitment. Your presence would be greatly missed to family, specially, in my mind for lifetime.

TABLE OF CONTENTS

	Page
Abstract of Dissertation	iii
Acknowledgments	vii
Table of Contents	x
List of Tables	xiii
List of Figures	xvi
List of Symbols	xxiii
Chapter 1 INTRODUCTION	
1.1 Background.....	1.1
1.2 Goals and Objectives of Research.....	1.6
1.3 References.....	1.9
Chapter 2 LITERATURE REVIEW	
2.1 Field Evidence of Membrane Behavior.....	2.1
2.2 Laboratory Evidence of Membrane Behavior.....	2.8
2.2.1 Hyperfiltration Flow-Through Tests.....	2.9
2.2.2 Chemico-Osmotic Flow-Through Tests.....	2.19
2.2.3 Chemico-Osmotic No-Flow Tests.....	2.39
2.3 Osmotic Effects on Mechanical Properties of Clays.....	2.45
2.4 Theoretical Considerations of Membrane Behavior.....	2.52
2.5 Literature Indirectly Related to Membrane Research.....	2.60
2.6 References.....	2.64
Chapter 3 ISOTROPIC CONSOLIDATION OF A GEOSYNTHETIC CLAY LINER	
3.1 Introduction.....	3.2
3.2 Materials and Experimental Methods.....	3.3
3.2.1 Materials.....	3.3
3.2.2 Specimen Assembly and Preparation.....	3.4
3.3 Results.....	3.6
3.3.1 Measured Hydraulic Conductivity.....	3.6
3.3.2 Strain versus Time.....	3.7
3.3.3 Stress versus Strain.....	3.8
3.3.4 Coefficients of Consolidation.....	3.9
3.3.5 Theoretical Hydraulic Conductivity.....	3.12
3.3.6 Secondary Compression.....	3.13

3.4	Discussion	3.14
3.4.1	Compression Index.....	3.14
3.4.2	Coefficient of Consolidation.....	3.15
3.4.3	Theoretical versus Measured Hydraulic Conductivity.....	3.16
3.5	Summary and conclusions.....	3.17
3.6	References.....	3.20

Chapter 4 CLAY MEMBRANE TESTING USING A FLEXIBLE-WALL CELL UNDER CLOSED-SYSTEM BOUNDARY CONDITIONS

4.1	Introduction.....	4.2
4.2	Background.....	4.4
4.2.1	Boundary Conditions.....	4.4
4.2.2	Types of Cells.....	4.5
4.3	Descriptions of Testing Apparatus and Procedures.....	4.7
4.3.1	Testing Apparatus.....	4.7
4.3.2	Calculation of Membrane Efficiency.....	4.11
4.4	Evaluation of Testing Apparatus.....	4.15
4.4.1	Materials.....	4.15
4.4.2	Specimen Assembly and Preparation.....	4.16
4.4.3	Membrane Testing Procedures.....	4.18
4.4.4	Testing Program.....	4.19
4.5	Results.....	4.20
4.5.1	Specimen Flushing and Consolidation.....	4.20
4.5.2	Electrical Conductivities.....	4.21
4.5.3	Boundary Pressures.....	4.23
4.5.4	Induced Chemico-Osmotic Pressures.....	4.25
4.5.5	Induced Membrane Efficiencies.....	4.26
4.5.6	Volume Changes.....	4.26
4.6	Discussion.....	4.30
4.7	Summary and Conclusion	4.32
4.8	References.....	4.35

Chapter 5 EFFECT OF CONSOLIDATION STRESS ON GCL MEMBRANE BEHAVIOR

5.1	Introduction.....	5.2
5.2	Materials and Experimental Methods.....	5.3
5.2.1	Materials.....	5.3
5.2.2	Specimen Assembly and Preparation.....	5.5
5.2.3	Membrane Testing Procedures and Program.....	5.6
5.2.4	Correlation of Solute Concentrations with Electrical Conductivity.....	5.7
5.3	Results.....	5.7
5.3.1	Specimen Flushing and Consolidation.....	5.7
5.3.2	Strain versus Time.....	5.9
5.3.3	Coefficients of Consolidation.....	5.9
5.3.4	Electrical Conductivities.....	5.10

5.3.5	Boundary Pressures.....	5.11
5.3.6	Induced Chemico-Osmotic Pressures.....	5.13
5.3.7	Induced Membrane Efficiencies.....	5.13
5.3.8	Volume Changes.....	5.15
5.4	Discussion.....	5.16
5.5	Summary and Conclusion.....	5.18
5.6	References.....	5.20

Chapter 6 MEMBRANE BEHAVIOR OF COMPACTED CLAY LINER MATERIALS

6.1	Introduction.....	6.2
6.2	Materials and Experimental Methods.....	6.3
6.2.1	Materials.....	6.3
6.2.2	Permeant Liquids.....	6.4
6.2.3	Compacted Specimen of NFC.....	6.4
6.2.4	Development of Acceptable Zones.....	6.5
6.2.5	Specimen Preparation and Assembly.....	6.7
6.2.6	Testing Program	6.9
6.3	Results.....	6.10
6.3.1	Flushing Stage of Specimens.....	6.10
6.3.2	Electrical Conductivities.....	6.11
6.3.3	Boundary Pressures.....	6.12
6.3.4	Induced Membrane Efficiencies.....	6.12
6.3.5	Volume Changes.....	6.13
6.4	Discussion.....	6.14
6.5	Summary and Conclusion.....	6.16
6.6	References.....	6.18

Chapter 7 SUMMARY AND CONCLUSIONS

7.1	Summary.....	7.1
7.2	Conclusions.....	7.2
7.2.1	Consolidation Behavior of a Geosynthetic Clay Liner.....	7.2
7.2.2	Development and Evaluation of Flexible-Wall Cell for Membrane Behavior.....	7.5
7.2.3	Influence of Effective Consolidation Stress on GCL Membrane Behavior.....	7.7
7.2.4	Membrane Efficiency of Compacted Clay Liner Materials.....	7.9

Appendix A - Calibration between KCl concentrations and electrical conductivity

Appendix B - Variation in laboratory temperature during membrane testing

Appendix C - Flushing, consolidation, and volume change data during membrane testing

Appendix D - Hydraulic conductivity test data for compacted clay materials

Appendix E - Membrane test data in flexible-wall cell

Appendix F - Hydraulic conductivity test data for porous stainless steel disk

LIST OF TABLES

	Page
Chapter 3	
3.1 Sequence of stress conditions imposed on test specimens.....	3.23
3.2 Summary of measured hydraulic conductivity and coefficient of consolidation values for two specimens of a geosynthetic clay liner (GCL).	3.24
3.3 Values for the secondary compression ratio (R_{α}) and secondary compression index (C_{α}) based on both vertical and volumetric strains for two specimens of a geosynthetic clay liner (GCL) consolidated under isotropic conditions.....	3.25
Chapter 4	
4.1 Results of multi-stage membrane testing using flexible-wall cell for two specimens of a geosynthetic clay liner at an effective confining stress of 241 kPa (35.0 psi).....	4.42
Chapter 5	
5.1 Properties of bentonite in a geosynthetic clay liner.....	5.25
5.2 Sequence of stress conditions imposed on test specimens.....	5.26
5.3 Testing series for membrane efficiency of the GCL specimens.....	5.27
5.4 Summary of measured hydraulic conductivity and coefficient of consolidation values for the specimens of a geosynthetic clay liner (GCL).....	5.28
5.5 Initial and final properties of 10-mm-thick specimens of the geosynthetic clay liner tested for membrane behavior in this study.....	5.29
5.6 Results of multi-stage membrane testing for specimens of the geosynthetic clay liner at each effective confining stress.....	5.30
Chapter 6	
6.1 Physical and chemical properties and mineralogical compositions of constituent soils used for model backfill mixtures.....	6.22
6.2 Testing series for membrane efficiency of Nelson Farm Clay (NFC) and NFC plus 5 % bentonite specimens.....	6.23
6.3 Results of compaction.....	6.24
6.4 Range of measured hydraulic conductivities for each compacted soil.....	6.25

6.5	Results of multi-stage membrane testing using flexible-wall cell for compacted specimens of Nelson Farm Clay (NFC) and NFC plus 5 % bentonite.....	6.26
6.6	Comparison for evaluation of factors affecting membrane efficiency according to soil types and specimen thicknesses used in previous research.....	6.27

LIST OF FIGURES

	Page
Chapter 3	
3.1 Measured hydraulic conductivity versus effective confining stress for two specimens of a geosynthetic clay liner (GCL) permeated with de-ionized water.....	3.26
3.2 Measured hydraulic conductivity versus void ratio for two specimens of a geosynthetic clay liner (GCL) permeated with de-ionized water during consolidation/permeation stage of testing: (a) logarithmic k_{measured} ; (b) arithmetic k_{measured}	3.27
3.3 Vertical (left) and volumetric (right) strain versus logarithm of time for consolidation of two specimens of a geosynthetic clay liner (GCL).....	3.28
3.4 Vertical (left) and volumetric (right) strain versus square root of time for consolidation of two specimens of a geosynthetic clay liner (GCL).....	3.29
3.5 Consolidation test data based on (a) vertical strain, (b) volumetric strain, and (c) void ratio versus effective consolidation stress for two specimens of a geosynthetic clay liner (GCL).....	3.30
3.6 Coefficients of consolidation based on vertical strain for two specimens of a geosynthetic clay liner (GCL) as function of average effective consolidation stress.....	3.31
3.7 Coefficients of consolidation based on volumetric strain for two specimens of a geosynthetic clay liner (GCL) as function of average effective consolidation stress.....	3.32
3.8 Coefficients of volume compressibility based on (a) vertical strain and (b) volumetric strain for two specimens of a geosynthetic clay liner (GCL) as function of average effective consolidation stress.....	3.33
3.9 Coefficients of compressibility based on (a) vertical strain and (b) volumetric strain for two specimens of a geosynthetic clay liner (GCL) as function of average effective consolidation stress.....	3.34
3.10 Effect of type of strain on the coefficients of consolidation, c_v , based on (a) Casagrande method and (b) Taylor method for two specimens of a geosynthetic clay liner (GCL) as function of average effective consolidation stress.....	3.35
3.11 Effect of method of analysis on the coefficients of consolidation, c_v , based on (a) vertical strain and (b) volumetric strain for two specimens of a geosynthetic clay liner (GCL) as function of average effective consolidation stress.....	3.36
3.12 Theoretical hydraulic conductivity versus average effective stress based on c_v by Casagrande method and m_v by (a) vertical strain and (b) volumetric strain for two specimens of a geosynthetic clay liner (GCL)...	3.37

3.13	Theoretical hydraulic conductivity versus average effective stress based on c_v by Taylor method and m_v by (a) vertical strain and (b) volumetric strain for two specimens of a geosynthetic clay liner (GCL).....	3.38
3.14	Secondary compression ratio based on (a) vertical strain and (b) volumetric strain versus effective consolidation stress for two specimens of a geosynthetic clay liner (GCL).....	3.39
3.15	Secondary compression index based on (a) vertical strain and (b) volumetric strain versus effective consolidation stress for two specimens of a geosynthetic clay liner (GCL).....	3.40
3.16	Ratio of secondary compression ratio and index based on vertical strain relative to that based on volumetric strain versus effective consolidation stress for two specimens of a geosynthetic clay liner (GCL).....	3.41
3.17	Measured hydraulic conductivity versus theoretical hydraulic conductivity for two specimens of a geosynthetic clay liner (GCL) permeated with de-ionized water: (a) c_v by Casagrande method and m_v by vertical strain; (b) c_v by Casagrande method and m_v by volumetric strain; (c) c_v by Taylor method and m_v by vertical strain; (d) c_v by Taylor method and m_v by volumetric strain.....	3.42

Chapter 4

4.1	Schematic cross-section of flexible-wall testing apparatus.....	4.43
4.2	Pictorial views of flexible-wall cell (top) and cell with entire testing apparatus (bottom).....	4.44
4.3	Electrical conductivity (a) and hydraulic conductivity (b) versus elapsed time for two specimens of a geosynthetic clay liner (GCL) permeated with de-ionized water during flushing stage of test.....	4.45
4.4	Electrical conductivity (EC) in circulation outflows from top and bottom boundaries of flexible-wall cell during membrane testing for two specimens of a geosynthetic clay liner (GCL) [$EC_0 = EC$ of KCl source solution].....	4.46
4.5	Boundary pressures and effective stresses in specimen GCL1 during membrane testing in flexible-wall cell.....	4.47
4.6	Boundary pressures and effective stresses in specimen GCL2 during membrane testing in flexible-wall cell.....	4.48
4.7	Measured chemico-osmotic pressure differences across specimens GCL1 and GCL2 during membrane testing in flexible-wall cell.....	4.49
4.8	Measured chemico-osmotic pressure differences versus elapsed time for two specimens of a geosynthetic clay liner (GCL) during multi-stage membrane testing in flexible-wall cell.....	4.50
4.9	Comparison of measured membrane efficiencies versus elapsed time based on (a) initial concentration differences ($\Delta\pi_0$) and (b) average concentration differences ($\Delta\pi_{ave}$) for two specimens of a geosynthetic clay liner (GCL) during multi-stage membrane testing in flexible-wall cell.....	4.51

4.10	Incremental (a) and cumulative (b) changes in cell volume for two specimens of a geosynthetic clay liner (GCL) during membrane testing in flexible-wall cell.....	4.52
4.11	Incremental (a) and cumulative (b) volumetric strains for two specimens of a geosynthetic clay liner (GCL) during membrane testing in a flexible-wall cell.....	4.53
4.12	Boundary pressures and stresses for a preliminary test with valves closed after sampling and refilling syringes.....	4.54
4.13	Steady-state membrane efficiencies versus average of difference in initial (source) KCl concentrations for two GCL specimens: (a) ω_{ss} values based initial concentration differences ($\Delta\pi_0$), $\omega_{ss,0}$, versus average concentration differences ($\Delta\pi_{ave}$), $\omega_{ss,ave}$; (b) ratio of ω_{ss} based on $\Delta\pi_{ave}$ relative to ω_{ss} based on $\Delta\pi_0$	4.55
4.14	Membrane efficiency coefficients at steady state based on (a) initial concentration differences ($\Delta\pi_0$) and (b) average concentration differences ($\Delta\pi_{ave}$) as a function of the average of the difference in initial source KCl concentrations and the type of cell used in the measurement.....	4.56
4.15	Membrane efficiency coefficients at steady state versus void ratio as a function of the type of cell used in the measurement (rigid-wall data from Malusis and Shackelford 2002b).....	4.57

Chapter 5

5.1	Schematic cross section of manufactured geosynthetic clay liner evaluated in this study (after Malusis et al. 2002).....	5.31
5.2	Wet (hydrometer) and dry (mechanical sieve) grain-size distributions for the bentonite in the geosynthetic clay liner evaluated in this study (after Malusis and Shackelford 2002).....	5.32
5.3	Electrical conductivity (a) and hydraulic conductivity (b) versus elapsed time for specimens of a geosynthetic clay liner permeated with de-ionized water during flushing stage of test prior to consolidation to initial effective stresses of 34.5, 103, 172, and 241 kPa (5.0, 15.0, 25.0, and 35.0 psi).....	5.33
5.4	Volumetric strain versus (a) logarithm of time and (b) square root of time for specimens of a geosynthetic clay liner consolidated to initial effective stresses of 103, 172, and 241 kPa (15.0, 25.0, and 35.0 psi) prior to membrane testing in flexible-wall cell.....	5.34
5.5	Effect of method of analysis on the coefficients of consolidation, c_v , based on volumetric strain for the specimens of a geosynthetic clay liner as function of average effective consolidation stress.....	5.35
5.6	Electrical conductivity values in outflows from top and bottom boundaries of specimens of a geosynthetic clay liner consolidated to an initial effective stress of 103, 172, and 241 kPa (15.0, 25.0, and 35.0 psi) resulting from the chemico-osmotic stage in flexible-wall cell.....	5.36

5.7	Boundary pressures and effective stresses for a specimen of a geosynthetic clay liner consolidated to an initial effective stress of 34.5 kPa (5.0 psi) during membrane testing in flexible-wall cell.....	5.37
5.8	Boundary pressures and effective stresses for a specimen of a geosynthetic clay liner consolidated to an initial effective stress of 103 kPa (15.0 psi) during membrane testing in flexible-wall cell.....	5.38
5.9	Boundary pressures and effective stresses for a specimen of a geosynthetic clay liner consolidated to an initial effective stress of 172 kPa (25.0 psi) during membrane testing in flexible-wall cell.....	5.39
5.10	Boundary pressures and effective stresses for a specimen of a geosynthetic clay liner consolidated to an initial effective stress of 241 kPa (35.0 psi) during membrane testing in flexible-wall cell.....	5.40
5.11	Measured chemico-osmotic pressure differences across for specimens of a geosynthetic clay liner consolidated to initial effective stresses of 34.5, 103, 172, and 241 kPa (5.0, 15.0, 25.0, and 35.0 psi) during membrane testing in flexible-wall cell.....	5.41
5.12	Induced differential pressure versus time for specimens of a geosynthetic clay liner as a function of effective stress, σ' , during multi-stage membrane testing in flexible-wall cell.....	5.42
5.13	Elapsed time versus membrane efficiency coefficients for specimens of a geosynthetic clay liner as a function of effective stress, σ' , during multi-stage membrane testing in flexible-wall cell.....	5.43
5.14	Comparison of measured membrane efficiencies versus elapsed time based on (a) initial concentration differences ($\Delta\pi_0$) and (b) average concentration differences ($\Delta\pi_{ave}$) for specimens of a geosynthetic clay liner as a function of effective stress, σ' , during multi-stage membrane testing in flexible-wall cell.....	5.44
5.15	Incremental (a) and cumulative (b) changes in cell volume for specimens of a geosynthetic clay liner as a function of effective stress, σ' , during multi-stage membrane testing in flexible-wall cell.....	5.45
5.16	Incremental (a) and cumulative (b) volumetric strains for specimens of a geosynthetic clay liner as a function of effective stress, σ' , during multi-stage membrane testing in flexible-wall cell.....	5.46
5.17	Effect of potassium chloride (KCl) source concentration on steady-state membrane efficiency coefficients for specimens of a geosynthetic clay liner as a function of effective stress, σ' , during multi-stage membrane testing in flexible-wall cell.....	5.47
5.18	Effect of effective stress on steady-state membrane efficiency coefficients for specimens of a geosynthetic clay liner subjected to different source concentrations, C_{ot} , of potassium chloride (KCl).....	5.48
5.19	Comparison of steady-state membrane efficiency coefficients for specimens of a geosynthetic clay liner measured in this study using a flexible-wall cell as a function of effective stress, σ' , versus those reported by Malusis and Shackelford (2002b) using a rigid-wall cell with different specimen thicknesses, L	5.49

5.20	Steady-state membrane efficiency coefficients, ω_{ss} , versus average of difference in initial (source) KCl concentrations for specimens of a geosynthetic clay liner: (a) ω_{ss} values based initial concentration differences ($\Delta\pi_0$), $\omega_{ss,0}$, versus average concentration differences ($\Delta\pi_{ave}$), $\omega_{ss,ave}$; (b) ratio of ω_{ss} based on $\Delta\pi_{ave}$ relative to ω_{ss} based on $\Delta\pi_0$	5.50
5.21	Comparison of membrane efficiency coefficients at steady state based on (a) initial concentration differences ($\Delta\pi_0$) and (b) average concentration differences ($\Delta\pi_{ave}$) measured in this study using a flexible-wall cell as a function of effective stress, σ' , versus those reported by Malusis and Shackelford (2002b) using a rigid-wall cell.....	5.51
5.22	Comparison of membrane efficiency coefficients measured in this study using a flexible-wall cell as a function of effective stress, σ' , versus those previously measured in a rigid-wall cell reported by Malusis and Shackelford (2002b).....	5.52
5.23	History of void ratios during consolidation and membrane testing for specimens of a geosynthetic clay liner consolidated to different effective stress, σ'	5.53
5.24	History of porosities during consolidation and membrane testing for specimens of a geosynthetic clay liner consolidated to different effective stress, σ'	5.54

Chapter 6

6.1	A schematic diagram for the flushing and hydraulic conductivity test for compacted specimens of Nelson Farm Clay (NFC) and NFC plus 5 % bentonite.....	6.28
6.2	Pictorial view of permeating compacted specimens of Nelson Farm Clay (NFC) and NFC plus 5 % bentonite.....	6.29
6.3	Pictorial views for different stage for setting up compacted specimens of Nelson Farm Clay (NFC) and NFC plus 5 % bentonite in flexible-wall cell for membrane testing (clockwise from top left): (a) permeating; (b) extruding; (c) specimen setup; (d) membrane and top cap; (e) flexible-wall cell; and (f) membrane testing system.....	6.30
6.4	Grain-size distributions for Nelson Farm Clay (NFC) and bentonite used in this study (after Yeo et al. 2005).....	6.31
6.5	Compaction curves for Nelson Farm Clay (NFC) and NFC plus 5 % (dry weight) bentonite (B): (a) standard compaction curve (ASTM D 698) (b) modified compaction curve (ASTM D 1557); (c) reduced compaction curve (Eng. Manual EM-1110-2-1906).....	6.32
6.6	Initial water contents versus hydraulic conductivity of compacted specimens of (a) Nelson Farm Clay (NFC) (b) NFC plus 5 % bentonite compacted by standard compaction (ASTM D 698), modified compaction (ASTM D 1557), and reduced compaction (Eng. Manual EM-1110-2-1906).....	6.33

6.7	Acceptable zones for Nelson Farm Clay (NFC) based on (a) the traditional design approach (b) the hydraulic conductivity approach proposed by Daniel and Benson (1990).....	6.34
6.8	Acceptable zones for Nelson Farm Clay (NFC) plus 5 % bentonite based on (a) the traditional design approach (b) the hydraulic conductivity approach proposed by Daniel and Benson (1990).....	6.35
6.9	Electrical conductivity (a) and hydraulic conductivity (b) versus elapsed time for compacted specimens of Nelson Farm Clay (NFC) and NFC plus 5 % bentonite (B) permeated with de-ionized water during flushing stage of test prior to membrane testing.....	6.36
6.10	Electrical conductivity (EC) in circulation outflows from top and bottom boundaries of flexible-wall cell during membrane testing for compacted specimens of Nelson Farm Clay (NFC) and NFC plus 5 % bentonite (B) [$EC_0 = EC$ of KCl source solution]: (a) NFC multi-stage; (b) NFC plus 5 % B multi-stage; and NFC plus 5 % B single-stage at (c) 3.9 mM KCl (d) 8.7 mM KCl, and (e) 20 mM KCl concentration differences.....	6.37
6.11	Boundary pressures and effective stresses for a compacted specimen of Nelson Farm Clay (No.1) at an initial effective stress of 34.5 kPa (5.0 psi) during membrane testing in flexible-wall cell.....	6.38
6.12	Boundary pressures and effective stresses for a compacted specimen of Nelson Farm Clay (NFC) plus 5 % bentonite (No. 2) at an initial effective stress of 34.5 kPa (5.0 psi) during membrane testing in flexible-wall cell.....	6.39
6.13	Boundary pressures and effective stresses for a compacted specimen of Nelson Farm Clay (NFC) plus 5 % bentonite (No. 3) at an initial effective stress of 34.5 kPa (5.0 psi) during membrane testing in flexible-wall cell.....	6.40
6.14	Boundary pressures and effective stresses for a compacted specimen of Nelson Farm Clay (NFC) plus 5 % bentonite (No. 4) to an initial effective stress of 34.5 kPa (5.0 psi) during membrane testing in flexible-wall cell.....	6.41
6.15	Boundary pressures and effective stresses for a compacted specimen of Nelson Farm Clay (NFC) plus 5 % bentonite (No. 5) at an initial effective stress of 34.5 kPa (5.0 psi) during membrane testing in flexible-wall cell.....	6.42
6.16	Measured chemico-osmotic pressure differences across compacted specimens of (a) Nelson Farm Clay (NFC; No. 1) and (b) and (c) NFC plus 5 % bentonite (Nos. 2 and 3) at an initial effective stress of 34.5 kPa (5.0 psi) during membrane testing in flexible-wall cell.....	6.43
6.17	Measured chemico-osmotic pressure differences across compacted specimens of (d) and (e) NFC plus 5 % bentonite (Nos. 4 and 5) at an initial effective stress of 34.5 kPa (5.0 psi) during membrane testing in flexible-wall cell.....	6.44

6.18	Elapsed time versus membrane efficiency coefficients for compacted specimens of Nelson Farm Clay (NFC) during multi-stage membrane testing in flexible-wall cell.....	6.45
6.19	Comparison of measured membrane efficiencies versus elapsed time based on (a) initial concentration differences ($\Delta\pi_0$) and (b) average concentration differences ($\Delta\pi_{ave}$) for a compacted specimen of Nelson Farm Clay (NFC) during multi-stage membrane testing in flexible-wall cell.....	6.46
6.20	Elapsed time versus membrane efficiency coefficients for compacted specimens of Nelson Farm Clay (NFC) plus 5 % bentonite soils during multi-stage membrane testing in flexible-wall cell.....	6.47
6.21	Comparison of measured membrane efficiencies versus elapsed time based on (a) initial concentration differences ($\Delta\pi_0$) and (b) average concentration differences ($\Delta\pi_{ave}$) for compacted specimens of Nelson Farm Clay (NFC) plus 5 % bentonite soils during multi-stage membrane testing in flexible-wall cell.....	6.48
6.22	Incremental (a) and cumulative (b) changes in cell volume for compacted specimens of Nelson Farm Clay (NFC) and NFC plus 5 % bentonite (B) during membrane testing in a flexible-wall cell.....	6.49
6.23	Incremental (a) and cumulative (b) volumetric strains for compacted specimens of Nelson Farm Clay, NFC (No. 1), and NFC plus 5 % bentonite (Nos. 2, 3, 4, and 5) during membrane testing in a flexible-wall cell.....	6.50
6.24	Comparison of steady-state membrane efficiency coefficients for compacted specimens of Nelson Farm Clay (NFC) and NFC plus 5 % bentonite (B) measured in this study using a flexible-wall cell as a function of effective stress, σ' , versus those reported by Malusis and Shackelford (2002b) using a rigid-wall cell with different specimen thicknesses, L.....	6.51
6.25	Steady-state membrane efficiencies, ω_{ss} , versus average of difference in initial (source) KCl concentrations for compacted specimens of Nelson Farm Clay (NFC) and NFC plus 5 % sodium bentonite (B): (a) ω_{ss} values based initial concentration differences ($\Delta\pi_0$), $\omega_{ss,0}$, versus average concentration differences ($\Delta\pi_{ave}$), $\omega_{ss,ave}$; (b) ratio of ω_{ss} based on $\Delta\pi_{ave}$ relative to ω_{ss} based on $\Delta\pi_0$	6.52
6.26	Comparison of membrane efficiency coefficients at steady state based on (a) initial concentration differences ($\Delta\pi_0$) and (b) average concentration differences ($\Delta\pi_{ave}$) measured in this study using a flexible-wall cell as a function of effective stress, σ' , versus those reported by Malusis and Shackelford (2002b) using a rigid-wall cell.....	6.53

LIST OF SYMBOLS

A	= cross-sectional area of the specimen [L^2]
a_v	= coefficient of compressibility [$M^{-1}Lt^2$]
C	= solute concentration [$M \cdot L^{-3}$ or $mol \cdot L^{-3}$]
C_c	= compression index [dimensionless]
C_s	= salt concentration [$M \cdot L^{-3}$]
C_o	= source solute concentration [$mol \cdot L^{-3}$]
C_α	= secondary compression index [dimensionless]
c_v	= the coefficient of consolidation [L^2t^{-1}]
D	= bulk diffusion coefficient [L^2t^{-1}]
D^*	= effective diffusion coefficient [L^2t^{-1}]
e	= void ratio [dimensionless]
e_o	= initial void ratio [dimensionless]
g	= acceleration of gravity [Lt^{-2}]
G_s	= specific gravity [dimensionless]
h	= hydraulic head [L]
I	= electrical current [Coulomb $\cdot L^{-2} t^{-1}$]
J	= total solute flux [$mol \cdot L^{-2}t^{-1}$]
J_d	= diffusive flux of solute [$mol \cdot L^{-2}t^{-1}$]
k_e	= electro-osmotic conductivity [$L^2t^{-1}Volt^{-1}$]
k_h	= hydraulic conductivity [Lt^{-1}]
L	= specimen thickness [L]
m_v	= coefficient of volume compressibility [$M^{-1}Lt^2$]
n	= specimen porosity [dimensionless]
P	= hydraulic (or liquid) pressure [$ML^{-1}T^{-2}$]
P_e	= effective or net pressure measured across specimen [$ML^{-1}T^{-2}$]
q	= total hydraulic liquid flux [Lt^{-1}]
q_h	= hydraulic liquid flux [Lt^{-1}]
q_π	= chemico-osmotic liquid flux [Lt^{-1}]
Q	= volumetric flow ratio [L^3t^{-1}]
R	= universal gas constant [$8.314 J \cdot mol^{-1} \cdot K^{-1}$]
R_c	= compression ratio [dimensionless]
R_d	= retardation factor [dimensionless]
R_α	= secondary compression ratio [dimensionless]
ss	= subscript denoting "steady state"

T	= absolute temperature [K]
t	= elapsed time to steady state [t]
u	= pore-water pressure [$ML^{-1}T^{-2}$]
V	= volume [L^3]
ϵ_{vert}	= vertical strain [dimensionless]
ϵ_{vol}	= volumetric strain [dimensionless]
μ	= chemical potential of solute [$ML^2mol^{-1}t^{-2}$]
ν	= number of ions per molecule of salt
π	= chemico-osmotic pressure [$ML^{-1}t^{-2}$]
ρ	= soil density [ML^{-3}]
τ	= tortuosity factor [dimensionless]
σ_c	= confining stress [$ML^{-1}T^{-2}$]
σ'	= effective consolidation stress [$ML^{-1}T^{-2}$]
σ'_{ave}	= average effective consolidation stress [$ML^{-1}T^{-2}$]
ω or σ	= chemico-osmotic efficiency coefficient [dimensionless]

CHAPTER 1

INTRODUCTION

1.1 BACKGROUND

The potential significance of membrane behavior in clay barriers, which results in hyperfiltration and chemico-osmosis, has become an important consideration in terms of the use of such barriers in waste containment systems and for *in situ* remediation applications (Kemper and Rollins 1966, Bresler 1973, Greenberg et al. 1973, Mitchell et al. 1973, Fritz and Marine 1983, Olsen 1985, Barbour and Fredlund 1989, Yeung and Mitchell 1993, Keijzer et al. 1997, Neuzil 2000, Malusis et al. 2002, Shackelford et al. 2003, Yeo et al. 2005, Henning et al. 2006). The extent to which a soil acts as a semi-permeable membrane is quantified in terms of a chemico-osmotic efficiency coefficient, ω (Mitchell 1993, Malusis et al. 2002, Shackelford et al. 2003), also referred to as the reflection coefficient, σ (Staverman 1952, Kemper and Rollins 1966, Olsen et al. 1990, Keijzer et al. 1997), which ranges zero ($\omega = 0$), representing no solute restriction (i.e., no membrane behavior), to unity ($\omega = 1$), representing complete solute restriction (i.e., an "ideal" membrane). In most cases, the pores in soils that exhibit membrane behavior vary over a range of sizes such that not all of the pores are restrictive. In such cases, $0 < \omega < 1$, and the soils exhibiting membrane behavior typically are referred to as "non-ideal" membranes (Kemper and Rollins 1966, Olsen 1969, Bresler 1973, Barbour 1986, Barbour and Fredlund 1989, Mitchell 1993, and Keijzer et al. 1997, Malusis et al. 2002, Shackelford et al. 2003).

The ability of clays to act as semi-permeable membranes that inhibit the passage

of solutes relative to liquid has been well documented (McKelvey and Milne 1962, Kemper and Rollins 1966, Olsen 1969, Marine and Fritz 1981, and Olsen et al. 1990, Malusis et al. 2002, Shackelford et al. 2003). In particular, evidence exists in the literature indicating that subsurface geological formations can exist as semipermeable membranes, resulting in the development of osmotic pressure, differences in electrical potential, and salt sieving or ultrafiltration and ion exclusion due to the net electrical charge deficiency in clay minerals (Mackay 1946, Hanshaw 1972). For example, aquitards have been shown to act as an effective pollution barrier to the movement of salts (e.g., NaCl) between overlying salt-water aquifers and underlying fresh-water aquifers typical of coastal regions (Greenberg et al. 1973). Also, the existence of anomalous hydraulic heads in geologic formations has been attributed to the existence of osmotic pressures generated by differences in chemical potential of a solution across a semi-permeable membrane (Marine and Fritz 1981, Fritz 1986, Neuzil 2000).

Membrane behavior in clays typically has been measured in the laboratory using either flow-through or no-flow test procedures. For the flow-through test procedure, two approaches have commonly been employed (McKelvey et al. 1962, Kemper and Evans 1963, Kemper and Quirk 1972, Hanshaw and Coplen 1973, Kharaka and Smalley 1976, Fritz et al. 1983, Whitworth and Fritz 1994, Ishiguro et al. 1995, Keijzer et al. 1999, Henning et al. 2006). The first approach, which is far more common, involves forcing a salt solution through the clay under an applied hydraulic pressure difference (hydraulic gradient) and determining how much of the salt has been filtered out of solution (referred to as filtrate) by the clay due to membrane behavior (McKelvey et al. 1962, Hanshaw and Coplen 1973, Kharaka and Smalley 1976, Fritz et al. 1983, Whitworth and Fritz 1994).

This type of test often is referred to as a hyperfiltration test. The second approach involves determining the membrane efficiency from the measured amount of chemico-osmotic counter flow (Kemper and Evans 1963, Kemper and Quirk 1972, Ishiguro et al. 1995, Keijzer et al. 1999, Henning et al. 2006). This second approach is less common because of the greater difficulty in accurately measuring the small quantities of chemico-osmotic counter flow that typically result.

In the no-flow test procedure, solution flow is prevented resulting in the build up of a chemico-osmotic pressure difference across the specimen to counteract the tendency for chemico-osmotic flow, and the membrane efficiency (ω) is determined based on the magnitude of the pressure buildup and the salt concentrations at the boundaries (Olsen 1969, Elrick et al. 1976, Olsen 1984, Malusis et al. 2001, Malusis and Shackelford 2002, Shackelford and Lee 2003, Yeo et al. 2005). In this case, differences in test results can occur depending on how well the salt concentrations at the boundaries are maintained constant during the test.

The results of flow-through tests conducted on a variety of soils and synthetic porous media and under a variety of conditions have provided insight into the factors affecting membrane behavior in such tests. For example, McKelvey et al. (1957) studied salt filtering using two synthetic granular ion-exchange resins and a synthetic ion-exchange membrane, and concluded that the salt was filtered by virtue of electrolytic dissociation and the ionic nature of the ion-exchange resins and membrane. McKelvey et al. (1962) also studied the salt filtering ability of compacted Wyoming bentonite and a disaggregated shale using solutions of sodium chloride (NaCl) and concluded that the increased desalting ability of both the bentonite and shale could be attributed to lower

porosity. Hanshaw and Coplen (1973) studied the existence and extent of ultrafiltration (i.e., hyperfiltration or ion exclusion) of 10 clay specimens consisting of Na-montmorillonite by forced passage of NaCl solutions, and concluded that the extent or degree of ion exclusion depends upon the ion exchange capacity of the clay. Kharaka and Smalley (1976) performed filtration experiments using chloride solutions with compacted bentonite and kaolinite clay, and concluded that the chemistry of natural water is influenced strongly by the membrane behavior of sedimentary rocks. Finally, Whitworth and Fritz (1994) provided experimental results indicating that increasing electrolyte flux into a compacted smectite (i.e., montmorillonite) membrane resulted in greater permeability of the membrane as the influx of electrolyte into the membrane pores decreases the diffuse double layer (DDL) thickness associated with the clay particles.

Membrane behavior in soils also results in chemico-osmosis, or the movement of liquid in response to a solute concentration gradient. For example, Kemper (1960) studied the potential effects of the electrostatic charge and the DDL on the movement of NaCl solutions and concluded that the electrostatic charge and DDL have considerable effect on the movement of solution through films with thicknesses encountered at moisture contents less than field capacity. Kemper and Evans (1963) also conducted experimental studies involving restriction of solutes by membranes and the consequent effects on the movement of water, and concluded that repulsion of anions from the vicinity of negatively charged mineral surfaces causes an increase in the membrane efficiency (σ). Kemper and Rollins (1966) conducted experiments to measure ω due to a variety of concentration differences for solutions of NaCl, Na₂SO₄, CaCl₂ and CaSO₄ and a variety of hydraulic pressure differences, and concluded that salt gradients may become a major

factor causing solution movement under unsaturated conditions. Olsen (1969, 1972) studied the simultaneous fluxes of liquid and charge under hydraulic, electrical, and electrolyte concentration gradients, and concluded that not only hydraulic gradients but also osmotic and possibly electro-chemical gradients should be considered in evaluating subsurface flow of liquids at depth. Ishiguro et al. (1995) evaluated the membrane behavior of a Wyoming bentonite and concluded that montmorillonite clay can be used effectively as a reverse osmosis membrane for the rejection of electrolyte solutes. Finally, Keijzer et al. (1997, 1999) and Shackelford and Lee (2003) noted that the measurement of low measured membrane efficiencies in flow-through systems may be due to a decrease in the boundary salt concentrations resulting in lower observed chemico-osmotic pressure differences that also decrease with time as opposed to a decrease in the actual membrane efficiency of the specimens.

Chemico-osmotic, no-flow tests also have been conducted by maintaining the concentrations at the boundaries constant, or nearly constant, during the test. For example, Malusis and Shackelford (2002) used the no-flow testing apparatus that includes a rigid-wall testing cell developed by Malusis et al. (2001) to study the membrane behavior of a geosynthetic clay liner (GCL) containing granular bentonites. Malusis and Shackelford (2002) found the GCL behaved as a semipermeable membrane and concluded that the existence of the membrane behavior in the GCLs has important ramifications with respect to the evaluation of the hydraulic and contaminant transport performance of GCLs used in waste containment applications. Shackelford and Lee (2003) used the no-flow procedure described by Malusis et al. (2001) to evaluate the potentially destructive role of diffusion of invading salt cations on the ability of a GCL to

act as a semipermeable membrane. Yeo et al. (2005) used the no-flow testing procedure described by Malusis et al. (2001) to evaluate the ability of soil-bentonite (SB) backfills to behave as semipermeable membranes and concluded that chemico-osmotic liquid flux due to membrane behavior could reduce the total liquid flux through an SB vertical cutoff wall. Finally, Henning et al. (2006) used the same approach as Yeo et al. (2006) to evaluate the existence of membrane behavior in two soil-bentonite backfills obtained from two field-constructed vertical cutoff walls. Henning et al. (2006) concluded that membrane behavior in such materials could be significant, depending on the void ratio and clay content of the backfill.

Membrane behavior also has been shown to affect the mechanical properties of clays. For example, Mitchell et al. (1973) studied chemico-osmotic consolidation of clays and concluded that such consolidation was detectable only in highly compressible, active clays such as bentonite. Barbour et al. (1989) also studied the effects of membrane behavior on the consolidation of clays and concluded that the dominant mechanism of volume change associated with brine contamination was osmotic consolidation. Finally, Di Maio (1996) performed consolidation tests using salt solutions and reported that changes in the thickness of the DDL were produced by ions diffusing into or out of the clay, and that specific chemical treatment may be a way to cause a lasting improvement in the mechanical properties of active clays.

1.2 GOALS AND OBJECTIVES OF RESEARCH

Although membrane behavior has been shown to exist in bentonite-based barrier materials used in waste containment applications, such as GCLs and soil-bentonite

backfills in vertical cutoff walls, the existence of membrane behavior in compacted natural clays commonly used as liners in waste containment applications has not been evaluated. Therefore, the primary goal of this study was the evaluation of the potential existence of membrane behavior in a compacted natural clay soil that is similar to those typically used as compacted clay liners in waste containment applications. This goal was achieved by measuring the membrane efficiency for compacted specimens of a local clay, known as Nelson Farm Clay (NFC), as well as compacted specimens of the NFC amended with 5 % (dry wt.) of a sodium bentonite. The measured hydraulic conductivity values of compacted specimens of both of these soils were found to be sufficiently low (i.e., $< 10^{-7}$ cm/s) such that both soils qualified for use as compacted clay liners for typical waste containment applications, including those for municipal solid waste and hazardous waste landfills.

A secondary goal of this study pertains to the development of a flexible-wall testing apparatus for the measurement of clay membrane behavior under closed-system (i.e., no-flow) boundary conditions. Although flexible-wall apparatuses have been used in the past to measure membrane behavior of fine-grained porous media, such as clays, dredged soils and shales (e.g., Keijzer et al. 1997, 1999, Keijzer and Loch 2001, Rahman et al. 2005), either open-system boundary conditions have been employed, such that hydraulic and chemico-osmotic flow are allowed to occur (Keijzer et al. 1997, 1999, Keijzer and Loch 2001), or the control on the hydraulic boundary conditions for the system has been poorly defined (Rahman et al. 2005). A primary advantage of closed-system boundary conditions relative to open-system boundary conditions is that the former is based on measurement of chemico-osmotic pressure difference developed

during the test due to the prevention of liquid flux, which is more sensitive and easier to measure than the small magnitudes of liquid flux that typically result under open-system boundary conditions. Thus, development of a closed system, flexible-wall apparatus with well-defined boundary conditions represents a novel contribution to the open literature pertaining to equipment used to measure membrane behavior of clay soils.

The third goal pertains to the evaluation of the influence of an isotropic state-of-stress (SOS) on the membrane behavior of a GCL. Although the effect of SOS has been evaluated for a specially prepared kaolin clay using a rigid-wall apparatus (Olsen 1972) as well as a naturally occurring shale using a flexible-wall apparatus (Rahman et al. 2005), the evaluation of the potential influence of an isotropic SOS on the membrane behavior of a GCL has not heretofore been evaluated.

These goals will be accomplished by achieving the following objectives:

- (1) Develop a flexible-wall testing apparatus and procedures to be able to consider stress conditions such as effective stress, back pressure, and consolidation in the laboratory for measuring the chemico-osmotic efficiency of clay soils in the presence of electrolyte solutions;
- (2) Evaluate the performance of the testing apparatus for measuring the chemico-osmotic efficiency coefficient (ω) for a given soil, solute, and boundary conditions by comparing the results obtained with the flexible-wall apparatus with those previously reported based on an existing rigid-wall testing apparatus on the same GCL;
- (3) Evaluate the potential effect of effective stress on the membrane behavior of the same GCL used in (2) through consolidation of the GCL using the same testing

- apparatus as described in (1);
- (4) Determine the existence and potential significance of membrane behavior of compacted natural clays that could be considered for use as a compacted clay liner for waste containment applications (e.g., landfills); and
 - (5) Evaluate the effect of effective stress and bentonite addition on the ability of the natural clay used in (4) on the existence and potential significance of membrane behavior for the clay.

The results of this study are expected to advance our present understanding of membrane behavior sufficiently to allow a more rational basis for potentially incorporating membrane behavior into the design of clay barriers for waste containment applications, such as compacted clay liners, geosynthetic clay liners, and soil-bentonite vertical cutoff walls. In addition, the results may have significant implications with respect to the relationships among effective stress, void ratio, hydraulic conductivity, consolidation stress, and membrane behavior for such clay barriers.

1.3 REFERENCES

- Bader, S. and Heister, K. (2006). "The effect of membrane potential on the development of chemical osmotic pressure in compacted clay." *Journal of Colloid and Interface Science*, 297, 329-340.
- Barbour, S. L. and Fredlund, D. G. (1989). "Mechanisms of osmotic flow and volume change in clay soils." *Canadian Geotechnical Journal*, Vol. 26, No. 4, 551-562.
- Bresler, E. (1973). "Simultaneous transport of solutes and water under transient

- unsaturated flow conditions." *Water Resources Research*, Vol. 9, No. 4, 975-986.
- Di Maio, C. (1996). "Exposure of bentonite to salt solution: osmotic and mechanical effects." *Geotechnique*, Vol. 46, No. 4, 695-707.
- Elrick, D. E., Smiles, D. E., Baumgartner, N., And Groenevelt, P. H. (1976). "Coupling phenomena in saturated homo-ionic montmorillonite: I. Experimental." *Soil Science Society of America Journal*, Vol. 40, No. 4, 490-491.
- Evans, J. C., Costa, M., and Cooley, B. (1995). "The state of stress in soil-bentonite slurry trench cutoff walls." *Geoenvironment 2000, Geotechnical special publication No. 46*, Y. B. Acar and D. E. Daniel, eds., ASCE, New York, 1173-1191.
- Filz, G. M. (1996). "Consolidation stresses in soil-bentonite backfilled trenches." *Proc., 2nd Int. Congress on Environmental Geotechnics*, M. Kamon, ed., A. A. Balkema, Rotterdam, The Netherlands, 497-502.
- Filz, G. M., Baxter, D. Y., Bentler, D. J., and Davidson, R. R. (1999). "Ground deformation adjacent to a soil-bentonite cutoff wall." *Proc., GeoEngineering for Underground Facilities*, ASCE, Reston, Va., 121-139.
- Fritz, S. J. (1986). "Ideality of clay membranes in osmotic process: a review." *Clays and Clay Minerals*, Vol. 34, No. 2, 214-223.
- Fritz, S. J. and Marine, I. W. (1983). "Experimental support for a predictive osmotic model of clay membranes." *Geochimica et Cosmochimica Acta*, Vol. 47, No. 8, 1515-1522.
- Gleason, M. H., Daniel, D. E., and Eykholt, G. R. (1997). "Calcium and sodium bentonite for hydraulic containment application." *Journal of Geotechnical and*

Geoenvironmental Engineering, Vol. 123, No. 5, 438-445.

Greenberg, J. A., Mitchell, J. K., and Witherspoon, P. A. (1973). "Coupled salt and water flows in a groundwater basin." *Journal of Geophysical Research*, Vol. 78, No. 27, 6341-6353.

Groenevelt, P. H. and Elrick, D. E. (1976). "Coupling phenomena in saturated homo-ionic montmorillonite: II. Theoretical." *Soil Science Society of America Journal*, Vol. 40, No. 6, 820-823.

Hanshaw, B. B. (1972). "Natural-membrane phenomena and subsurface waste emplacement." *The American Association of Petroleum Geologists*, Vol. 18, No. 6, 308-317.

Hanshaw, B. B. and Coplen, T. B. (1973). "Ultrafiltration by a compacted clay membrane – II. Sodium ion exclusion at various ionic strengths." *Geochimica et Cosmochimica Acta*, Vol. 37, No. 10, 2311-2327.

Heister, K., Keijzer, Th. J. S. and Loch, J. P. G. (2004). "Stability of clay membranes in chemical osmosis." *Soil Science Society of America Journal*, Vol. 169, No. 9, 632-639.

Henning, J. T., Evans, J. C., and Shackelford, C. D. (2006). "Membrane behavior of two backfills from field-constructed soil-bentonite cutoff walls." *Journal of Geotechnical and Geoenvironmental Engineering*, Vol. 132, No. 10, 1243-1249.

Ishiguro, M., Matsuura, T., and Detellier, C. (1995). "Reverse osmosis separation for a montmorillonite membrane." *Journal of Membrane Science*, Vol. 107, No. 1, 87-92.

Keijzer, Th. J. S., Kleingeld, P. J., and Loch, J. P. G. (1997). "Chemical osmosis in

- compacted clayey material and the prediction of water transport." *Geoenvironmental Engineering, Contaminated Ground: Fate of Pollutants and Remediation*, R. N. Yong and H. R. Thomas, eds., University of Wales, Cardiff, U. K., Sept. 6-12, Thomas Telford Publ., London, 199-204.
- Keijzer, Th. J. S., Kleingeld, P. J., and Loch, J. P. G. (1999). "Chemical osmosis in compacted clayey material and the prediction of water transport." *Engineering Geology*, Vol. 53, No. 2, 151-159.
- Keijzer, Th. J. S. and Loch, J. P. G. (2001). "Chemical osmosis in compacted dredging sludge." *Soil Science Society of America Journal*, Vol. 65, No. 4, 1046-1055.
- Kemper, W. D. (1960). "Water and ion movement in thin films as influenced by the electrostatic charge and diffuse layer of cations associated with clay mineral surfaces." *Soil Science Society of America Proc.*, Vol. 24, 10-16.
- Kemper, W. D. (1961). "Movement of water as effected by free energy and pressure gradients: II. Experimental analysis of porous systems in which free energy and pressure gradients act in opposite directions." *Soil Science Society of America Proceedings*, Vol. 25, No. 4, 260-265.
- Kemper, W. D. and Evans N. A. (1963). "Movement of water as effected by free energy and pressure gradients: III. Restriction of solutes by membranes." *Soil Science Society of America Proceedings*, Vol. 27, No. 5, 485-490.
- Kemper, W. D. and Quirk, J. P. (1972). "Ion mobilities and electric charge of external clay surfaces inferred from potential differences and osmotic flow." *Soil Science Society of America Proc.*, Vol. 36, No. 3, 426-433.
- Kemper, W. D. and Rollins, J. B. (1966). "Osmotic efficiency coefficients across

- compacted clays." *Soil Science Society of America Proceedings*, Vol. 30, No. 5, 529-534.
- Kharaka, Y. K. and Berry, F. A. F. (1973). "Simultaneous flow of water and solutes through geological membranes – I. Experimental investigation." *Geochimica et Cosmochimica Acta*, Vol. 37, No. 12, 2577-2603.
- Kharaka, Y. K. and Smalley, W. C. (1976). "Flow of water and solutes through compacted clays." *The American Association of Petroleum Geologists Bulletin*, Vol. 60, No. 6, 973-980.
- MacKay, R. A. (1946). "The control of impounding structures on ore deposition." *Economic Geology and the Bulletin of the Society of Economic Geologists*, The Economic Geology Publ. Co., New Haven, CT, Vol. 41, 13-46.
- Malusis, M. A. (2001). *Membrane Behavior and Coupled Solute Transport through a Geosynthetic Clay Liner*. PhD Dissertation, Colorado State University, Fort Collins, CO.
- Malusis, M. A. and Shackelford, C. D. (2002). "Chemico-osmotic efficiency of a geosynthetic clay liner." *Journal of Geotechnical and Geoenvironmental Engineering*, Vol. 128, No. 2, 97-106.
- Malusis, M. A., Shackelford, C. D., and Olsen, H. W. (2001). "A laboratory apparatus to measure chemico-osmotic efficiency coefficients for clay soils." *Geotechnical Testing Journal*, Vol. 24, No. 3, 229-242.
- Malusis, M. A., Shackelford, C. D., and Olsen, H. W. (2003). "Flow and transport through clay membrane barriers." *Engineering Geology*, Vol. 70, No. 3, 235-248.
- Manassero, M., and Dominijanni, A. (2003). "Modeling the osmosis effect on solute

- migration through porous media." *Geotechnique*, Vol. 53, No. 5, 481-492.
- Marine, I. W. (1974). "Geohydrology of a buried Triassic basin at Savannah River plant, South Carolina." *The American Association of Petroleum Geologists Bulletin*, Vol. 58, No. 9, 1825-1837.
- Marine, I. W. and Fritz, S. J. (1981). "Osmotic model to explain anomalous hydraulic heads." *Water Resources Research*, Vol. 17, No. 1, 73-82.
- McKelvey, J. G. and Milne, I. H. (1962). "The flow of salt solutions through compacted clay." *Proceedings, Ninth National Conference on Clays and Clay Minerals*, Lafayette, Indiana, Oct. 5-8, 1960, Pergamon Press, New York, 248-259.
- McKelvey, J. G., Spiegler, K. S. and Wyllie, M. R. J. (1957). "Salt filtering by ion-exchange grains and membranes." *The Journal of Physical Chemistry*, Vol. 61, No. 2, 174-178.
- Mitchell, J. K., Greenberg, J. A., and Witherspoon, P. A. (1973). "Chemico-osmotic effects in fine-grained soils." *Journal of the soil mechanics and foundations division*, Vol. 99, SM 4, 307-322.
- Neuzil, C. E. (2000). "Osmotic generation of 'anomalous' fluid pressures in geological environments." *Nature*, Vol. 403, No. 6766, 182-184.
- Olsen, H. W. (1966). "Darcy's law in saturated kaolinite." *Water Resources Research*, Vol. 12, No. 2, 287-295.
- Olsen, H. W. (1969). "Simultaneous fluxes of liquid and charge in saturated kaolinite." *Soil Science Society of America Proceedings*, Vol. 33, No. 3, 338-344.
- Olsen, H. W. (1972). "Liquid movement through kaolinite under hydraulic, electric, and osmotic gradients." *The American Association of Petroleum Geologists Bulletin*,

Vol. 56, No. 10, 2022-2028.

- Olsen, H. W. (1985). "Osmosis: A cause of apparent deviations from Darcy's law." *Canadian Geotechnical J.*, Vol. 22, No. 2, 238-241.
- Olsen, H. W., Yearsley, E. N., and Nelson, K. R. (1990). "Chemico-osmosis versus diffusion-osmosis." *Transportation Research Record No. 1288*, Transportation Research Board, Washington D.C., 15-22.
- Rahman, M. M., Chen, S., and Rahman, S. S. (2005). "Experimental investigation of shale membrane behavior under tri-axial condition." *Petroleum Science and Technology*, 23, 1265-1282.
- Shackelford, C. D. and Lee, J.-M. (2003). "The destructive role of diffusion on clay membrane behavior." *Clays and Clay Minerals*, CMS, Vol. 51, No. 2, 186-196.
- Shackelford, C. D., Malusis, M. A., and Olsen, H. W. (2003). "Clay membrane behavior for geoenvironmental containment." *Soil and Rock America Conference 2003* (Proceedings of the joint 12th Panamerican Conference on Soil Mechanics and Geotechnical Engineering and the 39th U.S. Rock Mechanics Symposium), P. J. Culligan, H. H. Einstein, and A. J. Whittle, eds., Verlag Glückauf GMBH, Essen, Germany, Vol. 1, 767-774.
- Staverman, A. J. (1952). "Non-equilibrium thermodynamics of membrane processes." *Transactions of the Faraday Society*, Vol. 48, No. 2, 176-185.
- Whitworth, T. M. and Fritz, S. J. (1994). "Electrolyte-induced solute permeability effects in compacted smectite membranes." *Applied Geochemistry*, Vol. 9, No. 5, 533-546.
- Yeo, S.-S., Shackelford, C. D., and Evans, J. C. (2005). "Membrane behavior of model

soil-bentonite backfills." *Journal of Geotechnical and Geoenvironmental Engineering*, Vol. 131, No. 4, 418-429.

Yeung, A. T. and Mitchell, J. K. (1993). "Coupled fluid, electrical, and chemical flows in soil." *Geotechnique*, Vol. 43, No. 1, 121-134.

CHAPTER 2

LITERATURE REVIEW

2.1 FIELD EVIDENCE OF MEMBRANE BEHAVIOR

Mackay (1946) discusses the phenomenon whereby subsurface geological structures exist as semipermeable membranes that essentially cause metals in solution to be deposited within the structure while simultaneously allowing the solvent or ore carrying fluid (e.g., ground water) to pass through the structure. The phenomenon responsible for the impedance was referred to as "exosmosis" if the metal is in true solution, and dialysis (ultrafiltration or hyperfiltration) if the metal is in colloidal form. The factors that determine whether a structure will be permeable or not to a substance are the effective pore sizes and properties of the substance. Effective size of pores refers to the actual size as modified by adsorption effects, and properties of the substance indicate the molecular size, the degree of ionization, the rate of penetration, and the valence.

Whether a specific dissolved substance or dispersed solid can be separated from the ambient liquid by impedance is mainly a matter of pore size, and this constitutes semi-permeability. The pore size necessary for the retention of a given substance is related to the particle size for hyperfiltration and the molecular size and hydrated ionic volume (i.e., instead of discrete particle size) for "exosmosis". The actual pore size is reduced to an effective pore size by adsorption effects, and the divergence between actual and effective pore size increases in the lower size ranges. The greater the molecular size, the less the penetrability through a given membrane.

Both the chemical environment and changing temperature and pressure conditions contribute to deposition. Also, deposition cannot take place without impedance except in small amounts of mixed minerals. Impoundment is necessary to accumulate appreciable amounts of the commonest hydrothermal metals (Hg, Pb, Cu, Sn, Zn) and to separate the more easily impeded metals from the less easily impeded metals. Furthermore, if hyperfiltration can take place in a geological environment, the structure must be capable of concentrating more mineral than that due to a decrease in temperature or pressure. For the hydrothermal minerals relatively little impedance is required, whereas for mercury a very complete barrier is essential.

Hanshaw (1972) noted that differences in the chemical potential of water across semipermeable clay membranes can result in the development of osmotic pressure, differences in electrical potential, and salt sieving or ultrafiltration. If a chemical, electrical, or thermal gradient is imposed across a semipermeable membrane, movement of water in response to the gradient will be resulted in order to equalize the chemical potential of water on the two sides of the membrane.

Hanshaw (1972) also discussed the widely held hypothesis that ion exclusion occurs in semipermeable clay membranes as a result of the net electrical-charge deficiency in the clay minerals structure, which can result due to: (1) broken bonds, (2) removal of the hydrogen of an exposed hydroxyl group, (3) removal of structural cations under certain conditions, and (4) substitution of lower-valence cations for cations of higher valence within the mineral structure (i.e., isomorphic substitution). In order to maintain electrical neutrality, the material adsorbs a large number of cations and some anions into pores of material and produces a diffuse double layer. The flow of water

through the membrane to establish osmotic equilibrium is accompanied by ion-exclusion (ultrafiltration) effects that increase the salinity of the solution on the low-pressure side of the membrane. Because the solution that passes through the membrane is less saline than solution on either side, the salinity on the high-pressure side of the membrane will tend to decrease. Hanshaw (1972) noted that the existence of semipermeable membrane behavior could have significant practical effects.

For example, injection of liquid wastes in a subsurface aquifer system likely could upset the state of dynamic equilibrium causing (1) chemical reactions with the existing fluid and rocks, (2) thermal changes, and (3) increased pressure on the aqueous phase. Ultrafiltration can result if pressure is increased simply as a result of emplacement of waste, and if the increased pressure exceeds the pressure required for osmotic balance. The effect would be to cause flow across the shale and increase the chemical concentration of the filtrate in the emplacement aquifer beyond the planned amount.

Greenberg et al. (1973) analyzed the migration of ground water and salt in a 9.1-m (30-ft)-thick subterranean aquitard within a multiple aquifer system in the Oxnard coastal basin (Ventura County, California), where lateral invasion of seawater into the upper Oxnard aquifer threatened the quality of freshwater in an underlying Mugu aquifer separated by the aquitard. The analysis was performed using equations describing simultaneous flows of salt and water in a sediment-solution system including coupling to derive two simultaneous partial differential equations based on the postulates of irreversible thermodynamics and conservation of mass of salt and water. The resulting equations contained quantitative factors that can be used to discern three different types of coupling in sediment-solution systems, including (1) chemico-osmotic coupling

representing the movement of water induced by salt concentration gradients; (2) drag coupling representing the movement of salt induced by hydrostatic pressure gradients; and (3) void ratio coupling representing the movement of salt induced by void ratio changes within sediment. The analysis included two possible consequences of the seawater intrusion, including an osmotic pressure drop in the aquifer caused by salt intrusion that would "suck" pore fluid out of adjacent aquitards and induce chemico-osmotic consolidation of the aquitards, and an increase of NaCl concentration in the Oxnard aquifer that would impose a NaCl concentration drop across the aquitard. Three cases were simulated corresponding to different imposed hydraulic gradient due to pumping, including the baseline case of no pumping, and pumping freshwater from the Mugu aquifer resulting in 3.05- and 9.14-m drawdown.

The results indicated that chemico-osmotic consolidation followed by rebound in the aquitard resulted from the initially high NaCl concentration in the Oxnard aquifer, causing water to be released from the aquitard by chemico-osmosis. After 25 years, diffusion of NaCl into the aquitard was appreciable, and a chemico-osmotic suction of salt water back into the aquitard caused the consolidation to cease and rebound to begin. Pumping from the Mugu would cause a downward flow of seawater into and through the aquitard under a hydraulic gradient, producing a more rapid and higher level of degradation. The rates of salt inflow in both the aquitard and the Mugu aquifer also were found to be sensitive to the thickness of the aquitard, as a 0.305-m-thick aquitard offered little or no protection from degradation by seawater, even though the aquitard was of very low permeability ($< 1 \times 10^{-9}$ m/s), due to diffusion of salt through the aquitards. As a result, the overall effectiveness of the aquitard as a barrier between freshwater and

salt water is critically dependent on the location of the thinnest sections.

The authors concluded that the aquitard could act as an effective pollution barrier to the downward movement of NaCl into and through the aquitard for very long periods of time, and salt movement in the aquitard depended primarily on aquitard thickness, hydraulic permeability, and drawdown in overlying and underlying aquifers. Theoretical considerations indicated that the tightness of an aquitard to salt movement improves as void ratio and the hydraulic permeability of the aquitard decrease. Coupling effects that move salt (i.e., drag and void ratio coupling), increased as the tightness of an aquitard decreases, whereas chemico-osmotic coupling, which moves water, increased as the tightness of an aquitard increases.

Marine and Fritz (1981) proposed chemico-osmosis as an explanation for the existence of anomalous heads in the Dunbarton Triassic basin at the Savannah River plant near Aiken, South Carolina. The Dunbarton Triassic basin is overlain by 330 m of coastal plain sediments which contain freshwater. The heads in two wells penetrating Triassic sediments in the Dunbarton basin were 80.4 and 132.4 m (114.3 and 188.3 psi) above the head in the coastal plain aquifer. The sediments in the Dunbarton basin consist of lenses of sand and clay. The clayey portions functioned as membranes, whereas the sandy portions served as the sources of the saline solution. The osmotic efficiencies for four clay mineral membranes using solutions of NaCl at four different concentrations (0.1, 0.6, 1.0, and 6.0 m) were estimated using an established theory and plotted as a function of porosity. The clay mineral membranes were considered to be composed of montmorillonite, chlorite, illite, or kaolinite with average cation exchange capacities of 1.0, 0.3, 0.2, and 0.08 meq/g, respectively.

The results of the study indicated that clay mineral membranes act as osmotic membranes, and that the magnitude of osmotically induced differential hydraulic pressure depends upon concentration differences across the membrane, type of ions, type of clay, and pore size. The more highly charged membranes like montmorillonite had higher osmotic efficiencies even at high concentration gradients, whereas the kaolinite membrane with the lowest charged was not efficient in excluding anions even at low porosities.

Based on the results, the authors proposed that the anomalous hydraulic heads in the Dunbarton Triassic basin could be explained as follows. First, saline ground water exists in the Triassic rocks as a result of previous hydrogeochemical process. Freshwater from the coastal plain sediments passed into the Triassic rock by chemico-osmosis through illite-rich membranes ranging from 30 to 300 m in thickness. When the fluid pressure in the Triassic increased to achieve osmotic equilibrium pressure, the net inflow of water into the Triassic basin stopped, with the continued existence of the osmotic equilibrium pressure suggesting that the physical integrity of the membrane had been maintained for a long time. In this condition, fluid confinement applies only to the net fluid flux, such that the solution continues to move slowly in both directions through the membrane. The freshwater influx decreases the salinities of water contained in the thick composite membrane at the margins of the Triassic basin, and because the membrane is not completely ideal, outward movement of salt and inward movement of freshwater creates a zone of decreased salt concentration.

Fritz (1986) described the high fluid pressures in the Dunbarton Triassic basin, South Carolina, as a good example osmotically induced potentials in a geologic system.

This unique osmotic cell was created by the juxtaposition of the fresh water in the overlying Coastal Plain sediments against the saline pore water housed within the pores of the membrane-functioning sediments of the Triassic basin. Sediment within the Triassic basin consists of intercalated lenses of fine sand and clay and the clay was mainly illite with 3.5 % average porosity of the sediments (Marine, 1974). By assuming that the illites with low porosity in the clay lenses of the Triassic sediments have a CEC of 20 meq/100g, the σ values for this membrane in contact with waters of two wells were calculated to be 0.95 and 0.97. Because wells penetrating the saline core of the basin show anomalously high heads relative to wells penetrating the basin margins, Fritz (1986) hypothesized that the longevity of this osmotic cell could be dictated by the rate at which salt diffuses out into the overlying fresh water aquifer.

Anomalous pressures existing in the subsurface commonly are considered to result from processes that alter the pore or fluid volume, which implies crustal changes happening at a rate too slow to observe directly. However, Neuzil (2000) noted that such pressure anomalies also could be due to the existence of osmotic pressures generated by differences in chemical potential of a solution across a semi-permeable membrane. Although the notion of osmotic pressures in the subsurface has been regarded skeptically, Neuzil (2000) noted many anomalous pressures also are associated with areas of high total dissolved solids (TDS).

In support of his argument, Neuzil (2000) conducted tests in the Cretaceous-age Pierre Shale in central South Dakota. The shale at the site was saturated with a permeability ranging from 10^{-21} to 10^{-20} m² and a clay content ranging from 70 to 80 % of which about 80 % is mixed-layer smectite-illite. The pore water of the shale contains up

to 3.5 g/L NaCl. Four boreholes spaced at 15-m intervals were drilled 80 m into the shale, and the test was started by adding waters with different TDS to the boreholes. The water levels for nine years were monitored with an electrical sounding cable, and samples of the borehole waters were collected for analysis. Since osmotic pressure decays when TDS differences dissipate by diffusion, the longevity of osmotic pressure is controlled by effective ionic diffusion coefficient of the membrane.

The testing results obtained under *in situ* conditions were consistent with the generation by shales of osmotic pressures as high as 20 MPa, and the sustainability of these osmotic pressures over a nine-year period is consistent with maintaining the pressure for geologically significant periods of time. For example, the existence of osmotic pressures of 20 MPa could support a column of water extending 2 km above the land surface, and are sufficient to explain many observed anomalies. The results also indicate that shales may be able to generate high TDS solutions by retarding solute movement relative to water similar through a process that is similar to ultrafiltration.

Neuzil (2000) concluded that anomalous pressures are frequently encountered in sedimentary basins below 1-km depth, but have been attributed to continuing and undetected dynamic processes such as diagenesis, oil generation, and tectonic deformation. Also, in many cases, anomalous pressures could be derived osmotically from pre-existing chemical potential differences in the pore water.

2.2 LABORATORY EVIDENCE OF MEMBRANE BEHAVIOR

Membrane behavior of clays typically has been measured using either the flow-through or no-flow test procedures. For the flow-through test procedure, two approaches

have commonly been employed. The first approach, which is far more common, involves forcing a salt solution through the clay under an applied hydraulic pressure difference (hydraulic gradient) and determining how much of the salt has been filtered out of solution (referred to as filtrate) by the clay due to membrane behavior. This type of test often is referred to as a hyperfiltration test. The second approach, which is far less common, involves determining the membrane efficiency from the measured amount of chemico-osmotic counter flow. This approach is less common because of the greater difficulty in accurately measuring the small quantities of flow that typically result.

In contrast, flow of solution through the test specimen is prevented from occurring in the no-flow test procedure. As a result of preventing solution flow, a chemico-osmotic pressure difference builds up across the specimen to counteract the tendency for chemico-osmotic flow, and the membrane efficiency (ω) is determined based on the magnitude of the pressure buildup and the salt concentrations at the boundaries. In this regard, differences in test results can occur depending on how well the salt concentrations at the boundaries are maintained constant during the test.

2.2.1 Hyperfiltration Flow-Through Tests

McKelvey et al. (1957) evaluated salt filtering through porous media using two synthetic, granular ion-exchange resins and a synthetic ion-exchange membrane. The resins included Dowex 50, a sulfonated polystyrene cation exchanger, and Amberlite IRA 411, a quaternary amine anion exchanger, with particle sizes ranging from 20 to 50 mesh (wet U.S. Standard Screen). The salt solutions included sea water from the Gulf of Mexico (chlorinity 17.9 ‰) and 0.204 N magnesium chloride (MgCl_2). The resins were

equilibrated with the respective salt solution, filtered, and then were loaded into a steel cylinder and subjected to pressure by means of a steel piston to squeeze liquid from the resins. For 150 g of Dowex 50, the initial and final volumes of resin bed were 160 and 74 mL, respectively, and the total volume of squeezed solution was 32.2 mL. For 58 g of Amberlite IRA-411, initial and final volumes of the resin bed were 80 and 40 mL, respectively, and the total volume of squeezed solution was 20.8 mL.

For the experiment involving squeezing of the cation-exchange resin equilibrated with sea water, the ratio of sodium to potassium in the squeezed solution stayed relatively constant throughout the experiment, while the ratio of magnesium to calcium initially was higher than that in the sea water, but eventually decreased to a much lower value than that in the sea water. The concentration of salt in the squeezed solution decreased gradually, and the ratios of the concentrations of the various dissolved salts also changed with increased compression.

A synthetic cation-exchange membrane Permaplex C-10 (United Water Softeners, Ltd., London), also was used in this study. At the start of the experiment, the membrane was in the sodium form after equilibration with a 0.099 N sodium chloride solution. The effective membrane area was 9.0 cm and the thickness 0.06 cm. The membrane was held at one end of a "Lucite" tube and supported against a high-pressure differential of about 1500 psi by a micro-metallic porous disc. The Lucite cylinder was partially filled with 45 mL of a 0.099 N sodium chloride solution. The salt filtering effect was demonstrated by collecting and analyzing the solution filtered through the membrane over 45 d. After about four-fifths of the original solution had been filtered, the pressure cell was disassembled and the remaining solution was analyzed.

Several additional experiments conducted at pressures below 100 psi indicated that the membrane contained pores that allow passage of salt and water at low pressures, but become reduced in size at high pressure resulting in reduction in the passage of salt. Experiments with membranes of similar chemical composition, but different hydraulic permeability, indicated that the desalting effect is critically dependent on the hydraulic permeability of the membrane with membranes of lower hydraulic permeability producing greater desalting effects.

The results of the study showed that the process of salt removal depends upon the large excess charge attached to the membrane, which prevents the passage of like charged ions, and that separation occurred because of the electrical properties rather than the size of the solute. Thus, the salt was filtered by virtue of its electrolytic dissociation and the ionic nature of the ion-exchange membrane.

McKelvey et al. (1962) evaluated the salt filtering ability of compacted Wyoming bentonite and a disaggregated shale composed of calcite, quartz, montmorillonite, illite and kaolinite using solutions of NaCl at three different concentrations (0.1, 1.03 and 1.5 N). Two bentonite specimens at different porosities (0.34 and ~0.39-0.41) and one shale specimen at a porosity of 0.24 were tested. The hydraulic conductivities ranged from 4.2×10^{-11} m/s to 5.8×10^{-11} m/s for the bentonite and from 1.0×10^{-10} m/s to 1.5×10^{-10} m/s for the shale.

The bentonite specimens were prepared by compressing from 15 to 30 g of bentonite between the pistons and the confining steel cylinders for 24 h under different hydraulic pressure conditions of 5,000 and 10,000 psi. The resulting thickness of the specimens was 0.51 cm with an area of 20 cm² and gravimetric water contents ranging

from 16 to 19 %. The shale specimen was prepared in the same manner resulting in a thickness of 0.41 cm, an area of 20 cm² and a water content of 10.7 %.

The specimens were tested by forcing solutions with different concentration of NaCl through the specimens under a hydraulic gradient, and measuring the amount of filtrated solute. The ratio of input-to-output solution concentration was as high as 8 for the thinner bentonite specimen permeated with dilute (0.164 N NaCl) solutions, and decreased with increased input concentration and with increased porosity, whereas the ratio for the shale specimen was 1.7 with an input concentration of 0.129 N NaCl. Experiments with the thicker bentonite specimen in which NaCl was allowed to accumulate at the input face of the clay did not provide a meaningful ratio of filtrate to concentrate normalities. Streaming potential differentials of approximately 1 mV per 100 psi were measured during the flow experiments, and the potential differential was highest with the shale material and showed a decrease with increasing salt concentration.

The authors showed that the increased desalting ability of both the bentonite and shale at lower input flow pressure was due to lower porosity as substantiated by the observed lower flow rate at lower hydraulic pressures. However, they also noted that there was a fundamental difference in terms of membrane behavior among thickness, water content, and initial porosity of these specimens.

Kharaka and Berry (1973) performed filtration experiments to investigate the relative retardation by geological membranes of cations and anions generally present in subsurface waters using chloride solutions of alkali and alkaline earth metals with a powdered Wyoming bentonite (Belle Fourche, S. Dakota, USGS No. 65CM200), illite (Morris, Illinois API standard No. 36), and a disaggregated shale (Kettleman North Dome

Oil Field, California). The bentonite contained 92 percent montmorillonite, the illite clay contained 90 percent illite mineral, and the shale contained 30 percent montmorillonite and 30 percent illite. The exchange capacities of the powdered bentonite and illite clay were 88 and 24 meq/100g, respectively. Illite and shale samples were dried at about 100 °C for 10 min and ball-milled to pass through a 325 mesh (44 µm) sieve. Approximately 40 g of all three soils were dispersed and equilibrated in about 400 mL of a chemical solution resembling sea water. In some cases, samples of Wyoming bentonite also were dispersed in 150 mL of the chloride solution to eliminate the effects of ion complexing. The resulting slurries were stirred for at least 4 h before centrifuging for 15 min, and then the supernatant was discarded. The entire procedure was repeated 7 times. Test specimens of the three clays dispersed in the chemical solutions (either sea water or the chloride solution) were transferred to a plastic filtration cell and compressed under pressures of 4,138 to 34,483 kPa (600 to 5,000 psi) at temperatures 20 and 70 °C, resulting in a diameter of 10.16 cm and a thickness of approximately 0.25 cm.

The measured membrane efficiencies were found to increase with increase in the exchange capacity of the soil and decrease in the concentration of the input solution. The efficiency of a given membrane increased with increasing compaction pressure and decreased slightly at higher temperatures for solutions of the same ionic concentration. The decrease in membrane efficiency observed at the higher temperature was attributed to two factors. First, flow rates at elevated temperatures are higher because of the decrease in water viscosity. Second, ionic association generally increases at higher temperatures, resulting in lower membrane efficiencies.

The experimental results also indicated that the retardation sequences varied

depending on the material used and the experimental conditions. The sequences for monovalent and divalent cations at laboratory temperatures generally were in the orders $\text{Li}^+ < \text{Na}^+ < \text{NH}_4^+ < \text{K}^+ < \text{Rb}^+ < \text{Cs}^+$ and $\text{Mg}^{2+} < \text{Ca}^{2+} < \text{Sr}^{2+} < \text{Ba}^{2+}$, respectively. The retardation selectivity sequences obtained for anions at room temperature were variable, but the retardation selectivity sequence at 70 °C was in the orders $\text{HCO}_3^- < \text{I}^- < \text{H}_2\text{BO}_3^- < \text{SO}_4^{2-} < \text{Cl}^- < \text{Br}^-$. The authors concluded that monovalent cations generally were retarded with respect to divalent cations. The relative passage rates obtained for the dissolved species could be explained in terms of (1) the concentration of the dissolved species in the pore solution, (2) the interaction of the dissolved species with the negative sites on the clay particles, and (3) the "streaming potential" due to the drag on the diffuse double layer induced by water transport resulting in selectivity sequences that depend on the ionic charge, hydrated radii, and degree of dissociated and complex formation of the dissolved species.

Hanshaw and Coplen (1973) evaluated the existence and extent of ultrafiltration (i.e., hyperfiltration or ion exclusion) of 10 clay specimens consisting of Na-montmorillonite with particle sizes less than 5 μm , by forced passage of NaCl solutions through the membranes under a pressure difference of 10,000 kPa (100 bars) and at ambient temperature ($22^\circ \pm 2^\circ\text{C}$). The 100-mm-diameter specimens were compacted under a hydraulic pressure of 33,000 kPa (330 bars) to a thickness 10 mm resulting in porosity of 0.35. The input solutions contained concentrations of NaCl ranging from 0.001 to 1.65 m. Samples of the residual solutions (influent) and the ultrafiltrate (effluent) were collected at 10-day intervals for about 200 days.

The results of the study showed that ion exclusion depended upon the ion

exchange capacity of the clay. The author also noted that, when the concentrations of the input solution is high, then the concentration of anions admitted into the clay pore is also high such that the extent of ion exclusion diminishes as the concentration of the input solution increases, and the ultrafiltrate concentration approaches the residual solution concentration. Based on the results of the study, Hanshaw and Coplen (1973) concluded that the ultrafiltration phenomena due to the formation of subsurface brines and mineral deposits should be taken into consideration in any proposal for subsurface waste emplacement in an environment containing large quantities of clay minerals.

Kharaka and Smalley (1976) performed filtration experiments using chloride solutions of alkali and alkaline earth metals with bentonite and kaolinite clay compacted under pressures of 48,300 to 69,000 kPa (7,000 to 10,000 psi) at temperatures from 25 to 85 °C. The bentonite was powdered and consisted of 92 percent smectite, and the kaolinite clay consisted of 97 percent kaolinite mineral. The exchange capacities of the powdered bentonite and kaolinite clay were 98 and 15 meq/100g, respectively. Test specimens had diameters of 10.2 cm and thicknesses of 0.25 cm and 1.50 cm for the bentonite and kaolinite, respectively. The test specimens were confined in a filtration cell consisting of a plastic cylinder and pistons.

The measured hydraulic conductivity was found to decrease with increasing compaction pressures, but increase with increasing hydraulic pressure gradient and temperature. The membrane efficiencies for monovalent cations generally decreased with decreasing flow rates, whereas those for divalent cations generally increased with increasing flow rates. The retardation of bentonite decreased with increasing temperature. Divalent cations were retarded to a greater extent than monovalent cations, and the

retardation of Cs, Rb, and K decreased significantly at the higher temperatures.

The selective transport of the cations was attributed to charge attraction of the cations to the negative sites on the clay particles and to the dynamic force (the hydraulic drag) exerted on the cations by the flowing water. The relative retardation of Ca and Na were reversed with respect to temperature, with Ca being retarded to a greater extent than Na at 85 °C, and vice versa at 53 °C. The variations in the relative retardation of cations with temperature were attributed to changes in the degree and nature of hydration of cations.

The results of the study demonstrated the ability of natural materials to behave as semipermeable membranes at temperatures, compactions, and hydraulic pressures encountered in subsurface situations. Also, the efficiency of geologic membranes is a function of the difference between the cation and anion exchange capacities of the materials, and is highest for shale composed of smectite. Finally, the results support the concept that the chemistry of natural water is influenced strongly by the membrane behavior of sedimentary rocks.

Fritz et al. (1983) evaluated the membrane behavior of Na-bentonite using solutions of NaCl at six different concentrations and two specimens at different porosities (0.59 and 0.41) and hydraulic conductivities (1.5×10^{-11} cm/s and 7.3×10^{-12} cm/s), but the same thickness (0.7 cm) and area (81.07 cm²). The cation exchange capacity (CEC) of the bentonite was 98 meq/100g. The membrane behavior in the form of the reflection coefficient, σ , was determined by hyperfiltrating solutions of NaCl at different concentrations through the specimens under a constant applied hydraulic pressure difference, ΔP , of 17.5 Mpa and a constant temperature of 23 °C.

The test apparatus included a high pressure, precision syringe pump that sequentially forced the NaCl solutions through the specimens. The outflow from the specimen was collected in a pre-weighed 250-mL flask, and a valve on the inflow side of the specimen was periodically opened to allow collection of the solution and to insure no build-up of solute concentration at this interface, commonly referred to as the concentration polarization effect.

The value of σ was defined as:

$$\sigma = \left(\frac{C_0 - C_e}{C_0 + C_e} \right) \quad (2.1)$$

where C_0 is the concentration of solute entering the specimen, and C_e is the concentration of solute exiting the specimen. The values of σ measured for Na-bentonite ranged from 0.30 to 0.87, with the higher values of σ being correlated with lower NaCl concentrations in the source solution and/or lower specimen porosity. The authors concluded that, if the concentration gradient across the clay membrane is very high, then the osmotic pressure difference across the membrane, $\Delta\pi$, is also high, but the low σ value of the membrane renders $\sigma\Delta\pi$ low, and vice versa.

Whitworth and Fritz (1994) provided experimental results that increasing electrolyte flux into a compacted smectite membrane resulted in greater permeability of the membrane as the influx of electrolyte into the membrane pores decreases the diffuse double layer (DDL) thickness, reducing the clay's ability to exclude anions. The experimental procedure consisted of forcing a NaCl solution through compacted smectite membranes (National Western Bentonite, Wyoming) using a syringe pump with 500-mL

capacity syringes, and periodically collecting effluent samples. The syringe pump was set for a constant flow of 1.80 mL/h and 0.35 mL/h for two compacted Na-bentonite specimens with thicknesses of 2.74 mm and 8.10 mm, porosities of 0.448 and 0.620, and average permeabilities using capillary tube permeability measuring device of 4.17×10^{-14} and 9.32×10^{-15} cm³/dyne/s, respectively. The clay used to construct the membrane was beneficiated to achieve an average particle size of 30 μm by means of an air separator. Following separation, the fine fraction was slurried with 1 M NaCl solution, dialyzed to remove excess solute and finally freeze-dried. After the clay paste was placed between two piston assemblies in the cell, the clay was compressed by application of a hydraulic pressure.

The experimental results indicated that the addition of electrolytes to a clay-water system compresses the DDL and reduces the repulsive forces between platelets. The DDL compression results in flocculation of clay-water systems upon electrolyte addition. Reduction of DDL thickness, even in well-compressed clays, has the effect of increasing the permeability of the clay to solutes because of the reduced anion exclusion effect. As a result, the concentration polarization layer (CPL), i.e., the layer of elevated solute concentrations resulting from solute restriction at the inflow side of the membrane, diminished such that the effluent concentration eventually equaled the solute concentration of the feed solution and a true steady-state condition was achieved. Whitworth and Fritz (1994) hypothesized that the fact that membrane efficiency decreases as pore solute concentration increases could explain why conclusive trends attributable to membrane effects in geologic formations (e.g., shales) have not been more commonly observed in the subsurface.

2.2.2 Chemico-Osmotic Flow-Through Tests

Kemper (1960) evaluated experimentally the potential effects of the electrostatic charge and the diffuse double layer (DDL) of ions adjacent to particle surfaces on the movement of solution through thin films of such particles at moisture contents less than field capacity. A partial separation of the solute and solvent (salt sieving) might be expected as the solution passes through these thin films, since the ions in the solution are charged but the water is not. When water moves in thin films between negatively charged clay particles, there is an initial tendency for more cations than anions to be carried to the low pressure side because of the greater number of cations relative to free anions in the system. This tendency causes a buildup of positive charge at the low pressure end, and a decrease of positive charge at the high pressure end.

Three 0.5-L portions of saturated Na-bentonite (Volclay) suspension containing solutions of NaCl at different concentrations (0.01 N, 0.1 N and 0.94 N) were placed in pressure membrane cells using Visking sausage casing as the membrane (see: <http://www.visking.com/home.html>). A pressure of 1,013 kPa (10 atm) was applied in the cells to push the solution out of the suspension through the membrane. The pressure membrane cells were opened three days later after solution flow had stopped. Then, 0.3-L solutions containing NaCl at different concentrations (0.01 N, 0.1 N and 0.94 N) were poured into the respective cells and the cells were closed. A pressure of 1,013 kPa (10 atmospheres) was applied in the cells again, forcing the fresh solutions through the clay paste and the cellulose membranes. The concentrations and amounts of the solutions emanating from the membrane cells were checked periodically until about 0.15 L of

solution had been collected. The cells then were opened, and the concentration of NaCl in solution on top of the clay paste was determined. The thickness of the clay paste was measured and moisture content was determined.

The results indicated that the NaCl concentration in the solution emanating from the cell was lower than that in the input solution and also that salt had accumulated in the solution on top of the clay layer. The reductions in the salt content for solutions with initial NaCl concentrations of 0.01 N, 0.1 N, and 0.94 N NaCl were 32 %, 10 %, and from 3 % to 4 %, respectively. The experimental results also indicated that increases in apparent intrinsic permeability with increasing hydraulic pressure gradients in clay systems could be explained by the "salt-sieving" phenomena.

Diffusion and movement of ions with water being pulled into the plants by transpiration were considered to be the major factors in the mechanisms by which ions are brought to the plant root surfaces. In this regard, salt-sieving would be expected to be an important factor in calculating the amount of salt moving with the transpiration stream at moisture contents less than field capacity. The negative adsorption of anions from thin films suggests that diffusion in thin films was strongly affected by the electrostatic charge and the ions associated with clay particles. The effect of the DDL on the diffusion of ions across clay membranes would be able to clarify the significance of potentials across clay membranes. The author concluded that as a result of salt-sieving action, successive increments of solution emanating from a pressurized membrane might be expected to have higher salt concentrations despite the negative adsorption of salts by clays. However, the electrostatic charge and DDL of associated ions would have considerable effect on the movement of solution through films of thickness encountered at moisture

contents less than field capacity.

Kemper (1961) conducted an experimental analysis to evaluate the validity of the theory governing viscous and diffusive flows of water in thin films of porous media. The porous media included ground Pierre shale, and a fine fraction of Pierre shale obtained by grinding and sedimentation, and Wyoming bentonite with cation-exchange capacities of 18.0, 30.5, and 94 meq/100g, respectively. The exchange complexes of the clays were saturated with Na^+ by washing the clays four times in 1 N NaCl solution. The flocculated clays then were mixed with distilled water in centrifuge tubes, shaken, centrifuged, and then the supernatant liquids were poured off. This specimen preparation procedure was repeated until the concentration of the supernatant liquids was less than 0.02 N NaCl based on electrical conductivity measurements.

Osmotic pressures measured across compacted specimens of the clays were compared with theoretical pressures calculated using tortuosities, effective thicknesses of films, hydraulic conductivities and salt diffusion data. Specimens of the Pierre shale, fine fraction of Pierre shale, and bentonite were each compacted into a stainless steel cylinder using a pressure of 34,483 kPa (5,000 psi) resulting in thicknesses of 0.83, 1.00, and 0.81 cm, and porosities of 0.21, 0.24, and 0.39, respectively. Saturated NaCl solution containing 5 g of solid salt was poured into the cylinder, and the clay and salt were compressed again to equilibrium under 5,000 psi pressure. Distilled water was circulated through two ports in a bottom porous ceramic disk until the pressure and rate of salt diffusion were practically constant with time. Saturated NaCl solution then was passed through the lower disk until the viscous flow that resulted in response to the pressure gradient dissipated the pressure difference. The rate of movement of solution through a

calibrated capillary tube attached to the open port was used to determine rates of flow through the compacted clays.

Sodium chloride movement through the compacted clays was determined by measuring the amount and electrical conductivity of solution that had been circulated through the lower porous ceramic disk. Water diffused from the bottom to the top of the compacted specimens in response to a free energy gradient resulting from a high salt content of water on the top of the clay layer. Diffusion of water to the top of the clay layer built up pressure in the water in the top porous disk that was measured using a pressure gage. The hydraulic pressure difference was attributed to viscous flow from the top to the bottom of the clay. The results indicated that the bentonite, which was the finest of the three clays, developed higher steady state pressures and took longer to reach maximum pressures. The pressure buildup increased rapidly to a maximum and then declined slowly. The slow decline was assumed to be due to solid-phase salt dissolving into solution, and diffusing through the compacted specimen and out of the bottom of the cell, resulting in expansion of the clay into the volume formerly occupied by the salt. The expansion of the clay caused the average width of pores in the clay to be larger and increase the rate of viscous flow downward at given pressure gradient. The author concluded that salt gradients may be a major factor in the movement of the water.

Kemper and Evans (1963) conducted experimental studies involving restriction of solutes by membranes and consequent effects on the movement of water, and developed equations that include the sizes of the solute molecules and the pores to predict the rate at which osmotic pressure differences move water through uncharged porous media. The experimental results were based on the use of a dialysis membrane and solutions of

polyethylene glycols, also commonly known as "carbowaxes". The concentrations of the carbowaxes (by mass) were 0.8, 1.5, 5.7, and 5.8 % for the carbowaxes with molecular weights of 200, 600, 6,000, and 20,000, respectively. Water movement due to solute concentration differences across a membrane was established by placing the membrane between two reservoirs, one containing a solution and the other containing water. Hydraulic pressures on the two sides were kept to within 1 mm of water of each other. Samples of the solution from each side were taken for two hours after filling the cells. The volumetric moisture content of the membranes was 0.6, and the thickness of the membrane when wet was 0.005 cm. The viscosity of water at 25 °C was 0.9×10^{-3} Pa·s (0.009 poises), and the self-diffusion coefficient, D_0 , of water was taken as 2.35×10^{-5} cm²/s.

The solution flow rates due to osmotic and hydraulic pressure differences were practically the same. Less than 4 % of the observed solution flow was attributed to diffusive flow of water molecules. Thus, the results indicated that viscous flow was the major mechanism by which water moves through membranes in response to osmotic and hydraulic pressure gradients. Osmotic pressure and hydraulic pressure differences were equally effective in moving water through a membrane when the solutes were completely restricted by the membrane. When the solutes were not completely restricted through membranes, osmotic pressure differences were less effective than hydraulic pressure differences in moving water through membranes. The authors concluded that repulsion of anions from the vicinity of negatively charged mineral surfaces which reduces the number of solute molecules impacting on the solution could cause an increase in the reflection coefficient, σ , and estimations using diffuse double layer theory indicated that

the value of σ resulting from such repulsion could account for the hydraulic pressures resulting from solute concentration differences. However, the broad range of solution concentrations encountered within the clay in each experimental system might prevent quantitative calculations.

Kemper and Rollins (1966) conducted experimental results of osmotic efficiency coefficient due to concentration differences and hydraulic pressure differences of NaCl, Na₂SO₄, CaCl₂ and CaSO₄ solution to evaluate the degree to which electrostatic interaction causes osmotic pressure gradients to move solution through clay-water-ion systems. In soil-water systems, electrostatic interactions occur between the ions and the dominantly negative charge of the clay particles. Movement of solution through clays in response to both salt concentration differences and hydraulic pressure differences was measured.

Wyoming bentonites particles less than 2 μm were separated from the coarser fraction by sedimentation, and saturated with Na⁺ by washing with 1 N NaCl solutions. Subsequently, the clay was dried at 105 °C and ground to pass a 30 mesh sieve. Clay and distilled water were then mixed in amounts necessary to give pastes with 20, 33, and 40 % clay contents by weight. After equilibration in containers for one week, these pastes were used to fill retainer rings 2-mm deep and 63 mm in diameter. Porous stainless steel plates were placed on each side of the rings. Rates of flow were measured from the rates of movement of the menisci in the calibrated capillary tubes attached to the test cells.

Sodium chloride (NaCl) concentrations ranging from 0.001 to 1.0 N were used with the concentration of NaCl on the low concentration side being about one-third of that on the high concentration side. Rates of solution movement in response to the

“osmotic pressure” gradient were measured, the solutions were removed, and changes in concentration on the two sides were determined conductometrically. The NaCl solution was replaced by 0.01 N Na₂SO₄ solution, 0.01 N CaCl₂ solution and 0.01 N CaSO₄ solution, and then osmotic flow and hydraulic conductivity were determined as with NaCl solutions.

The measured osmotic efficiency coefficients increased when the clay was saturated with monovalent rather than divalent cations, divalent anions rather than monovalent anions were used, the water content of the clay plug decreased, and the average salt concentration of the across the specimen decreased. The measured osmotic efficiency coefficients were found to be lower than the calculated coefficients.

The osmotic efficient coefficient was calculated with the paired osmotic pressure and hydraulic pressure conductivity data:

$$\sigma = \frac{-\Delta q_0 \Delta P}{\Delta q \Delta \pi} \quad (2.2)$$

where Δq_0 is the amount of flow per unit cross section due to the osmotic pressure, ΔP is the pressure differential forcing the solution through the clay paste, Δq is the amount of flow per unit cross section in the time interval, and $\Delta \pi$ is the osmotic pressure difference across the specimen with thickness, x .

One possible reason is due to concentration gradients within the porous stainless steel plates which enclosed the clay membrane. As solution is pulled through the clay from the low to the high concentration side, some salt filtering takes place at the porous steel-clay interface. The salt accumulates, raises the concentration at the porous steel-clay

interface, and tends to diffuse back through the porous steel to the solution. Diffusion of the salts tends to raise the concentration of salt in the pores of the stainless steel to concentration in the solution. The effect on both sides is to make the concentration difference across the clay lower than the difference in concentration between the solutions.

The rate at which salt moved from the high to the low concentration side was measured. These measured rates together with the velocities of solution through the porous plates, the diffusion coefficients of salt in the steel plates, and the thickness of the steel plates provided sufficient data to calculate the actual concentration difference across the clays. The remaining discrepancy between the measured and calculated osmotic efficiency may be attributed to imperfections in the assumptions used in the theory and calculations, or errors in the data.

The films of water in soil are not uniform in thickness, and the geometry of the water phase probably involves relatively large capillary "puddles" of water interconnected by thin films adsorbed on and between mineral surfaces. Under these probable conditions, negative adsorption of free electrolyte from the thin films likely causes some restriction of the electrolyte as it diffuses from puddle to puddle. Such restriction would result in appreciable osmotic efficiency of the soil and in viscous movement of the solution in response to a salt concentration gradient in the soil.

Throughout the soil moisture range encountered by growing plants, salt concentration gradients will not be an important factor causing movement of soil solution. However, at evaporating surfaces or freezing surfaces in soils, salt concentration gradients may be large and water film thicknesses may be very thin. Therefore, under

unsaturated conditions salt gradients may become a major factor causing solution movement.

Olsen (1969) provided experimental results showing that the simultaneous fluxes of liquid and charge under hydraulic, electrical, and electrolyte concentration gradients obey the macroscopic rate laws derived from the irreversible thermodynamics of discontinuous systems, except that the experimental flux versus driving force relations possess hydraulic and electrical potential intercepts. The experimental results were derived from testing specimens of kaolinite clay (type hydrite 121, Georgia Kaolin Co.) with a diameter of 10.16 cm and thicknesses ranging from 1.0 to 3.0 cm. The kaolinite clay was prepared to be homoionic with sodium by saturation via equilibration with 10^{-3} N NaCl solution, with chloride as the anion. This preparation was desired together with silver-silver chloride electrodes to allow current to be passed through the system by means of simple electrolytic transport, without extraneous electrochemical reactions and gas generation taking place at the electrodes. The test cell underwent successive increments of consolidation under loads ranging from 3.4 to 680 kg/cm² for transport measurement before being unloaded to 13.6 kg/cm². The porosities of the specimen ranged from 0.114 to 0.590 during the loading stage and from 0.159 to 0.213 during the unloading stage. The primary purposes of the study were to determine the relative magnitudes of the hydraulic, osmotic, and electro-osmotic conductivities as a function of the consolidation load and specimen porosities, and to evaluate the validity of the postulates of irreversible thermodynamics in a system in which the porosity and the average pore diameter were small.

The values for the reflection coefficient, σ , measured with 10^{-3} N NaCl solution

ranged from 0.014 to 0.453 for the loading stage and from 0.445 to 0.476 for the unloading stage. Because the reflection coefficients increase with the specimen density, the author proposed that dissolved salts filtered in the specimen were not uniformly distributed during consolidation increments and formed a concentration gradient within the specimen, and that internal concentration gradients induced by the consolidation process contributed to the hydraulic and electrical potential intercepts. The results of the study indicated that the electrical potential intercepts arise from electrolyte concentration gradients within the specimen, generated by differential salt filtering at the specimen during consolidation increments.

Olsen (1972) evaluated the relative importance of osmotic and electro-osmotic flow versus hydraulic flow through confining beds at different depths of burial by determining the hydraulic, osmotic, and electro-osmotic conductivities of sodium kaolinite measured as a function of compaction pressure. The experimental results were derived from testing specimens of sodium kaolinite clay (type hydrite 121, Georgia Kaolin Co.) with a diameter of 10 cm and thicknesses ranging from 1.0 to 3.0 cm. The kaolinite clay was prepared to be homoionic with sodium by saturation via equilibration with 0.001 N NaCl solution, with chloride as the anion. The test cell underwent several increments of consolidation and rebound under loads ranging from 1 to 608 bars corresponding to overburden depths ranging from 3 to 3048 m (10 to 10,000 ft). The hydraulic (k_H), osmotic (k_C) and electro-osmotic (k_E) conductivities were determined by measuring the difference of hydraulic head (ΔH) as a function of the flow rate (Q/t), dissolved solids concentration (ΔC), and electrical potential (ΔE) as functions of externally imposed electric currents (I) through the clay system while maintaining $I = \Delta C$

= 0, $Q = I = 0$, and $Q = \Delta C = 0$ respectively.

The results of the study indicated that osmotic and electro-osmotic flow become increasingly more significant relative to hydraulic flow with increasing depth of overburden, and the magnitude of hydraulic flow decreases more rapidly with depth than the osmotic and electro-osmotic flows. The author concluded that not only hydraulic gradients but also osmotic and possibly electro-chemical gradients should be considered in evaluating subsurface flow of liquids at depth because Darcy's law is not a sufficient basis for predicting either the magnitudes or the directions of liquid movement through deep confining beds.

Kemper and Quirk (1972) evaluated the membrane behavior of several clays including kaolinite (Mesa Ata, New Mexico, API 9) with a measured CEC of 5 meq/100g and specific surface area of 17 m²/g, Fithian illite (Fithian, Illinois, API 35) with a measured CEC of 22 meq/100g and specific surface area of 100 m²/g, Willalooka illite extracted from solonetz soils (South Australia) with a measured CEC of 32 meq/100g and specific surface area of 180 m²/g, and bentonite (Upton, Wyoming) with a measured CEC of 80 meq/100g and specific surface area of 720 m²/g. Specimens of the kaolinite, Fithian illite, Willalooka illite, bentonite were made homoionic with either sodium (Na⁺) or calcium (Ca²⁺) and mixed with distilled water to form clay pastes with volumetric water contents 0.53, 0.59, 0.72, and 0.84 or 0.91, respectively. The pastes were packed between porous stainless steel plates of a clay compartment such that the thickness and diameter of the specimens were 2 mm and 63 mm, respectively. The compacted specimens then were placed between reservoirs containing chloride solutions of the respective cations, and the rates of osmotic flow, electric potentials in the solutions, and streaming potentials

across the specimens were measured. Diffuse double layer (DDL) theory was used to estimate the concentration ranges assuming the measured external potential differences were not appreciably different from the respective potentials of the solution inside the clay specimens.

The standard procedure for sodium homo-ionized clay was to fill one side of the cell with 1 N NaCl and the other with 0.3 N NaCl. Osmotic flow was determined by measuring the rate of water movement in capillary tubes, and the electric potential between Ag:AgCl electrodes in the end compartments was determined. The rate of solution movement was monitored by the movement of the air bubble which generally traveled 2 to 10 cm through capillary tube during a measurement. Solution pairs of 1 to 0.3 N, 0.3 to 0.1 N, 0.1 to 0.03 N, 0.03 to 0.01 N, 0.01 to 0.003 N, and 0.003 to 0.001 N NaCl were placed in the end compartments, and osmotic potential and hydraulic conductivity measurements were repeated. The end compartments were then filled with 1 N CaCl₂ which was replaced twice daily for at least 4 d. Analysis of the solution at the end of each dialysis period showed no Na⁺ coming out of the clay at the end of 4 d, and the clays was assumed to be saturated by Ca²⁺. Solutions in the end compartments were then changed from 1.0 to 0.001 N CaCl₂ on the high concentration side and from 1.0 to 0.0003 N CaCl₂ on the low concentration side, and all measurements were performed using the same procedure with the sodium homo-ionized clay. The calcium homo-ionized clay also was tested using an additional solution pair of 0.001 to 0.0003 N CaCl₂ along with the solution pairs previously described for the sodium homo-ionized clay.

The results of the study indicated that the measured osmotic efficiency coefficients increased when the clay was saturated with monovalent sodium versus

divalent calcium. The osmotic flow was often from the high salt to low salt concentration side and was generally in the direction of more negative potential, indicating electro-osmosis as the mechanism involved in osmotic flow as opposed to chemico-osmosis, since chemico-osmosis would be expected to result in solution flow from low to high salt concentration. The "mobile" fraction of the adsorbed cations appeared to decrease for divalent calcium relative to monovalent sodium as the equilibrium solution concentration decreased.

The authors concluded that when anions are largely excluded from compressed clay membranes, a concentration gradient of the mobile adsorbed cation forms. The concentration gradient causes the cations to diffuse to the low concentration side, creating an electrical potential difference which pushes the mobile adsorbed cations and the water lattice. The authors suggested that the electro-osmotic force is the mechanism causing most of the "osmotic" movement across clay membranes. The portion of the adsorbed ions dissociated into the DDL decreases as salt concentration decreases. Even though relatively small portions of adsorbed multivalent cations (Na^+ , Ca^{2+} , La^{3+}) participate in the DDL on external mineral surfaces, adsorbed multivalent cations are in mobile form to cause electro-osmotic movement and to be an important factor in general transport phenomena involving ions and water.

Elrick et al. (1976) evaluated the effects of a salt concentration difference on salt migration through a 10-mm-thick, compacted layer of sodium bentonite using solutions of NaCl at different concentrations (0.1 and 1.0 mM) under isothermal conditions. The differences in water pressure (ΔP) and voltage (ΔV) resulting from imposing a difference in NaCl concentration (ΔC) across the compacted bentonite under the condition of zero

net flux of liquid were measured continuously with a differential pressure transducer and a differential amplifier, respectively. The concentration difference also was measured by calibration with electrical conductivity measurements using a pair of radiometer conductivity meters.

Samples of the bentonite separated by sedimentation were shaken with a sequence of 1.0 M NaCl solutions and then dialyzed to eliminate the excess NaCl and then equilibrated at 0.1 mM NaCl in a stainless steel pressure membrane cell using 1.5 MPa air pressure. Silver membranes (Selas Flotronics Corp. Springhouse, Pa) with average pore sizes of 0.8 μm were coated with silver chloride in a saturated KCl solution using an external direct current voltage of 1.5 V, resulting in a voltage difference of approximately 59 mV for a 10-fold change in NaCl concentration using a standard calomel reference electrode. The clay paste containing 11.4 g of dry clay per 100 g of water was placed in 14 cylindrical cavities of a sample holder. Each cavity was 0.38-cm long with a cross-sectional area of 1.29 cm^2 . The clay cylinders were supported by the silver-silver chloride membranes. A concentration difference was imposed across the clay plug (0.1 and 1.0 mM NaCl) and ΔC , ΔP , and ΔV were observed for $0 < t < 20$ h. After 20 h the reversible electrodes were "short circuited", and ΔC and ΔP were recorded for $20 < t < 28$ h.

The results of the study indicated that ΔV contributed to the concentration difference across the membrane and the difference in transference number based on the ionic mobility of cations (Na^+) and anions (Cl^-). Thus, ΔV decreased with time since ΔC diminished as a consequence of ionic diffusion. For the non-short-circuited portion of the test, the ratio of ΔP and ΔC appeared to be constant, whereas for short-circuiting the rate of transfer of salt increased immediately, because the ion that limits the rate of flow (Cl^-) no

longer must physically traverse the clay membrane. The change in sign of ΔP following short-circuiting of the reversible electrodes represented the drag effect exerted on the liquid by the cations whose movement is no longer restricted because of the relative immobility of the anions. The authors concluded that the magnitude of the drag effect was related to the concentration difference and the effect was reversible, and that the forces of pressure difference, concentration difference, and voltage difference were intricately linked due to the permiselective properties of the bentonite.

Ishiguro et al. (1995) provided experimental results for the rejection of salt and non-ionized organic solutes to investigate the full potential of a montmorillonite layer as a reverse osmosis membrane. The authors evaluated the membrane behavior of a crude montmorillonite (Wyoming bentonite) with a measured CEC of 83 meq/100g, specific surface area of 646 m²/g, a clay fraction by particle size (< 2 μ m) of more than 90 %, and a density of 2.72 g/cm³. The montmorillonite was purified by sedimentation and processed such that the exchange complex was saturated with sodium. The purified clay in the sodium form was prepared as a clay paste in the form of 25 g of water for each 1 g of dry clay, and placed on a porous stainless steel plate with a diameter of 4 cm. The thickness of the clay membrane with volumetric water content of 59 % was 0.5 mm. The tests were conducted in apparatus specially constructed to conduct reverse osmosis experiments by forcing a feed solution through the clay specimens under an operating pressure of 3 MPa. The feed concentrations used for the experiments were 1, 10 and 100 mM for NaCl, and 100 mg/L of carbon for organic solutes.

Based on the permeation rate and solute separation, the results indicated that inorganic electrolyte solutes and non-ionized organic solutes were fractionated to greater

extent by the montmorillonite membrane relative to previous results reported in the literature for negatively charged polymeric membranes. The difference was explained on the basis of the structure of the two types of membranes in that polymeric membranes involve long polymer chains that are entangled whereas montmorillonite membranes consist of laminated sheets that are compacted under a high pressure. However, the montmorillonite membrane fractionated the sodium chloride to a greater extent than the non-ionized organic solutes. This difference was attributed to the solute separation of sodium chloride being governed by the differences between the charges of sodium and chloride ions versus the charge of the montmorillonite.

The decrease in the separation of electrolyte solutes with an increase in the feed solute concentration is one of the typical characteristics of charged membranes based on the diffuse double layer theory. The decrease in the permeation rate with an increase in the feed solute concentration was attributed to the effect of osmotic pressure and electrical potential. The authors concluded that a montmorillonite layer exhibited the characteristics typical of a charged membrane by rejecting sodium chloride solute less effectively with increasing solute concentration and was effective as a reverse osmosis membrane for the rejection of electrolyte solutes.

Keijzer et al. (1997, 1999) evaluated the membrane behavior of compacted Ankerpoort Na-bentonite (Ankerpoort Colclay A90 batch 61203 from the Netherlands), with a measured CEC of 64 meq/100g, primary specific surface area of 120 m²/g, a clay fraction by particle size (< 2µm) of 98 %, and a mineralogical composition of 99 % smectite for the clay fraction. Two compacted 50-mm-diameter Ankerpoort Na-bentonite specimens with thicknesses of 2.3 mm and 3.4 mm were tested. Each specimen was

tested in a flexible-wall permeameter under a cell pressure of 100 kPa by simultaneously subjecting the specimen to a hydraulic gradient ranging from 100 to 125, and a chemical concentration gradient ranging from 0.1 to 0.6 M NaCl. The porosities of the specimens were 0.638 and 0.671 after saturation, and the hydraulic conductivities using a falling head permeability test were $7.6 \pm 0.9 \times 10^{-12}$ m/s and $2.9 \pm 0.9 \times 10^{-12}$ m/s.

The membrane efficiency in the form of σ was determined using the following expression (Keijzer et al. 1997, 1999):

$$J_w = \sigma KA \frac{\Delta\pi}{\Delta x} \quad (2.3)$$

where J_w is the measured water flux, K is the hydraulic conductivity, A is the area of the specimen, and $\Delta\pi$ is the osmotic pressure difference across the specimen with thickness, x . The hydraulic pressure difference between two reservoirs connected to either side of the specimen, one containing salt water and one containing fresh water, was measured using pressure transducers after closing the reservoirs. The water flux from the fresh-water reservoir to the salt-water reservoir was also gravimetrically measured at regular time intervals for each specimen when the experiment was run with open reservoirs. The osmotic pressure difference across a semi-permeable membrane was calculated using the van't Hoff equation, or (Keijzer et al. 1997, 1999):

$$\Delta\pi = \frac{RT}{\bar{V}_w} \ln \frac{a_{fresh}}{a_{salt}} \quad (2.4)$$

where R is the universal gas constant ($8.31451 \text{ J mol}^{-1}\text{K}^{-1}$), T is the absolute temperature, \bar{V}_w is the mean partial molar volume of water and a is the activity of the fresh water or salt water at either side of the membrane.

Although the results indicated that the Ankerpoort Na-bentonite exhibited membrane behavior for the conditions imposed in the test, the measured values for σ of 0.003 and 0.001 were quite low. Keijzer et al. (1997, 1999) noted that changes in the induced chemico-osmotic pressures across the compacted bentonite specimens were attributed to time-dependent changes in the boundary salt concentrations, resulting in a time-dependent decrease in the concentration gradient across the specimen. These boundary concentration changes were attributed to the net migration of water in a direction of decreasing concentration gradient due to the process of diffusion-osmosis (Olsen et al. 1990). As a result, the low measured σ values reported by Keijzer et al. (1997, 1999) could be attributed to the decrease in observed pressure difference as opposed to a decrease in membrane efficiency of the specimens (Shackelford and Lee, 2003).

Keijzer et al. (2001) evaluated the membrane behavior of a Wyoming bentonite and two dredged sludges from the Port of Rotterdam, the Netherlands. The bentonite had a CEC of $68.3 \pm 1.3 \text{ meq/100g}$, primary specific surface area of $556 \pm 13 \text{ m}^2/\text{g}$, and a clay fraction by particle size ($< 2 \mu\text{m}$) of 98 %, with smectite dominating the mineralogical composition of clay fraction. The two dredged sludges had CECs of 24.2 ± 0.3 and $14.9 \pm 0.5 \text{ meq/100g}$, primary specific surface areas of 167 ± 1 and $184 \pm 14 \text{ m}^2/\text{g}$, and clay fractions by particle size ($< 2 \mu\text{m}$) of 56 and 26 %, respectively. One sludge was comprised primarily of smectite, kaolinite, and illite minerals, whereas the other sludge

consisted primarily of kaolinite and illite. The test apparatus and procedures used by Keijzer et al. (2001) were the same as those previously described by Keijzer et al. (1997, 1999), and included a flexible-wall cell connected to a fresh-water reservoir and a salt-water reservoir on either side of the specimen. Each specimen was subjected to a cell pressure of less than 500 kPa, with a 0.01 M NaCl solution in the fresh water reservoir and 0.1 M NaCl solution in the salt water reservoir. The porosity after saturation for the specimen of Wyoming bentonite was 0.555, and the hydraulic conductivity was $1.2 \pm 0.7 \times 10^{-12}$ m/s. For specimens of the two dredged sludges, the porosities were 0.505 and 0.339 and the hydraulic conductivities were $5.2 \pm 1.6 \times 10^{-12}$ m/s and $21 \pm 4 \times 10^{-12}$ m/s respectively.

The measured values for σ were determined using two different approaches. One approach involved using Eq. 2.2 with the average measured water flux during the first 48 h of the experiment, and applying an analogue of Darcy's law when hydraulic pressure differences are still negligible (Barbour and Fredlund 1989, Keijzer et al. 1999, Keijzer 2000). A second approach involved using the following expression for σ (Staverman 1952):

$$\sigma = \left(\frac{\Delta P}{\Delta \pi_0} \right)_{J_v=0} \quad (2.5)$$

where $\Delta \pi_0$ is the maximum possible osmotic pressure based on the difference between the initial boundary salt concentrations on either side of the specimen in accordance with van't Hoff's expression, and ΔP is the actual induced osmotic pressure as a result of the specimen behaving as a semipermeable membrane.

The values of σ measured for the Wyoming bentonite were 0.015 based on

measured pressure difference (Eq. 2.4), and 0.030 based on measured water flux (Eq. 2.2). For the dredged sludge with 56 % clay content, σ was 0.022 based on the measured pressure difference, and 0.019 based on measured water flux. No membrane behavior (i.e., $\sigma = 0$) was observed for the dredged sludge with 26 % clay content.

The authors concluded that the experimental values for σ obtained by the two different approaches were in good agreement, but noted that there is a fundamental difference between their experiments performed under the condition of reverse osmosis and the direct measurement of osmotic water transport. In a typical reverse osmosis experiment, the sample is generally confined in a rigid-wall permeameter and subjected to an axially applied overburden pressure to ensure a good specimen-to-wall contact. But because reverse osmosis normally is applied over a short period of time, the time is too short for the potential detrimental effects resulting from salt diffusion into the specimen to be observed (e.g., see Shackelford and Lee 2003).

Henning et al. (2006) evaluated the existence of membrane behavior of two soil-bentonite backfills obtained from two vertical cutoff walls, one in Delaware and one in New Jersey. Both backfills were designed as a mixture of dry bentonite (3-4 % by dry weight) and the locally excavated soil blended with bentonite water slurry to provide slumps ranging from 100 to 150 mm (from 4 to 6 in). The Delaware backfill was classified as poorly graded, clayey sand (SP-SC) with a cation exchange capacity (CEC) of 15.0 meq/100g and electrical conductivity (EC) of 86 mS/m at 25 °C, whereas the New Jersey backfill was classified as clayey sand with a CEC of 14.4 meq/100g and an EC of 510 mS/m. Specimens of the two backfills were tested at void ratios ranging from 0.40 to 1.53 for the Delaware backfill and from 0.55 to 0.89 for the New Jersey backfill.

The chemico-osmotic efficiency coefficient, ω , which is analogous to the reflection coefficient (see Eq. 2.5), was determined by imposing a constant concentration difference across the specimen while maintaining a constant volume inside a closed system testing apparatus (Malusis et al. 2001) such that ω was determined in accordance with Eq. 2.5.

The results indicated that the magnitude of ω increases with decreasing void ratio. However, the magnitudes of the ω values for these construction-site backfills, which ranged from 0.0019 to 0.0172 for the Delaware backfill and from 0.0119 to 0.0140 for the New Jersey backfill, were lower than those previously reported for model backfills prepared in the laboratory (Yeo et al. 2005). The difference in the membrane behavior was attributed in part to a lower percentage of clay in the construction-site backfills relative to the model backfills. Nevertheless, the authors estimated that the existence of the membrane behavior in the two cutoff walls could result in as much as 1-10 % decreases in the total liquid flux for the cutoff wall in Delaware and 7-8 % for the cutoff wall in New Jersey, depending on the void ratio, relative to the case where membrane behavior does not exist. Thus, the results of this study suggest that membrane behavior in field-constructed cutoff wall can be significant, depending on the void ratio and clay content of the backfill.

2.2.3 Chemico-Osmotic No-Flow Tests

Malusis et al. (2001) describe a unique laboratory apparatus for measuring the chemico-osmotic efficiency coefficient for clay soils. The testing cell consisted of an acrylic cylinder (71.1-mm diameter) and top and bottom pedestals with embedded porous stones through which separate electrolyte solutions could be continuously circulated to

establish and maintain a constant concentration difference across the specimen. An advantage of the apparatus was the capability of circulating the electrolyte solutions at identical rates such that volume changes through the system were prevented resulting in no-flow conditions. The entire testing cell could be placed in a load frame such that the thickness of the specimen could be controlled through the movable top pedestal. The effective diffusion coefficient (D^*) and retardation factors (R_d) of the solutes (K^+ and Cl^-) also could be determined simultaneously by measuring the diffusive solute mass flux through the specimen until steady-state diffusion was achieved.

Some example results illustrating the performance of the testing apparatus were presented based on two tests performed using circular specimens of a geosynthetic clay liner (GCL) with thicknesses of 10 mm exposed to chemical concentration differences of 8.7 and 47 mM potassium chloride (KCl). The porosities of the specimens were 0.79 and 0.78 respectively. The chemico-osmotic efficiency coefficient, ω , was derived from a measured pressure difference induced across the specimen in response to the applied concentration difference and was determined in accordance with Eq. 2.5.

The GCL was found to act as semipermeable membrane, with ω values at steady state, ω_{ss} , of 0.49 and 0.14 for the 8.7 and 47 mM KCl differences, respectively. The resulting values of the effective diffusion coefficient, D^* , for Cl^- and K^+ were $1.16 \times 10^{-10} \text{ m}^2/\text{s}$ and $0.907 \times 10^{-10} \text{ m}^2/\text{s}$ respectively, and the measured values of the retardation factor, R_d , for Cl^- and K^+ were 1.4 and 9.1 respectively. The results of chemico-osmotic tests conducted on GCL specimens in the presence of KCl solutions indicated that the differential pressure response may be influenced by time-dependent changes in chemico-osmotic efficiency due to soil-solution interactions, and the circulation rate of the

electrolyte solutions at the specimen boundaries relative to the rate of solute diffusion through of soil. The time required to achieve a steady-state response in induced pressure difference was related to the time required to achieve steady-state diffusion of all solutes, and may have been affected by the circulation rate at the specimen boundaries. The authors concluded that ω should be evaluated using the induced pressure difference at steady state, and the circulation rate should be sufficiently rapid to minimize changes in the boundary concentration due to diffusion, but sufficiently slow to allow measurement of solute mass flux at the lower concentration boundary for evaluating D^* and R_d .

Malusis and Shackelford (2002) evaluated the membrane behavior of a geosynthetic clay liner (GCL) containing granular bentonite (71 % montmorillonite) with a measured CEC of 47.7 meq/100g. The tests were performed using the same testing procedure and apparatus as described in detail by Malusis et al. (2001), and the chemico-osmotic efficiency coefficients, ω , were determined in accordance with Eq. 2.5. Circular specimens of the GCL with nominal diameters of 71.1 mm and thicknesses of 8, 10, and 13 mm were tested in a rigid, acrylic cylindrical cell by applying a chemical concentration difference ranging from 3.9 to 47 mM potassium chloride (KCl) under no-flow conditions. Both single-stage and multiple-stage chemico-osmotic tests were conducted. In the single-stage tests, the differential pressure induced by introducing a single KCl solution (i.e., 3.9, 8.7, 20, or 47 mM) was measured until steady-state conditions were achieved. The multiple-stage tests consisted of five individual stages in which differential pressures corresponding to five different source KCl solutions (i.e., 3.9, 6.0, 8.7, 20, and 47 mM) introduced sequentially through the top piston were measured across the same GCL specimen. The porosities of the specimens were 0.74 and 0.86 for

multiple-stage tests, and ranged from 0.78 to 0.80 for single-stage tests. The initial hydraulic conductivities of the specimens ranged from 1.63×10^{-11} m/s to 8.73×10^{-12} m/s for single-stage tests, and were 2.98×10^{-11} m/s and 3.86×10^{-12} m/s for the multiple-stage tests.

The GCL was found to act as semipermeable membrane, with ω values at steady state, ω_{ss} , ranging from 0.08 to 0.69. The ω_{ss} values decreased with increasing porosity and increasing KCl concentration. The decrease in ω_{ss} with increasing KCl concentration was attributed to compression of the diffuse double layers surrounding the clay particles, which was reflected by a time-dependent decrease in the induced differential pressure as well as an increase in the hydraulic conductivity of the specimen. The authors concluded that existence of the membrane behavior in the GCLs has important ramifications with respect to the evaluation of the hydraulic and contaminant transport performance of GCLs used in waste containment applications.

Shackelford and Lee (2003) illustrated the destructive role of diffusion on the ability of a geosynthetic clay liner (GCL) to act as a semipermeable membrane using the same testing procedure and apparatus as described by Malusis et al. (2001), and Malusis and Shackelford (2002). The GCL contained Na-bentonite (78 % montmorillonite) with a measured CEC of 69.4 meq/100g. The measured porosity of the GCL specimen with a nominal diameter of 71.1 mm and average measured thickness of 5.6 mm was 0.718. The tests were conducted by maintaining a concentration difference of 5 mM CaCl_2 across the GCL specimen while preventing flow of electrolyte solution through the specimen. The time-dependent membrane efficiency was derived from measured pressure differences induced across the specimen in response to the applied concentration difference, and the

chemico-osmotic efficiency coefficients, ω , were determined in accordance with Eq. 2.5. The diffusive mass fluxes of the solutes (Cl^- and Ca^{2+}) through the specimen also were measured simultaneously.

The results of the test indicated an initial increase in induced pressure difference across the specimen to a maximum value of 19.3 kPa corresponding to a maximum membrane efficiency of 52 % after 9 days of testing followed by a gradual decrease in induced pressure difference to almost zero (0.6 kPa) corresponding to a membrane efficiency of only 1.6 % after 35 days of testing, and subsequently to zero after 48 days of testing. The effective destruction of the initially observed semipermeable membrane behavior after 35 days of testing correlated well with the time of 35 ± 2 d required to essentially achieve steady-state Ca^{2+} diffusion. The decrease in induced pressure difference is consistent with compression of diffuse double layers between clay particles and particle clusters due to diffusion of Ca^{2+} , resulting in concomitant increase in pore sizes and decrease in the membrane efficiency. Thus, the results of the study illustrate the potentially destructive role of diffusion of invading salt cations on the membrane behavior of clays.

Yeo et al. (2005) evaluated the ability of two model soil-bentonite (SB) backfills to behave as semipermeable membranes. The bases soils for the model backfills consisted of a natural clay referred to as Nelson Farm Clay (NFC) and a mixture of sand with 5 % dry sodium bentonite. The NFC was classified as low plasticity clay (CL) with 89 % fines and ~52 % clay-sized particles with a cation exchange capacity (CEC) of 10.1 meq/100g and electrical conductivity (EC) of 36 mS/m at 25 °C. The silica sand was poorly graded (SP) with 100 % sand-sized particles with an EC of 1.5 mS/m. The sodium bentonite was

a high plasticity clay (CH) with 100 % fines and ~94 % clay-sized particles with a CEC of 86.1 meq/100g and an EC of 193 mS/m. Specimens of both base soils were mixed with a sufficient amount of 5 % sodium bentonite-water slurry to correspond to 100-mm slumps in accordance with standard practice for SB vertical cutoff walls.

The chemico-osmotic tests were performed using the same testing procedure and apparatus as described in detail by Malusis et al. (2001) and Malusis and Shackelford (2002), and the chemico-osmotic efficiency coefficients, ω , were determined in accordance with Eq. 2.5.

Membrane behavior was evaluated by measuring values for ω resulting from maintaining a 3.88 mM KCl concentration difference across the specimens at void ratios ranging from 0.605 to 1.008 for NFC backfill and from 0.812 to 1.212 for the sand-bentonite backfill.

Both model backfills were found to act as semipermeable membranes, with ω ranging from 0.018 to 0.024 for the NFC backfill and from 0.118 to 0.166 for the sand-bentonite backfill. The difference in the range of ω values was attributed to the significantly higher amount of high-swelling bentonite in the sand-bentonite backfill (i.e., 7.20 % versus 2.12 %). More significant membrane behavior (higher ω) correlated with higher consolidation stress, lower void ratio, and lower hydraulic conductivity. The results of this study provide the first quantitative evidence that SB vertical cutoff walls can behave as semipermeable membrane.

An example analysis to illustrate the potential significance of membrane behavior in a 1-m-thick SB vertical cutoff wall was provided based on the results of the study. The analysis showed that chemico-osmotic liquid flux due to membrane behavior could reduce the total liquid flux through an SB vertical cutoff walls in the case of a unit

outward hydraulic gradient to as low as 68 % of that which would occur in the absence of membrane behavior, whereas in the case of a unit inward hydraulic gradient, a chemico-osmotic liquid flux could contribute as much as 32 % of the hydraulic liquid flux to the total liquid flux through the wall.

2.3 OSMOTIC EFFECTS ON MECHANICAL PROPERTIES OF CLAYS

Mitchell et al. (1973) described theoretical and experimental approaches to evaluate the chemico-osmotic flow and consolidation process and enable identification and quantification of three types of coupling between the flow of salt and water: (1) chemico-osmotic coupling, (2) drag coupling, and (3) void ratio coupling. The theoretical approach included an analysis of chemico-osmotic consolidation to study the parameters important for understanding chemico-osmosis in soils. The results of the theoretical analysis indicated that (1) chemico-osmotic consolidation builds rapidly and smoothly to a maximum followed by a swelling, (2) the maximum amount of chemico-osmotic consolidation increases with increase in boundary salt concentration and soil compressibility, and (3) the time taken to reach equilibrium in the diffusion of both pore water and salt increase as soil void ratio decreases and soil compressibility increases.

A series of laboratory experiments also were conducted to measure the magnitude of chemico-osmotic coupling and consolidation for a wide range of soil-solution systems. Simple tests were designed to detect the existence of chemico-osmotic effects in soil-chemical solution systems. Thin thick disc-shaped specimens of soil were immersed in different solutions and weighed at various intervals for 2,000 min. Five different fine grained soils varying from a sandy clay to a highly active bentonite paste were tested.

Five different solutions ranging from a solution with high salt concentration NaCl to corn starch solution with low concentration 380 g/L triethylene glycol, polyethylene glycol 6000, polyethylene glycol 20000, and nadex 771 were used. Specimens of all five soils were consolidated to an effective stress of 98 kPa (1.0 kg/cm^2) in an ordinary consolidometer. The results of chemico-osmotic consolidation experiments on the same soils under a load increment of 98 kPa (1.0 kg/cm^2) to 196 kPa (2.0 kg/cm^2) indicated that chemico-osmotic consolidation was detectable only in highly compressible, active clays such as bentonite. Since high salt concentrations in contact with compressible, active clays can draw water from the clay, the authors noted that chemico-osmotic consolidation could serve as a technique for stabilizing compressible clays.

Barbour et al. (1989) provided an alternate macroscopic description of the osmotic volume change behavior of a clay soil undergoing changes in pore fluid chemistry. Theoretical descriptions are presented for two potential mechanisms of osmotic volume change, i.e., osmotic consolidation and osmotically induced consolidation. Laboratory testing was performed to establish the dominant mechanism of osmotic volume change in two clay soils, a natural soil referred to as Regina clay and an artificial soil mixture. The Regina clay is predominately a Ca-montmorillonite (45.2 % of the clay fraction) with a measured CEC of 31.7 meq/100g, specific surface area of $53 \text{ m}^2/\text{g}$, a clay fraction of 66 %, and a plasticity index of 51.2 %. The artificial soil mixture was comprised of 20 % sodium montmorillonite and 80 % Ottawa sand with a specific surface area ranging from 140 to $168 \text{ m}^2/\text{g}$, a clay fraction of 20 %, and liquid limit of 62.1 %. The initial thicknesses for the Regina clay and the soil mixture were 0.5-cm and 1.7-cm, respectively.

Each specimen was tested in a modified oedometer cell using standard incremental loading consolidation and was undergone osmotic consolidation of effective stresses of 100 kPa for Regina clay and 200 kPa for the soil mixture. However, after an elapsed time of 8000 min, the water along either the upper soil surface or both the top and bottom of the specimen was replaced with a solution containing 4.0 M NaCl to induce chemico-osmotic conditions. Experimental osmotic efficiencies based on test results were interpreted with theoretical osmotic efficiencies in order to determine the relative roles in producing volume change played by osmotic flow (osmotic efficiency) versus osmotic compressibility.

The analyses of the osmotic flow and pressure measurements indicated that osmotic consolidation was the predominate mechanism of osmotic volume change for both the Regina clay and the sand-montmorillonite mixture. However, the sand-montmorillonite specimen consolidated at a faster rate than the Regina clay specimen. This difference in consolidation rates was attributed to two possible reasons. First, based on the results of separate diffusion tests, the diffusion of NaCl was found to be slower in the Regina clay than the sand-montmorillonite mixture. Second, the osmotic compressibility of the sand-montmorillonite mixture was found to be greater than the osmotic compressibility of the Regina clay. Consequently, the time to the completion of osmotic consolidation for the Regina clay specimen was greater than that for the sand-montmorillonite specimen.

The results of this research showed that the dominant mechanism of volume change associated with brine contamination was osmotic consolidation that occurs as a result of a change in the electrostatic (repulsive-minus-attractive) stresses. Osmotically

induced consolidation that occurs because of chemico-osmotic liquid flow out of the clay in response to concentration gradient was of little significance with respect to volume change.

Di Maio (1996) evaluated the effect of chemico-osmosis on the mechanical behavior of a sodium bentonite exposed to NaCl, KCl, and CaCl₂ solutions ranging in concentration from 0.1 to 6.0 M. The liquid limit, shear strength, and consolidation behavior of saturated specimens of the Ponza bentonite (PI = 320, % < 2 μ m = 80) were measured using distilled water as well as the NaCl, KCl, and CaCl₂ solutions. Preliminary liquid limit tests whereby the salt solutions were used instead of water resulted in reduced liquid limits ranging from 60 to 200, indicating that diffusion of salts into the clay may result in noticeable changes in the mechanical behavior of the clay.

The residual shear strength was determined using a Casagrande direct shear box with specimens consolidated to about 400 kPa before being saturated with a salt solution and sheared within about 24 h at a displacement rate of 0.005 mm/min, and at several axial stresses ranging from 50 to 400 kPa. For the one-dimensional consolidation tests, 2.0-cm-thick specimens reconstituted by mixing the powdered clay with distilled water in a slurry were compressed in conventional oedometers to fixed axial stresses ranging from 40 kPa and 2,500 kPa, after each specimen was exposed to a salt solution by replacing the water in the cell. For comparisons of consolidation versus swelling, each specimen was unloaded to 40 kPa and then re-exposed to water.

The result of the residual shear strength indicated that pore fluid concentration had a noticeable influence not only on the values of the residual shear strength, but also on the shape of the curves. The residual shear strength against applied axial stress showed

that the greatest variations occurred at salt concentrations below 0.5 M, with negligible variations for salt concentration greater than 0.5 M. The residual shear strength increased about 1.7 times in 0.2 M salt concentration and about 2.3 times in 0.5 M salt concentration relative to that for distilled water, and the effects on the residual shear strength were found to be reversible when the specimens were re-exposed to water, whereas the effects of KCl and CaCl₂ persisted even after some months of continuous testing. The results of consolidation and swelling tests indicated that exposure of the clay to each of the solutions produced a decrease of in void ratio. The author concluded that changes in the thickness of the diffuse double layer were produced by ions diffusing into or out of the clay, and that a specific chemical treatment might cause a lasting improvement in the mechanical properties of active clays.

Gleason et al. (1997) evaluated the hydraulic conductivity (k) of sodium and calcium bentonite for hydraulic containment applications. Compacted sand-bentonite mixtures, a thin bentonite layer simulating a geosynthetic clay liner (GCL), and cement-bentonite mixtures simulating backfill for a vertical cutoff wall were permeated with tap water and a 0.25 M calcium chloride solution. Sodium and calcium bentonites consisted of 92 and from 75 to 80 percent smectite, respectively, and the measured liquid limits of the two bentonites were 603 and 124, respectively. The cation exchange capacities of the powdered sodium and calcium bentonites ranged from 100 to 110 and from 91 to 107 meq/100g, respectively. The sands used for this study included a uniform medium Ottawa sand, a broadly graded sand, and a naturally occurring silty sand with measured k values of 0.2, 0.003, and 1×10^{-5} cm/s, respectively.

The 0.25 M CaCl₂ solution reduced the swelling properties of both bentonites, and

caused a significant increase in k from 2×10^{-8} cm/s for calcium bentonite and 1×10^{-8} cm/s for sodium bentonite to 1×10^{-6} cm/s for both bentonites. The importance of grain size of the air-dry material was apparent from the difference in k values for the granular versus powdered sodium bentonite, with a k of 7×10^{-7} cm/s for the granular sodium bentonite, and a k of 1×10^{-8} cm/s for the powdered sodium bentonite. The results of this study showed that the hydraulic performance of calcium bentonite was not significantly better than that of sodium bentonite for either the clay-amended sand or the GCL application, and that the only advantage of the calcium bentonite relative to the sodium bentonite was a drained shear strength that was twice as high for the calcium bentonite.

Heister et al. (2004) evaluated the effect of gradually increasing salt solutions on the flocculation and hydraulic conductivity of a sodium bentonite (Ankerpoort Colclay A90 batch 61203 from the Netherlands) with a measured CEC of 68.3 meq/100g. Flocculation was evaluated visually via a series of sedimentation tests involving the settling of clay suspensions at densities ranging from 0.06 to 2 % by dry weight in sodium chloride (NaCl) solutions containing from 0.02 to 0.6 M NaCl. The results indicated that the minimum electrolyte concentration that caused flocculation of the bentonite was below 0.02 M NaCl. The hydraulic conductivities of specimens of the bentonite with a thickness of 2 mm and a diameter of 50 mm were measured using the falling-head method with flexible-wall permeameters and hydraulic gradients ranging from 149 to 327. During the experiments, a cell pressure of 400 kPa (58 psi) was applied to prevent swelling. The first hydraulic conductivity test was performed initially with tap water, then with increasingly more concentrated NaCl solutions ranging from 0.6 M and 1 M NaCl. A second experiment was performed by permeating first with de-ionized

water and subsequently with a 1 M NaCl solution.

The average, measured steady-state hydraulic conductivities were $2.3 \pm 0.9 \times 10^{-12}$ m/s and $2.4 \pm 0.2 \times 10^{-12}$ m/s for the first and second specimens, respectively, and remained relatively unchanged throughout the specimens, although the porosity of the specimen in the first experiment decreased from 0.56 before permeation to 0.39 after completion of permeation. Thus, the ionic strength of permeant liquid apparently had no influence on hydraulic conductivity. Although the "effective pore size" (i.e., the size of the fraction of the pores that participates in water flow) of clays likely would have increased due to the decrease in the thickness of the diffuse double layers of the clay platelets with increase in solution concentration, the applied cell pressure apparently was sufficient to consolidate the specimens and reduced the overall void ratio such that the effective pore-size distribution remained relatively unchanged. The authors surmised that the clay platelets apparently approached each other to the same degree as the diffuse double layers shrunk, resulting in no net effect. Therefore, rearrangement of the clay platelets due to flocculation or gelation apparently did not take place at the applied cell pressure. Based on the results of this study, the authors concluded that dissipation of osmotically induced hydraulic pressure differences in the chemical osmosis experiments reported by Keijzer and Loch (2001) under sufficiently high overburden pressure cannot be explained by flocculation.

2.4 THEORETICAL CONSIDERATIONS OF MEMBRANE BEHAVIOR

Staverman (1952) considered three types of driving forces existing across semi-permeable membranes, including an electrical potential difference (ΔE), a pressure difference (ΔP), and differences in the chemical potentials ($\Delta\mu$) of chemical species. The relationship between ΔE and $\Delta\mu$ results in the theory of membrane potentials (diffusion potentials), the relationship between ΔP and ΔE results in the process of electrokinetics, and the relationship between $\Delta\mu$ and ΔP results in process of chemico-osmosis.

Staverman (1952) noted that model theories not only lacked rigorous application of the macroscopic dielectric constant and viscosity to fields of molecular dimensions, but also usually ignored all of the secondary interaction effects, which amounts to neglecting all proportionality constants relating currents to forces. Staverman (1952) also noted that, since these theories include the static case with zero flow, the kinetic nature of the selection process induced by the membrane was not taken into account sufficiently by the theories. Knowledge of the various components of the liquid entering and leaving the membrane at a given rate of flow is required to calculate the excess charge contained in the membrane.

Staverman (1952) considered the apparent osmotic pressure in terms of a reflection coefficient, σ , and noted that σ has the advantage of being independent of the concentration in dilute solutions, and also of giving the very perspicuous result, that the measured osmotic pressure is σ times the thermostatic osmotic pressure. Finally, Staverman (1952) also noted the desire not only to measure for a given membrane one or two complex quantities like the membrane potential and the electrokinetic potential but also to obtain sufficient data to calculate all values in order to see how these change with

changing concentration, and to test theoretical assumption on these simple quantities rather than on the complex ones.

Groenevelt and Elrick (1976) presented a theory based on thermodynamic principles for the formulation of flux equations describing the transport of water, salt, and electrical charge through clays. Model considerations led to analytical expressions for the transport coefficients based on diffuse double layer theory. A macroscopic equation for the energy dissipation in an isothermal clay-water system was defined as follows (Groenevelt and Bolt, 1969):

$$T\sigma\Delta X = -j^v\Delta P - j^D\Delta\pi - I\Delta E^- \quad (2.6)$$

where $T\sigma$ is the energy dissipation, T is the absolute temperature, ΔX is the length of the macroscopic volume element in the flow direction, ΔP is the difference in hydrostatic pressure, $\Delta\pi$ is the difference in osmotic pressure, ΔE^- is the electric potential difference measured with electrodes reversible to the anions, j^v is the volume flux, j^D is the diffusion flux, and I is the electric current.

The difference between the proposed theory and former theories is that the proposed theory was based on electrodes that are reversible to the anions instead of the cations, such that the resulting impact of the difference in the magnitudes of the coefficients and the physico-chemical responses was formidable. The authors noted that the original definition of the reflection coefficient by Staverman (1951) was based on the reflection of polymers by membranes and dealt with only two forces in thermodynamic treatment, viz., the hydrostatic pressure difference (ΔP) and the osmotic pressure

difference ($\Delta\pi$). However, as also noted by authors, the reflection coefficient in the case of ions is also a function of the difference of the electrostatic potential (ΔE). Therefore, the authors suggested two different definitions: (1) the reflection coefficient at zero current ($I = 0$), in which there is no return passage for the electrons such that a streaming potential arises, and (2) the reflection coefficient with shorted electrodes reversible to the anions. This latter definition for the reflection coefficient is a property of the combination of the clay-water system and the shorted electrodes.

Fritz (1986) reviewed the existence and extent of membrane behavior in clays. He noted that the magnitude of generated osmotic pressures in geologic systems is governed by the theoretical osmotic pressure ($\Delta\pi$) calculated solely from solution properties based on van't Hoff's equation and by value of three phenomenological coefficients in the membranes, viz. the hydraulic permeability coefficient (L_p), the reflection coefficient (σ), and the solute permeability coefficient (ω). The hydraulic permeability coefficient L_p is defined as follows:

$$L_p = \frac{K}{\rho g x} \quad (2.7)$$

where K is the conventional permeability coefficient, ρ is the fluid density, g is the gravitational acceleration, and x is the thickness of the membrane. The reflection coefficient σ is related to the porosity and surface-charge density of the clay membrane, and the mean solute concentration on either side of the membrane. The solute permeability coefficient, ω , is a diffusion coefficient of the solute that is defined as follows:

$$\omega = \frac{J_s}{\Delta\pi} \quad (2.8)$$

where the ratio of the flux of solute, J_s , to $\Delta\pi$ (i.e., $\omega = J_s/\Delta\pi$). In general, lower values of L_p correspond to highly compacted membranes that have values of σ close to unity and ω values approaching 0.

Yeung and Mitchell (1993) developed the general formulation for coupled flows caused by hydraulic, electrical and chemical gradients under isothermal conditions. Thermally-induced flows were not included in the analysis, because temperature gradients are not likely to be great in most natural systems and thermally-induced flows in near saturated soils are usually small. An initial test of the theory was performed, and the computed concentration profiles of a cation and an anion were compared with the experimentally measured profiles to evaluate the proposed theory.

A laboratory testing program was developed to measure the migration of cations and anions in compacted clay under the influences of hydraulic, electrical and chemical gradients imposed simultaneously using the same testing procedure and apparatus as described in detail by Yeung (1990). The soil tested was grey-brown silty clay of moderate plasticity (CH) from Livermore, California, that was used as the compacted clay liner for a landfill at Altamont, California. The maximum dry density of the specimen was 176 kg/cm^3 (110 lb/ft^3) and optimum gravimetric water content was 17.4 % based on modified Proctor compaction procedure (ASTM D 1557). The measured liquid limit, plastic limit, and plasticity index (ASTM D 4318) of the soil were 52 %, 27 % and 25 %, respectively. Specimens were compacted directly into fixed-wall

permeameters at a water content of 21 %, and then saturated with tap water by back pressure. The hydraulic conductivities (k_h), coefficients of electro-osmotic permeability (k_{eo}) and electrical conductivities (κ) of the specimens were measured, and measured values ranged from 2.23×10^{-11} to 4.08×10^{-12} m/s for k_h , from 2.76×10^{-9} to 3.29×10^{-10} m²/V s for k_{eo} , and from 10.48 to 10.79 mS/m for κ .

A hydraulic gradient of 50 was applied continuously to a 0.022 M NaCl solution and an electrical gradient of 1 V/cm was applied for one hour per day in a direction that would cause electro-osmotic flow opposite to the hydraulic flow. One sample was sectioned for chemical analyses every five days, and concentration profiles of sodium ions Na⁺ and chloride ions Cl⁻ were measured. Based on the good agreement between the measured and predicted concentration profiles, the authors concluded that the developed coupled flow theory could reasonably predict the migration of cations and anions in saturated compacted clay under hydraulic, electrical and chemical gradients imposed simultaneously in a laboratory-scale experiment, and could be used as a basis for the prediction and evaluation of electrokinetic application for hazardous waste containment and site remediation.

Malusis et al. (2003) presented flux equations for liquid and solute migration through clay barriers that behave as semi-permeable membranes used in waste containment and remediation applications, referred to as clay membrane barriers (CMBs). The results of a simplified analysis of flow through a geosynthetic clay liner (GCL) using measured values for the chemico-osmotic efficiency coefficient (ω) of the GCL indicated that membrane behavior can result in a total liquid flux that counters the outward Darcy (hydraulic) liquid flux due to chemico-osmotic counter flow associated with clay

membrane behavior of the GCL. Also, the solute (contaminant) flux through the GCL was reduced relative to that which would occur in the absence of membrane behavior due to chemico-osmotic counter advection and solute restriction.

In the absence of an electrical current, the general expression for total solute (contaminant) flux, J , in a fine-grained soil that exhibits membrane behavior can be written for one-dimensional transport as follows (Malusis and Shackelford, 2002):

$$J = \underbrace{(1-\omega)q_h C}_{J_{ha}} + \underbrace{q_\pi C}_{J_\pi} + \underbrace{nD^* i_c}_{J_d} \quad (2.9)$$

where, ω = the chemico-osmotic efficiency coefficient, q_h = hydraulic liquid flux, q_π = chemico-osmotic liquid flux, n = specimen porosity, D^* = the effective salt-diffusion coefficient, i_c = the concentration gradient (>0), J_{ha} = hyperfiltrated advective solute flux, J_π = chemico-osmotic solute flux, and J_d = diffusive solute flux. Based on the flux equations for flow and transport through CMBs used in waste containment and remediation application, the effect of a CMB is to reduce the contaminant (solute) flux through the barrier relative to the contaminant flux that would occur in the absence of membrane behavior. This reduction in the contaminant flux results from two explicit mechanisms: (1) counter advection due to the chemico-osmosis inherent in the J_π term, and (2) solute restriction due to hyperfiltration inherent in J_{ha} term. The authors concluded that since diffusion commonly controls solute transport through GCLs and other low-permeability clay barriers, the implicit (empirical) correlation between the chemico-osmotic efficiency coefficient, ω , and the effective salt-diffusion coefficient, D^* , of the migrating contaminant is an important consideration with respect to contaminant

restriction in CMBs.

Manassero and Dominijanni (2003) performed a review of the coupled flow theory by Yeung and Mitchell (1993), and proposed a new set of equations to describe the osmosis effect on solute and solvent flows within fine-grained porous media. Mass flow equations could be derived from dissipation function by using the postulate of irreversible thermodynamics as follows (Katchalsky and Curran, 1965):

$$J_w = \alpha_{11}V_w \nabla(-P) + \alpha_{12} \frac{RT}{C} \nabla(-C) \quad (2.10 \text{ a})$$

$$J_d = \alpha_{21}V_w \nabla(-P) + \alpha_{22} \frac{RT}{C} \nabla(-C) \quad (2.10 \text{ b})$$

where, J_w = the mass flow rate of the solvent, J_d = the mass flow rate of the solute, V_w = the partial molar volume of the solvent, P = the hydraulic pressure, C = the molar concentration of the solute, R = the universal gas constant, T = the absolute temperature, and α_{ij} = phenomenological coefficients that relate the i th flow to the j th force. The following expression for α_{22} that is valid for the most general combination of flows and gradients could be derived as follows (Manassero and Dominijanni, 2003):

$$\alpha_{22} = C \left(\frac{nD}{RT} + \frac{Ck\omega^2}{\gamma} \right) \quad (2.11)$$

where, n = the porosity of the soil skeleton, D = the bulk diffusion coefficient, k = the hydraulic conductivity, ω = the osmotic efficiency, and γ = the unit weight of the solution.

This expression is different from the one which includes only the first term in the brackets proposed by Yeung and Mitchell (1993) that comes from an arbitrary extrapolation of the specific case of a counter-diffusion test where the osmotic effect is inhibited. Their proposed equations were based on fundamental principles of irreversible thermodynamics under the basic assumptions of incompressibility of the solid skeleton and the solvent, constant temperature, no electrical or electromagnetic gradients, and a sufficiently dilute solution. The proposed governing equations were tested using limiting conditions for the input parameters, including no osmotic efficiency ($\omega = 0$), perfect osmotic efficiency ($\omega = 1$), no water flow, and no external hydraulic gradient, to verify the consistency of the proposed equations in terms of the physical meaning of the governing parameters.

The proposed equations were used to reinterpret some experimental data taken from literature, and the results of the interpretation provided validation of the proposed equations in terms of osmotic efficiency (ω), an effective solute porosity (n^*), bulk diffusion coefficient (D) and tortuosity (τ). Nevertheless, the authors suggested that further experimental studies are necessary to assess independently the different transport parameters for a definitive validation of the proposed model and to obtain insight into the specific aspects whether the experimentally evaluated variations of the osmotic efficiency, ω , with solute concentration are due only to changes of the solid skeleton fabric and/or the diffuse double layer modifications due to the interaction with the contaminants at different concentrations in clayey soils. The authors noted that the proposed model could be used to assess the influence of the osmotic efficiency (ω) on the performance of mineral barriers for subsoil pollutant control, such as geosynthetic clay liners (GCL).

2.5 LITERATURE INDIRECTLY RELATED TO MEMBRANE RESEARCH

Olsen (1966) provided experimental results using a constant flow-rate apparatus consisting of a syringe pump (Harvard Apparatus Co. model 600-900 infusion-withdrawal pump) and a stainless steel syringe with a plunger to investigate the validity of Darcy's law at low gradients in a saturated sample of kaolinite clay (type hydrite MP, Georgia Kaolin Co.). Principal advantages of the apparatus were that the applied flow rates and the measured head differences did not require capillary tubes and, therefore, were not affected by air-water menisci, and that the time intervals needed to obtain head difference measurements were short (< 6 s). Constant flow rates were produced by driving or withdrawing the plunger of a syringe at 12 speeds ranging from about 1×10^{-1} to 2×10^{-5} cm/s. The experimental results were derived from testing specimens of the kaolinite clay with a diameter of 10.16 cm and thicknesses ranging from 1.0 to 3.0 cm. The specimens of kaolinite clay were prepared as a slurry with de-aired, distilled water (DDW). The test cell underwent successive increments of consolidation under loads ranging from 49 to 34,323 kPa (0.5 to 350 kg/cm²). The porosities of the specimen ranged from 0.225 to 0.588 during the loading stage, and the hydraulic conductivity ranged from 2.31×10^{-5} to 2.88×10^{-8} cm/s. The permeant solutions were changed during the experiments from DDW to either a 1 or 2 mN NaCl solution. Darcy's law was investigated after each consolidation increment by measuring the hydraulic head difference induced across the specimen by the applied flow rate with a differential pressure transducer. The corresponding values of hydraulic gradients and flow rates were calculated from the measured specimen thicknesses and the syringe calibrations.

The results of the study indicated that the relations between induced hydraulic

gradient versus flow rate were linear such that Darcy's law was obeyed with induced hydraulic gradients ranged from about 0.2 to 40 depending on the applied flow rate. The author concluded that Darcy's law is valid in many natural clays and clayey sediments, but that non-Darcy flow behavior may occur in very fine-grained clays, specifically clays containing significant amounts of high swelling montmorillonite (e.g., bentonites), and where high gradients are present in shallow unconfined sediments or in granular soils containing small amounts of clay.

Bresler (1973) developed theoretical and mathematical tools for analyzing transient one-dimensional (vertical) simultaneous transfer of non-interacting solute and water in unsaturated soils. The transient diffusion-convection equation was solved numerically by an approach that eliminates the effect of numerical dispersion. The numerical results were compared with some analytical solutions for steady water flow, and the results for transient infiltration were compared with field data reported by Warrick et al (1971).

Numerical solutions to the equation describing transient solute and water transfer in unsaturated soils had been used for evaluating that solute displacement can be predicted quantitatively. The numerical results indicated that a value of λ , an experimental constant on the characteristics of the porous media, from 0.3 to 0.5 cm is required to approximate field conditions. The value of the mechanical dispersion coefficient, D_h was greater than the molecular diffusion coefficient, D_p by 2 to 3 orders of magnitude, such that the molecular diffusion coefficient, D_p could be neglected.

The author noted that the molecular diffusion coefficient, D_p becomes more important than the mechanical dispersion as the solution flow velocity decreased during

the post-infiltration redistribution and the evaporation period. The highest D_p values and lowest D_h values were calculated at the soil surface and close to the wetting front during redistribution and in a zone above and below the horizontal plane at which there was no flow during the evaporation period. The numerical results were given for typical cases of infiltration, redistribution, and evaporation of water from the soil that effect on dispersion coefficients and salt concentration profiles.

Olsen (1984) reviewed the existing literature for evidence on the potential significance of osmosis, and showed that osmosis causes non-zero intercepts in flow rate versus hydraulic gradient relationships that are consistent with the observed deviations from Darcy's law at very low gradients. The magnitude of the intercepts in the continuous linear flow rate versus hydraulic gradient relationship can be varied by superimposing electrically driven and chemically driven osmosis in a specimen. Moreover, because a non-zero intercept exists when the electrolyte concentrations above and below the specimen are equal, Olsen (1984) concluded that an internal source of osmosis within the specimen was apparent.

Accordingly, Olsen (1984) proposed the hypothesis that chemico-osmosis can be generated within a specimen due to changes in the chemistry of the pore fluid over time, which is analogous to the previously proposed occurrence of electro-osmosis in nature generated by geochemical weathering reactions. The possible sources of this osmosis within the test specimens were identified as: (1) the existence of chemical reactions involved in aging effects within a specimen, (2) differential salt filtering originating from nonsymmetrical consolidation of the test specimen, due to variation in membrane efficiency with the size of soil pores, (3) divergence from chemical equilibrium owing to

differences in temperature and pressure between the laboratory and the location in nature, and (4) differences in chemical composition between soil pore fluids and the fluids brought into contact with specimens in the laboratory.

Shackelford et al. (2003) provided an overview of the primary factors affecting clay membrane behavior, illustrated the potential benefits resulting from the existence of clay membrane behavior, and elucidated the current issues associated with the evaluation of clay membrane behavior for use in the design of engineered containment barriers. In general, the efficiency of clay barriers being used for geoenvironmental containment applications can be improved by controlling the factors that trend to increase ω can enhance. These factors include increasing the state of stress on the clay, thereby decreasing the void ratio (porosity), and increasing the amount of high activity clays, such a bentonite used in the clay barrier. Enhancement of the adsorption capacity of such barriers through the addition of materials with relatively high cation exchange capacities, such as zeolites, may assist in increasing the time required to achieve steady-state diffusion of the invading cations, thereby prolonging the membrane behavior of the barrier. However, the potential effect of the additive constituents on the ability of the barrier to exhibit membrane behavior still would require evaluation.

2.6 REFERENCES

- Bader, S. and Heister, K. 2006. The effect of membrane potential on the development of chemical osmotic pressure in compacted clay. *Journal of Colloid and Interface Science*, 297, 329-340.
- Barbour, S. L. and Fredlund, D. G. 1989. Mechanisms of osmotic flow and volume change in clay soils." *Canadian Geotechnical Journal*, Vol. 26, No. 4, 551-562.
- Bresler, E. 1973. Simultaneous transport of solutes and water under transient unsaturated flow conditions. *Water Resources Research*, Vol. 9, No. 4, 975-986.
- Di Maio, C. 1996. Exposure of bentonite to salt solution: osmotic and mechanical effects. *Geotechnique*, Vol. 46, No. 4, 695-707.
- Elrick, D. E., Smiles, D. E., Baumgartner, N., And Groenevelt, P. H. 1976. Coupling phenomena in saturated homo-ionic montmorillonite: I. Experimental. *Soil Science Society of America Journal*, Vol. 40, No. 4, 490-491.
- Evans, J. C., Costa, M., and Cooley, B. 1995. The state of stress in soil-bentonite slurry trench cutoff walls. *Geoenvironment 2000, Geotechnical special publication No. 46*, Y. B. Acar and D. E. Daniel, eds., ASCE, New York, 1173-1191.
- Filz, G. M. 1996. Consolidation stresses in soil-bentonite backfilled trenches. *Proc., 2nd Int. Congress on Environmental Geotechnics*, M. Kamon, ed., A. A. Balkema, Rotterdam, The Netherlands, 497-502.
- Filz, G. M., Baxter, D. Y., Bentler, D. J., and Davidson, R. R. 1999. Ground deformation adjacent to a soil-bentonite cutoff wall. *Proc., GeoEngineering for Underground Facilities*, ASCE, Reston, Va., 121-139.
- Fritz, S. J. 1986. Ideality of clay membranes in osmotic process: a review. *Clays and*

Clay Minerals, Vol. 34, No. 2, 214-223.

Fritz, S. J. and Marine, I. W. 1983. Experimental support for a predictive osmotic model of clay membranes. *Geochimica et Cosmochimica Acta*, Vol. 47, No. 8, 1515-1522.

Gleason, M. H., Daniel, D. E., and Eykholt, G. R. 1997. Calcium and sodium bentonite for hydraulic containment application. *Journal of Geotechnical and Geoenvironmental Engineering*, Vol. 123, No. 5, 438-445.

Greenberg, J. A., Mitchell, J. K., and Witherspoon, P. A. 1973. Coupled salt and water flows in a groundwater basin. *Journal of Geophysical Research*, Vol. 78, No. 27, 6341-6353.

Groenevelt, P. H. and Elrick, D. E. 1976. Coupling phenomena in saturated homo-ionic montmorillonite: II. Theoretical. *Soil Science Society of America Journal*, Vol. 40, No. 6, 820-823.

Hanshaw, B. B. 1972. Natural-membrane phenomena and subsurface waste emplacement. *The American Association of Petroleum Geologists*, Vol. 18, No. 6, 308-317.

Hanshaw, B. B. and Coplen, T. B. 1973. Ultrafiltration by a compacted clay membrane – II. Sodium ion exclusion at various ionic strengths. *Geochimica et Cosmochimica Acta*, Vol. 37, No. 10, 2311-2327.

Heister, K., Keijzer, Th. J. S. and Loch, J. P. G. 2004. Stability of clay membranes in chemical osmosis. *Soil Science Society of America Journal*, Vol. 169, No. 9, 632-639.

Henning, J. T., Evans, J. C., and Shackelford, C. D. 2006. Membrane behavior of two backfills from field-constructed soil-bentonite cutoff walls. *Journal of*

- Geotechnical and Geoenvironmental Engineering*, Vol. 132, No. 10, 1243-1249.
- Ishiguro, M., Matsuura, T., and Detellier, C. 1995. Reverse osmosis separation for a montmorillonite membrane. *Journal of Membrane Science*, Vol. 107, No. 1, 87-92.
- Keijzer, Th. J. S., Kleingeld, P. J., and Loch, J. P. G. 1997. Chemical osmosis in compacted clayey material and the prediction of water transport. *Geoenvironmental Engineering, Contaminated Ground: Fate of Pollutants and Remediation*, R. N. Yong and H. R. Thomas, eds., University of Wales, Cardiff, U. K., Sept. 6-12, Thomas Telford Publ., London, 199-204.
- Keijzer, Th. J. S., Kleingeld, P. J., and Loch, J. P. G. 1999. Chemical osmosis in compacted clayey material and the prediction of water transport. *Engineering Geology*, Vol. 53, No. 2, 151-159.
- Keijzer, Th. J. S. and Loch, J. P. G. 2001. Chemical osmosis in compacted dredging sludge. *Soil Science Society of America Journal*, Vol. 65, No. 4, 1046-1055.
- Kemper, W. D. 1960. Water and ion movement in thin films as influenced by the electrostatic charge and diffuse layer of cations associated with clay mineral surfaces. *Soil Science Society of America Proc.*, Vol. 24, 10-16.
- Kemper, W. D. 1961. Movement of water as effected by free energy and pressure gradients: II. Experimental analysis of porous systems in which free energy and pressure gradients act in opposite directions. *Soil Science Society of America Proceedings*, Vol. 25, No. 4, 260-265.
- Kemper, W. D. and Evans N. A. 1963. Movement of water as effected by free energy and pressure gradients: III. Restriction of solutes by membranes. *Soil Science Society*

- of America Proceedings*, Vol. 27, No. 5, 485-490.
- Kemper, W. D. and Quirk, J. P. 1972. Ion mobilities and electric charge of external clay surfaces inferred from potential differences and osmotic flow. *Soil Science Society of America Proc.*, Vol. 36, No. 3, 426-433.
- Kemper, W. D. and Rollins, J. B. 1966. Osmotic efficiency coefficients across compacted clays. *Soil Science Society of America Proceedings*, Vol. 30, No. 5, 529-534.
- Kharaka, Y. K. and Berry, F. A. F. 1973. Simultaneous flow of water and solutes through geological membranes – I. Experimental investigation. *Geochimica et Cosmochimica Acta*, Vol. 37, No. 12, 2577-2603.
- Kharaka, Y. K. and Smalley, W. C. 1976. Flow of water and solutes through compacted clays. *The American Association of Petroleum Geologists Bulletin*, Vol. 60, No. 6, 973-980.
- MacKay, R. A. 1946. The control of impounding structures on ore deposition. *Economic Geology and the Bulletin of the Society of Economic Geologists*, The Economic Geology Publ. Co., New Haven, CT, Vol. 41, 13-46.
- Malusis, M. A. 2001. *Membrane Behavior and Coupled Solute Transport through a Geosynthetic Clay Liner*. PhD Dissertation, Colorado State University, Fort Collins, CO.
- Malusis, M. A. and Shackelford, C. D. 2002. Chemico-osmotic efficiency of a geosynthetic clay liner. *Journal of Geotechnical and Geoenvironmental Engineering*, Vol. 128, No. 2, 97-106.
- Malusis, M. A., Shackelford, C. D., and Olsen, H. W. 2001. A laboratory apparatus to measure chemico-osmotic efficiency coefficients for clay soils. *Geotechnical*

Testing Journal, Vol. 24, No. 3, 229-242.

Malusis, M. A., Shackelford, C. D., and Olsen, H. W. 2003. Flow and transport through clay membrane barriers. *Engineering Geology*, Vol. 70, No. 3, 235-248.

Manassero, M., and Dominijanni, A. 2003. Modeling the osmosis effect on solute migration through porous media. *Geotechnique*, Vol. 53, No. 5, 481-492.

Marine, I. W. 1974. Geohydrology of a buried Triassic basin at Savannah River plant, South Carolina. *The American Association of Petroleum Geologists Bulletin*, Vol. 58, No. 9, 1825-1837.

Marine, I. W. and Fritz, S. J. 1981. Osmotic model to explain anomalous hydraulic heads. *Water Resources Research*, Vol. 17, No. 1, 73-82.

McKelvey, J. G. and Milne, I. H. 1962. The flow of salt solutions through compacted clay. *Proceedings, Ninth National Conference on Clays and Clay Minerals*, Lafayette, Indiana, Oct. 5-8, 1960, Pergamon Press, New York, 248-259.

McKelvey, J. G., Spiegler, K. S. and Wyllie, M. R. J. 1957. Salt filtering by ion-exchange grains and membranes. *The Journal of Physical Chemistry*, Vol. 61, No. 2, 174-178.

Mitchell, J. K., Greenberg, J. A., and Witherspoon, P. A. 1973. Chemico-osmotic effects in fine-grained soils. *Journal of the soil mechanics and foundations division*, Vol. 99, SM 4, 307-322.

Neuzil, C. E. 2000. Osmotic generation of 'anomalous' fluid pressures in geological environments. *Nature*, Vol. 403, No. 6766, 182-184.

Olsen, H. W. 1966. Darcy's law in saturated kaolinite. *Water Resources Research*, Vol. 12, No. 2, 287-295.

- Olsen, H. W. 1969. Simultaneous fluxes of liquid and charge in saturated kaolinite. *Soil Science Society of America Proceedings*, Vol. 33, No. 3, 338-344.
- Olsen, H. W. 1972. Liquid movement through kaolinite under hydraulic, electric, and osmotic gradients. *The American Association of Petroleum Geologists Bulletin*, Vol. 56, No. 10, 2022-2028.
- Olsen, H. W. 1985. Osmosis: A cause of apparent deviations from Darcy's law. *Canadian Geotechnical J.*, Vol. 22, No. 2, 238-241.
- Olsen, H. W., Yearsley, E. N., and Nelson, K. R. 1990. Chemico-osmosis versus diffusion-osmosis. *Transportation Research Record No. 1288*, Transportation Research Board, Washington D.C., 15-22.
- Rahman, M. M., Chen, S., and Rahman, S. S. 2005. Experimental investigation of shale membrane behavior under tri-axial condition. *Petroleum Science and Technology*, 23, 1265-1282.
- Shackelford, C. D. and Lee, J.-M. 2003. The destructive role of diffusion on clay membrane behavior. *Clays and Clay Minerals*, CMS, Vol. 51, No. 2, 186-196.
- Shackelford, C. D., Malusis, M. A., and Olsen, H. W. 2003. Clay membrane behavior for geoenvironmental containment. *Soil and Rock America Conference 2003* (Proceedings of the joint 12th Panamerican Conference on Soil Mechanics and Geotechnical Engineering and the 39th U.S. Rock Mechanics Symposium), P. J. Culligan, H. H. Einstein, and A. J. Whittle, eds., Verlag Glückauf GMBH, Essen, Germany, Vol. 1, 767-774.
- Staverman, A. J. 1952. Non-equilibrium thermodynamics of membrane processes. *Transactions of the Faraday Society*, Vol. 48, No. 2, 176-185.

- Whitworth, T. M. and Fritz, S. J. 1994. Electrolyte-induced solute permeability effects in compacted smectite membranes. *Applied Geochemistry*, Vol. 9, No. 5, 533-546.
- Yeo, S.-S., Shackelford, C. D., and Evans, J. C. 2005. Membrane behavior of model soil-bentonite backfills. *Journal of Geotechnical and Geoenvironmental Engineering*, Vol. 131, No. 4, 418-429.
- Yeung, A. T. and Mitchell, J. K. 1993. Coupled fluid, electrical, and chemical flows in soil. *Geotechnique*, Vol. 43, No. 1, 121-134.

CHAPTER 3

ISOTROPIC CONSOLIDATION OF A GEOSYNTHETIC CLAY LINER

ABSTRACT: The consolidation behavior of a geosynthetic clay liner (GCL) was evaluated by consolidating duplicate specimens of the GCL under isotropic states of stress in a flexible-wall cell to a final effective consolidation stress, σ' , of 241 kPa (35.0 psi). The hydraulic conductivity, k , also was measured at the end of each loading increment. The results indicated that the GCL was normally consolidated for values of σ' greater than 34.5 kPa (5.0 psi), which correlates well with limited consolidation data reported in the literature based on one-dimensional consolidation. Values of the measured k , k_{measured} , for the GCL were low ($\leq 5.0 \times 10^{-9}$ cm/s) due to the sodium bentonite content of the GCL, and were within a factor of about two of the values of k based on consolidation theory, k_{theory} (i.e., $0.5 \leq k_{\text{theory}}/k_{\text{measured}} \leq 2.0$), suggesting that k_{theory} provided a good estimate of k_{measured} . Overall, the low k of the GCL dominated the consolidation behavior of the GCL. For example, values of the coefficient of consolidation, c_v , for the GCL ranged from 5.2×10^{-10} m²/s to 1.8×10^{-9} m²/s, which is among the lowest range of c_v values reported in the literature for clays. In addition, c_v for a given GCL specimen decreased with increasing σ' , albeit only slightly, primarily due to the decrease in k with increasing σ' . Finally, an estimate of the measured compression index, C_c , for the GCL based solely on empirical correlation with the liquid limit, LL, of the bentonite in the GCL (LL = 478 %) was found to be not only inaccurate but also conservative by about 300 %.

Key Words: compressibility, consolidation, geosynthetic clay liner, hydraulic conductivity

3.1 INTRODUCTION

Traditional (conventional) geosynthetic clay liners (GCLs) are thin (~ 5- to 10-mm thick), factory manufactured (prefabricated) hydraulic barriers (liners) that consist primarily of a processed clay, typically sodium bentonite, or other low permeability material that is either encased or "sandwiched" between two geotextiles or attached to a single polymer membrane (i.e., geomembrane) and held together by needle-punching, stitching, and/or gluing with an adhesive (Shackelford 2007). Over the past approximately two decades, GCLs have been used increasingly and extensively as barriers or components of barriers in hydraulic containment applications, such as municipal solid waste and hazardous waste landfills, surface impoundments (e.g., ponds and lakes, aeration lagoons, fly ash lagoons, tailings ponds, and other surface impoundments), canals, storage tanks, and secondary containment of above-grade fuel storage tanks (e.g., Bouazza 2002, Koerner 2005, Rowe 2005). The primary reasons for the increasing and extensive use of GCLs in such applications are savings in cost and technically equivalent performance relative to other hydraulic containment barriers, such as compacted clay liners and geomembrane liners.

In terms of technical equivalency, extensive research has been performed on both the hydraulic performance of GCLs to a variety of permeant liquids (e.g., Daniel et al. 1997, Shackelford et al. 2000, Rowe 2005, Shackelford 2007), as well as the shear strength of GCLs (e.g., Fox and Stark 2004). However, in contrast, very little research

has been performed on the consolidation behavior of GCLs. Accordingly, the primary purpose of this paper is to present the results of a study focused on assessing the consolidation behavior of a GCL subjected to isotropic states of stress. The study is believed to represent the first comprehensive attempt to quantify the consolidation behavior of a GCL subjected to an isotropic state of stress, and the results are among the few available pertaining to the consolidation behavior of a GCL.

3.2 MATERIALS AND EXPERIMENTAL METHODS

3.2.1 Materials

The GCL evaluated in this study is the same as that tested by Malusis and Shackelford (2002) for semi-permeable membrane behavior. The GCL ranges from about 5 to 10 mm in thickness in the air-dried (as-shipped) condition, and consists of sodium bentonite sandwiched between non-woven (non-patterned) and a woven (patterned) geotextiles and held together by needle punching with polymer fibers.

The physical and chemical properties as well as the mineralogical composition of the bentonite portion of the GCL were reported by Malusis and Shackelford (2002). In terms of mineralogy, the bentonite component of the GCL contained 71 % montmorillonite, 7 % mixed layer illite/smectite, 15 % quartz, and 7 % other minerals. The liquid limit (LL) and plastic limit (PL) measured in accordance with ASTM D4318 were reported as 478 % and 39 %, respectively, and the bentonite classified as a high plasticity clay (CH) based on the Unified Soil Classification System (ASTM D2487). The measured cation exchange capacity, or CEC, was reported as 47.7 meq/100 g (= 47.7 cmol/kg), and ~ 53 % of the exchange complex was reported as being comprised of

exchangeable sodium (i.e., sodium bentonite). Further details regarding the physical and chemical properties of the GCL bentonite are provided by Malusis and Shackelford (2002)

3.2.2 Specimen Assembly and Preparation

The GCL specimens were consolidated in this study in preparation for testing for membrane behavior (e.g., see Malusis and Shackelford 2002, Shackelford and Lee 2003). Accordingly, the specimen preparation consisted of two stages: (1) a flushing stage, and (2) a consolidation and permeation (consolidation/permeation) stage. The primary purpose of the flushing stage was to leach soluble salts from the GCL bentonite to enhance the potential for membrane behavior, since the membrane behavior of clays is known to increase with decreasing salt concentration (e.g., Shackelford et al. 2003). Secondary purposes included saturating the test specimens and measuring the initial hydraulic conductivity, k_{sat} , of the specimens. The primary purpose of the consolidation/permeation stage was to consolidate the specimens to a sufficiently high effective stress to again enhance the potential for membrane behavior. The secondary purpose was to measure k of the specimens for comparison with the k from the flushing stage and to evaluate the effect of consolidation on k .

For the flushing stage, circular specimens of the GCL with nominal diameters of 102 mm were permeated in standard flexible-wall permeameters (e.g., Daniel et al. 1985, Daniel 1994) at an average effective stress of 34.5 kPa (5.0 psi) with de-ionized water (DIW). The permeation with DIW continued until the electrical conductivity, EC, of the effluent from the specimen was ~ 50 % of the measured EC of 56.1 mS/m for the lowest

salt concentration (3.9 mM KCl) to be used in the subsequent membrane testing.

After completion of the flushing stage, the GCL specimens were transferred to separate but identical flexible-wall cells for the purpose of consolidating the specimens under isotropic loading conditions to a final effective stress of 241 kPa (35.0 psi) prior to membrane testing. After re-assembling the specimens in the flexible-wall cells, the specimens were initially consolidated back to an average effective stress of 34.5 kPa (5.0 psi) and then permeated with DIW for the purpose of providing a comparison of the measured k values after re-assembling versus those measured during flushing. After this initial consolidation stage, the specimens were subsequently consolidated in three 69.0-kPa (10.0-psi) increments until the desired, final average effective stress of 241 kPa (35.0 psi) had been achieved. Volume changes (ΔV) were monitored versus time via measuring changes in the air-water interface within the cell-water accumulator attached to the flexible-wall cell, and changes in the specimen height (ΔH) were determined using a telescope sighted to markings located on the specimen membrane located within the flexible-wall cell (see Daniel et al. 1985, Daniel 1994).

Values for k_{sat} were measured at the end of each incremental loading stage for the purposes of (1) evaluating the effect of consolidation stress on k , and (2) providing for a comparison of values of k based on consolidation theory, k_{theory} , with the measured k values, k_{measured} . With two exceptions, values of k_{measured} were determined in accordance with procedures in ASDTM D5084 (*Standard Test Methods for Measurement of the Hydraulic Conductivity of Saturated Porous Materials Using the Flexible Wall Permeameter*) using the falling headwater, rising tailwater procedure at an average effective stress of 34.5 kPa (5.0 psi). The two exceptions in procedures were the use of

DIW as the permeant liquid instead of the "standard water" specified in ASTM D5084, and the use of an average hydraulic gradient of 330. While this hydraulic gradient is higher than the maximum gradient (i.e., 30) stipulated in ASTM D 5084 for soils with low hydraulic conductivity ($k < 10^{-7}$ cm/s), hydraulic gradients ranging from 50 to 600 typically are used for measuring the k of GCLs due to the typically low k of GCLs. The k of GCLs has been shown to be affected to a greater extent by the average effective stress than by the magnitude of hydraulic gradient (Shackelford et al. 2000). The complete stress states for the GCL specimens during both the flushing and consolidation/permeation stages are summarized in Table 3.1.

3.3 RESULTS

3.3.1 Measured Hydraulic Conductivity

As shown in Fig. 3.1 and Table 3.2, the values for k_{measured} based on permeation with DIW after re-consolidating to the initial average effective stress of 34.5 kPa (5 psi) were slightly higher than those at the end of the flushing stage for both GCL specimens. For example, k_{measured} after reconsolidation of specimen GCL1 was 3.3×10^{-9} cm/s compared to the steady-state k value of 2.7×10^{-9} cm/s after flushing, whereas k_{measured} after reconsolidation of specimen GCL2 was 5.0×10^{-9} cm/s compared to the steady-state k value of 3.3×10^{-9} cm/s after flushing. Thus, both GCL specimens undoubtedly experienced some disturbance upon reassembly and reconsolidation, although the differences in k values are considered to be minor such that any disturbance to the specimens likely was minimal.

After the initial reconsolidation to 34.5 kPa (5.0 psi), values for k_{measured} for each GCL decreased with increasing effective consolidation stress, σ' , until the final σ' of 241

kPa (35.0 psi) was achieved. In the case of specimen GCL1, k_{measured} decreased from 3.3×10^{-9} cm/s at 34.5 kPa (5.0 psi) to 5.0×10^{-10} cm/s at 241 kPa (35.0 psi), whereas for specimen GCL2, k_{measured} decreased from 5.0×10^{-9} cm/s at 34.5 kPa (5.0 psi) to 6.4×10^{-10} cm/s at 241 kPa (35.0 psi). As illustrated in Fig. 3.2, the decrease in k_{measured} with increasing σ' is consistent with a decrease in void ratio with increasing σ' .

3.3.2 Strain versus Time

Plots of vertical strain (ϵ_{vert}) and volumetric strain (ϵ_{vol}) versus both logarithm of time ($\log t$) and square root of time ($t^{1/2}$) for each consolidation stage are shown for both specimens in Figs. 3.3 and 3.4, respectively. A comparison of the plots in Figs. 3.3 and 3.4 for a given stress indicates that values of ϵ_{vol} were slightly lower than values of ϵ_{vert} at a given time, which is consistent with smaller differences between vertical deformations, ΔH , versus volumetric deformations, ΔV , relative to the greater differences between initial specimen height, H_0 , versus initial specimen volume, V_0 (i.e., $8.23 \text{ mm} \leq H_0 \leq 8.86 \text{ mm}$ vs. $71,207 \text{ mm}^3 \leq V_0 \leq 75,170 \text{ mm}^3$). The closeness between ϵ_{vol} and ϵ_{vert} also suggests that the consolidation behavior of the GCL was anisotropic, such that ϵ_{vol} was dominated by vertical deformations (i.e., lateral deformations were relatively minor). This behavior undoubtedly is related to the geometry of the disk-like GCL specimens, with thicknesses on the order of only 8 % of the diameter (102 mm) of the specimens. In general, the volumetric deformations were considered to be more reliable than the vertical deformations, primarily because measurements of ΔV based on changes in the water level in the cell-water accumulator of the flexible-wall cell were easier and likely more accurate than were measurements of ΔH using a telescope due to the relative

difficulty in sighting the reference mark on the specimen membrane within the flexible-wall cell with the telescope.

3.3.3 Stress versus Strain

Stress-versus-strain (stress-strain) curves in the form of ϵ_{vert} , ϵ_{vol} , and void ratio (e) versus logarithm of σ' for both GCL specimens are shown in Fig. 3.5. Note that the stress-strain curve presented in terms of void ratio (Fig. 3.5c) is based only on volumetric strains (i.e., not vertical strains), because the specimens were not confined to only vertical deformation. Several observations are readily apparent from the stress-strain curves shown in Fig. 3.5.

First, all semi-log linear regressions of the data resulted in high values for the coefficient of determination, r^2 (i.e., $r^2 \geq 0.996$), indicating that the stress-strain curves were all indeed semi-log linear, such that no stress history is evident and the GCL specimens were normally consolidated. This observation follows from the fact that the maximum previous effective consolidation stress, σ'_{max} , of 34.5 kPa (5.0 psi) was applied during the flushing stage of the specimen preparation, such that applied effective consolidation stresses greater than 34.5 kPa (5.0 psi) should result in virgin compression of the specimens. These results are somewhat different from those shown in Shan (1993), who performed one-dimensional (consolidometer) consolidation tests on specimens of four different GCLs, in that all of the GCLs tested by Shan (1993) indicated stress history. However, the values of σ'_{max} for the tests performed by Shan (1993) were all less than about 38.3 kPa (5.6 psi), and less than 34.5 kPa (5.0 psi) for three of the four GCLs tested. Thus, virgin compression behavior also was evident in the majority of the results reported

by Shan (1993) for σ' greater than about 34.5 kPa (5.0 psi). In addition, differences between the results reported by Shan (1993) versus those reported herein may be due to differences between the types of GCLs tested as well as difference in the testing procedures (e.g., 1-D vs. 3-D consolidation, specimen preparation, etc.).

Second, the values for the compression ratios, R_c , and compression indexes, C_c , for both GCL specimens are reasonably close, with the R_c and C_c values for specimen GCL1 being slightly lower than those for specimen GCL2. For example, the ratios of R_c for specimen GCL2 to R_c for specimen GCL1 are 1.24 based on ϵ_{vert} and only 1.22 based on ϵ_{vol} , whereas the ratio of C_c for specimen GCL2 to C_c for specimen GCL1 is 1.20.

Third, values for R_c based on ϵ_{vert} tend to be slightly greater than those based on ϵ_{vol} for both GCL specimens. This difference in R_c is consistent with ϵ_{vert} being slightly greater than ϵ_{vol} as previously discussed.

3.3.4 Coefficients of Consolidation

Values for the coefficient of consolidation, c_v , based on the time-strain plots in Figs. 3.3 and 3.4 are summarized in Table 3.2, and plotted as a function of the average of σ' , σ'_{ave} , in Figs. 3.6 and 3.7 based on ϵ_{vert} and ϵ_{vol} , respectively. Note that σ'_{ave} is used here instead of the final σ' because values of c_v calculated in accordance with Casagrande's method are based on the time to achieve 50 % consolidation of the applied loading increment, such that only half of the applied loading increment has been transferred to effective stress.

In general, c_v for a given GCL specimen decreases with increasing σ'_{ave} , albeit only slightly. This trend is consistent with the previously discussed decrease in $k_{measured}$

with increasing σ' in accordance with the following standard correlation (e.g., Lambe and Whitman 1969):

$$c_v = \frac{k}{m_v \rho_w g} = \frac{k(1+e_o)}{a_v \rho_w g} \quad (3.1)$$

where m_v is the coefficient of volume compressibility, a_v is the coefficient of compressibility, e_o is the initial void ratio, ρ_w is the density of water, and g is the acceleration due to gravity. However, as shown in Figs. 3.8 and 3.9, the GCL compressibility (m_v or a_v) also decreases with increasing σ'_{ave} , which would tend to increase c_v with increasing σ'_{ave} in accordance with Eq. 3.1. The reason c_v decreases with increasing σ'_{ave} is that k decreases to a greater extent than either m_v or a_v with increasing σ'_{ave} , such that the overall trend is decreasing c_v with increasing σ'_{ave} .

For example, Yeo (2003) and Yeo et al. (2005) also found that k , m_v , and a_v all decreased with increasing σ'_{ave} for nine model soil-bentonite (SB) backfill mixtures for vertical cutoff walls consisting of natural clay-sand mixtures with backfill fines contents of 20, 40, 60, 75, and 89 percent by dry weight, and sand-bentonite mixtures with dry backfill bentonite contents of 2, 3, 4, and 5 percent. However, in contrast, Yeo (2003) and Yeo et al. (2005) found that c_v increased with increasing σ'_{ave} for their model SB backfill mixtures, because m_v and a_v decreased to a greater extent than did k with increasing σ'_{ave} . The difference between the two trends in c_v versus σ'_{ave} can be attributed to several factors, including generally lower compressibilities reported by Yeo (2003) (i.e., $1.6 \times 10^{-5} \text{ kPa}^{-1} \leq m_v \leq 6.1 \times 10^{-3} \text{ kPa}^{-1}$) relative to those determined in this study (i.e., 4.3×10^{-4}

$\text{kPa}^{-1} \leq m_v \leq 2.2 \times 10^{-3} \text{ kPa}^{-1}$), a much greater range of applied effective consolidation stresses for the model soil-bentonite backfills tested by Yeo (2003) and Yeo et al. (2005) relative to the GCLs tested in this study (i.e., $5 \text{ kPa} \leq \sigma' \leq 1280 \text{ kPa}$ vs. $103 \text{ kPa} \leq \sigma' \leq 241 \text{ kPa}$), and the difference between specimens being consolidated under isotropic conditions in this study versus under one-dimensional, confined compression conditions by Yeo (2003) and Yeo et al. (2005).

As indicated in Table 3.2, the value of c_v for specimen GCL2 tended to be greater than that of specimen GCL1 for a given σ' , regardless of whether the value was based on ϵ_{vert} versus ϵ_{vol} or whether the Casagrande or Taylor method was used for the analysis. For example, the ratio of the values for c_v for specimen GCL2 relative to those for specimen GCL1 range from 1.1 to 1.9. Also, the ratio of the values for c_v for specimen GCL2 relative to those for specimen GCL1 tended to be the greatest at a final value of σ' of 241 kPa (35.0 psi) relative to σ' of 103 kPa (15.0 psi) or 172 kPa (25.0 psi), regardless of type of strain (ϵ_{vert} vs. ϵ_{vol}) or method of analysis (Casagrande vs. Taylor).

The values of c_v based on ϵ_{vol} relative to those based on ϵ_{vert} (c_v based on $\epsilon_{\text{vol}}/c_v$ based on ϵ_{vert}) are plotted as a function of σ'_{ave} in Fig. 3.10. In all cases, the values of c_v based on ϵ_{vol} are greater than those based on ϵ_{vert} ($1.31 \leq c_v$ based on $\epsilon_{\text{vol}}/c_v$ based on $\epsilon_{\text{vert}} \leq 1.46$), although the difference is relatively minor ($1.06 \leq c_v$ based on $\epsilon_{\text{vol}}/c_v$ based on $\epsilon_{\text{vert}} \leq 1.12$) in the case of specimen GCL2 based on Taylor's method of analysis (Fig. 3.10b).

As shown in Fig. 3.11, values of c_v based on the Taylor method relative to those based on the Casagrande method, or $c_{v,\text{Taylor}}/c_{v,\text{Casagrande}}$, are practically the same for both GCL specimens regardless of the value of σ'_{ave} or whether the c_v values are based on

either ϵ_{vert} or ϵ_{vol} . For example, based on ϵ_{vert} (Fig. 3.11a), $c_{v,\text{Taylor}}/c_{v,\text{Casagrande}}$ ranges from 0.86 to 1.3 for specimen GCL1 and from 1.1 to 1.3 for specimen GCL2, whereas based on ϵ_{vol} (Fig. 3.11b), $c_{v,\text{Taylor}}/c_{v,\text{Casagrande}}$ ranges from 0.83 to 1.3 for specimen GCL1 and from 0.84 to 1.0 for specimen GCL2. These results suggest that method of analysis had a relatively minor effect on the determination of c_v for the GCL and test conditions evaluated in this study.

3.3.5 Theoretical Hydraulic Conductivity

Values of the theoretical hydraulic conductivity, k_{theory} , based on Eq. 3.1 are plotted as a function of σ'_{ave} in Figs. 3.12 and 3.13 based on the c_v values determined using the Casagrande method and the Taylor method, respectively. Consistent with the trends in both c_v and m_v (or a_v) with σ'_{ave} (Figs. 3.6–3.9), k_{theory} decreases with increasing σ'_{ave} . This trend in k_{theory} versus σ'_{ave} again is expected on the basis that k is expected to decrease with decreasing void ratio resulting from increasing σ' , as previously explained in connection with k_{measured} (Fig. 3.2 and Table 3.2). Also, the values of k_{theory} at a given value of σ'_{ave} for specimen GCL2 are always greater than or equal to those for specimen GCL1, regardless of method of analysis for c_v (i.e., Casagrande vs. Taylor) or basis of analysis for m_v (i.e., ϵ_{vert} vs. ϵ_{vol}).

Finally the values of k_{theory} range from a high of 4.1×10^{-9} cm/s for specimen GCL2 at a σ'_{ave} value of 69.0 kPa (10.0 psi) based on analysis using the Casagrande method for determining c_v and ϵ_{vol} for determining m_v (Fig. 3.12b), to a low of 2.1×10^{-10} cm/s for specimen GCL1 at a σ'_{ave} value of 207 kPa (30.0 psi) based on analysis using the Taylor method for determining c_v and ϵ_{vert} for determining m_v (Fig. 3.13a). Also,

there is little difference among the values of k_{theory} for a given GCL specimen at a given value of σ'_{ave} based on the different methods of analysis for c_v (i.e., Casagrande vs. Taylor) or m_v (i.e., ϵ_{vert} vs. ϵ_{vol}). For example, the four values of k_{theory} for specimen GCL2 at a σ'_{ave} value of 69.0 kPa (10.0 psi) range from 3.0×10^{-9} cm/s to 4.1×10^{-9} cm/s, whereas the four values of k_{theory} for specimen GCL1 at a σ'_{ave} value of 207 kPa (30.0 psi) range from 2.1×10^{-10} cm/s to 4.6×10^{-10} cm/s. Thus, the values of k_{theory} determined in this study for both GCL specimens are in good agreement with other measured values of k for GCLs based on permeation with water, which typically are on the order of $\leq 3.0 \times 10^{-9}$ cm/s (Daniel et al. 1997).

3.3.6 Secondary Compression

Values of the secondary compression ratio, R_{α} , and the secondary compression index, C_{α} , based on both ϵ_{vert} and ϵ_{vol} are summarized in Table 3.3 and plotted versus final σ' in Figs. 3.14 and 3.15, respectively, where R_{α} and C_{α} are defined as follows:

$$R_{\alpha, \text{vert}} = \frac{\Delta \epsilon_{\text{vert}}}{\Delta \log t} \quad ; \quad R_{\alpha, \text{vol}} = \frac{\Delta \epsilon_{\text{vol}}}{\Delta \log t} \quad (3.2)$$

and

$$C_{\alpha, \text{vert}} = \frac{-\Delta e_{\text{vert}}}{\Delta \log t} = R_{\alpha, \text{vert}} (1 + e_0) \quad ; \quad C_{\alpha, \text{vol}} = \frac{-\Delta e_{\text{vol}}}{\Delta \log t} = R_{\alpha, \text{vol}} (1 + e_0) \quad (3.3)$$

where Δe_{vert} and Δe_{vol} are the changes in void ratios corresponding to the changes in ϵ_{vert}

and ϵ_{vol} , respectively. As indicated in Table 3.3, the values of R_α and C_α for specimen GCL2 at a given σ' are always slightly higher than the corresponding values for specimen GCL1, regardless of whether R_α and C_α were based on ϵ_{vert} or ϵ_{vol} . In addition, the values of R_α and C_α for both GCL specimens decrease essentially linearly with increasing σ' .

Finally, as shown in Fig. 3.16, values of $R_{\alpha,vert}/R_{\alpha,vol}$ ($= C_{\alpha,vert}/C_{\alpha,vol}$) also tended to decrease approximately linearly as σ' increases from 103 kPa (15.0 psi) to 241 kPa (35.0 psi), although the correlation for specimen GCL2 is not as good as that for specimen GCL1. Also, values of R_α and C_α based on ϵ_{vert} (i.e., $R_{\alpha,vert}$ and $C_{\alpha,vert}$) tend to be slightly higher than values of R_α and C_α based on ϵ_{vol} (i.e., $R_{\alpha,vol}$ and $C_{\alpha,vol}$) at the lowest σ' of 103 kPa (15.0 psi), whereas the opposite is true at the highest σ' of 241 kPa (35.0 psi). At the intermediate σ' of 172 kPa (25.0 psi), $R_{\alpha,vert}$ and $C_{\alpha,vert}$ are virtually identical to $R_{\alpha,vol}$ and $C_{\alpha,vol}$.

3.4 DISCUSSION

3.4.1 Compression Index

The measured values for the compression index, C_c , for the two GCL specimens were previously shown in Fig. 3.5. To the best of the authors' knowledge, reports on the consolidation properties of GCLs are extremely limited. In fact, the only reference of which the authors are aware that contains consolidation results for GCLs is the PhD dissertation by Shan (1993). However, this reference does not report values of either C_c or c_v , as the primary purpose of the consolidation tests performed by Shan (1993) was to determine the times to achieve 50 % consolidation, or t_{50} , for use in determining the

strain rates to be used in shear strength testing of the GCLs. Also, Shan (1993) performed only one-dimensional consolidation testing in traditional consolidometers, i.e., as opposed to three-dimensional consolidation performed under isotropic states of stress imposed in this study. Therefore, some discussion of the C_c values measured in this study is warranted.

The measured values for C_c of 1.31 for specimen GCL1 and 1.57 for specimen GCL2 would be over estimated by factors of 3.2 and 2.7, respectively, based on the commonly used empirical expression between C_c and the liquid limit, LL, for normally consolidated clays (e.g. Holtz and Kovacs 1981, Terzaghi et al. 1996), or $C_c = 0.009(LL - 10)$, which results in a value for C_c of 4.2 for the measured LL of 478 % for the bentonite contained in the GCL evaluated in this study. Thus, estimates of C_c for the GCL based solely on the liquid limit of the bentonite in accordance with the aforementioned empirical expression are not only inaccurate but also conservative (high). Sridharan and Nagarj (2000) also concluded that liquid limit alone cannot be used to correlate with compression index, because other index properties such as the stress boundary conditions, specimen geometry, plastic limit, plasticity index, shrinkage limit, and shrinkage index also significantly influence the compression index.

3.4.2 Coefficient of Consolidation

Values of the coefficient of consolidation, c_v , for the two GCL specimens loaded under isotropic conditions in this study were summarized in Table 3.2, and range from 5.2×10^{-10} m²/s (specimen GCL1, ϵ_{vert} , Casagrande method) to 2.1×10^{-9} m²/s (specimen GCL2, ϵ_{vol} , Casagrande method). This range of c_v values is among the lowest range of c_v

values reported for clays, and can be attributed primarily to the relatively low magnitudes of k_{measured} for the two specimens (Table 3.2).

For example, Holtz and Kovacs (1981) report c_v values ranging from 4.0×10^{-9} m^2/s to 4.0×10^{-7} m^2/s for a wide range of naturally occurring silts and clays. Thus, the lowest value of c_v reported by Holtz and Kovacs (1981) is still about two times greater than the highest value of c_v measured in this study. More recently, Terzaghi et al. (1996) show c_v values for a wide range of clays ranging from about 6.4×10^{-9} m^2/s (0.2 m^2/yr) to about 6.4×10^{-7} m^2/s (20 m^2/yr). Thus, the lowest value of c_v reported by Terzaghi et al. (1996) is still about three times greater than the highest measured value of c_v for the GCL evaluated in this study.

3.4.3 Theoretical versus Measured Hydraulic Conductivity

The theoretical values of k , k_{theory} , based on Eq. 3.1 are compared with the measured values of k , k_{measured} , for each GCL specimen in Fig. 3.17. Overall, there is relatively good agreement between k_{theory} and k_{measured} , regardless of method of analysis (Casagrande vs. Taylor) or type of strain (ϵ_{vert} vs. ϵ_{vol}) used to calculate k_{theory} . For example, $k_{\text{theory}}/k_{\text{measured}}$ varies by only about a factor of two (i.e., $0.5 \leq k_{\text{theory}}/k_{\text{measured}} \leq 2.0$) for both GCL specimens, especially when k_{theory} was based on ϵ_{vol} (Figs. 3.17b and 3.17d).

In general, k_{measured} was expected to be somewhat lower than k_{theory} for a given loading increment (i.e., $k_{\text{theory}}/k_{\text{measured}} > 1$), since k_{measured} was determined at the end of the full loading increment corresponding to the lowest void ratio for the loading increment (i.e., after both primary consolidation and secondary compression), whereas

k_{theory} is based only on primary consolidation corresponding to a relatively higher void ratio. Nonetheless, the good agreement between k_{theory} and k_{measured} for the GCL and testing conditions imposed in this study (e.g., isotropic stress conditions, DIW as the permeant liquid, etc.) suggests that reasonably good approximations of k (i.e., within a factor of about two) can be obtained from the results of consolidation testing, i.e., without the need for direct measurement of k .

3.5 SUMMARY AND CONCLUSIONS

Duplicate specimens of a geosynthetic clay liner (GCL) were consolidated under isotropic states of stress in a flexible-wall cell after permeation at an effective stress, σ' , of 34.5 kPa (5.0 psi) to flush soluble salts from the soil pores in preparation to be tested for semi-permeable membrane behavior. The specimens were consolidated using a constant loading increment of 69.0 kPa (10.0 psi) to final effective stresses of 103 kPa (15.0 psi), 172 kPa (25.0 psi), and 241 kPa (35.0 psi). The hydraulic conductivity, k , also was measured at the end of each loading increment. The strain-versus-time data were analyzed in terms of both vertical strain (ϵ_{vert}) and volumetric strain (ϵ_{vol}) using both the Casagrande ($\log t$) and Taylor ($t^{1/2}$) methods to determine values for the coefficient of consolidation (c_v), the coefficients of volume compressibility (m_v) and compressibility (a_v), the theoretical hydraulic conductivity (k_{theory}), and the secondary compression ratio (R_α) and index (C_α). The results of the stress-strain curves were analyzed in terms of both ϵ_{vert} and ϵ_{vol} and void ratios to determine values for the compression ratio (R_c) and compression index (C_c), respectively. The study is believed to represent the first comprehensive attempt to quantify the consolidation behavior of a GCL subjected to an

isotropic state of stress, and the results are among the few available, if any, pertaining to the consolidation behavior of a GCL.

The stress-versus-strain curves for both GCL specimens were semi-log linear, such that the GCL specimens were considered to be normally consolidated with a maximum previous effective consolidation stress, σ'_{\max} , of 34.5 kPa (5.0 psi). This observation is consistent with limited published results based on conventional, one-dimensional (consolidometer) consolidation testing of four different GCLs indicating values for σ'_{\max} of ≤ 38.3 kPa (5.6 psi) for all four GCLs and ≤ 34.5 kPa (5.0 psi) for three of the four GCLs.

The coefficients of consolidation, c_v , for the two GCL specimens ranged from 5.2×10^{-10} m²/s to 2.1×10^{-9} m²/s, which is among the lowest range of c_v values reported in the literature for clays. In addition, c_v for a given GCL specimen decreased with increasing effective consolidation stress, σ' , albeit only slightly. Both of these observations were attributed primarily to the dominance of the relatively low magnitudes of k measured for the two specimens (i.e., $k_{\text{measured}} \leq 5.0 \times 10^{-9}$ cm/s). Finally, values of c_v calculated using different types of strain (ϵ_{vert} vs. ϵ_{vol}) or different methods of analysis (Casagrande vs. Taylor) varied by at most a factor of about two, such that type of strain or method of analysis had a relatively minor effect on determining c_v .

Values of the hydraulic conductivity measured as the end of each loading increment, k_{measured} , as well as those calculated on the basis of consolidation theory, k_{theory} , were found to generally decrease with increasing σ' , which is consistent with decreases in void ratio with increasing σ' . In addition, the range of values for k_{measured} was similar to that for k_{theory} (i.e., 5.0×10^{-10} cm/s $\leq k_{\text{measured}} \leq 5.0 \times 10^{-9}$ cm/s vs. 2.1×10^{-10} cm/s \leq

$k_{\text{theory}} \leq 4.1 \times 10^{-9}$ cm/s). The overall good agreement between k_{theory} and k_{measured} for the GCL and testing conditions imposed in this study (e.g., isotropic stress conditions, DIW as the permeant liquid, etc.) suggests that reasonably good approximations of k (i.e., within a factor of about two) can be obtained from the results of consolidation testing, i.e., without the need for direct measurement of k .

The values for the compression ratios, R_c , and compression indexes, C_c , for both GCL specimens were reasonably close, with better agreement between the R_c values of the two GCL specimens being obtained when ϵ_{vol} versus ϵ_{vert} was considered in the analysis. Also, the measured values for C_c for the two GCL specimens of 1.31 and 1.57 were significantly lower by factors of 3.2 and 2.7, respectively, relative to those based solely on empirical correlation with the liquid limit, LL, of the bentonite in the GCL (LL = 478). Thus, estimates of C_c for the GCL based solely on the liquid limit of the bentonite in accordance with the empirical correlation are likely to be not only inaccurate but also conservative (high).

Values of the secondary compression ratio, R_{α} , based on both ϵ_{vert} ($R_{\alpha,\text{vert}}$) and ϵ_{vol} ($R_{\alpha,\text{vol}}$), and the associated secondary compression index, C_{α} , were found to decrease essentially linearly as σ' increased from 103 kPa (15.0 psi) to 241 kPa (35.0 psi). Values of $R_{\alpha,\text{vert}}/R_{\alpha,\text{vol}}$ ($= C_{\alpha,\text{vert}}/C_{\alpha,\text{vol}}$) also tended to decrease approximately linearly with increasing σ' .

ACKNOWLEDGMENTS

Financial support for this study was provided by the U. S. National Science Foundation (NSF), Arlington, VA, under Grants CMS-0099430 entitled, "Membrane Behavior of

Clay Soil Barrier Materials" and CMS-0624104 entitled, "Enhanced Clay Membrane Barriers for Sustainable Waste Containment". The opinions expressed in this paper are solely those of the writers and are not necessarily consistent with the policies or opinions of the NSF.

3.6 REFERENCES

- Bouazza, A. 2002. Geosynthetic clay liners. *Geotextiles and Geomembranes*, 20(1), 3-17.
- Daniel, D.E. 1994. State-of-the-art: Laboratory hydraulic conductivity test for saturated soils. *Hydraulic Conductivity and Waste Contaminant Transport in Soil*, ASTM STP 1142, D.E Daniel and S.J. Trautwein, eds., ASTM, West Conshohoken, PA, 30-78.
- Daniel, D.E., Anderson, D.C., and Boynton, S.S. 1985. Fixed-wall versus flexible-wall permeameters. *Hydraulic Barriers in Soil and Rock*, ASTM STP 874, A. I. Johnson, R. K. Frobels, N. J. Cavalli, and C. B. Pettersson, eds., ASTM, West Conshohoken, PA, 107-126.
- Daniel, D.E., Bowders, J.J., and Gilbert, R.B. 1997. Laboratory hydraulic conductivity testing of GCLs in flexible-wall permeameters. *Testing and Acceptance Criteria for Geosynthetic Clay Liners*, ASTM STP 1308, L. Well, ed., ASTM, West Conshohocken, PA, 208-226.
- Fox, P. J. and Stark, T. D. 2004. State-of-the-art: GCL shear strength and its measurement. *Geosynthetics International*, 11(3), 141-175.
- Holtz, R.D. and Kovacs, W.D. 1981. *An Introduction to Geotechnical Engineering*, Prentice-Hall, Inc., Englewood Cliffs, New Jersey.

- Koerner, R. M. 2005. Geosynthetic Clay Liners, Chapter 6: *Designing with Geosynthetics*, 5th Ed., Pearson Prentice Hall, Upper Saddle River, New Jersey, USA 630-668.
- Lambe, T.W. and Whitman, R.V. 1969. *Soil Mechanics*. John Wiley and Sons, Inc., New York.
- MacKay, R.A. 1946. The control of impounding structures on ore deposition. *Economic Geology and the Bulletin of the Society of Economic Geologists*, The Economic Geology Publ. Co., New Haven, CT, Vol. 41, 13-46.
- Malusis, M.A. and Shackelford, C.D. 2002. Chemico-osmotic efficiency of a geosynthetic clay liner. *Journal of Geotechnical and Geoenvironmental Engineering*, 128(2), 97-106.
- Rowe, R.K. 2005. Long-term performance of contaminant barrier systems. *Géotechnique*, 55(9), 631-678.
- Shackelford, C.D. 2007. Selected issues affecting the use and performance of GCLs in waste containment applications. *21st Geotechnical Engineering Conference*, M. Manassero and A. Dominijanni, eds., Politecnico di Torino, Torino, Italy, Nov. 27-28, 2007, 1-45.
- Shackelford, C.D. and Lee, J.-M. 2003. The destructive role of diffusion on clay membrane behavior. *Clays and Clay Minerals*, 51(2), 186-196.
- Shackelford, C.D, Benson, C.H., Katsumi, T., Edil, T.B., and Lin, L. 2000. Evaluating the hydraulic conductivity of GCLs permeated with non-standard liquids. *Geotextiles and Geomembranes*, 18(2-4), 133-161.
- Shackelford, C.D., Malusis, M.A., and Olsen, H.W. 2003. Clay membrane behavior for

- geoenvironmental containment. *Soil and Rock America Conference 2003*, P. J. Culligan, H. H. Einstein, and A. J. Whittle, eds., Verlag Glückauf GMBH, Essen, Germany, Vol. 1, 767-774.
- Shan, H.-Y. 1993. *Stability of Final Covers Placed on Slopes Containing Geosynthetic Clay Liners*. Ph.D. Dissertation, University of Texas, Austin, Texas.
- Sridharan, A. and Nagaraj, H.B. 2000. Compressibility behaviour of remoulded, fine-grained soils and correlation with index properties. *Canadian Geotechnical Journal*, 37(3), 712-722.
- Terzaghi, K., Peck, R.B., and Mesri, G. 1996. *Soil Mechanics in Engineering Practice*, 3rd Edition. John Wiley & Sons, Inc., New York
- Yeo, S.-S. 2003. *Hydraulic Conductivity, Consolidation, and Membrane Behavior of Model Backfill-Slurry Mixtures for Vertical Cutoff Walls*. M.S. Thesis, Colorado State University, Fort Collins, Colorado.
- Yeo, S.-S., Shackelford, C. D., and Evans, J. C. 2005. Consolidation and hydraulic conductivity of nine model soil-bentonite backfills. *Journal of Geotechnical and Geoenvironmental Engineering*, 131(10), 1189-1198.

Table 3.1 – Sequence of stress conditions imposed on test specimens.

Stage No.	Testing Stage	Confining Stress, σ_c [kPa (psi)]	Applied Back Pressures, u_{bp} [kPa (psi)]		Effective Stress, $\sigma'^{(a)}$ [kPa (psi)]
			Top, $u_{bp,top}$	Bottom, $u_{bp,bottom}$	
1	Flushing	207 (30.0)	155 (22.5)	189 (27.5)	34.5 (5.0)
2	Consolidation	207 (30.0)	172 (25.0)	172 (25.0)	34.5 (5.0)
	Permeation	207 (30.0)	155 (22.5)	189 (27.5)	34.5 (5.0)
3	Consolidation	275 (40.0)	172 (25.0)	172 (25.0)	103 (15.0)
	Permeation	275 (40.0)	155 (22.5)	189 (27.5)	103 (15.0)
4	Consolidation	344 (50.0)	172 (25.0)	172 (25.0)	172 (25.0)
	Permeation	344 (50.0)	155 (22.5)	189 (27.5)	172 (25.0)
5	Consolidation	413 (60.0)	172 (25.0)	172 (25.0)	241 (35.0)
	Permeation	413 (60.0)	155 (22.5)	189 (27.5)	241 (35.0)

^(a) Final effective stress at the end of consolidation and average effective stress during permeation.

Table 3.2. Summary of measured hydraulic conductivity and coefficient of consolidation values for two specimens of a geosynthetic clay liner (GCL).

Testing Stage	Effective Stress, σ' ^(a) [kPa (psi)]	Measured Hydraulic Conductivity, k_{measured} (10^{-9} cm/s)		Coefficient of Consolidation, c_v (10^{-9} m ² /s)							
		GCL1	GCL2	Casagrande Method			Taylor Method				
				Vertical Strain	Volumetric Strain		Vertical Strain	Volumetric Strain			
Flushing	34.5 (5.0)	2.7	3.3	-----	-----	-----	-----	-----	-----	-----	-----
		3.3	5.0	-----	-----	-----	-----	-----	-----	-----	-----
Consolidation/ Permeation	103 (15.0)	1.3	2.2	1.4	1.5	1.8	2.1	1.2	1.6	1.6	1.8
		172 (25.0)	0.76	1.4	1.1	1.3	1.6	1.8	1.0	1.4	1.3
	241 (35.0)	0.50	0.64	0.52	1.0	0.96	1.3	0.69	1.3	1.2	1.4

^(a) Final effective stress at the end of consolidation and average effective stress during permeation.

Table 3.3. Values for the secondary compression ratio (R_{α}) and secondary compression index (C_{α}) based on both vertical and volumetric strains for two specimens of a geosynthetic clay liner (GCL) consolidated under isotropic conditions.

Effective Stress, σ' [kPa (psi)]	$R_{\alpha} (10^{-2})$				$C_{\alpha} (10^{-2})$			
	Vertical Strain, $R_{\alpha,vert}$		Volumetric Strain, $R_{\alpha,vol}$		Vertical Strain, $C_{\alpha,vert}$		Volumetric Strain, $C_{\alpha,vol}$	
	GCL1	GCL2	GCL1	GCL2	GCL1	GCL2	GCL1	GCL2
103 (15.0)	1.3	1.5	1.2	1.3	7.4	8.6	7.0	7.4
172 (25.0)	0.91	0.95	0.87	0.99	5.2	5.3	5.0	5.6
241 (35.0)	0.45	0.61	0.63	0.68	2.6	3.4	3.6	3.8

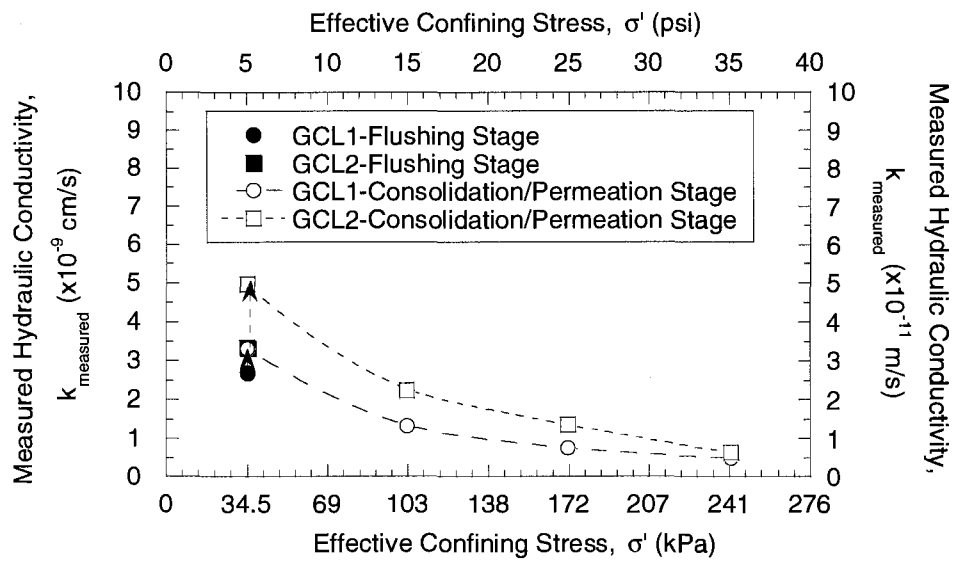


Fig. 3.1 – Measured hydraulic conductivity versus effective confining stress for two specimens of a geosynthetic clay liner (GCL) permeated with de-ionized water.

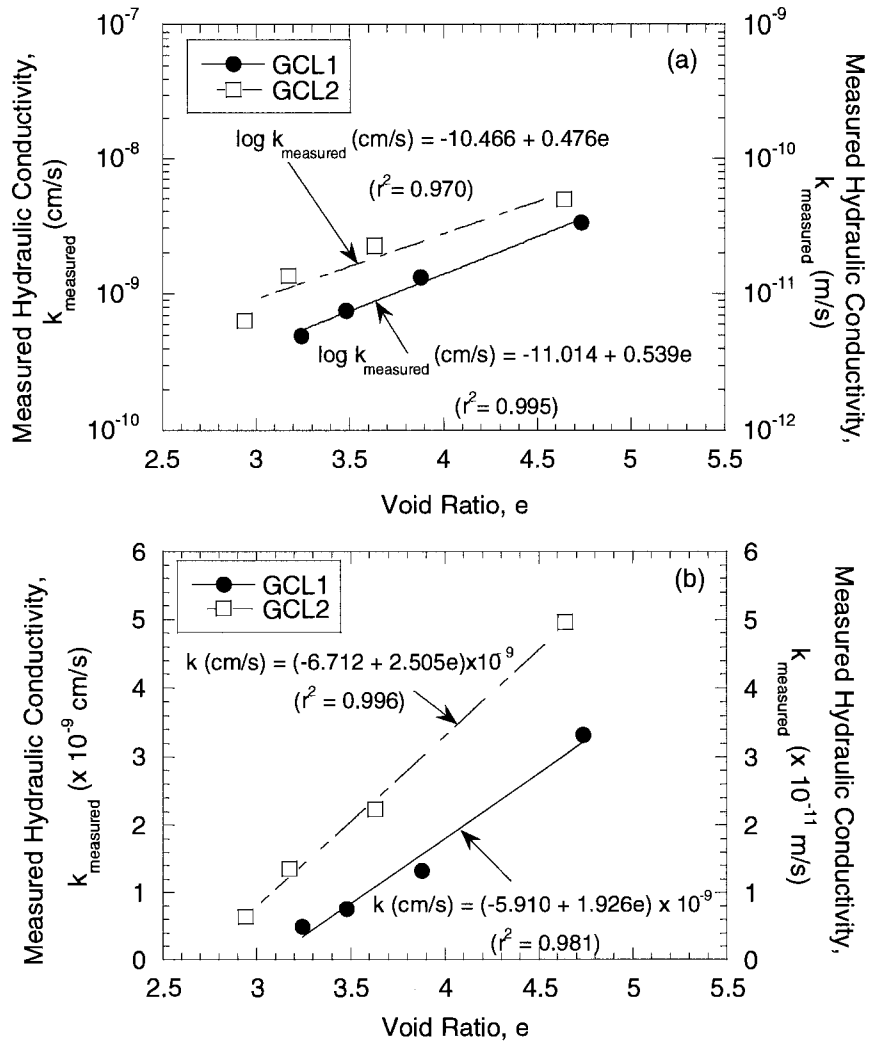


Fig. 3.2 – Measured hydraulic conductivity versus void ratio for two specimens of a geosynthetic clay liner (GCL) permeated with de-ionized water during consolidation/permeation stage of testing: (a) logarithmic k_{measured} ; (b) arithmetic k_{measured} .

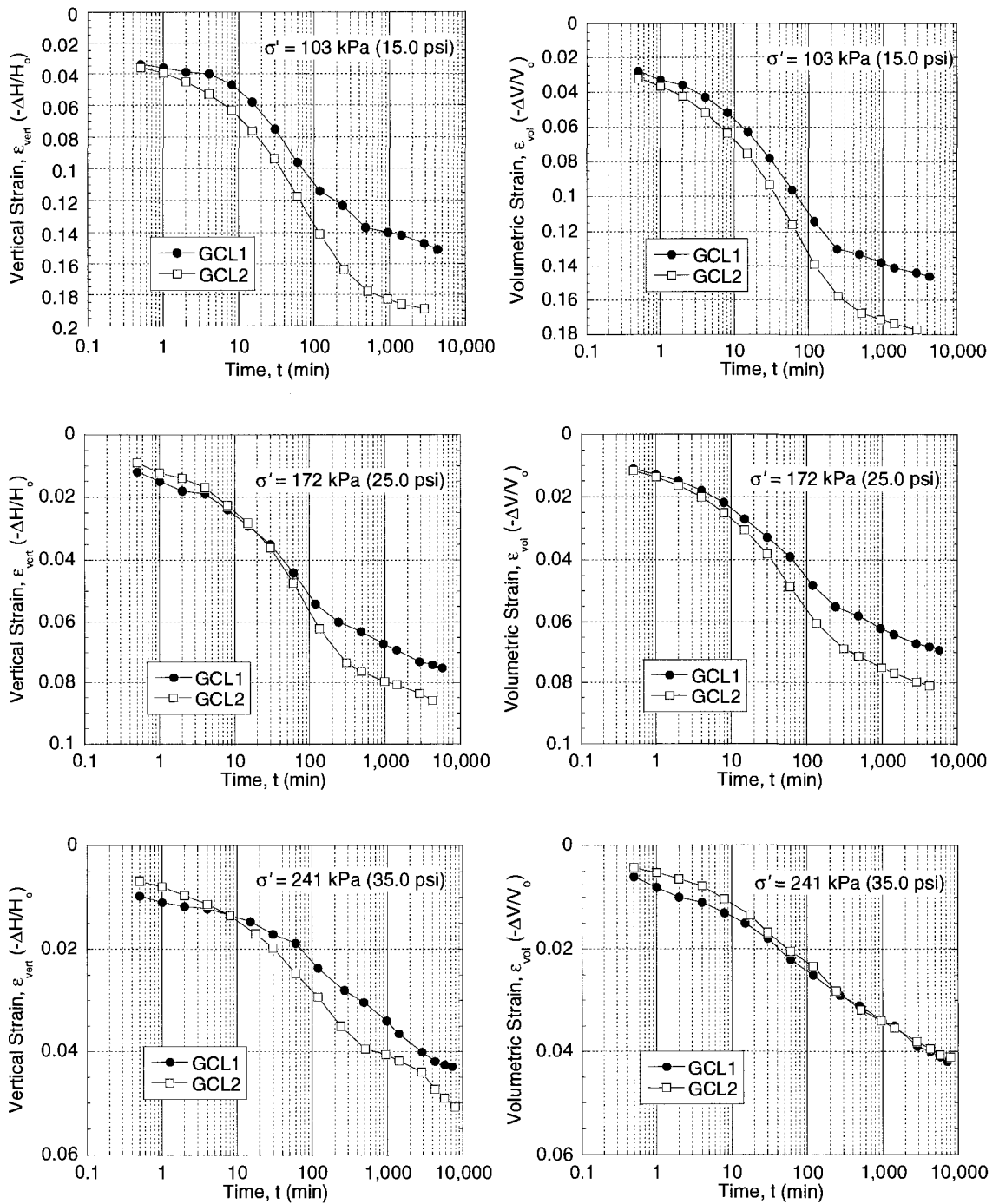


Fig. 3.3 – Vertical (left) and volumetric (right) strain versus logarithm of time for consolidation of two specimens of a geosynthetic clay liner (GCL).

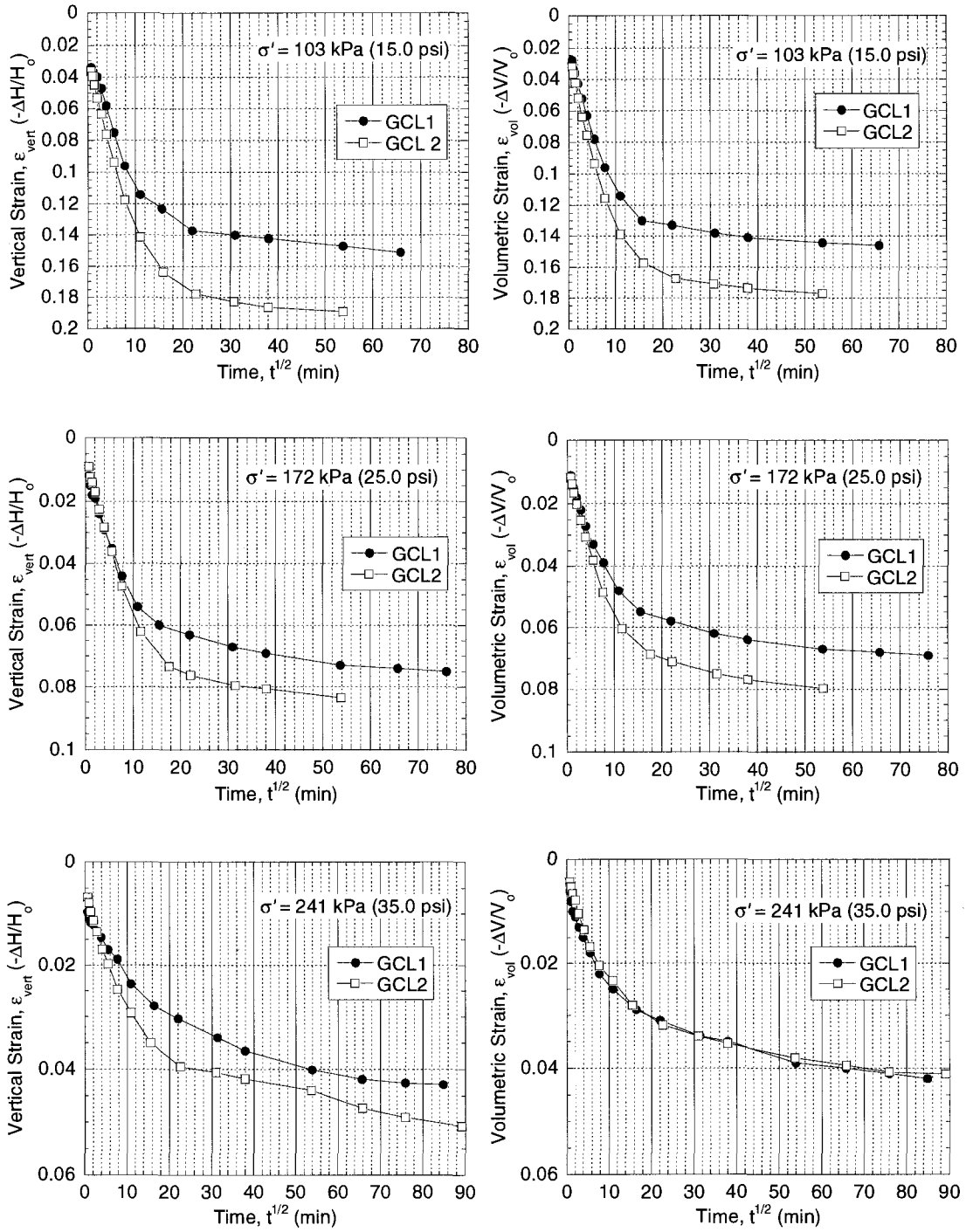


Fig. 3.4 – Vertical (left) and volumetric (right) strain versus square root of time for consolidation of two specimens of a geosynthetic clay liner (GCL).

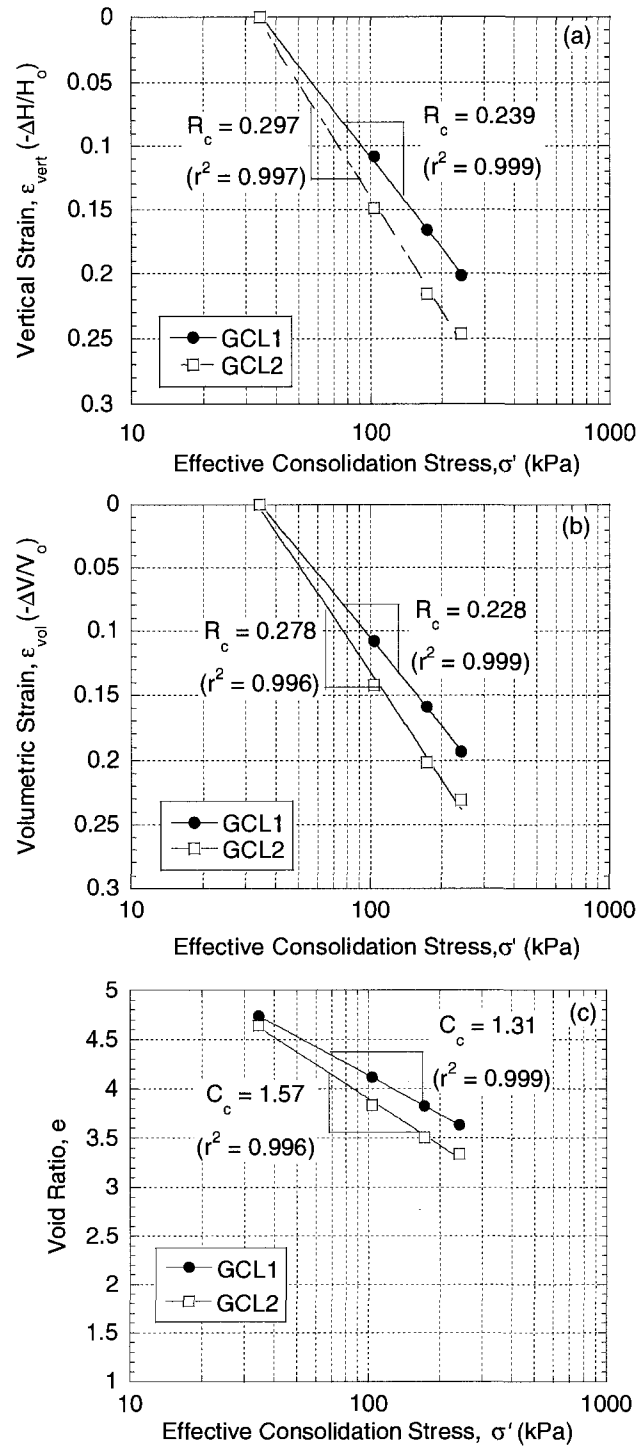


Fig. 3.5 – Consolidation test data based on (a) vertical strain, (b) volumetric strain, and (c) void ratio versus effective consolidation stress for two specimens of a geosynthetic clay liner (GCL).

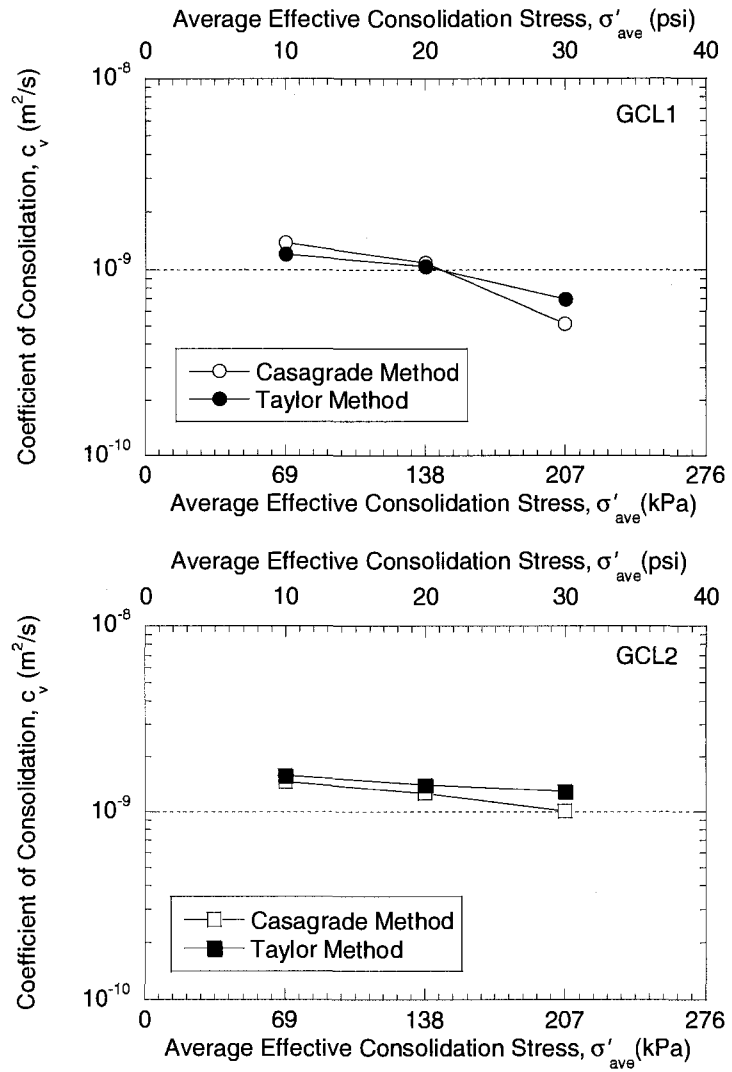


Fig. 3.6 – Coefficients of consolidation based on vertical strain for two specimens of a geosynthetic clay liner (GCL) as function of average effective consolidation stress.

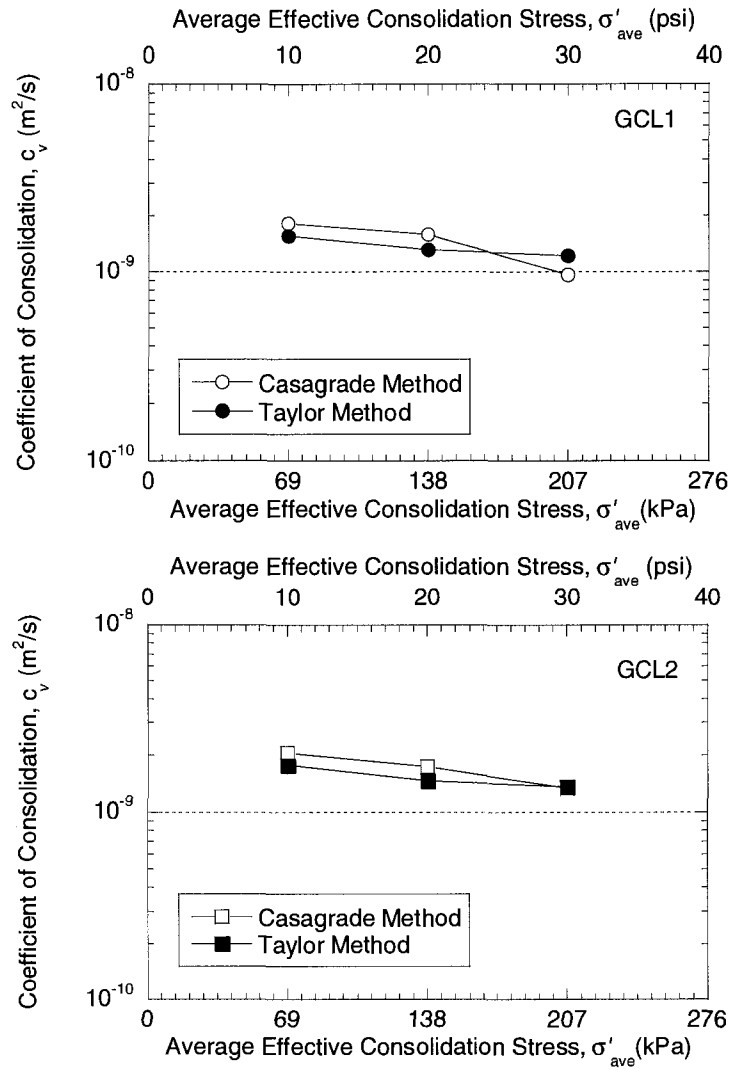


Fig. 3.7 – Coefficients of consolidation based on volumetric strain for two specimens of a geosynthetic clay liner (GCL) as function of average effective consolidation stress.

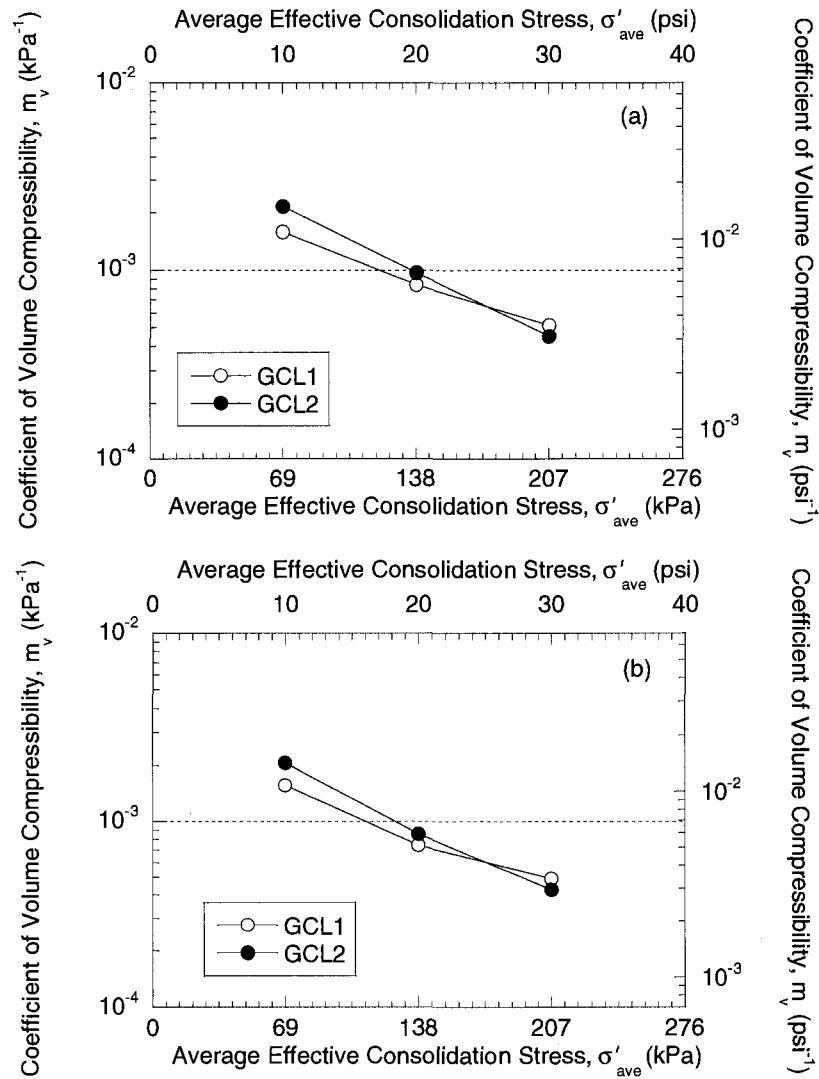


Fig. 3.8 – Coefficients of volume compressibility based on (a) vertical strain and (b) volumetric strain for two specimens of a geosynthetic clay liner (GCL) as function of average effective consolidation stress.

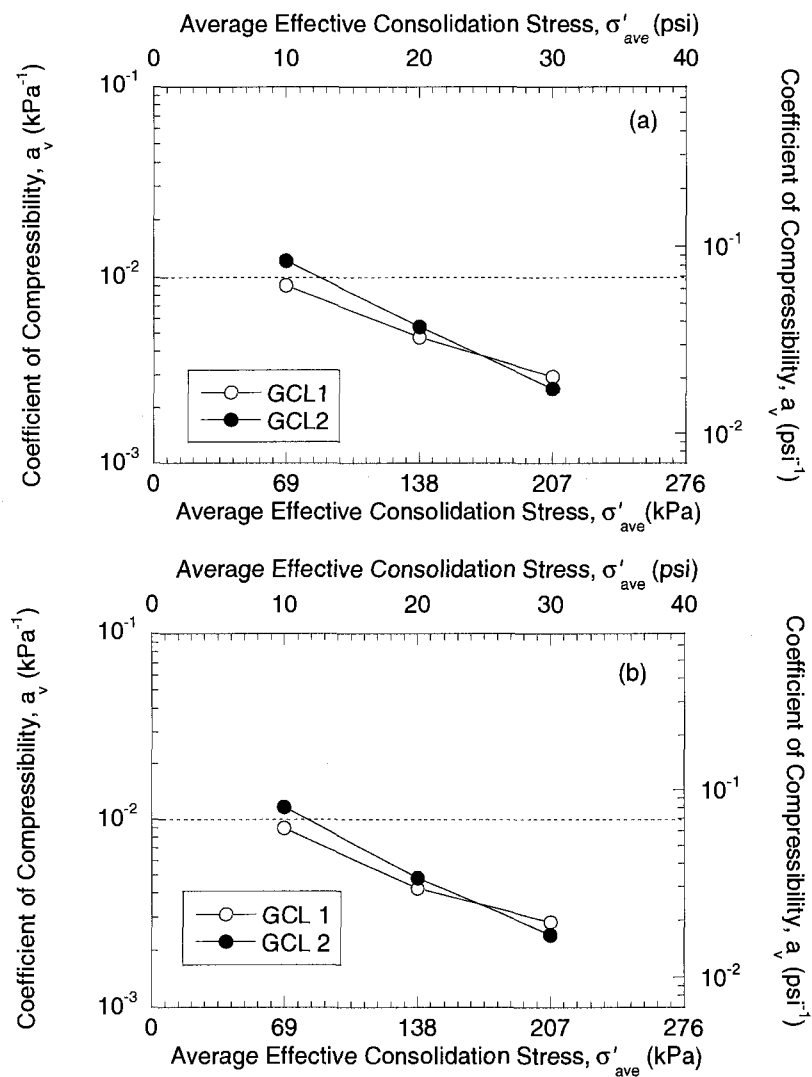


Fig. 3.9 – Coefficients of compressibility based on (a) vertical strain and (b) volumetric strain for two specimens of a geosynthetic clay liner (GCL) as function of average effective consolidation stress.

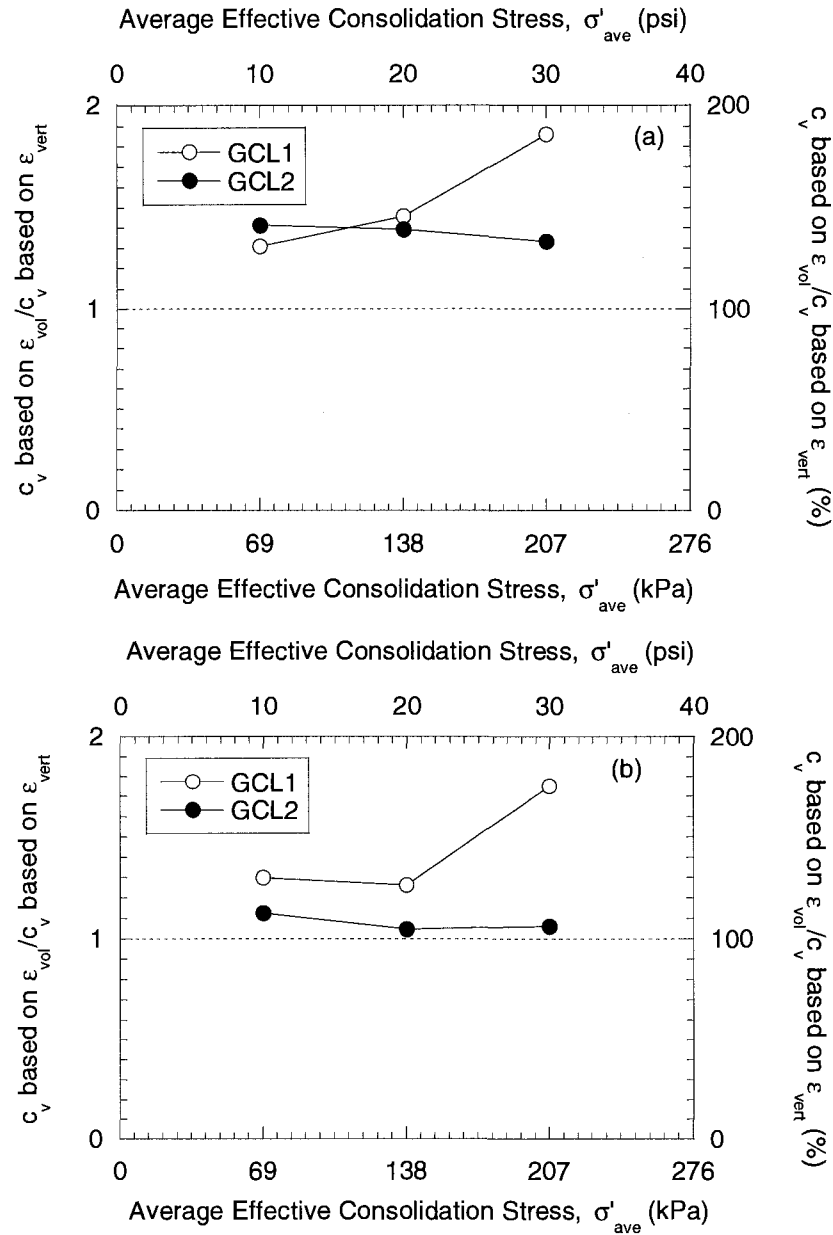


Fig. 3.10 – Effect of type of strain on the coefficients of consolidation, c_v , based on (a) Casagrande method and (b) Taylor method for two specimens of a geosynthetic clay liner (GCL) as function of average effective consolidation stress.

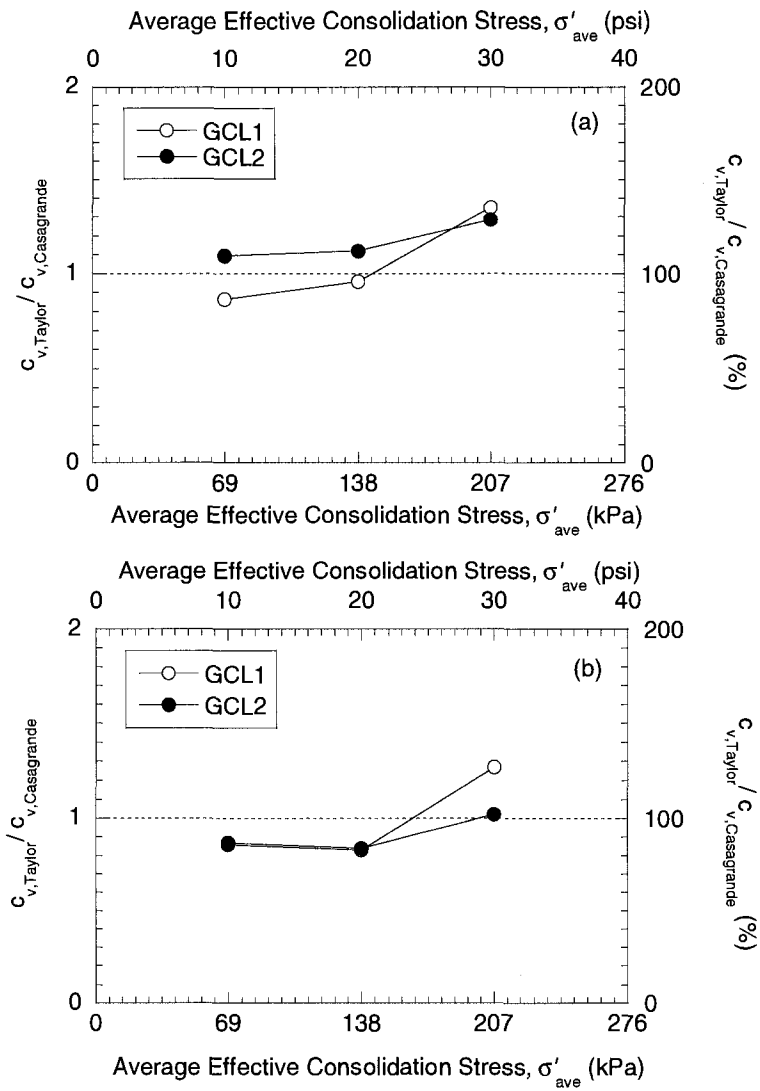


Fig. 3.11 – Effect of method of analysis on the coefficients of consolidation, c_v , based on (a) vertical strain and (b) volumetric strain for two specimens of a geosynthetic clay liner (GCL) as function of average effective consolidation stress.

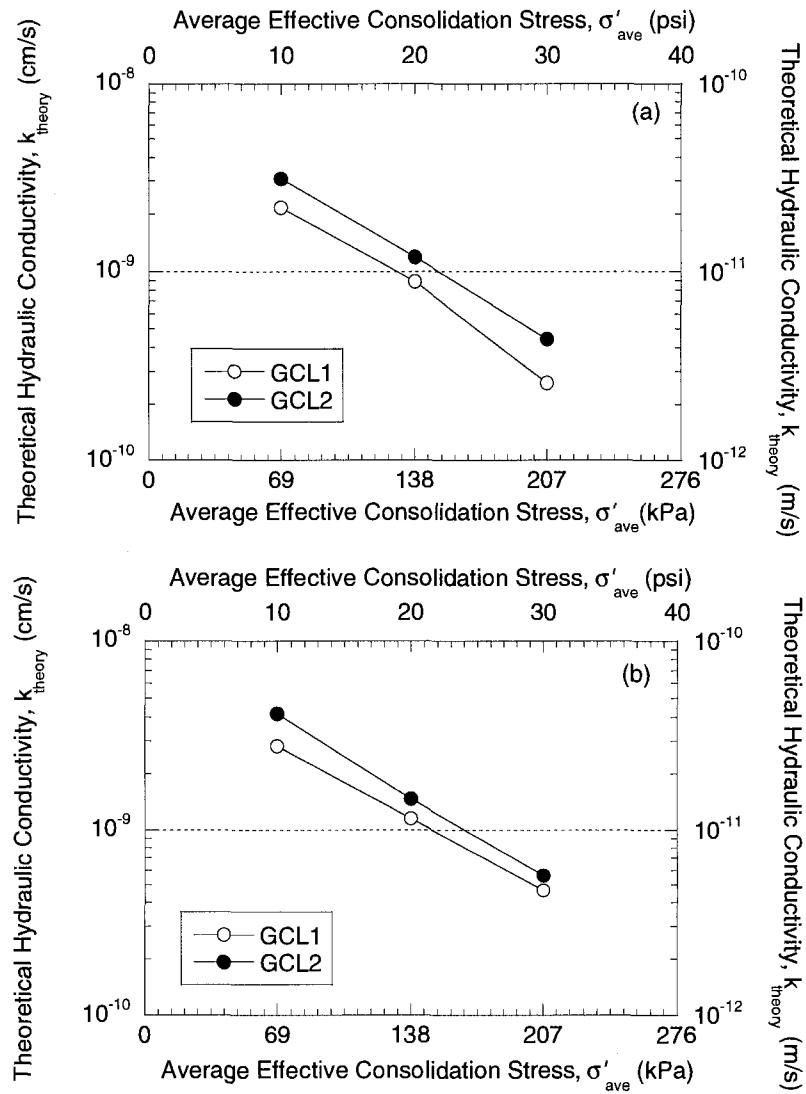


Fig. 3.12 – Theoretical hydraulic conductivity versus average effective stress based on c_v by Casagrande method and m_v by (a) vertical strain and (b) volumetric strain for two specimens of a geosynthetic clay liner (GCL).

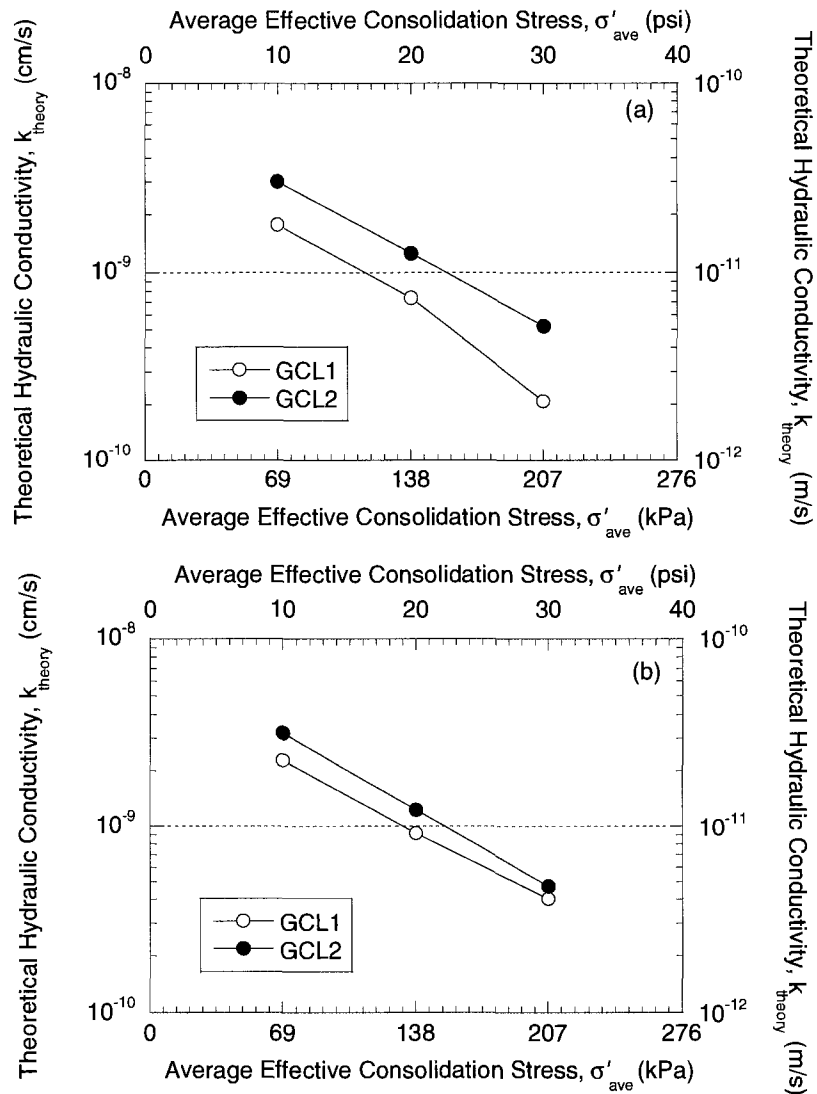


Fig. 3.13 – Theoretical hydraulic conductivity versus average effective stress based on c_v by Taylor method and m_v by (a) vertical strain and (b) volumetric strain for two specimens of a geosynthetic clay liner (GCL).

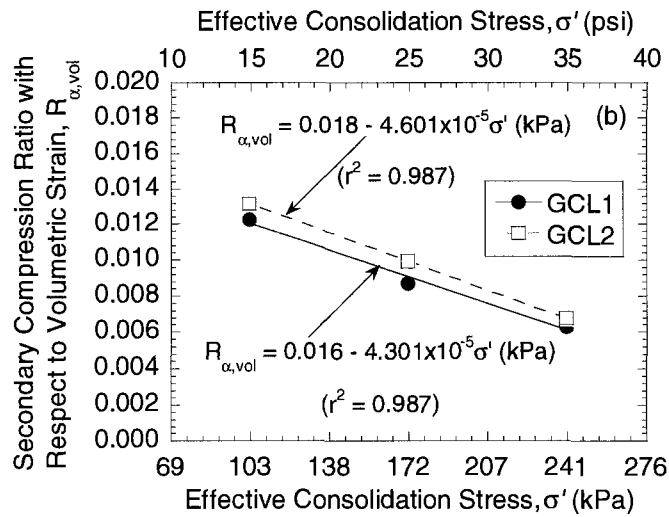
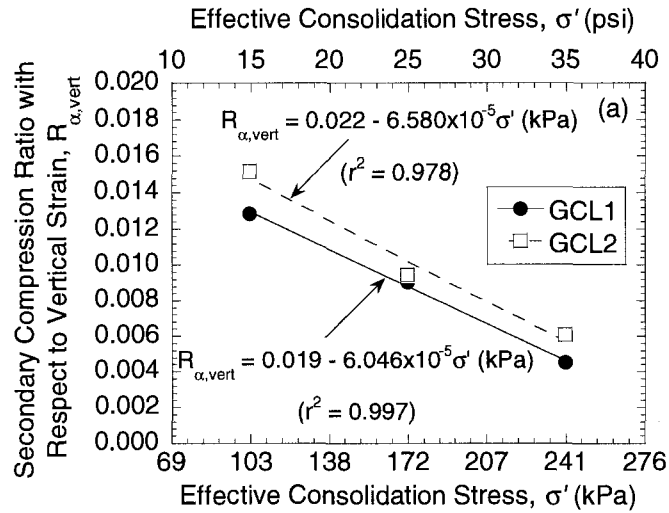


Fig. 3.14 – Secondary compression ratio based on (a) vertical strain and (b) volumetric strain versus effective consolidation stress for two specimens of a geosynthetic clay liner (GCL).

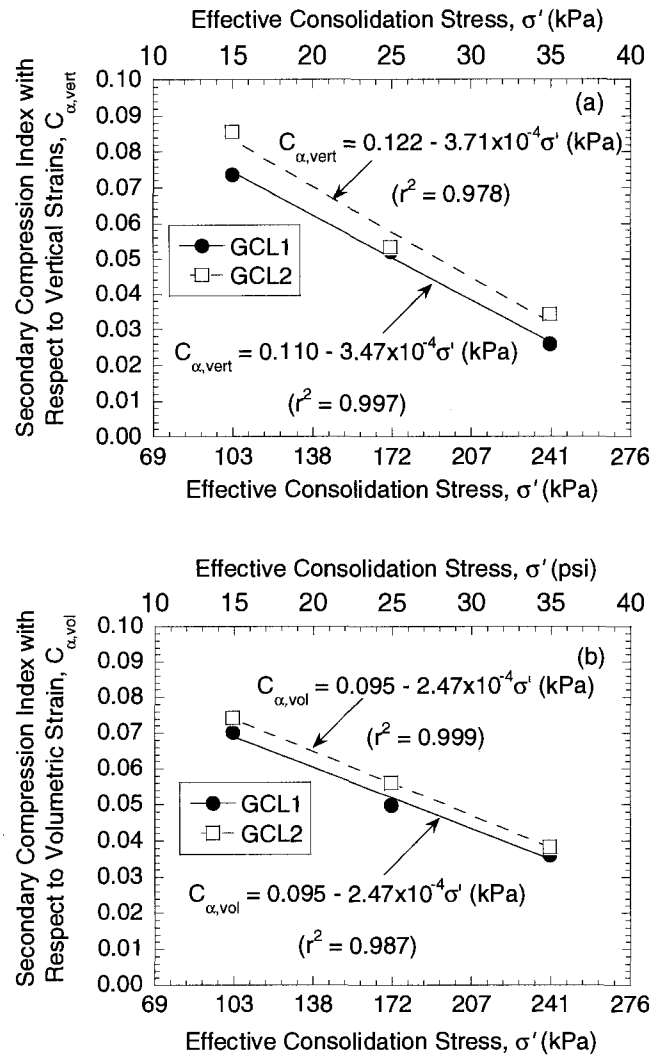


Fig. 3.15 – Secondary compression index based on (a) vertical strain and (b) volumetric strain versus effective consolidation stress for two specimens of a geosynthetic clay liner (GCL).

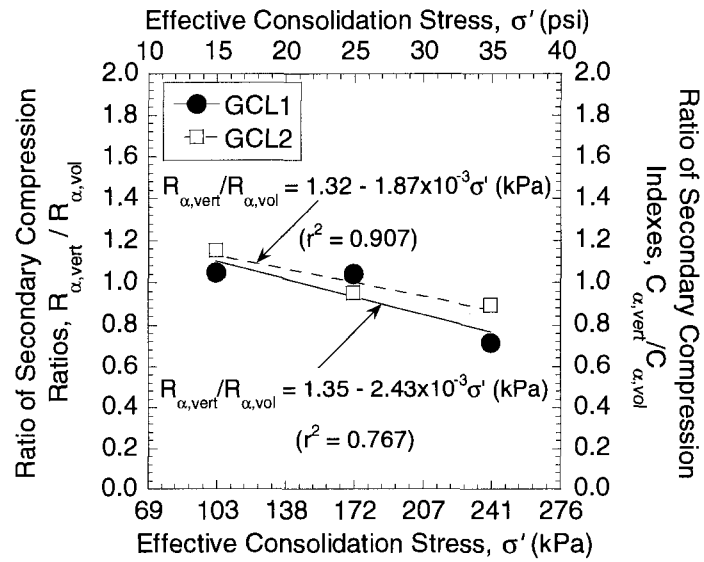


Fig. 3.16 – Ratio of secondary compression ratio and index based on vertical strain relative to that based on volumetric strain versus effective consolidation stress for two specimens of a geosynthetic clay liner (GCL).

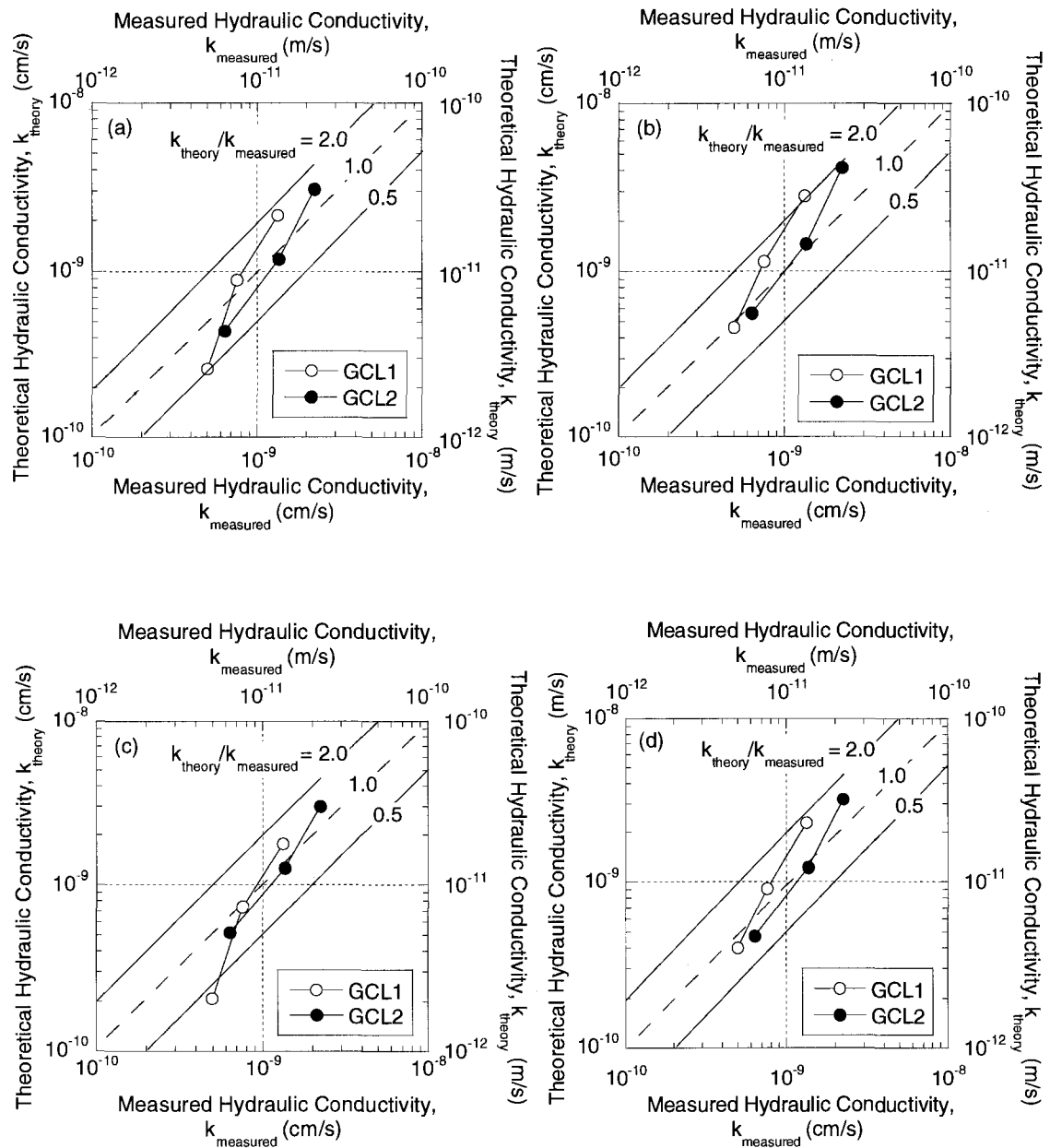


Fig. 3.17 – Measured hydraulic conductivity versus theoretical hydraulic conductivity for two specimens of a geosynthetic clay liner (GCL) permeated with de-ionized water: (a) c_v by Casagrande method and m_v by vertical strain; (b) c_v by Casagrande method and m_v by volumetric strain; (c) c_v by Taylor method and m_v by vertical strain; (d) c_v by Taylor method and m_v by volumetric strain.

CHAPTER 4

CLAY MEMBRANE TESTING USING A FLEXIBLE-WALL CELL UNDER CLOSED-SYSTEM BOUNDARY CONDITIONS

ABSTRACT: Membrane behavior represents the ability of porous media to restrict the migration of solutes, leading to the existence of chemico-osmosis, or the flow of liquid in response to a chemical concentration gradient. Membrane behavior is an important consideration with respect to clay soils with small pores and interactive electric diffuse double layers associated with individual particles, such as bentonite. The results of recent studies indicate the existence of membrane behavior in bentonite-based hydraulic barriers used in waste containment applications. Thus, measurement of the existence and magnitude of membrane behavior in such clay soils is becoming increasingly important. In this regard, the development and evaluation of a flexible-wall cell used to measure the membrane behavior of clay soils under closed-system boundary conditions is described. The advantages of a flexible-wall cell include complete control over the state of stress existing within the test specimen and the ability to back-pressure saturate and consolidate the specimen prior to membrane testing. Use of the developed flexible-wall cell is illustrated via tests conducted to measure the membrane behavior of a geosynthetic clay liner (GCL), a manufactured hydraulic barrier containing sodium bentonite. The results indicate that the membrane efficiencies of duplicate specimens of the GCL measured using the flexible-wall cell are both reproducible and similar to, but somewhat lower than, those previously reported for the same GCL using a rigid-wall cell under the same

closed-system boundary conditions.

4.1 INTRODUCTION

Membrane behavior in soils refers to the restricted migration of solutes through the soil resulting in the buildup of solute concentration at the influent side of the soil such that a concentration difference across the soil is developed. The existence of the concentration difference resulting from membrane behavior leads to a concentration gradient that drives two processes, viz., flow of the solvent (e.g., water) via chemico-osmosis in a direction from low solute concentration (high water activity) to high solute concentration (low water activity), and solute diffusion in a direction from high solute concentration to low solute concentration. In the case where all the solutes are inhibited from migration corresponding to perfect or ideal membrane behavior, all solute diffusion is prevented, but the chemico-osmotic flow of the solvent in response to the concentration gradient can still occur. For this reason, soils that exhibit membrane behavior are often referred to as semi-permeable membranes, because such soils are permeable to the solvent regardless of the degree of solute restriction. However, because the pores in soils are distributed over a range of sizes, most naturally occurring soil membranes are non-ideal or imperfect. As a result, both chemico-osmosis and diffusion occur simultaneously in most soil membranes, although the diffusion process becomes increasingly more restricted as the level or degree of solute restriction increases (Malusis and Shackelford 2002a).

Restriction of solutes from migration occurs when the pores of the soil are small relative to the size of the migrating solutes. Because the sizes of the pores required to

restrict solute migration are necessarily small, membrane behavior typically is observed in soils that are dominated with clay-sized particles, such that soils exhibiting membrane behavior are often referred to as clay membranes. In addition to particle size, the mineralogy of the soil also can play an important role in determining the existence and extent of membrane behavior. In particular, membrane behavior tends to be more prevalent in soils whose behavior is dominated by the existence of high swelling, active clay minerals, such as the sodium smectites (e.g., sodium montmorillonite) (Kemper and Rollins 1966, Fritz and Marine 1983, Fritz 1986, Olsen et al. 1990, Shackelford et al. 2003).

Interest in clay membrane behavior historically has been focused primarily in the soil and geological sciences. Studies in soil science have focused on the migration of nutrients to plant roots (e.g., Kemper 1960, 1961, Kemper and Evans 1963, Kemper and Quirk 1972), whereas studies in the geological sciences have focused on the ability of natural clay formations, such as aquitards and aquicludes, to exhibit membrane behavior (MacKay 1946, Olsen 1972, Hanshaw 1972, Greenberg et al. 1973, Marine 1974, Marine and Fritz 1981, Fritz 1986, Neuzil 1986, 2000, Cey et al. 2001, Soler 2001, Hart and Whitworth 2005). The results of relatively recent research also have indicated that membrane behavior can be substantial in bentonite-based barriers used for hydraulic containment applications (Malusis 2001, Shackelford et al. 2003, Malusis et al. 2001a, 2003, Malusis and Shackelford 2002a,b, Yeo 2003, Yeo et al. 2005, Derrington et al. 2006, Henning et al. 2006, Evans et al. 2008).

As a result of the above considerations, interest has increased recently in the ability to measure membrane behavior in clays, in general, and clays used in engineered

barriers for hydraulic containment applications, in particular. Accordingly, the purpose of this paper is to present the development and evaluation of a flexible-wall cell in a closed (no-flow) system that can be used to measure the membrane behavior of clays.

4.2 BACKGROUND

4.2.1 Boundary Conditions

When measuring the membrane behavior of clays in the laboratory, two considerations are paramount, viz. the boundary conditions to be imposed during testing, and the type of cell to be used for the test specimen. In terms of boundary conditions, measurement of membrane behavior can be conducted using either open or closed systems. For open systems, two approaches have commonly been employed. The first approach, which has been far more common, involves forcing a salt solution through the clay under an applied hydraulic pressure difference (hydraulic gradient) and determining how much of the salt has been filtered out of solution (referred to as filtrate) by the clay due to membrane behavior (e.g., McKelvey et al. 1957, McKelvey and Milne 1962, Kemper 1960, Kharaka and Berry 1973, Hanshaw and Coplen 1973, Kharaka and Smalley 1976, Fritz and Marine 1983, Whitworth and Fritz 1994, Ishiguro et al. 1995, Hart and Whitworth 2005, Derrington et al. 2006). This type of test often is referred to as a filtration, hyperfiltration, or ultrafiltration test.

The second, less common open-system approach involves determining the membrane efficiency from the measured amount of chemico-osmotic flow (Kemper 1961, Kemper and Evans 1963, Kemper and Rollins 1966, Kemper and Quirk 1972, Keijzer et al. 1997, 1999, Keijzer and Loch 2001). This approach probably has been less common

because of the greater difficulty in accurately measuring the small quantities of flow that typically result. This difficulty has been overcome to some extent via the use of flow-pump (syringe) systems that depend on measurement of potential differences using transducers during forced passage of small liquid fluxes through specimens via mechanical drive mechanisms (e.g., Olsen 1969, 1972).

In contrast, for membrane testing involving a closed system, liquid flow through the test specimen is prevented from occurring (Elrick et al 1976, Malusis et al. 2001b, Malusis and Shackelford 2002a,b, Shackelford and Lee 2003, Yeo et al. 2005, Henning et al. 2006). As a result of preventing solution flow, a chemico-osmotic pressure difference develops across the specimen to counteract the tendency for chemico-osmotic flow, and the membrane efficiency is determined based on the measured magnitude of the pressure buildup and the salt concentrations at the boundaries. In this regard, differences in test results can occur depending on how well the salt concentrations at the boundaries are maintained constant during the test (e.g., Malusis et al. 2001b, Shackelford and Lee 2003).

4.2.2 Types of Cells

The types of cells that have been used for clay membrane testing can be classified broadly into two categories, viz., rigid-wall (fixed-wall) cells and flexible-wall or triaxial cells. The primary difference between the two types of cells is that the volume of the test specimen is controlled during testing in rigid-wall cells, whereas the state of stress on the specimen is controlled in flexible-wall (triaxial) cells. The advantages and disadvantages of each type of cell in terms of hydraulic conductivity testing were identified by Daniel et al. (1985).

For rigid-wall cells used as permeameters, Daniel et al. (1985) identified the major advantages as lower cost, simplicity, greater adaptability to testing compacted soils, compatibility with a wide range of chemicals used as permeant liquids, and the lack of need to apply high confining pressures. The major disadvantages of rigid-wall cells were identified by Daniel et al. (1985) as incomplete control over imposed stress conditions, inability to measure deformations in most fixed-wall cells, difficulty in trimming soil samples into the containing ring, and the potential for side-wall leakage.

For flexible-wall cells used as permeameters, Daniel et al. (1985) identified the advantages as minimization of side-wall leakage, control over vertical and horizontal stresses, measurement of vertical and horizontal deformations, ability to back-pressure saturate soil specimens prior to testing, and adaptability to testing undisturbed soil samples recovered from field borings. Disadvantages of flexible-wall cells included higher cost, compatibility problems between the flexible confining membrane and some chemical solutions used as permeant liquids, and the need to apply significant confining pressures when testing soil specimens under high hydraulic gradients.

Although both rigid-wall and flexible-wall cells have been used extensively for hydraulic conductivity testing (e.g., Daniel 1994), only a few studies have employed the use of flexible-wall cells for membrane testing of clays (e.g., Keijzer et al. 1997, 1999, Keijzer and Lock 2001, Heister et al. 2004, 2005, Rahman et al. 2005). In the majority of these studies (e.g., Keijzer et al. 1997, 1999, Keijzer and Lock 2001, and Heister et al. 2004, 2005), open-system boundary conditions were imposed using the same hydraulic control apparatus, whereas in the study by Rahman et al. (2005), the system used to control the boundary conditions is not adequately described. To the authors' knowledge,

no study has reported the use of a flexible-wall cell in conjunction with closed-system boundary conditions. Such an apparatus offers the advantages of a flexible-wall cell, principally the ability to control the state of stress in the soil specimen, with the advantage of precise and accurate measurement of chemico-osmotic pressure buildup offered by a closed system (e.g., Malusis et al. 2001b). Thus, the objective of this study was to develop and evaluate a flexible-wall testing apparatus consisting of a flexible-wall cell and a hydraulic control system that imposes closed-system boundary conditions for measurement of the membrane behavior of clay soils. The evaluation was based primarily on the results of duplicate tests to measure the membrane behavior of a geosynthetic clay liner (GCL), a manufactured hydraulic barrier containing sodium bentonite.

4.3 DESCRIPTIONS OF TESTING APPARATUS AND PROCEDURES

4.3.1 Testing Apparatus

The flexible-wall cell developed in this study and the associated hydraulic control system are shown schematically in Fig. 4.1, and photographs of the flexible-wall cell and the complete testing apparatus are shown in Fig. 4.2. The hydraulic control system is essentially the same as that described in detail by Malusis et al. (2001b) except for three primary differences. First, the syringe/actuator flow pump and associated hydraulic system for control of the boundary conditions is connected to a flexible-wall cell as opposed to the rigid-wall cell used by Malusis et al. (2001b). Second, two in-line pressure transducers (Model PX181-100G5V, OMEGA, Stamford, Connecticut), designated as T1 and T2 in Fig. 4.1, are installed on either side of the differential pressure transducer (Model DP15, Validyne Engineering Sales Corp., Northridge, California), designated as

T3 in Fig. 4.1, used to measure the chemico-osmotic pressure difference, ΔP , to provide an independent measurement of the liquid pressure at the top (u_{top}) and the bottom (u_{bottom}) of the specimen, respectively, as well as an independent check of the chemico-osmotic pressure difference, $-\Delta P (= u_{\text{top}} - u_{\text{bottom}})$. Note that, since the positive x -direction is assumed downward from the top of the specimen, $-\Delta P > 0$ and $u_{\text{top}} > u_{\text{bottom}}$. Third, the cell-water accumulator (designated as CWA in Fig. 4.1) is included to provide an air-water interface for (1) filling the chamber (annulus space between the soil specimen and the cylindrical cell) with water, (2) measuring specimen volume change (i.e., changes in water level), and (3) applying the cell or confining pressure to the specimen via connection with a controlled source of air pressure (air compressor). Back pressure is controlled through lines connected to the refilling and sampling reservoirs to a similar controlled source of air pressure. The effective stress at the boundaries of a saturated soil specimen is represented by the difference between the total stress applied as the cell (confining) stress, σ_c , and the boundary water pressures (u_{top} and u_{bottom}) as measured by in-line transducers T1 and T2 (Fig. 4.1).

The flexible-wall cell consists of a clear, plastic (acrylic), cylindrical cell that is held together between top and bottom plates by four threaded tie rods at 90 degree spacings. O-rings contained within grooved cavities machined into the top and bottom plates together with vacuum grease provide water tight seals between the top and bottom plates and the cylindrical cell.

Prior to connecting the cylindrical cell to the top and bottom plates, the soil specimen is placed on top of a base pedestal that contains a porous plastic (acrylic) disk (1/8-in thick, 10 μm pore size, GenPore®, Reading, Pennsylvania) and is fastened to the

bottom plate with screws. Filter paper (Whatman No. 2) is placed between the pedestal and the soil specimen to keep the porous disk from clogging with soil particles. A soil specimen with a maximum diameter of 102 mm and maximum thickness of 100 mm can be tested with the current system, although smaller sized specimens also are possible by using smaller diameter top caps and bottom pedestals and/or thinner specimen thicknesses. After placing the soil specimen on the base pedestal, filter paper and a plastic top cap containing a porous plastic disk are placed on top of the specimen. The sides of the bottom pedestal and top cap are coated with a thin film of vacuum grease, and a standard elastic or flexible (polymer) membrane (e.g., see Daniel et al. 1984) is stretched over the bottom pedestal, soil specimen and top cap to isolate the soil specimen from the annulus space between the specimen and the outer cylindrical cell walls. O-rings then are applied around the stretched flexible membrane to provide a water-tight seal between the membrane and the base pedestal and top cap. The chamber then can be filled with de-aired water via the cell-water accumulator (CWA) and pressurized up to a maximum pressure 689 kPa (100 psi) to ensure intimate contact between the membrane and soil specimen and to apply a desired confining (total) stress.

The top cap and base pedestal also are equipped with ports that enable drainage of water from the soil specimen during consolidation, permeation of water through the specimen, and/or circulation of separate electrolyte solutions through the porous disks at the specimen boundaries as described by Malusis et al. (2001b) to establish and maintain a constant concentration difference (ΔC) across the specimen. Additional ports are installed in the top cap and base pedestal to allow for measurement of the pressure difference across the specimen via the differential pressure transducer, T3 (Fig. 4.1).

Consolidation can be induced with or without back-pressure by applying an elevated cell (confining) stress via the CWA, opening valve 5 that connects the CWA to the water-filled chamber of the cell, and opening valves 1-4 such that water drains from the specimen into the sampling/refilling reservoirs. Permeation can be induced by increasing and/or decreasing applied back pressures (with the appropriate valves being opened) to induce liquid flow upward or downward through the specimen as desired. For permeation, care must be taken to ensure that the back pressure does not exceed the cell (confining) stress for fear of blowing out the flexible membrane (see Daniel et al. 1984).

For membrane testing, electrolyte solutions are circulated continuously through the porous disks at the ends of the specimen using the flow-pump system described by Malusis et al. (2001b). This system includes a dual-carriage syringe pump (Model 944, Harvard Apparatus, South Natick, MA) equipped with two customized actuators (i.e., syringes) as shown in Fig. 4.2. In this case, valves 1 and 2 are open while valves 3 and 4 connecting the sampling and refilling reservoirs to the syringe/actuators are closed, such that the top and bottom circulation systems represent closed circuit loops (see Fig. 4.1).

In general, solutions containing initial concentrations of a given electrolyte (designated as C_{ot} and C_{ob} in Fig. 4.1) are expelled from each of the two syringes/actuators at the same, constant rate via the plunger that is attached to the flow-pump drive (Fig. 4.2), and subsequently are infused through the porous disks across the top and bottom boundaries of the specimen. Circulation outflow from the boundaries (designated as C_t and C_b in Fig. 4.1) is simultaneously collected at the same rate in order to maintain a constant volume inside the testing cell (i.e., $\Delta V_{cell} = 0$) and prevent liquid flux through the soil.

Typically, the initial electrolyte (salt) concentration circulated through the top boundary is controlled to be greater than that circulated through the bottom barrier (i.e., $C_{ot} > C_{ob}$) to establish the initial concentration difference, $-\Delta C_o (= C_{ot} - C_{ob})$ across the test specimen, although the reverse situation (i.e., $C_{ot} < C_{ob}$) is also possible. However, in the case of imperfect soil membranes, such that solutes are able to migrate through some soil pores, solute diffusion also occurs simultaneously in response to this concentration difference (Malusis et al. 2001b). In the case where $C_{ot} > C_{ob}$, solute diffusion occurs from the top to the bottom of the specimen, such that $C_t < C_{ot}$ and $C_b \geq C_{ob}$ (see Malusis et al. 2001b)

4.3.2 Calculation of Membrane Efficiency

As previously described, the volume of liquid infused into either end of the testing cell is equal to the volume of liquid withdrawn during circulation such that no flux of liquid can enter or exit the specimen boundaries during the test. Also, all actuator parts, fittings, valves, and tubing are constructed with grade 316 stainless steel to minimize volume change in the system (see Fig. 4.2 and Malusis et al. 2001b). As a result, the volume change occurring in the circulation systems during membrane testing should be nil (i.e., $\Delta V_{\text{circulation}} = 0$). In addition, in the case where the soil specimen is saturated with water prior to membrane testing, the total volume of the specimen cannot change during the test (i.e., $\Delta V_{\text{specimen}} = 0$). This situation is analogous to triaxial shear testing of saturated soil specimens under undrained conditions. Thus, for practical purposes, the entire testing apparatus represents a closed system during membrane testing (i.e., $\Delta V_{\text{cell}} = \Delta V_{\text{circulation}} + \Delta V_{\text{specimen}} = 0$). Finally, electrical current is not applied across the specimen,

and the non-conductive materials used in the construction of the cell prevent short circuiting of the specimen.

Under these conditions, the membrane efficiency, ω , is defined as follows (Groenevelt and Elrick 1976, Malusis et al. 2001b):

$$\omega = \frac{\Delta P}{\Delta \pi} \Big|_{\Delta V=0} \quad (4.1)$$

where ΔP (<0) is the measured chemico-osmotic pressure difference induced across the specimen as a result of prohibiting chemico-osmotic flux of solution, and $\Delta \pi$ (<0) is the theoretical chemico-osmotic pressure difference across an "ideal" semi-permeable membrane (i.e., $\omega = 1$) subjected to an applied difference in solute (electrolyte) concentration (e.g., Olsen et al. 1990). In essence, ω as defined by Eq. 1 represents the ratio of the actual to maximum chemico-osmotic pressure differences that occur across a membrane in a closed system in response to an applied concentration difference (i.e., as $\Delta P \rightarrow \Delta \pi$ as $\omega \rightarrow 1$). Thus, ω is calculated based on the measured pressure difference, ΔP , resulting from the difference in solute concentration established across the specimen, and knowledge of the boundary electrolyte (salt) concentrations.

As previously noted, ΔP is measured directly using a differential pressure transducer (T3 in Fig. 4.1), and also calculated independently as the difference between the pressures measured independently by the two in-line pressure transducers (T1 and T2 in Fig. 4.1). The theoretical chemico-osmotic pressure difference, $\Delta \pi$, in Eq. 1 for a single-salt system can be calculated based on the salt concentrations at the specimen

boundaries in accordance with the van't Hoff expression (Katchalsky and Curran 1965),
or

$$\Delta\pi = \nu RT\Delta C = \nu RT(C_2 - C_1) \quad (4.2)$$

where ν is the number of ions per molecule of the salt, R is the universal gas constant [8.314 J mol⁻¹K⁻¹], T is the absolute temperature (K), C is the salt concentration (M), and subscripts 1 and 2 represent the individual compartments on either side of the soil specimen. For example, for 1:1 electrolyte solutions (e.g., NaCl, KCl), $\nu = 2$ in Eq. 4.2, whereas for 2:1 electrolyte solutions (e.g., CaCl₂), $\nu = 3$ in Eq. 4.2. The van't Hoff expression is based on the limiting assumption that the electrolyte solutions are ideal and dilute and, therefore, provides only approximate values of the maximum chemico-osmotic pressure difference. However, Fritz (1986) notes that the error associated with the van't Hoff expression is low (< 5 %) for 1:1 electrolytes (e.g., NaCl, KCl) and concentrations ≤ 1.0 M.

The initial difference in chemico-osmotic pressure, $\Delta\pi_0$, can be computed in accordance with Eq. 4.2 based on the initial salt concentrations, C_{ot} and C_{ob} , and assuming the positive x-direction downward from the top of the specimen as follows:

$$\Delta\pi_0 = \nu RT(C_{ob} - C_{ot}) \quad (4.3)$$

The value $\Delta\pi_0$ based on Eq. 4.3 represents the maximum possible value of $\Delta\pi$ that can be maintained across the specimen during the test. Calculation of chemico-osmotic

efficiency based on $\Delta\pi_0$ is appropriate for "perfectly flushing" boundary conditions in which the circulation rate is sufficiently rapid relative to the diffusive rate through the specimen, such that changes in boundary salt concentrations due to diffusion are negligible. However, when the circulation rate is not sufficiently rapid, changes in the boundary concentrations due to diffusion may result in a time-dependent reduction in $\Delta\pi$ (Malusis et al. 2001b).

This potential effect of diffusion may be taken into account by basing the determination of ω on the average boundary salt concentrations of a solute species, $C_{t,ave}$ and $C_{b,ave}$, defined as follows (Malusis et al. 2001b):

$$C_{t,ave} = \frac{C_{ot} + C_t}{2} \quad ; \quad C_{b,ave} = \frac{C_{ob} + C_b}{2} \quad (4.4)$$

Based on these average concentrations, an average chemico-osmotic pressure difference, $\Delta\pi_{ave}$ can be written as follows:

$$\Delta\pi_{ave} = vRT(C_{t,ave} - C_{b,ave}) \quad (4.5)$$

Since $C_{t,ave} < C_{ot}$ and $C_{b,ave} \geq C_{ob}$, $\Delta\pi_{ave}$ given by Eq. 4.5 will be less than $\Delta\pi_0$ given by Eq. 4.3. Thus, for the same measured chemico-osmotic pressure difference, ΔP , values of ω based on $\Delta\pi_{ave}$, or ω_{ave} , will be greater than those based on $\Delta\pi_0$, or ω_0 , in accordance with Eq. 4.1 (Malusis et al. 2001b, Malusis and Shackelford 2002b). In the limit as $\omega \rightarrow 1$, solutes cannot enter or exit the specimen, such that $C_{t,ave} \rightarrow C_{ot}$ and $C_{b,ave} \rightarrow C_{ob}$ and

$\omega_{ave} \rightarrow \omega_0$.

4.4 EVALUATION OF TESTING APPARATUS

4.4.1 Materials

The flexible-wall cell was evaluated by performing duplicate membrane tests on specimens of the same geosynthetic clay liner (GCL) as tested by Malusis and Shackelford (2002a,b) using a rigid-wall cell and the same closed-system boundary conditions. The results reported by Malusis and Shackelford (2002a,b) indicated that the GCL behaved as a semi-permeable membrane with membrane efficiencies ranging from 8 to 69 % (i.e., $0.08 \leq \omega \leq 0.69$) for KCl concentrations differences ranging from 3.9 to 47 mM. The liquids used in the current evaluation also were the same as those used by Malusis and Shackelford (2002a,b) to facilitate comparison of results between the two studies. These liquids included de-ionized water (DIW) and solutions of DIW and potassium chloride (KCl) (certified A.C.S.; Fisher Scientific, Fair Lawn, New Jersey) dissolved in DIW at measured concentrations of 3.9, 6.0, 8.7, 20, and 47 mM.

The GCL ranges from about 5 to 10 mm in thickness in the air-dried (as-shipped) condition, and consists of sodium bentonite sandwiched between non-woven (non-patterned) and a woven (patterned) geotextiles and held together by needle punching with polymer fibers. The geotextiles provide no hydraulic resistance, but rather serve to contain the sodium bentonite which is the principal hydraulic resistance component of the GCL. The physical and chemical properties as well as the mineralogical composition of the bentonite portion of the GCL were reported by Malusis and Shackelford (2002b). In terms of mineralogy, the bentonite component of the GCL contained 71 %

montmorillonite, 7 % mixed layer illite/smectite, 15 % quartz, and 7 % other minerals. The liquid limit (LL) and plastic limit (PL) measured in accordance with ASTM D 4318 were reported as 478 % and 39 %, respectively, and the bentonite classified as a high plasticity clay (CH) based on the Unified Soil Classification System (ASTM D 2487). The measured cation exchange capacity, or CEC, was reported as 47.7 meq/100 g (= 47.7 cmol_c/kg), and ~ 53 % of the exchange complex was reported as being comprised of exchangeable sodium (i.e., sodium bentonite). Further details regarding the physical and chemical properties of the GCL bentonite are provided by Malusis and Shackelford (2002b)

4.4.2 Specimen Assembly and Preparation

For the GCL specimens evaluated in this study, the specimen assembly and disassembly consisted of three stages: (1) a flushing stage, (2) a consolidation stage, and (3) a membrane stage. The primary purpose of the flushing stage was to leach soluble salts from the pores of the GCL bentonite to enhance the potential for membrane behavior, since the membrane behavior of clays is known to increase with decreasing salt concentration (Olsen et al. 1990, Malusis and Shackelford 2002a,b, Shackelford and Lee 2003, Shackelford et al. 2003, Yeo et al. 2005). Secondary purposes included saturating the test specimens and measuring the initial hydraulic conductivity, k . The purpose of the consolidation stage was to consolidate the specimens to a sufficiently high effective stress to again enhance the potential for membrane behavior. Finally, the purpose of the membrane stage was to evaluate the measurement of the membrane efficiency of the GCL specimens using the developed flexible-wall membrane cell.

Because only one complete flexible-wall membrane cell was available for measuring membrane behavior, and the duration of each test could be lengthy (6 or more months), the flushing and consolidation stages of the procedure were conducted in separate flexible-wall cells similar to those commonly used for hydraulic conductivity testing (e.g., see Daniel et al. 1985, Daniel 1994), and then the specimen was transferred to and reconsolidated directly within the flexible-wall cell specifically designed in this study for membrane testing. Although this procedure resulted in unloading and re-loading of the test specimen, the procedure allowed for the simultaneous flushing and consolidation of a second specimen while the first specimen was being tested for membrane behavior.

For the flushing stage, circular specimens of the GCL with nominal diameters of 102 mm were permeated in standard flexible-wall permeameters at an average effective stress of 34.5 kPa (5.0 psi) with DIW until the electrical conductivity, EC, of the effluent from the specimen was ~ 50 % of the measured EC of 56.1 mS/m for the 3.9 mM KCL solution, which was the lowest KCl concentration to be used during the membrane stage of the test.

After completion of the flushing stage, the specimen was transferred to a separate, standard flexible-wall cell for the consolidation stage. After re-assembling the specimen, the specimen was consolidated to a final effective stress of 241 kPa (35.0 psi). Upon completion of the consolidation stage, the specimen was unloaded to zero confining stress, the specimen cell was disassembled, and the specimen was transferred to the flexible-wall membrane cell used to measure membrane behavior. Upon re-assembling the specimen in the flexible-wall membrane cell, the cylinder was filled with DIW to

confine the specimen, and confining and back pressures of 207 kPa (30.0 psi) and 172 kPa (25.0 psi), respectively, were applied with the drainage valves open. The confining stress then was increased incrementally in 69.0-kPa (10.0-psi) increments until a final confining stress of 413 kPa (60.0 psi) was achieved to provide the desired final effective stress of 241 kPa (35.0 psi). After equilibrium had been re-established, the drainage valves were closed to start the membrane testing stage

4.4.3 Membrane Testing Procedures

Prior to subjecting the confined test specimen to a solute concentration difference, DIW was circulated through the top cap and bottom pedestal of the specimen at a flow rate of $4.2 \times 10^{-10} \text{ m}^3/\text{s}$ to establish a steady baseline differential pressure. This displacement rate was the same as that used by Malusis et al. (2001b) for membrane testing using the same closed-system apparatus connected to a rigid-wall cell, and resulted in the need to refill the syringes/actuators with source solutions once every 24 h. Following the establishment of a baseline pressure difference across the specimen, source solutions with different initial concentrations of the same salt, C_{ot} and C_{ob} , were simultaneously injected from the syringes/actuators into the porous disks bounding the specimen through valves 1 and 2 (see Fig. 4.1), with the condition that valves 3 and 4 were closed, in order to establish a concentration difference, $-\Delta C (= C_{ot} - C_{ob} > 0)$, across the specimen. Buildup of a pressure difference in response to $-\Delta C$ was recorded via a personal computer (not shown) equipped with a data acquisition system (Labview software and Omega Model 100A DAQ Board), as described by Malusis et al (2001b). The electrolyte solutions from each of the two syringes/actuators were expelled after

complete displacement of the syringe/actuator, which is a function of the displacement rate of the plunger for the syringe/actuator and the volume of the liquid in the syringe/actuator (Malusis et al. 2001b).

After complete displacement of the syringe in the actuator, the specimen was isolated by closing valves 1 and 2, valves 3 and 4 were opened, and the direction of the syringe was reversed to allow sampling and refilling via the sampling and refilling reservoirs (see Fig. 4.1). The rate of displacement for sampling and refilling was significantly faster than that used during injection, such that refilling and sampling required only a fraction of the time (usually ≤ 2 mins) required for displacement during circulation (i.e., ~ 24 h). The electrical conductivity (EC) of individual samples recovered from the sampling reservoirs was measured as an indication of the boundary conditions (e.g., see Shackelford and Lee 2003), and to provide an estimate via calibration of the salt (KCl) concentrations in the circulation outflows from the top (C_t) and bottom (C_b) of the specimen (see Fig. 4.1). The variation in the cell volume also monitored through the cell-water accumulator (CWA in Fig. 4.1). Upon completion of sampling and refilling, valves 3 and 4 are closed, valves 1 and 2 were opened, and the syringe was displaced at the injection rate (i.e., $4.2 \times 10^{-10} \text{ m}^3/\text{s}$) to repeat another daily cycle for measurement of the membrane efficiency.

4.4.4 Testing Program

Duplicate multiple-stage membrane tests were conducted in this study to evaluate the flexible-wall cell. Multiple-stage tests are tests where a single specimen is subjected to progressively greater source concentration differences, $-\Delta C (= C_{ot} - C_{ob})$, in separate

but sequential stages, such that one membrane efficiency is measured per stage, thereby providing for a direct determination of the effect of concentration on the membrane efficiency of the specimen (Malusis and Shackelford 2002b). In both tests, DIW was circulated across the bottom of the specimen, such that $-\Delta C$ was the same as C_{ot} (i.e., $C_{ob} = 0$). Both tests included at least four stages involving circulation of source KCl solutions across the top of the specimen, with source KCl concentrations, C_{ot} , of 3.9 mM, 6.0 mM, 8.7 mM, and 20 mM. However, one test was extended to include a fifth stage with $C_{ot} = 47$ mM KCl. These source KCl concentrations were chosen to allow comparison of the results obtained with the flexible-wall cell with those previously reported by Malusis and Shackelford (2002b) based on the use of rigid-wall cell with the same boundary conditions and GCL. Each stage was conducted until a steady differential pressure response across the specimen was observed (i.e., $-\Delta P = \text{constant}$) and EC was constant.

4.5 RESULTS

4.5.1 Specimen Flushing and Consolidation

The results of the flushing stages of the tests for both GCL specimens are shown in Fig. 4.3. Both specimens were permeated with DIW until the electrical conductivity, EC, in the effluent from the specimens was only a fraction of that associated with the lowest KCl concentration of 3.9 mM of the source solutions used in the membrane stage of the test. As previously mentioned, this flushing stage was employed primarily to enhance the probability that membrane behavior would be observed in the test specimens (e.g., see Malusis et al 2001b, Malusis and Shackelford 2002b, Shackelford and Lee

2003). In the case of specimen GCL1, the specimen was flushed for 161 d resulting in an effluent EC of 30.5 mS/m, or 54.4 % of the EC of 56.1 mS/m associated with a 3.9 mM KCl solution. In the case of specimen GCL2, the specimen was flushed for 171 d resulting in an effluent EC of 22.2 mS/m, or 39.6 % of the EC of 56.1 mS/m associated with a 3.9 mM KCl solution.

The hydraulic conductivity, k , of the two GCL specimens was also measured during the flushing stage. As shown in Fig. 4.3, despite somewhat initial erratic behavior in the measured k values, permeation with DIW at a 34.5 kPa (5.0 psi) average effective stress eventually resulted in measured steady-state k values for specimens GCL1 and GCL2 of 2.69×10^{-9} cm/s and 3.34×10^{-9} cm/s, respectively. Both of these k values are representative of those typically measured for GCLs permeated with DIW in flexible-wall permeameters and similar effective stresses (see Daniel et al. 1997).

4.5.2 Electrical Conductivities

After reconsolidating the specimens in the flexible-wall membrane cell to an effective stress, σ' , of 241 kPa (35.0 psi), the drainage lines (valves 3 and 4 in Fig. 4.1) were shut, and deionized water (DIW) was circulated through both the top and bottom porous disks to mark the beginning of the membrane testing stage. Following establishment of the baseline pressure differences resulting from circulating DIW through both the top and bottom of the specimen, the DIW circulated through the top boundary of each specimen was replaced with electrolyte solutions containing increasingly higher concentrations of KCl, while maintaining circulation of DIW through the bottom boundary, to establish the concentration difference for measurement of the chemico-

osmotic pressure difference resulting from specimen membrane behavior.

The resulting values for the electrical conductivity measured in the circulation outflows from the top (EC_{top}) and bottom (EC_{bottom}) boundaries during the membrane testing stage are shown in Fig. 4.4. These measured EC values reflect the boundary conditions imposed in the tests. For example, the relatively low values for EC_{top} and EC_{bottom} during the initial circulation stage with DIW reflect the low ionic strength associated with DIW, and the lack of a substantial difference between EC_{top} and EC_{bottom} during this stage reflects the fact that DIW was circulated simultaneously through both the top and bottom. The increasing magnitude of EC_{top} upon replacing the DIW with the KCl solutions directly reflects the progressively greater increase in ionic strength of the KCl solutions resulting from the circulation of solutions with progressively higher KCl concentrations. The lower values for EC_{top} relative to the EC values for the source solutions, EC_o (i.e., $EC_{top} < EC_o$), are consistent with the loss of solute mass from the source solutions due to solute diffusion into the specimens, whereas the eventual increase in the values of EC_{bottom} with time is consistent with the gain of solute mass in the bottom circulation outflow due to solute diffusion through the specimen. Finally, leveling off of the values for both EC_{top} and EC_{bottom} during the 7-d periods applied for each stage of the test reflects the establishment of steady-state conditions with respect to EC in both the top and bottom boundaries. All of these observations are consistent with those previously reported for membrane tests involving rigid-wall cells (e.g., Malusis et al. 2001, Malusis and Shackelford 2002a,b, Shackelford and Lee 2003).

4.5.3 Boundary Pressures

The water pressures occurring at the top (u_{top}) and bottom (u_{bottom}) of the boundaries of the specimens measured with in-line transducers T1 and T2 (see Fig. 4.1), respectively, during the multiple-stage membrane tests are presented in Figs. 4.5a and 4.6a for specimens GCL1 and GCL2, respectively. Although there are some differences in the temporal trends in the water pressures between the two GCL specimens, the trends are also consistent between the two specimens in at least three ways.

First, during the initial stage of the tests where DIW is circulated through both the top and bottom boundaries, the values of u_{top} are virtually identical to the values of u_{bottom} (i.e., $u_{\text{top}} \approx u_{\text{bottom}}$). Second, upon replacing the DIW with the KCl solutions for circulation across the top boundary of the specimen, values of u_{bottom} are consistently lower than values of u_{top} (i.e., $u_{\text{top}} > u_{\text{bottom}}$). Third, after introduction of the KCl solutions, values of u_{bottom} tend to be slightly lower than the back pressure, u_{bp} , of 172 kPa (25.0 psi), whereas values of u_{top} tend to be slightly higher than u_{bp} (i.e., $u_{\text{bottom}} < u_{\text{bp}} < u_{\text{top}}$). A plausible explanation for these consistent trends follows.

During the initial stage of the tests when DIW is circulated both top and bottom, the chemical potential of the water on both sides of the specimens is the same, such that u_{top} should equal u_{bottom} and there is no potential for chemico-osmotic flow of water (H_2O) through the specimen, i.e., since a salt concentration gradient across the specimen has not been established. Upon introduction of the KCl solutions through the top boundary, a salt concentration difference across the specimen is established resulting in the two phenomena expected for semi-permeable membranes, viz., a tendency for chemico-osmotic flow of water from low salt concentration (bottom) to high salt

concentration (top), and diffusion of salt (i.e., KCl) from high salt concentration (top) to low salt concentration (bottom). As diffusion of KCl occurs, both chloride (Cl⁻) and potassium (K⁺) ions exit the bottom boundary of the specimen into the circulating DIW, such that the concentration of KCl in the circulation outflow from the bottom, C_b , is greater than that for the circulation inflow for the bottom, C_{ob} ($= 0$), or $C_b > C_{ob}$ (e.g., see Fig. 4.1). This increasing salt concentration at the bottom boundary of the specimen tended to reduce the chemical potential of water (e.g., Mitchell and Soga 2005), such that the measured water pressure at the bottom of the specimen was slightly lower than the back pressure (i.e., $u_{bottom} < u_{bp}$). This tendency of decreasing chemical potential for the water with increasing salt concentration also holds true for the top circulation boundary, such that one might expect the chemical potential of the water in the top boundary to also have been lower than that for the bottom boundary (i.e., $u_{top} < u_{bottom}$), i.e., since the salt concentrations in the KCl solutions being circulated through the top boundary were greater than those occurring in the bottom boundary (e.g., Fig. 4.4). This expectation would be true in an open system, whereby water could readily flow from bottom to top via chemico-osmosis. However, since the system being evaluated is closed, such that chemico-osmotic flow is prevented, a chemico-osmotic pressure difference, $-\Delta P$ (> 0), builds up across the specimen to counteract the tendency for chemico-osmotic flow, such that the water pressure at the top boundary, u_{top} [$= u_{bottom} + (-\Delta P)$], is greater than the back pressure, u_{bp} (i.e., $u_{top} > u_{bp} > u_{bottom}$).

Since the confining stress, σ_c , of 414 kPa (60.0 psi) is maintained constant during the tests, the variation in u_{top} and u_{bottom} with time also influenced the effective stresses at the top, σ'_{top} ($= \sigma_c - u_{top}$), and bottom, σ'_{bottom} ($= \sigma_c - u_{bottom}$), of the specimen, as shown

in Figs. 4.5b and 6b. As a result, the average effective stresses in the specimens, $\sigma'_{ave} [= (\sigma'_{top} + \sigma'_{bottom})/2]$, were not constant and also were not equal to 241 kPa (35.0 psi), as typically would be assumed on the basis of the constant back pressure (Figs. 4.5c and 4.6c).

4.5.4 Induced Chemico-Osmotic Pressures

The measured induced chemico-osmotic pressure differences, $-\Delta P (> 0)$, measured by the differential pressure transducer (T3 in Fig. 4.1) as well as the differences between the pressures measured at the top and bottom of the specimen by the in-line transducers (T1 and T2 in Fig. 4.1), $-\Delta u (= u_{top} - u_{bottom})$, are shown in Fig. 4.7 for both GCL specimens. As shown, differences between $-\Delta u$ and $-\Delta P$ were virtually imperceptible for both GCL specimens (i.e., $-\Delta u \approx -\Delta P$). The fact that $-\Delta u$ was virtually identical to $-\Delta P$ indicates that $-\Delta P$ is accurate, and also provides a measure of credibility to the previous explanation as to why $u_{top} > u_{bp} > u_{bottom}$ [i.e., if $-\Delta u (= u_{top} - u_{bottom}) = -\Delta P$, then $u_{top} = u_{bottom} + (-\Delta P)$]. The results shown in Fig. 4.7 also indicate that, whereas virtually no membrane behavior was observed during circulation of DIW through both the top and bottom boundaries of the specimens, significant and sustained membrane behavior occurred in both specimens virtually immediately upon replacing the DIW circulating through the top boundary with KCl solutions. Finally, as shown in Fig. 4.8, close agreement between the values of $-\Delta P$ for the two duplicate GCL specimens was achieved during both DIW circulation and circulation with the KCl solutions.

4.5.5 Induced Membrane Efficiencies

As shown in Fig. 4.9, the close agreement between values of $-\Delta P$ for the two duplicate GCL specimens shown in Fig. 4.8 correlates with close agreement between the values of the membrane efficiency coefficients, ω , for the duplicate GCL specimens, regardless of whether the ω values are based on $\Delta\pi$ values using Eq. 4.3 (Fig. 4.9a) or Eq. 4.5 (Fig. 4.9b). In calculating the values for ω shown in Fig. 4.9, net or "effective" values of $-\Delta P$ (i.e., $-\Delta P_e$) were used corresponding to the measured values of $-\Delta P$ based on circulation with the KCl solutions minus the initial measured values of $-\Delta P$ based on circulation with DIW through both top and bottom boundaries (e.g., see Malusis et al 2001b).

As shown in Fig. 4.9, the values of ω tended to decrease with increasing KCl concentration, which is consistent with previous results based on rigid-wall cells that attributed decreasing ω with increasing salt concentration to a progressively greater collapse of the diffuse double layers (DDLs) surrounding individual clay particles, resulting in larger pores and correspondingly less restriction of solutes (e.g., Malusis et al. 2001a, Malusis and Shackelford 2002b, Shackelford et al. 2003). Also, the values of ω were relatively constant over any interval of time corresponding to a given KCl concentration, implying that steady-state conditions were achieved during the 7-d circulation periods.

4.5.6 Volume Changes

Volume changes were recorded during the membrane testing stage via the cell-wall accumulator (CWA in Fig. 4.1) as a check on the assumption of undrained

conditions. As shown in Fig. 4.10, some incremental volume changes, ΔV ($\leq \pm 0.33$ mL), were recorded during the membrane testing stage, resulting in cumulative volume changes, $\Sigma(\Delta V)$, of -2.52 mL and -4.78 mL for specimens GCL1 and GCL2, respectively. The vast majority of these volume changes were negative, corresponding to decreases in the specimen volumes (i.e., compression), and occurred primarily during the circulation of the KCl solutions as opposed to during circulation of only DIW. As shown in Fig. 4.11, these volume changes corresponded to incremental volumetric strains ($\Delta V/V_0$) of $\leq \pm 0.6$ % and cumulative volumetric strains ($\Sigma(\Delta V)/V_0$) of ≤ -4.9 % and ≤ -9.5 % for specimens GCL1 and GCL2, respectively.

The existence of volume changes when none were expected led to the need to answer two questions. First, since the specimens were back-pressure saturated before testing, and all the drainage lines (i.e., valves 3 and 4 in Fig. 4.1) were closed during testing, how did drainage of liquid from the specimens occur during the testing? Second, since the specimens were consolidated to an equilibrium, final effective stress, σ' , of 241 kPa (35.0 psi) prior to testing, and no additional change in effective stress was imposed during testing, how did volume change occur in the absence of any apparent change in effective stress? Plausible answers to both of these questions follow.

In terms of how drainage could have occurred, the answer lies in the daily sampling and refilling procedure of the syringes. As previously described, the syringes were sampled and refilled daily, requiring a brief period (≤ 2 min) for reversal of the plunger direction (Fig. 4.1). As a result, the initial refilling/sampling approach considered to minimize the possibility of volume change during this brief period involved closing valves 1 and 2, opening valves 3 and 4, and reversing the direction of the plunger until

existing circulation liquid in the plunger was expelled into the sampling reservoir, and fresh liquid (DIW at the bottom and KCl solution at the top) was infused back into the syringe/actuator. After sampling/refilling, valves 3 and 4 were then closed, and valves 1 and 2 were opened, and the plunger direction was again reversed to inject liquid for circulation across the top and bottom boundaries. This procedure was expected to minimize the possibility for drainage of liquid from the specimen, i.e., since no continuous drainage path was ever left open during the procedure. However, preliminary testing indicated that this procedure resulted in "locked in" boundary water pressures that significantly affected the stress conditions on the specimens, as illustrated in Fig. 4.12. As a result, a decision was made to alter the initial procedure such that, after sampling/refilling the syringes, all four valves leading to the syringes (i.e., valves 1-4 in Fig. 4.1) were momentarily opened to re-establish the back pressure of 172 kPa (25.0 psi) before then closing valves 3 and 4 and starting the plunger to begin the next injection. This reestablishment of the back pressure before each injection stage is the reason for the daily, rapid decrease and increase in temporal distributions of the chemico-osmotic pressure differences established during circulation to the back pressure of 172 kPa (25.0 psi), as previously shown in Figs. 4.5-4.7, and likely represents the period during which small amounts of liquid could have drained from the specimen.

In terms of how volume changes could have occurred in the absence of any applied change in applied effective stress, the most likely explanation relates to an increment in effective stress resulting from physico-chemico interactions between the pore water in the bentonite and the individual particles of bentonite comprising the GCL specimens. Such physico-chemico interactions are more likely to be influential in clays

such as bentonite comprised of significant amounts of highly active clay minerals, such as sodium montmorillonite (Mitchell and Soga 2005). Theoretically, an increase in salt concentration in the pore water results in an increase in the adsorptive forces relative to the repulsive forces between individual soil particles (i.e., so-called R – A effect), such that the effective stress in the soil also increases resulting in compression of the soil (i.e., provided drainage is allowed). Such an increase in salt concentration in the pore water of the GCL specimens is consistent with diffusion of the KCl into the specimens as previously described, and with the observation that the cumulative changes in volume tended to increase with increasing KCl concentration for both GCL specimens (Figs. 4.10 and 4.11).

Thus, even though volume change was prevented from occurring during the actual measurement of the membrane efficiency of the GCL specimens (i.e., during KCl circulation between sampling/refilling periods), some volume change did occur as a result of the sampling/refilling procedure and the desire to re-establish the reference (back) pressure before each daily circulation event. The resulting volume changes that did occur tended to be relatively low ($\leq -9.5\%$), although the magnitude of the impact of these volume changes on the measured membrane efficiencies cannot be quantified. In general, a decreasing specimen volume results in decreasing pore (void) space, which would be expected to increase solute restriction and, therefore, increase membrane efficiency (ω). This trend tends to contradict the trend of decreasing ω with increasing test duration previously shown in Fig. 4.9. However, as noted by Shackelford et al. (2000) in their evaluation of the effects of inorganic salt solutions on the hydraulic conductivity of GCLs, pore size, as opposed to pore volume, is the key factor affecting solute restriction,

such that effect of physico-chemico interactions on the actual pore sizes as opposed to that on the overall specimen void (pore) volume likely have dominated the membrane efficiencies of the GCL specimens.

4.6 DISCUSSION

The final, or steady-state, values of ω for each KCl concentration, ω_{ss} , along with the values of $-\Delta P_e$, $-\Delta\pi_o$, and $-\Delta\pi_{ave}$ used to calculate ω_{ss} , are summarized in Table 4.1. The resulting values of ω_{ss} are plotted as a function of the average difference in the initial KCl concentrations, or $-\Delta C_{o,ave}$ [$= -\Delta C_o/2 = (C_{ot} - C_{ob})/2 = C_{ot}/2$], in Fig. 4.13a.

As expected, values of ω_{ss} based on $-\Delta\pi_o$, or $\omega_{ss,o}$, are more conservative (lower) than values of ω_{ss} based on $-\Delta\pi_{ave}$, or $\omega_{ss,ave}$, i.e., since $-\Delta\pi_o > -\Delta\pi_{ave}$. In fact, as shown in Fig. 4.13b, values of $\omega_{ss,ave}/\omega_{ss,o}$ increased virtually semi-log linearly with $-\Delta C_{o,ave}$. For example, $\omega_{ss,ave}/\omega_{ss,o}$ increased from 1.16 to 1.28 as $-\Delta C_{o,ave}$ increased from 1.95 mM to 10 mM, respectively, for specimen GCL1, whereas $\omega_{ss,ave}/\omega_{ss,o}$ increased from 1.19 to 1.33 as $-\Delta C_{o,ave}$ increased from 1.95 mM to 23.5 mM, respectively, for specimen GCL2.

Values of ω_{ss} measured in this study using the flexible-wall cell under closed-system boundary conditions are compared in Fig. 4.14 with values of ω_{ss} previously reported by Malusis and Shackelford (2002b) for the same GCL and same source KCl concentrations measured using a rigid-wall cell under closed-system boundary conditions. As expected and previously discussed, the membrane efficiencies decrease with increasing KCl concentration regardless of whether the flexible-wall or rigid-wall cell is used in the measurement. However, at least two distinct differences in the membrane efficiencies based on the flexible-wall cell versus those based on the rigid-wall

cell are apparent. First, except for the values of $\omega_{ss,ave}$ at the lowest $\Delta C_{o,ave}$ concentration of 1.95 mM KCl (i.e., $C_{ot} = 3.9$ mM KCl), all of the membrane efficiencies based on the flexible-wall cell are lower than those based on the rigid-wall cell at any given value of $\Delta C_{o,ave}$. Second, whereas the membrane efficiency of the GCL based on the rigid-wall cell decreases essentially semi-log linearly with increasing $\Delta C_{o,ave}$, the decrease in the membrane efficiency of the GCL with increasing logarithm of $\Delta C_{o,ave}$ is non-linear.

As shown in Fig. 4.15, these observed differences in the membrane efficiencies based on the flexible-wall cell versus those based on the rigid-wall cell cannot be attributed entirely to differences in the void ratios of the specimens, since for any given concentration of KCl in the source solution (i.e., C_{ot}), the void ratios for the GCL specimens tested in the flexible-wall cell were at or lower than the lower range of void ratios for the same GCL tested in the rigid-wall cell. Other possible reasons for the difference between the membrane efficiencies of the GCL measured in this study using the flexible-wall cell relative to those measured previously using rigid-wall cell include the differences in the stress conditions induced in the specimens in the two types of cells, as well as the differences in the specimen preparation procedures. With respect to specimen preparation procedures, the GCL specimens tested using the rigid-wall cell were flushed, compressed, and tested for membrane behavior entirely within the same rigid-wall cell, whereas the GCL specimens tested in this study were flushed, consolidated, and tested for membrane behavior in three different flexible-wall cells. In any event, further evaluation will be required before more conclusive statements can be made on the causes for the noted differences in the membrane efficiencies measured in the two different types of cells. Nonetheless, the membrane efficiencies of duplicate

specimens of a GCL measured with the flexible-wall cell under closed-system conditions evaluated in this study were both reproducible and similar to, albeit somewhat less than, those measured previously with a rigid-wall cell for the same GCL and boundary conditions.

4.7 SUMMARY AND CONCLUSIONS

The development of a flexible-wall testing apparatus consisting of a flexible-wall cell and a hydraulic control system that imposes closed-system boundary conditions for measurement of the membrane behavior of clay soils was described. The advantages of a flexible-wall cell include complete control over the state of stress existing within the test specimen and the ability to back-pressure saturate and consolidate the specimen prior to membrane testing. Use of the developed flexible-wall cell was illustrated via tests conducted to measure the membrane behavior of a geosynthetic clay liner (GCL). The GCL specimens were consolidated to a final effective stress, σ' , of 241 kPa (35.0 psi) prior to the start of membrane testing. Membrane testing consisted of multi-stage tests, whereby de-ionized water (DIW) was first circulated across both the bottom and the top of the specimens to establish a baseline pressure difference, $-\Delta P (> 0)$, of the specimen, followed by circulation of source KCl solutions across the top of the specimen (while maintaining DIW circulation across the bottom of the specimen) with sequentially higher source concentrations, C_{ot} , of KCl to establish the salt concentration differences, $-\Delta C (= C_{ot})$, required to evaluate the potential for membrane behavior.

The results indicated that the GCL behaved as a semi-permeable membrane, with measured membrane efficiencies at steady state, ω_{ss} , based on the difference in initial

(source) concentrations, $\omega_{ss,o}$, ranging from 0.068 (one specimen) at C_{ot} of 47 mM KCl to 0.539 ± 0.015 (two specimens) at C_{ot} of 3.9 mM KCl, and ω_{ss} values based on the average of the difference in boundary concentrations, $\omega_{ss,ave}$, ranging from 0.091 (one specimen) at C_{ot} of 47 mM KCl to 0.636 ± 0.025 (two specimens) at C_{ot} of 3.9 mM KCl. Also, both $\omega_{ss,o}$ and $\omega_{ss,ave}$ decreased with increasing C_{ot} , which is consistent with previous findings based on the use of a rigid-wall cell and attributable to progressively greater collapse of the electrostatic diffuse double layers surrounding individual clay particles with increasing salt concentration in the pore water. Finally, $\omega_{ss,ave}$ was always greater than $\omega_{ss,o}$, with values for the ratio of $\omega_{ss,ave}$ to $\omega_{ss,o}$, or $\omega_{ss,ave}/\omega_{ss,o}$, increasing with increasing average difference in the initial KCl concentrations, or $-\Delta C_{o,ave}$ [$=C_{ot}/2$]. For example, $\omega_{ss,ave}/\omega_{ss,o}$ for specimen GCL1 increased from 1.16 to 1.28 as $-\Delta C_{o,ave}$ increased from 1.95 mM to 10 mM, respectively, whereas $\omega_{ss,ave}/\omega_{ss,o}$ for specimen GCL2 increased from 1.19 to 1.33 as $-\Delta C_{o,ave}$ increased from 1.95 mM to 23.5 mM, respectively.

Although the membrane efficiencies of the GCL specimens were measured under closed (no-flow) conditions, some volume changes were recorded during the tests. These volume changes resulted in cumulative volumetric strains of $\leq -4.9\%$ and $\leq -9.5\%$ for specimens GCL1 and GCL2, respectively, and were attributed to drainage that occurred during the brief (≤ 2 min), daily sampling and refilling procedures for the syringes as opposed to during the circulation periods for measurement of membrane behavior, which lasted ~ 24 h.

Values of ω_{ss} measured in this study using the flexible-wall cell under closed-system boundary conditions were compared with values of ω_{ss} for the same GCL previously measured using a rigid-wall cell under the same closed-system boundary

conditions. As expected, the membrane efficiencies decrease with increasing KCl concentration regardless of whether the flexible-wall or rigid-wall cell was used in the measurement. Except for the values of $\omega_{ss,ave}$ at the lowest $-\Delta C_{o,ave}$ concentration of 1.95 mM KCl (i.e., $C_{ot} = 3.9$ mM KCl), all of the membrane efficiencies based on the flexible-wall cell were lower than those based on the rigid-wall cell at any given value of $\Delta C_{o,ave}$. Also, whereas the membrane efficiency of the GCL based on the rigid-wall cell decreased essentially semi-log linearly with increasing $\Delta C_{o,ave}$, the decrease in the membrane efficiency of the GCL with increasing logarithm of $\Delta C_{o,ave}$ was non linear in the case of the flexible-wall cell. These differences in measured membrane efficiencies based on the flexible-wall cell versus the rigid wall cell can be attributed, in part, to the difference in the stress conditions induced in the specimens in the two types of cells, as well as the difference in specimen preparation procedures. Despite these differences, the membrane efficiencies measured with the flexible-wall cell evaluated in this study were both reproducible and similar to, albeit somewhat less than, those measured previously with a rigid-wall cell.

ACKNOWLEDGMENTS

Financial support for this study was provided by the U. S. National Science Foundation (NSF), Arlington, VA, under Grants CMS-0099430 entitled, "Membrane Behavior of Clay Soil Barrier Materials" and CMS-0624104 entitled, "Enhanced Clay Membrane Barriers for Sustainable Waste Containment". The opinions expressed in this paper are solely those of the writers and are not necessarily consistent with the policies or opinions of the NSF. The authors also express appreciation to Dr. Jae-Myung Lee of the

California Department of Transportation for his assistance in the early stages of the development of the flexible-wall testing apparatus.

4.8 REFERENCES

- Cey, B.D., Barbour, S.L., and Hendry, M.J. 2001. Osmotic flow through a Cretaceous clay in southern Saskatchewan, Canada. *Canadian Geotechnical Journal*, 38(5), 1025-1033.
- Daniel, D.E. 1994. State-of-the-art: Laboratory hydraulic conductivity test for saturated soils. *Hydraulic Conductivity and Waste Contaminant Transport in Soil*, ASTM STP 1142, D.E Daniel and S.J. Trautwein (Eds.), ASTM, West Conshohoken, PA, 30-78.
- Daniel, D.E., Anderson, D.C., and Boynton, S.S. 1985. Fixed-wall versus flexible-wall permeameters. *Hydraulic Barriers in Soil and Rock*, ASTM STP 874, A. I. Johnson, R. K. Frobel, N. J. Cavalli, and C. B. Pettersson (Eds.), ASTM, West Conshohoken, PA, 107-126.
- Daniel, D.E., Bowders, J.J., and Gilbert, R.B. 1997. Laboratory hydraulic conductivity testing of GCLs in flexible-wall permeameters. *Testing and Acceptance Criteria for Geosynthetic Clay Liners*, ASTM STP 1308, L. Well (Ed.), ASTM, West Conshohocken, PA, 208-226.
- Derrington, D., Hart, M. and Whitworth, T. M. 2006. Low head sodium phosphate and nitrate hyperfiltration through thin kaolinite and smectite layers – Application to engineered systems. *Applied Clay Science*, 33(1), 52-58.
- Elrick, D.E., Smiles, D.E., Baumgartner, N., And Groenevelt, P.H. 1976. Coupling

- phenomena in saturated homo-ionic montmorillonite: I. Experimental. *Soil Science Society of America Journal*, 40(4), 490-491.
- Evans, J.C., Shackelford, C.D., Yeo, S.-S., and Henning, J. 2008. Membrane behavior of soil-bentonite slurry-trench cutoff walls. *Soil and Sediment Contamination*, 17(4), 316-322.
- Fritz, S.J. 1986. Ideality of clay membranes in osmotic process: A review. *Clays and Clay Minerals*, 34(2), 214-223.
- Fritz, S.J. and Marine, I.W. 1983. Experimental support for a predictive osmotic model of clay membranes. *Geochimica et Cosmochimica Acta*, 47(8), 1515-1522.
- Greenberg, J.A., Mitchell, J.K., and Witherspoon, P.A. 1973. Coupled salt and water flows in a groundwater basin. *Journal of Geophysical Research*, 78(27), 6341-6353.
- Groenevelt, P.H. and Elrick, D.E. 1976. Coupling phenomena in saturated homo-ionic montmorillonite: II.Theoretical. *Soil Science Society of America Journal*, 40(6), 820-823.
- Hanshaw, B.B. 1972. Natural-membrane phenomena and subsurface waste emplacement. *The American Association of Petroleum Geologists*, 18(6), 308-317.
- Hanshaw, B.B. and Coplen, T.B. 1973. Ultrafiltration by a compacted clay membrane – II. Sodium ion exclusion at various ionic strengths. *Geochimica et Cosmochimica Acta*, 37(10), 2311-2327.
- Hart, M. and Whitworth, T.M. 2005. Hyperfiltration of potassium nitrate through clay membranes under relatively low-head conditions. *Geochimica et Cosmochimica Acta*, 69(2), 4817-4823.

- Heister, K., Keijzer, Th.J.S. and Loch, J.P.G. 2004. Stability of clay membranes in chemical osmosis. *Soil Science Society of America Journal*, 169(9), 632-639.
- Heister, K., Kleingeld, P. J., Keijzer, Th.J.S., and Loch, J.P.G. 2005. A new laboratory set-up for measurements of electrical, hydraulic, and osmotic fluxes in clays. *Engineering Geology*, 77(3-4), 295-303.
- Henning, J.T., Evans, J.C., and Shackelford, C.D. 2006. Membrane behavior of two backfills from field-constructed soil-bentonite cutoff walls. *Journal of Geotechnical and Geoenvironmental Engineering*, 132(10), 1243-1249.
- Ishiguro, M., Matsuura, T., and Detellier, C. 1995. Reverse osmosis separation for a montmorillonite membrane. *Journal of Membrane Science*, 107(1), 87-92.
- Katchalsky, A. and Curran, P.F. 1965. *Nonequilibrium Thermodynamics in Biophysics*. Harvard University Press, Cambridge, Massachusetts, 248 pp.
- Keijzer, Th.J.S., Kleingeld, P.J., and Loch, J.P.G. 1997. Chemical osmosis in compacted clayey material and the prediction of water transport. *Geoenvironmental Engineering, Contaminated Ground: Fate of Pollutants and Remediation*, R. N. Yong and H. R. Thomas (Eds.), University of Wales, Cardiff, U. K., Sept. 6-12, Thomas Telford Publ., London, 199-204.
- Keijzer, Th.J.S., Kleingeld, P.J., and Loch, J.P.G. 1999. Chemical osmosis in compacted clayey material and the prediction of water transport. *Engineering Geology*, 53(2), 151-159.
- Keijzer, Th.J.S. and Loch, J.P.G. 2001. Chemical osmosis in compacted dredging sludge. *Soil Science Society of America Journal*, 65(4), 1046-1055.
- Kemper, W.D. 1960. Water and ion movement in thin films as influenced by the

- electrostatic charge and diffuse layer of cations associated with clay mineral surfaces. *Soil Science Society of America Proceedings*, 24(1), 10-16.
- Kemper, W.D. 1961. Movement of water as effected by free energy and pressure gradients: II. Experimental analysis of porous systems in which free energy and pressure gradients act in opposite directions. *Soil Science Society of America Proceedings*, 25(4), 260-265.
- Kemper, W.D. and Evans N.A. 1963. Movement of water as effected by free energy and pressure gradients: III. Restriction of solutes by membranes. *Soil Science Society of America Proceedings*, 27(5), 485-490.
- Kemper, W.D. and Quirk, J.P. 1972. Ion mobilities and electric charge of external clay surfaces inferred from potential differences and osmotic flow. *Soil Science Society of America Proceedings*, 36(3), 426-433.
- Kemper, W.D. and Rollins, J.B. 1966. Osmotic efficiency coefficients across compacted clays. *Soil Science Society of America Proceedings*, 30(5), 529-534.
- Kharaka, Y.K. and Berry, F.A.F. 1973. Simultaneous flow of water and solutes through geological membranes – I. Experimental investigation. *Geochimica et Cosmochimica Acta*, 37(12), 2577-2603.
- Kharaka, Y.K. and Smalley, W.C. 1976. Flow of water and solutes through compacted clays. *The American Association of Petroleum Geologists Bulletin*, 60(6), 973-980.
- MacKay, R.A. 1946. The control of impounding structures on ore deposition. *Economic Geology and the Bulletin of the Society of Economic Geologists*, The Economic Geology Publ. Co., New Haven, CT, Vol. 41, 13-46.

- Malusis, M.A. 2001. *Membrane Behavior and Coupled Solute Transport through a Geosynthetic Clay Liner*. PhD Dissertation, Colorado State University, Fort Collins, Colorado.
- Malusis, M.A. and Shackelford, C.D. 2002a. Coupling effects during steady-state solute diffusion through a semipermeable clay membrane. *Environmental Science and Technology*, 36(6), 1312-1319.
- Malusis, M.A. and Shackelford, C.D. 2002b. Chemico-osmotic efficiency of a geosynthetic clay liner. *Journal of Geotechnical and Geoenvironmental Engineering*, 128(2), 97-106.
- Malusis, M.A., Shackelford, C.D., and Olsen, H.W. 2001a. Flow and transport through clay membrane barriers. *Geoenvironmental Engineering: Geoenvironmental Impact Management*, R. N. Young and H. R. Thomas (Eds.), Thomas Telford Ltd., London, 334-341.
- Malusis, M.A., Shackelford, C.D., and Olsen, H.W. 2001b. A laboratory apparatus to measure chemico-osmotic efficiency coefficients for clay soils. *Geotechnical Testing Journal*, 24(3), 229-242.
- Malusis, M.A., Shackelford, C.D., and Olsen, H.W. 2003. Flow and transport through clay membrane barriers. *Engineering Geology*, 70(3), 235-248.
- Marine, I.W. 1974. Geohydrology of a buried Triassic basin at Savannah River plant, South Carolina. *The American Association of Petroleum Geologists Bulletin*, 58(9), 1825-1837.
- Marine, I.W. and Fritz, S.J. 1981. Osmotic model to explain anomalous hydraulic heads. *Water Resources Research*, 17(1), 73-82.

- McKelvey, J.G. and Milne, I.H. 1962. The flow of salt solutions through compacted clay. *Proceedings, Ninth National Conference on Clays and Clay Minerals*, Lafayette, Indiana, Oct. 5-8, 1960, Pergamon Press, New York, 248-259.
- McKelvey, J.G., Spiegler, K.S. and Wyllie, M.R.J. 1957. Salt filtering by ion-exchange grains and membranes. *The Journal of Physical Chemistry*, 61(2), 174-178.
- Mitchell, J.K. and Soga, K. 2005. *Fundamentals of Soil Behavior*, 3rd Ed. John Wiley and Sons, Inc., New York.
- Neuzil, C.E. 1986. Groundwater flow in low-permeability environments. *Water Resources Research*, 22(8), 1163-1195.
- Neuzil, C.E. 2000. Osmotic generation of 'anomalous' fluid pressures in geological environments. *Nature*, 403(6766), 182-184.
- Olsen, H.W. 1969. Simultaneous fluxes of liquid and charge in saturated kaolinite. *Soil Science Society of America Proceedings*, 33(3), 338-344.
- Olsen, H.W. 1972. Liquid movement through kaolinite under hydraulic, electric, and osmotic gradients. *The American Association of Petroleum Geologists Bulletin*, 56(10), 2022-2028.
- Olsen, H.W., Yearsley, E.N., and Nelson, K.R. 1990. Chemico-osmosis versus diffusion-osmosis. *Transportation Research Record No. 1288*, Transportation Research Board, Washington D.C., 15-22.
- Rahman, M.M., Chen, S., and Rahman, S.S. 2005. Experimental investigation of shale membrane behavior under tri-axial condition. *Petroleum Science and Technology*, 23(9-10), 1265-1282.
- Shackelford, C.D, Benson, C.H., Katsumi, T., Edil, T.B., and Lin, L. 2000. Evaluating

- the hydraulic conductivity of GCLs permeated with non-standard liquids. *Geotextiles and Geomembranes*, 18(2-4), 133-161.
- Shackelford, C.D. and Lee, J.-M. 2003. The destructive role of diffusion on clay membrane behavior. *Clays and Clay Minerals*, 51(2), 186-196.
- Shackelford, C.D., Malusis, M.A., and Olsen, H.W. 2003. Clay membrane behavior for geoenvironmental containment. *Soil and Rock America Conference 2003*, P. J. Culligan, H. H. Einstein, and A. J. Whittle (Eds.), Verlag Glückauf GMBH, Essen, Germany, Vol. 1, 767-774.
- Soler, J.M. 2001. The effect of coupled transport phenomena in the Opalinus Clay and implications for radionuclide transport. *Journal of Contaminant Hydrology*, 53(1), 63-84.
- Whitworth, T.M. and Fritz, S.J. 1994. Electrolyte-induced solute permeability effects in compacted smectite membranes. *Applied Geochemistry*, 9(5), 533-546.
- Yeo, S.-S. 2003. *Hydraulic Conductivity, Consolidation, and Membrane Behavior of Model Backfill-Slurry Mixtures for Vertical Cutoff Walls*. M. S. Thesis, Colorado State University, Fort Collins, Colorado.
- Yeo, S.-S., Shackelford, C.D., and Evans, J.C. 2005. Membrane behavior of model soil-bentonite backfills. *Journal of Geotechnical and Geoenvironmental Engineering*, 131(4), 418-429.

Table 4.1. Results of multi-stage membrane testing using flexible-wall cell for two specimens of a geosynthetic clay liner at an effective confining stress of 241 kPa (35.0 psi).

KCL Source Concentration, C_{ot} (mM)	Specimen Designation	Differences in Chemo-Osmotic Pressures ^(a) [kPa (psi)]			Membrane Efficiencies at Steady State, ω_{ss}	
		$-\Delta P_e$	$-\Delta\pi_0$	$-\Delta\pi_{ave}$	$\omega_{ss,0}$ ($=\Delta P_e/\Delta\pi_0$)	$\omega_{ss,ave}$ ($=\Delta P_e/\Delta\pi_{ave}$)
3.9	GCL1	9.979 (1.447)	19.011 (2.757)	16.324 (2.368)	0.525	0.611
	GCL2	10.531 (1.527)	19.011 (2.757)	15.930 (2.310)	0.554	0.661
	Average	10.255 (1.487)	19.011 (2.757)	16.127 (2.339)	0.539±0.015	0.636±0.025
6.0	GCL1	10.248 (1.486)	29.247 (4.242)	24.767 (3.592)	0.350	0.414
	GCL2	11.317 (1.641)	29.247 (4.242)	24.271 (3.520)	0.387	0.466
	Average	10.783 (1.564)	29.247 (4.242)	24.519 (3.556)	0.369±0.019	0.440±0.026
8.7	GCL1	10.490 (1.521)	42.408 (6.151)	34.762 (5.042)	0.247	0.302
	GCL2	11.007 (1.596)	42.408 (6.151)	35.123 (5.094)	0.260	0.313
	Average	10.749 (1.559)	42.408 (6.151)	34.943 (5.068)	0.253±0.007	0.308±0.008
20.0	GCL1	11.814 (1.713)	97.490 (14.140)	75.969 (11.018)	0.121	0.156
	GCL2	12.821 (1.860)	97.490 (14.140)	75.337 (10.927)	0.132	0.170
	Average	12.318 (1.787)	97.490 (14.140)	75.653 (10.972)	0.126±0.006	0.163±0.007
47.0	GCL1	-----	-----	-----	-----	-----
	GCL2	15.655 (2.271)	229.101 (33.228)	172.157 (24.969)	0.068	0.091
	Average	15.655 (2.271)	229.101 (33.228)	172.157 (24.969)	0.068	0.091

^(a) $-\Delta P_e$ = effective or net pressure difference measured across specimen at steady state; $-\Delta\pi_0$ = theoretical maximum pressure difference based on difference in initial (source) concentrations; $-\Delta\pi_{ave}$ = theoretical maximum pressure difference based on difference in average boundary concentrations at steady state

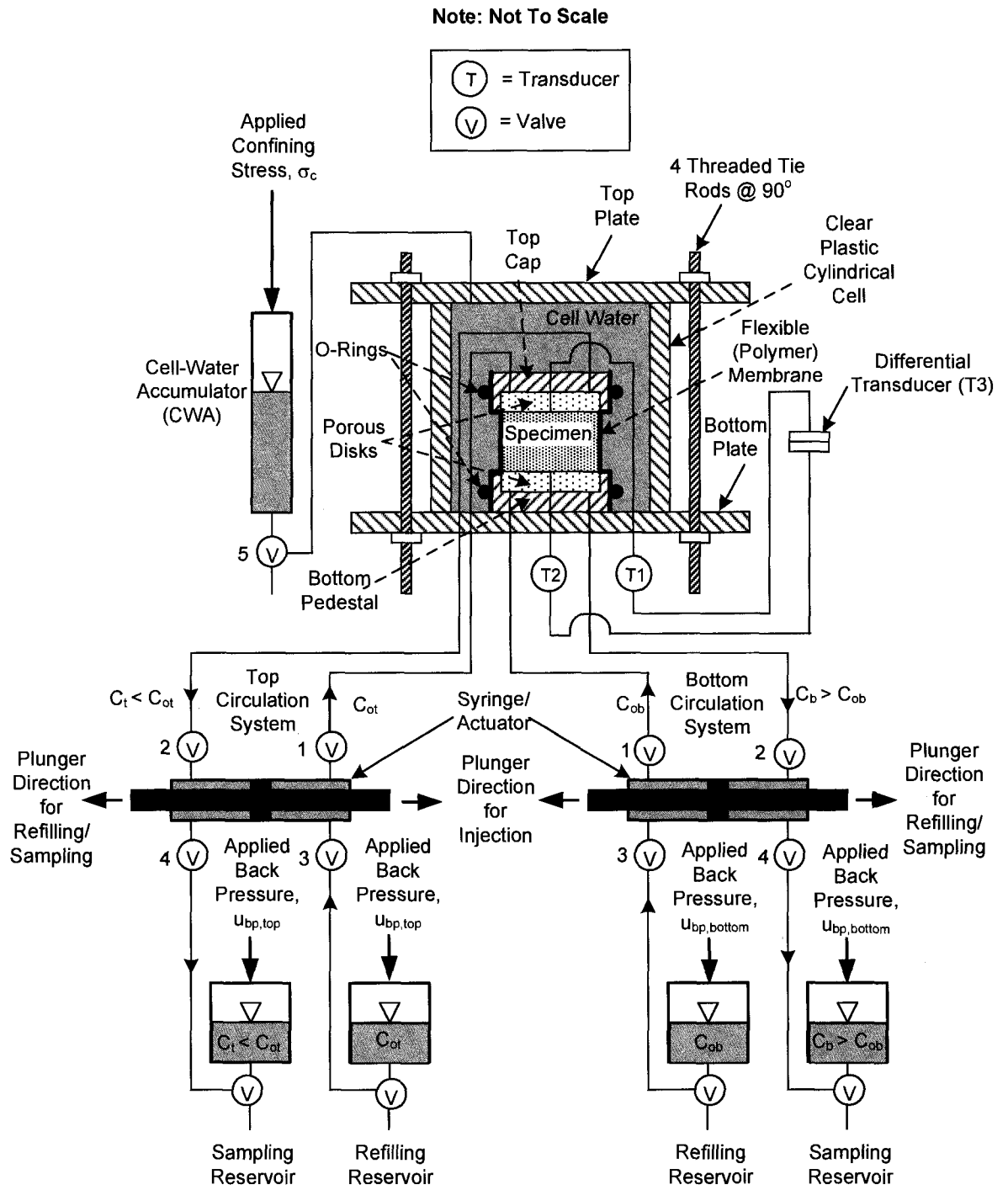


Fig. 4.1 – Schematic cross-section of flexible-wall testing apparatus.

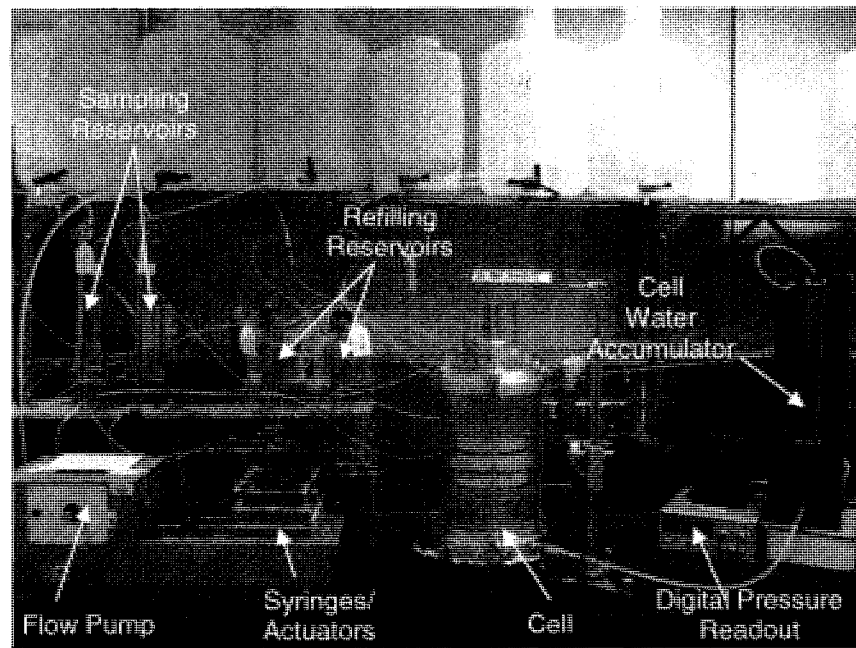
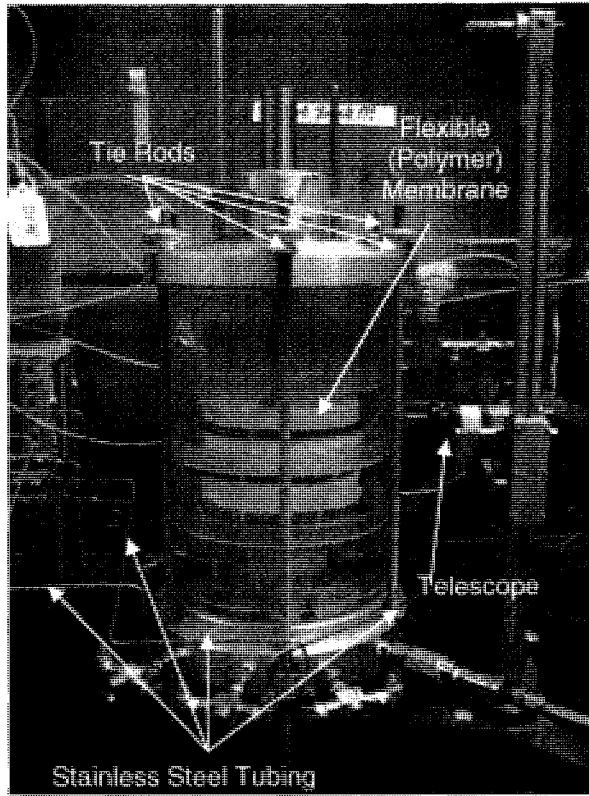


Fig. 4.2 – Pictorial views of flexible-wall cell (top) and cell with entire testing apparatus (bottom).

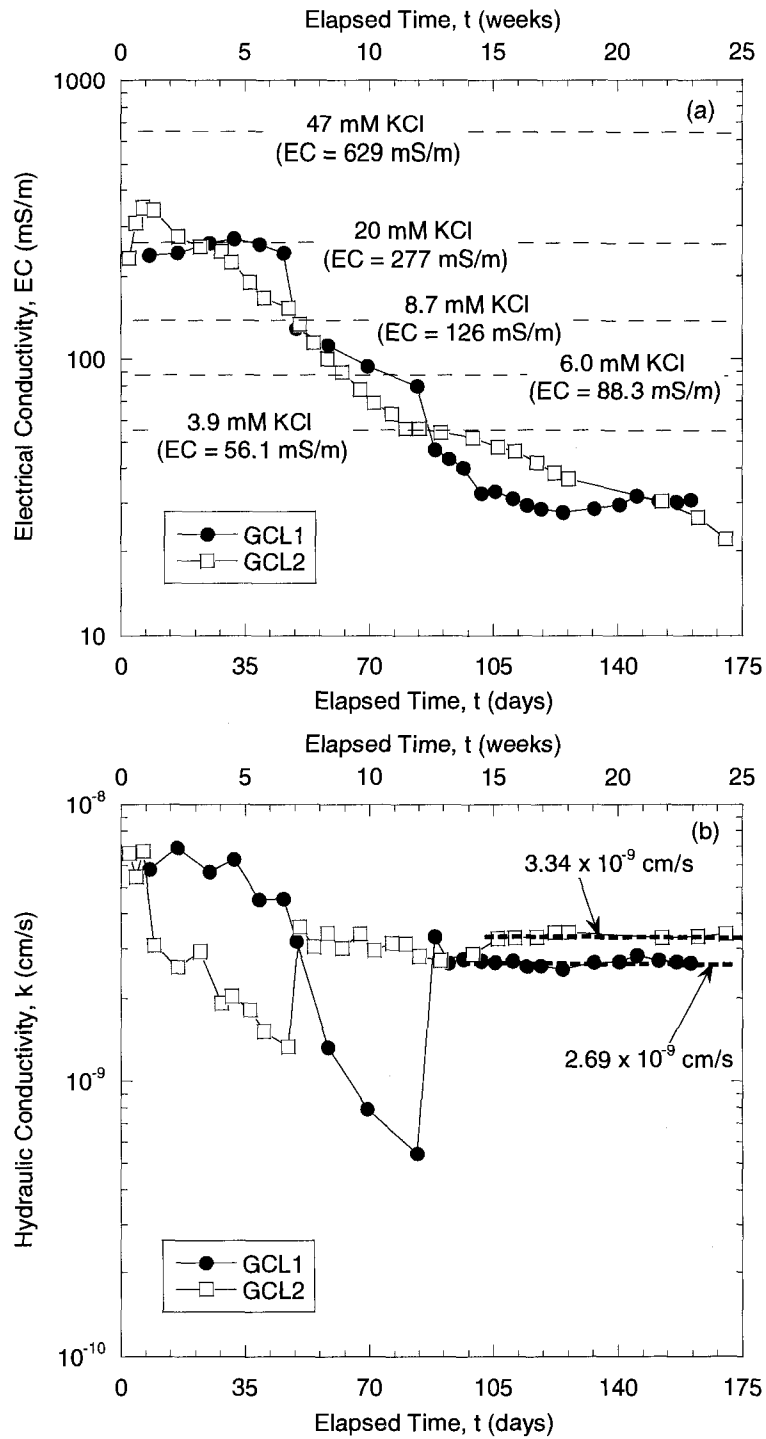


Fig. 4.3 – Electrical conductivity (a) and hydraulic conductivity (b) versus elapsed time for two specimens of a geosynthetic clay liner (GCL) permeated with de-ionized water during flushing stage of test.

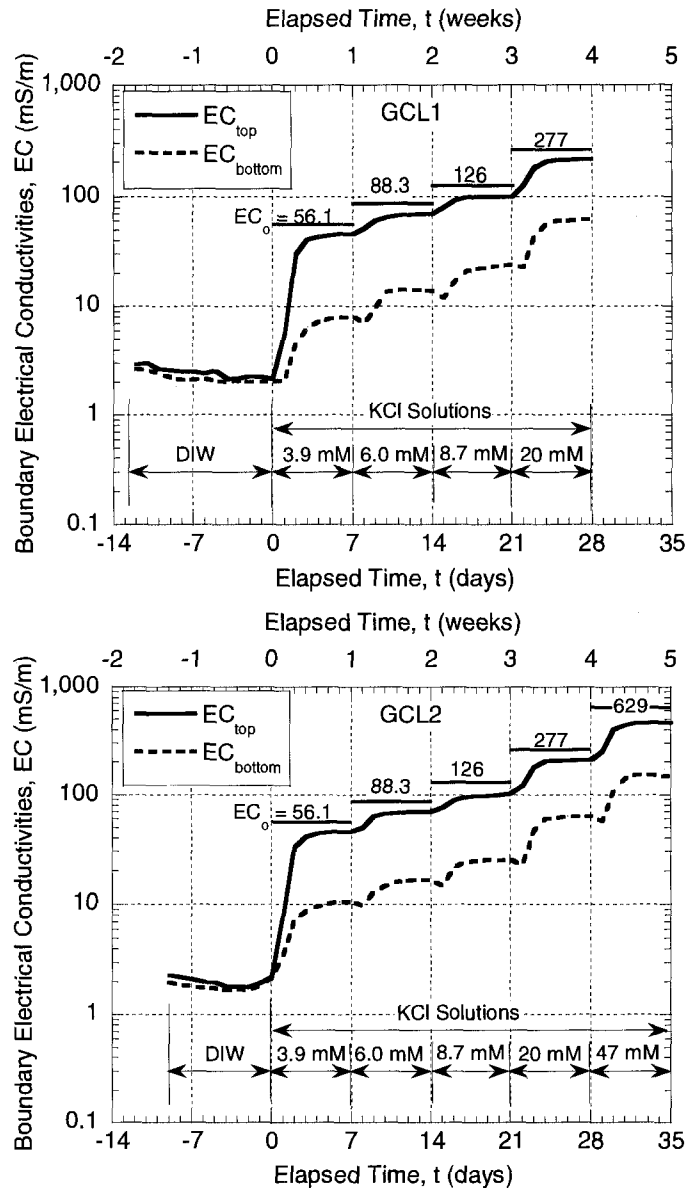


Fig. 4.4 – Electrical conductivity (EC) in circulation outflows from top and bottom boundaries of flexible-wall cell during membrane testing for two specimens of a geosynthetic clay liner (GCL) [$EC_0 = EC$ of KCl source solution].

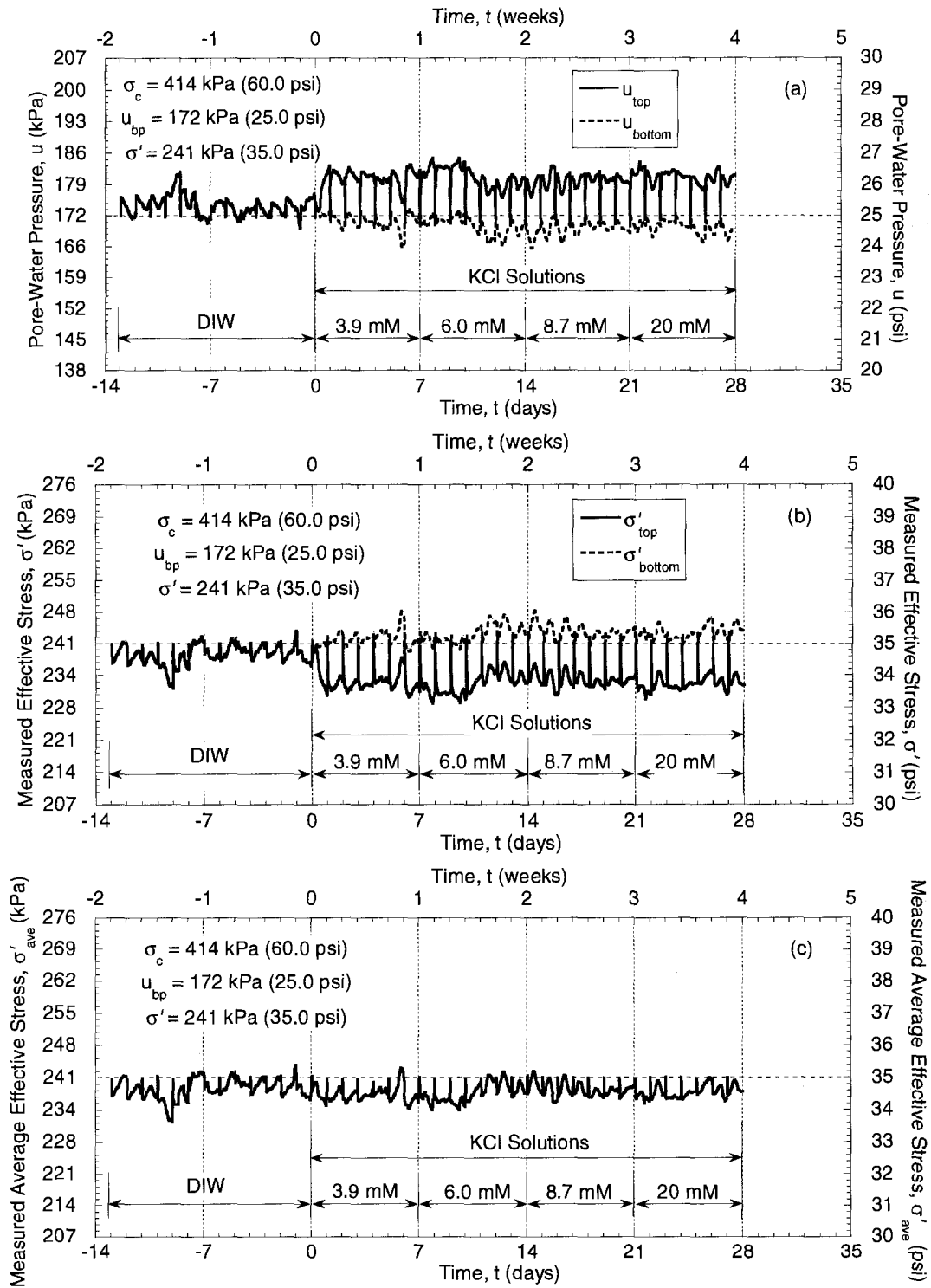


Fig. 4.5 – Boundary pressures and effective stresses in specimen GCL1 during membrane testing in flexible-wall cell.

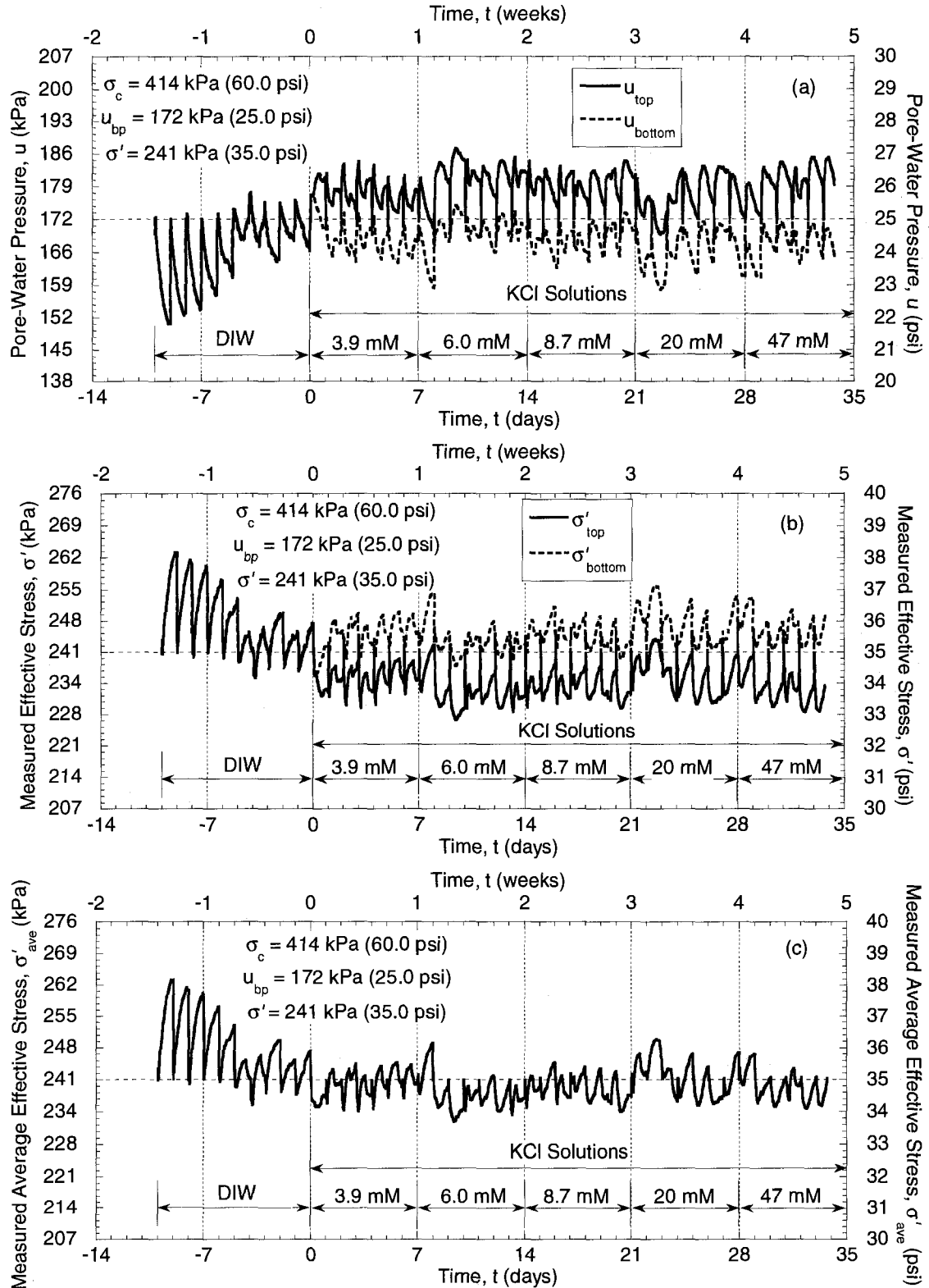


Fig. 4.6 – Boundary pressures and effective stresses in specimen GCL2 during membrane testing in flexible-wall cell.

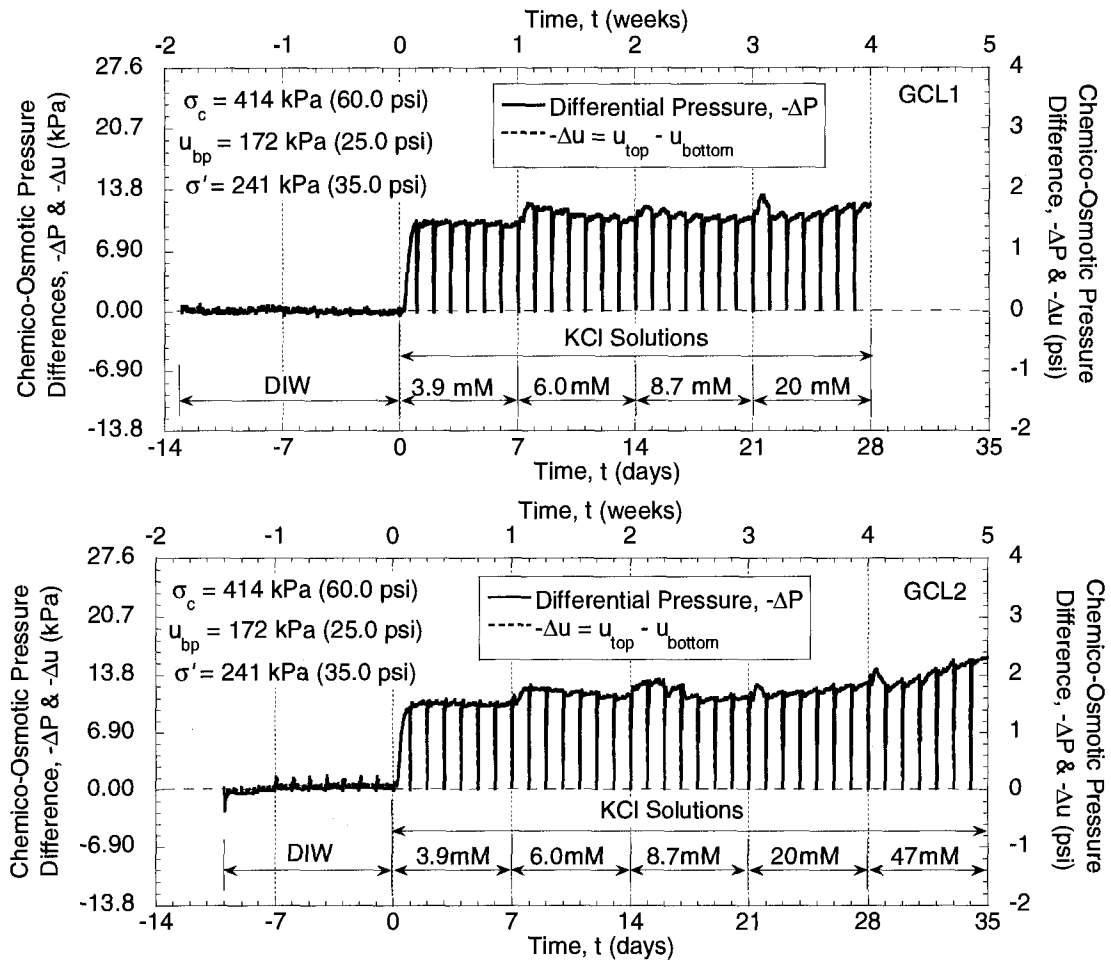


Fig. 4.7 – Measured chemico-osmotic pressure differences across specimens GCL1 and GCL2 during membrane testing in flexible-wall cell.

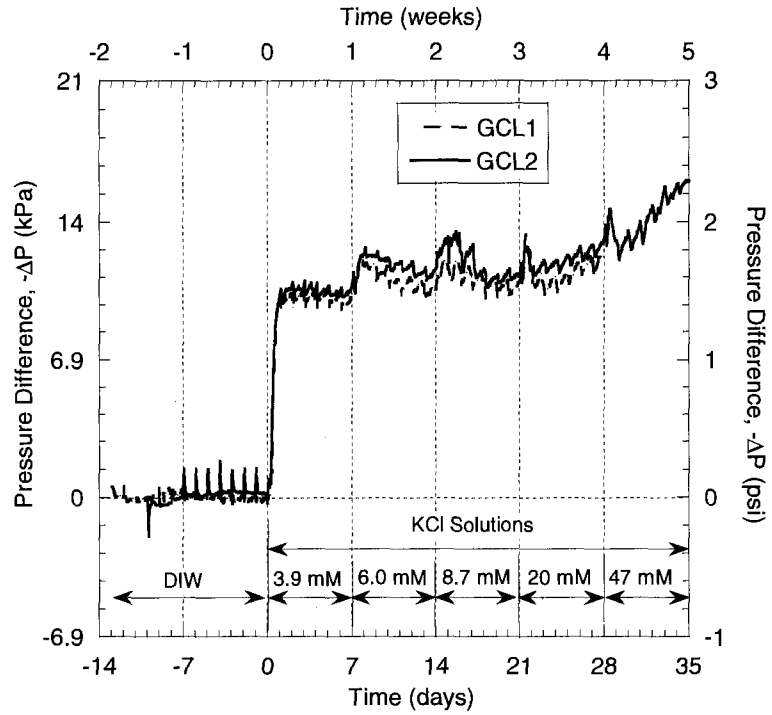


Fig. 4.8 – Measured chemico-osmotic pressure differences versus elapsed time for two specimens of a geosynthetic clay liner (GCL) during multi-stage membrane testing in flexible-wall cell.

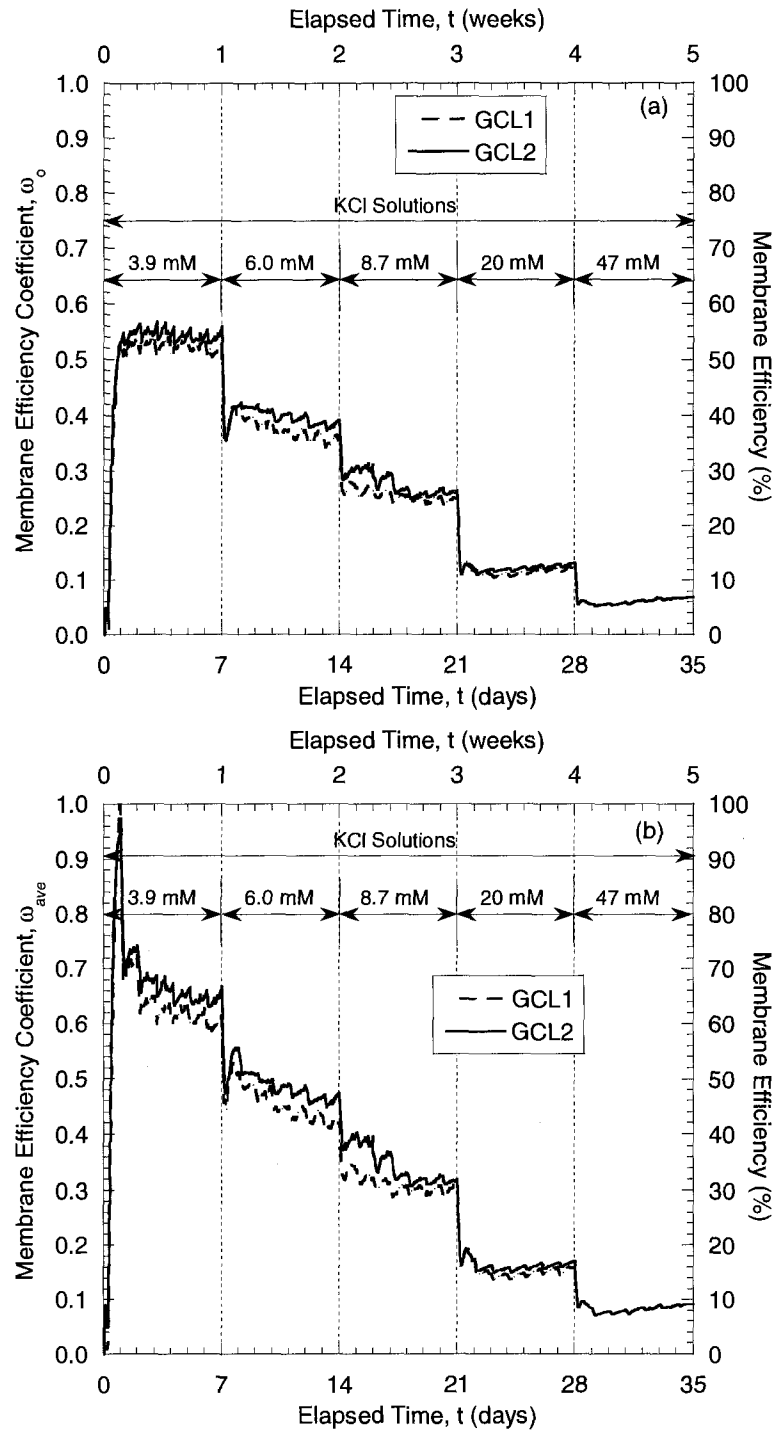


Fig. 4.9 – Comparison of measured membrane efficiencies versus elapsed time based on (a) initial concentration differences ($\Delta\pi_0$) and (b) average concentration differences ($\Delta\pi_{ave}$) for two specimens of a geosynthetic clay liner (GCL) during multi-stage membrane testing in flexible-wall cell.

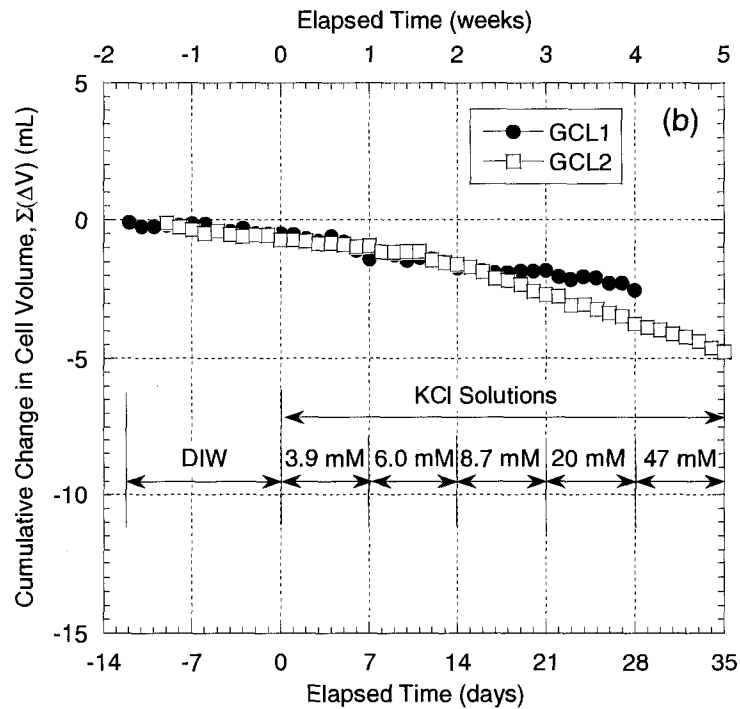
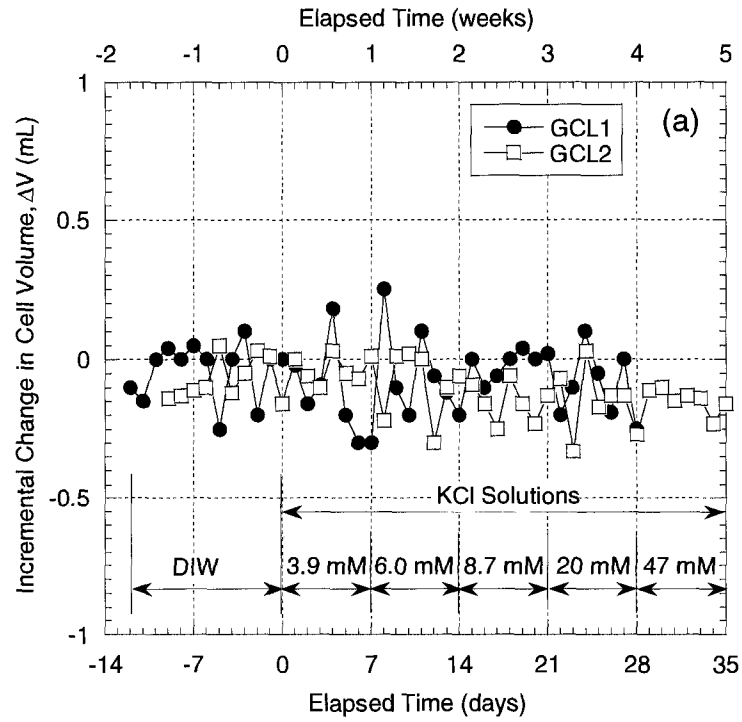


Fig. 4.10 – Incremental (a) and cumulative (b) changes in cell volume for two specimens of a geosynthetic clay liner (GCL) during membrane testing in flexible-wall cell.

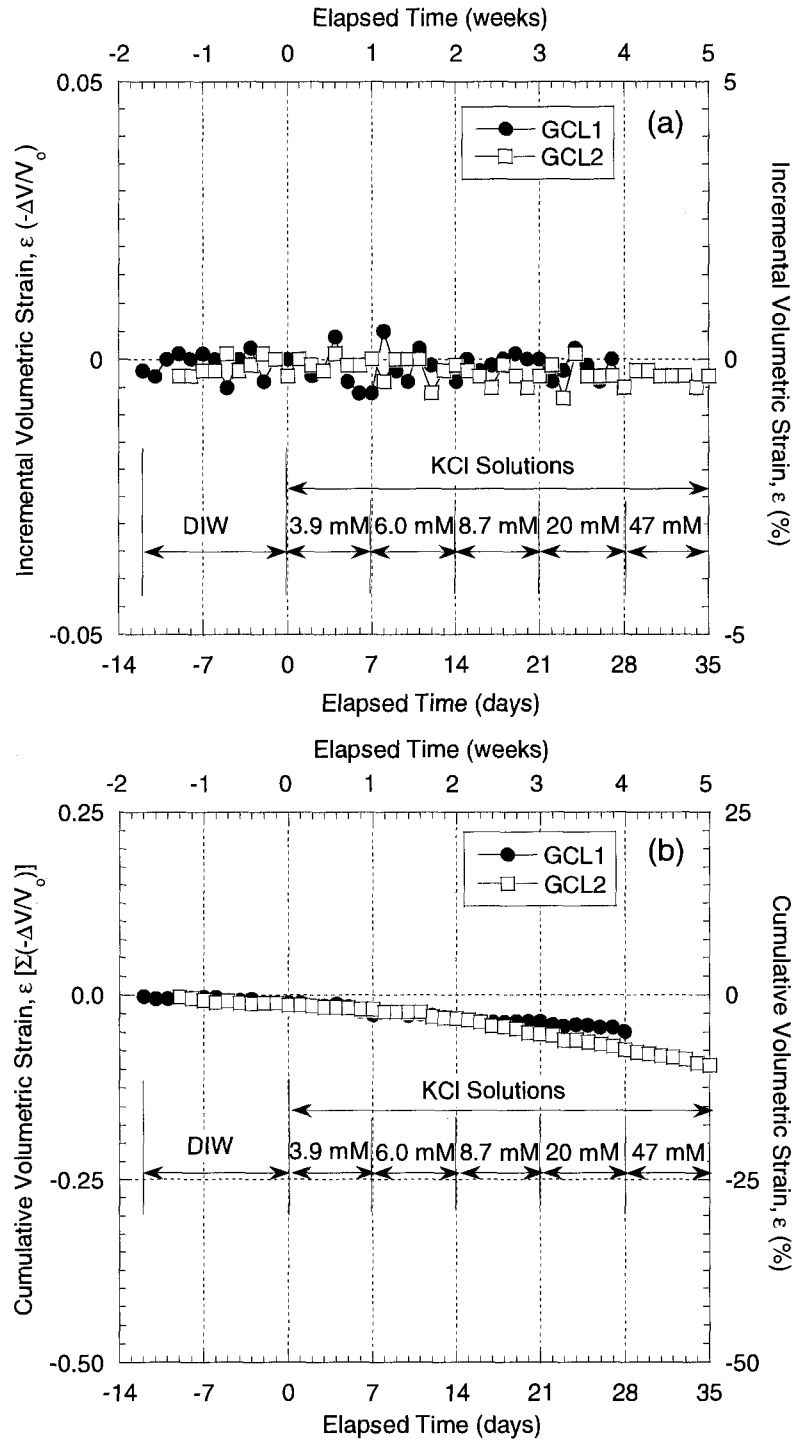


Fig. 4.11 – Incremental (a) and cumulative (b) volumetric strains for two specimens of a geosynthetic clay liner (GCL) during membrane testing in a flexible-wall cell.

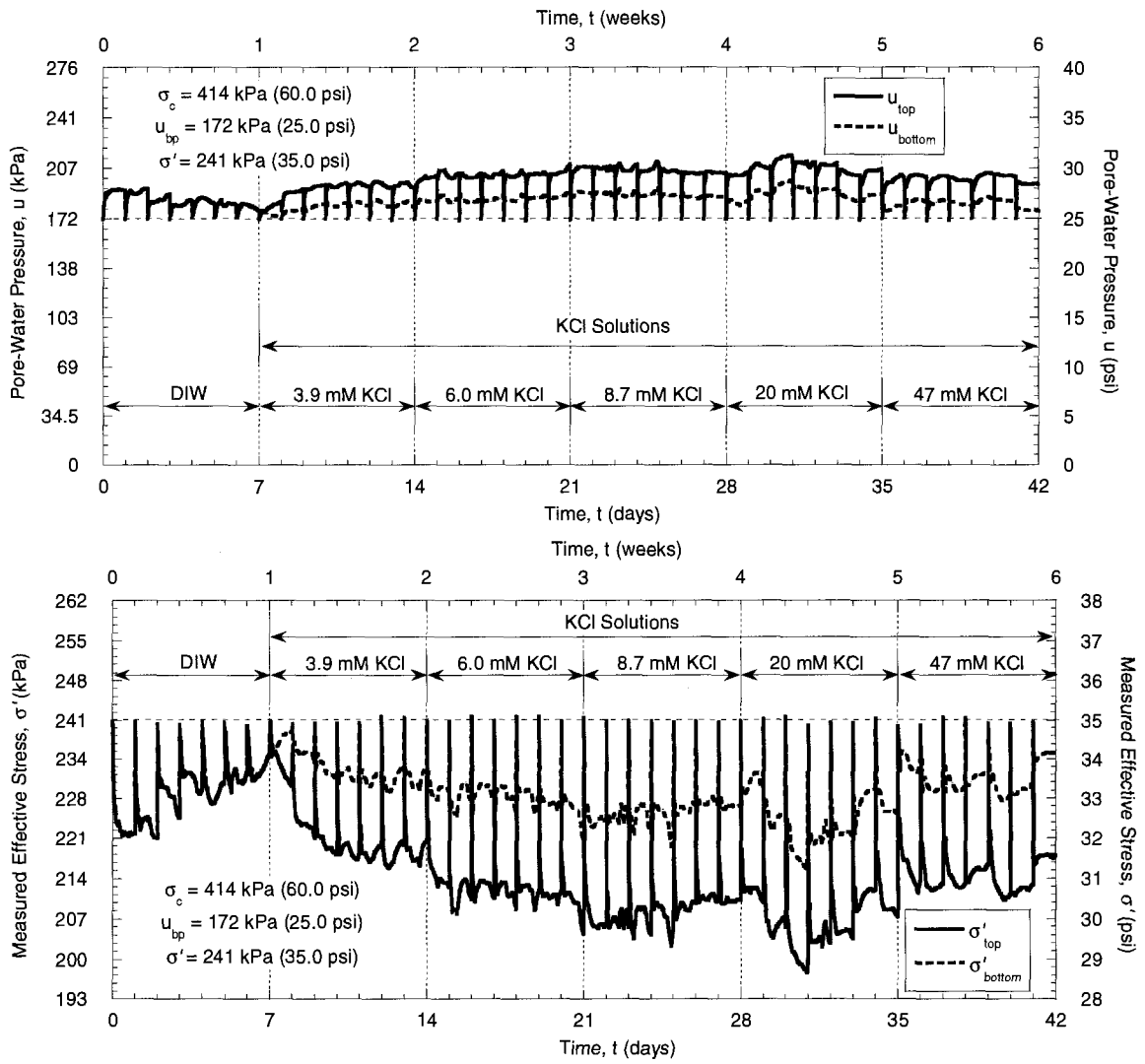


Fig. 4.12 – Boundary pressures and stresses for a preliminary test with valves closed after sampling and refilling syringes.

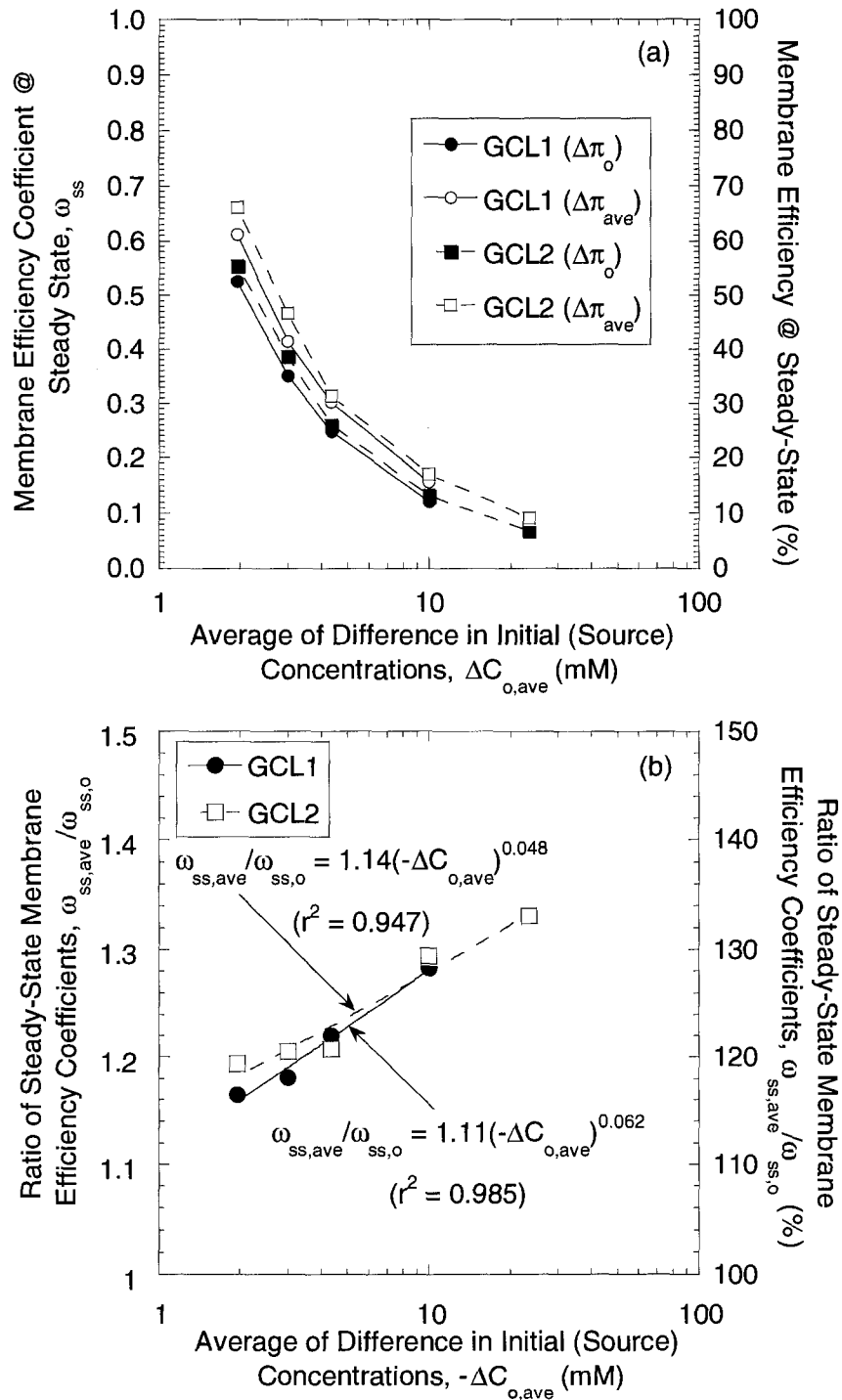


Fig. 4.13 – Steady-state membrane efficiencies versus average of difference in initial (source) KCl concentrations for two GCL specimens: (a) ω_{ss} values based initial concentration differences ($\Delta\pi_o$), $\omega_{ss,o}$, versus average concentration differences ($\Delta\pi_{ave}$), $\omega_{ss,ave}$; (b) ratio of ω_{ss} based on $\Delta\pi_{ave}$ relative to ω_{ss} based on $\Delta\pi_o$.

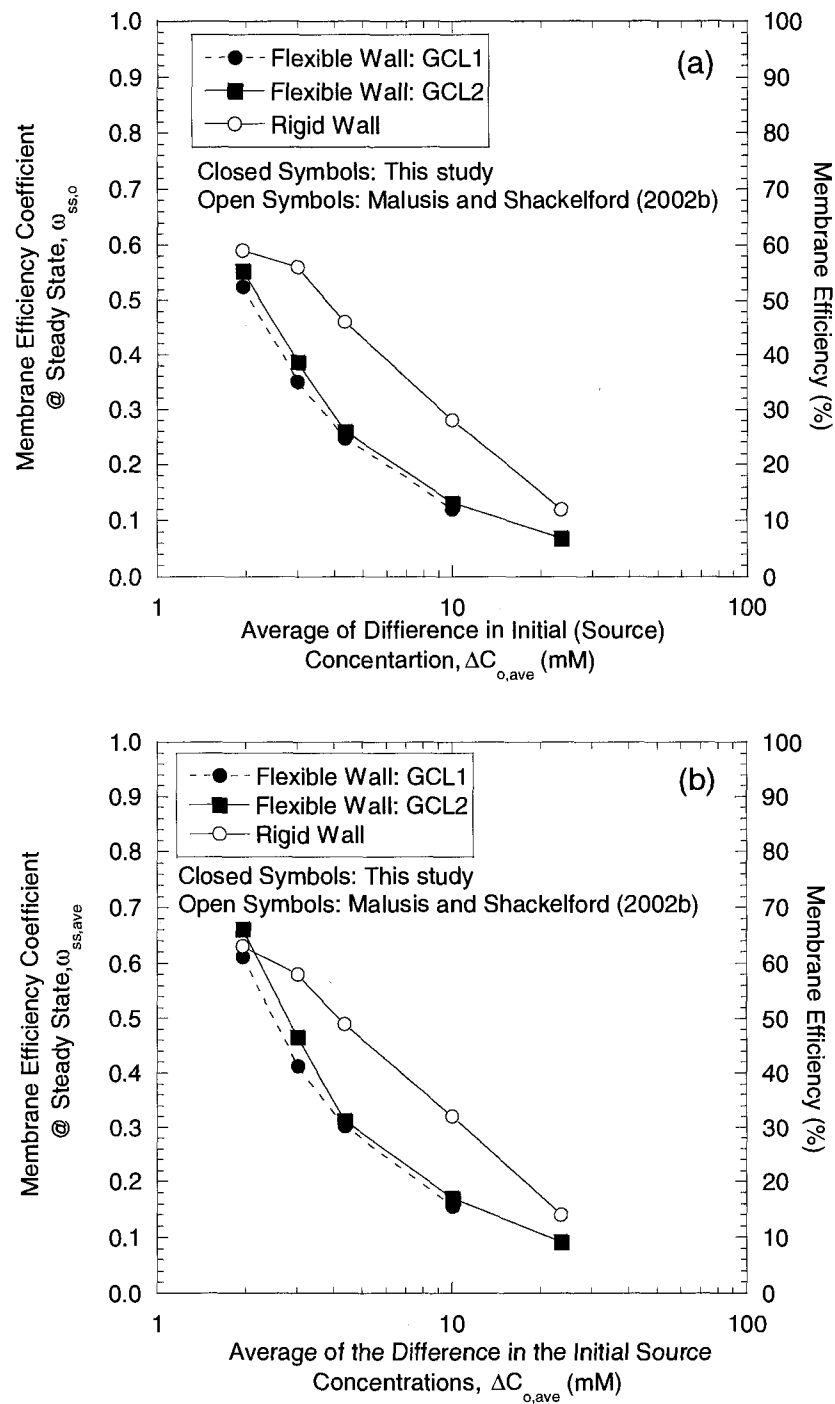


Fig. 4.14 – Membrane efficiency coefficients at steady state based on (a) initial concentration differences ($\Delta\pi_0$) and (b) average concentration differences ($\Delta\pi_{ave}$) as a function of the average of the difference in initial source KCl concentrations and the type of cell used in the measurement.

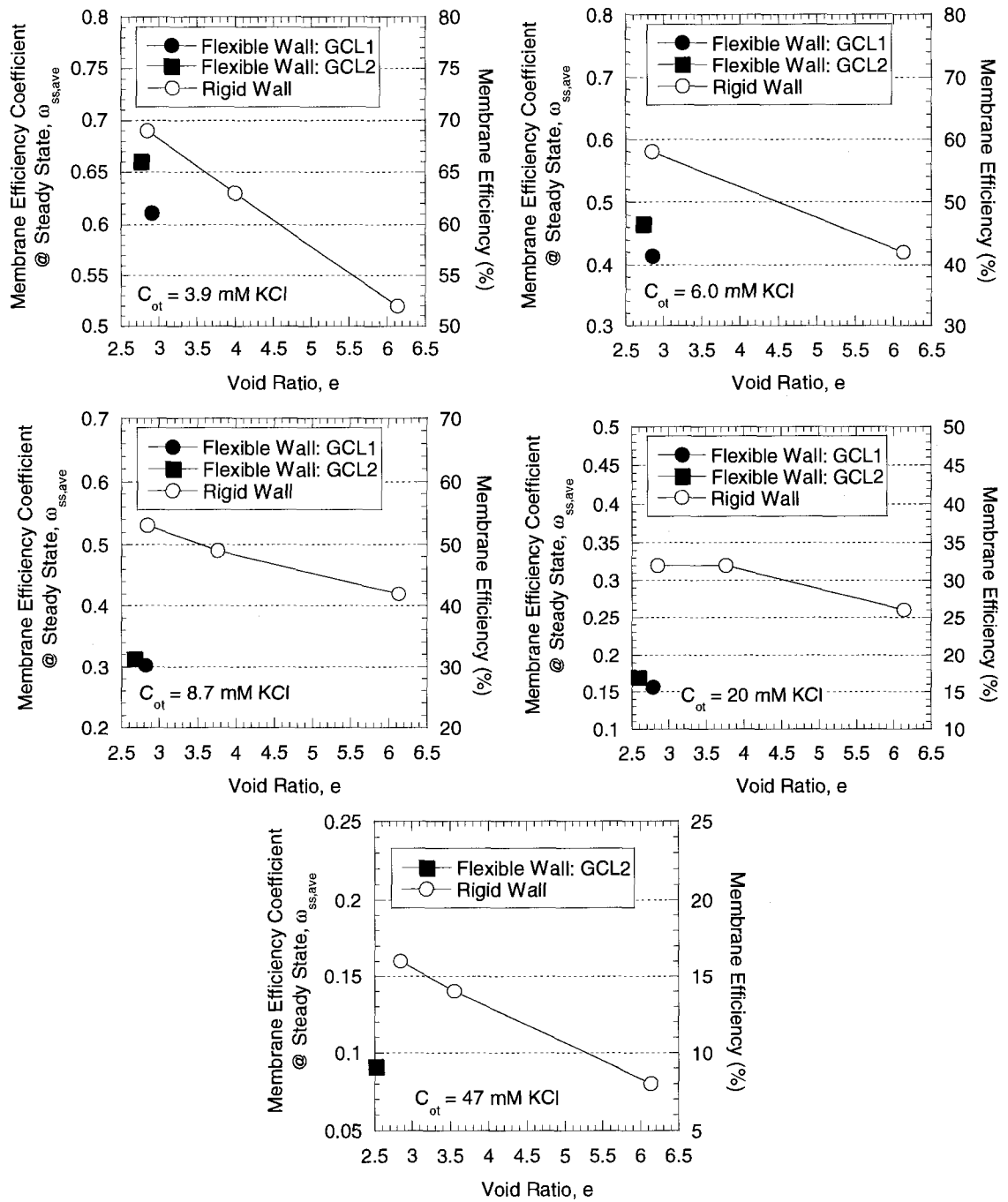


Fig. 4.15 – Membrane efficiency coefficients at steady state versus void ratio as a function of the type of cell used in the measurement (rigid-wall data from Malusis and Shackelford 2002b).

CHAPTER 5

EFFECT OF CONSOLIDATION STRESS ON GCL MEMBRANE BEHAVIOR

ABSTRACT: Semi-permeable membrane behavior in clay soils is a function of mechanical, physical, and chemical factors. In particular, the stress-strain behavior and the state of stress in the clay soil can be important in terms of both the existence and magnitude of clay membrane behavior. Thus, the influence of factors affecting clay membrane behavior such as the applied effective stress can be important. In this regard, the potential effect of effective consolidation stress, σ' , on the membrane efficiency coefficient, ω , of a geosynthetic clay liner (GCL) containing sodium bentonite was evaluated in the laboratory using a flexible-wall membrane cell. Membrane behavior was evaluated by establishing steady KCl concentration differences of 3.9 mM, 6.0 mM, 8.7 mM, 20 mM, and 47 mM across specimens of the GCL under closed-system boundary conditions. The results indicated that an increase in σ' from 34.5 kPa (5.0 psi) to 241 kPa (35.0 psi) resulted in a decrease in void ratio, e , from 1.896 to 4.049 a corresponding increase in ω from 0.015 (1.5 %) to 0.784 (78.4 %), respectively. These trends among σ' , e , and ω are consistent with expected behavior in that lower void ratios correlate with smaller pores and greater restriction in solute migration. The membrane efficiencies measured in this study at relatively high values for σ' of 172 kPa (25.0 psi) and 241 kPa (35.0 psi) also were similar to those previously reported for the same GCL using a rigid-wall cell at unknown states of stress.

Key Words: chemico-osmosis, consolidation, effective stress, geosynthetic clay liner, membrane efficiency, semi-permeable membrane, void ratio

5.1 INTRODUCTION

Geosynthetic clay liners (GCLs) are manufactured hydraulic barriers typically consisting of a thin layer (~ 5 to 10 mm) of natural or treated sodium bentonite sandwiched between two geotextiles or glued to a geomembrane (Daniel 1993, Koerner 1995). The primary differences among GCLs are the mineralogy (e.g., high vs. low content of montmorillonite) and form (e.g., powdery vs. granular) of bentonite used in the GCL, the type of geotextile (e.g., woven vs. non-woven), the hydration condition (e.g., non-prehydrated vs. prehydrated), and the bonding method (Daniel 1993, Koerner 1995, Shackelford et al. 2000, Lee and Shackelford 2005). The structural integrity of GCLs is maintained by one of several bonding methods, such as by stitching, needle punching, and/or adding a chemical adhesive to the bentonite to provide protected handling and installation and enforced in-plane shear strength (Estornell and Daniel 1992, Daniel 1993). The use of GCLs as liners for waste containment has increased over the past decade due to several advantages, including relatively easy installation, invulnerability to weathering, low cost, and low hydraulic conductivity to water (i.e., $\leq 10^{-8}$ cm/s) (Estornell and Daniel 1992, Daniel 1993, Koerner 1995, Lee and Shackelford 2005).

Recent research has indicated that GCLs can behave as semi-permeable membranes, thereby restricting the migration of solutes (e.g., contaminants) (Malusis and Shackelford 2002a,b). Since the purpose of clay soil barriers used in waste containment and *in situ* remediation applications is to restrict the migration of aqueous miscible

contaminants (i.e., solutes), the existence of membrane behavior in GCLs represents a potentially significant beneficial aspect in the use of GCLs for such applications.

In general, semi-permeable membrane behavior in clay soils is a function of mechanical, physical, and chemical factors (Shackelford et al. 2003). For example, Mitchell et al. (1973) studied chemico-osmotic consolidation of clays and concluded that such consolidation was detectable only in highly compressible, active clays such as bentonite. Barbour et al. (1989) also studied the effects of membrane behavior on the consolidation of clays and concluded that the dominant mechanism of volume change associated with brine contamination was osmotic consolidation. Di Maio (1996) performed consolidation tests using salt solutions and reported that changes in the thickness of the DDL were produced by ions diffusing into or out of the clay, and that specific chemical treatment may be a way to cause a lasting improvement in the mechanical properties of active clays. Finally, Olsen (1969) showed that the membrane behavior of kaolin clay could be enhanced by consolidation, with increases in effective consolidation stress corresponding to increases in solute restriction as reflected by increases in membrane efficiency. Thus, the influence of factors affecting clay membrane behavior such as the applied effective stress can be important.

In this regard, the purpose of this study was to evaluate the influence of effective consolidation stress, σ' , on the membrane efficiency coefficient, ω , of a geosynthetic clay liner (GCL) containing sodium bentonite. The GCL evaluated in this study was previously shown to possess semi-permeable membrane behavior (Malusis and Shackelford 2002a,b), but because the measured membrane behavior was based on the use of a rigid-wall cell, the complete states of stress in the GCL specimens were not

known. Accordingly, the membrane behavior of the GCL in this study was based on the use of a newly developed flexible-wall membrane cell (Chapter 4) that allowed for complete control of the state of stress in the GCL specimens, thereby permitting the evaluation of the effect of σ' on ω . As a result, the results of this study represent the first attempt to quantify the potential effect of applied consolidation stress on the membrane behavior of a GCL.

5.2 MATERIALS AND EXPERIMENTAL METHODS

5.2.1 Materials

The GCL tested in this study is the same as that used by Malusis and Shackelford (2002a,b) and is marketed commercially under the trade name Bentomat[®] (Colloid Environmental Technologies Company (CETCO), Lovell, WY). A schematic cross-section of the Bentomat[®] GCL is shown in Fig. 5.1. The physical and chemical properties and the mineralogical composition for the bentonite portion of the GCL are given in Table 5.1.

The GCL is approximately 8-mm thick in an air-dried (i.e., as-shipped) condition. Based on the results of a hydrometer (wet) analysis (ASTM D 422) shown in Fig. 5.2, the GCL bentonite is classified as a high-plasticity clay (CH) according to the Unified Soil Classification System (ASTM D 2487), or USCS. However, the results from the mechanical sieve analysis (ASTM D 421) of the dry bentonite indicate that the dry bentonite actually consists of assemblages or granules of individual clay particles and, therefore, is classified as poorly graded sand (SP) (Malusis and Shackelford, 2002a,b).

The physical and chemical properties as well as the mineralogical composition of

the bentonite portion of the GCL were reported by Malusis and Shackelford (2002a,b). In terms of mineralogy, the bentonite component of the GCL contained 71 % montmorillonite, 7 % mixed layer illite/smectite, 15 % quartz, and 7 % other minerals. The liquid limit (LL) and plastic limit (PL) measured in accordance with ASTM D4318 were reported as 478 % and 39 %, respectively, and the bentonite classified as a high plasticity clay (CH) based on the Unified Soil Classification System (ASTM D2487). The measured cation exchange capacity, or CEC, was reported as 47.7 meq/100 g (= 47.7 cmol_c/kg), and ~ 53 % of the exchange complex was reported as being comprised of exchangeable sodium (i.e., sodium bentonite). Further details regarding the physical and chemical properties of the GCL bentonite are provided by Malusis and Shackelford (2002)

5.2.2 Specimen Assembly and Preparation

Specimen assembly and disassembly consisted of three stages: a flushing stage, a consolidation stage, and a membrane testing stage. For the flushing stage, circular specimens of the Bentomat[®] with nominal diameters of 102 mm were cut from a larger GCL sheet and placed on the base pedestal in the flexible-wall permeameter. Each GCL specimen was permeated under 172 kPa (25.0 psi) backpressure at an average effective stress 34.5 kPa (5.0 psi) with DIW before consolidation testing to saturate the specimen, remove the excess soluble salts, and measure the initial hydraulic conductivity, k .

After completion of the flushing stage, the GCL specimen was transferred to the flexible-wall membrane cell described in Chapter 4 and consolidated to a desired effective stress. A total of four separate GCL specimens were consolidated in a single

loading step to four separate final effective stresses of 34.5, 103, 172, and 241 kPa (5.0, 15.0, 25.0, and 35.0 psi). During the consolidation stage, volume changes were measured via measuring changes in the air-water interface within the cell-water accumulator for the purpose of determining the stress-versus-strain relationship, and to calculate the coefficient of consolidation, c_v , under each effective stress condition.

At the end of consolidation, the drainage lines were close, and the membrane stage of the test started by circulating DIW through the top and bottom boundaries of the specimen at a circulation rate of $4.2 \times 10^{-10} \text{ m}^3/\text{s}$ for approximately seven days to establish a steady baseline differential pressure (Malusis et al. 2000). The membrane efficiency measurements then were initiated by circulating KCl solution through the top piston (i.e., $C_{ot} > 0$) while continuing circulation of DIW in the base pedestal. Thus, in this study, the initial concentration of solute in the base pedestal was maintained at zero (i.e., $C_{ob} = 0$). At the completion of the membrane stage of testing, the cell was disassembled, and the water content of the specimen was measured to determine the final degree of saturation of the specimen. The complete states of stress for each GCL specimen during the flushing, consolidation, and membrane testing stages are summarized in Table 5.2.

5.2.3 Membrane Testing Procedures and Program

Membrane testing procedures was performed using the same procedures as previously described in Chapter 4 (Section 4.4.3). Multiple-stage (MS) membrane tests were conducted. The MS tests consisted of five individual stages in which differential pressures corresponding to five different source KCl solutions (i.e., $C_{ot} = 3.9 \text{ mM}$, 6.0

mM, 8.7 mM, 20 mM, or 47 mM) were measured across the same GCL specimen. These five different source KCl solutions were the same as those previously used by Malusis and Shackelford (2002) for the same GCL and circulation control system but using a rigid-wall membrane cell instead of the flexible-wall membrane cell developed in this study (Chapter 4). Each stage was conducted until a steady differential pressure response across the specimen was observed (i.e., $\Delta P = \text{constant}$ and $EC = \text{constant}$). The complete testing program for this study for determination of the potential membrane behavior for the GCL specimens is shown in Table 5.3.

5.2.4 Correlation of Solute Concentrations with Electrical Conductivity

The KCl concentrations in the circulation outflow at steady state were determined based on electrical conductivity (EC) measurements of the electrolyte solutions in the circulation outflow from the specimen boundaries at steady state in accordance with the calibration shown in Appendix A (Fig. A.1 and Table A.1). This determination is based on the assumption that the only contributions to the EC in the circulation outflow from the specimen boundaries were due solely to the chloride (Cl^-) and potassium (K^+). This assumption was expected to have been reasonably accurate since the GCL specimens were permeated with DIW prior to membrane testing to remove excess soluble salts from the pore water of the specimens.

5.3 RESULTS

5.3.1 Specimen Flushing and Consolidation

The results of the flushing stage of the tests are shown in Fig. 5.3 (a). Specimens

were permeated with DIW until the electrical conductivity, EC, in the effluent from the specimens was only a fraction of that associated with the lowest KCl concentration of 3.9 mM of the source solutions used in the membrane stage of the test. As previously mentioned, this flushing stage was employed primarily to enhance the probability that membrane behavior would be observed in the test specimens (e.g., see Malusis et al 2001b, Malusis and Shackelford 2002b, Shackelford and Lee 2003). In the case of the 34.5 kPa (5.0 psi) average effective stress, the specimen was flushed for 199 d resulting in an effluent EC of 23.4 mS/m, or 41.7 % of the EC of 56.1 mS/m associated with a 3.9 mM KCl solution. In the case of 103 kPa (15.0 psi) average effective stress, the specimen was flushed for 209 d resulting in an effluent EC of 19.5 mS/m, or 34.8 % of the EC of 56.1 mS/m associated with a 3.9 mM KCl solution. In the case of 172 kPa (25.0 psi) average effective stress, the specimen was flushed for 105 d resulting in an effluent EC of 20.8 mS/m, or 37.1 % of the EC of 56.1 mS/m associated with a 3.9 mM KCl solution. In the case of 241 kPa (35.0 psi) average effective stress, the specimen was flushed for 231 d resulting in an effluent EC of 9.5 mS/m, or 16.9 % of the EC of 56.1 mS/m associated with a 3.9 mM KCl solution.

The hydraulic conductivity, k , of the GCL specimens also was measured during the flushing stage. As shown in Fig. 5.3 (b), despite somewhat initial erratic behavior in the measured k values, permeation with DIW eventually resulted in measured steady-state k values of 3.06×10^{-9} cm/s, 2.63×10^{-9} cm/s, 2.41×10^{-9} cm/s, and 3.34×10^{-9} cm/s for specimens consolidated to final effective stresses of 34.5, 103, 172, and 241 kPa (5.0, 15.0, 25.0, and 35.0 psi), respectively. These k values are representative of those typically measured for GCLs permeated with DIW in flexible-wall permeameters and similar

effective stresses (see Daniel et al. 1997).

5.3.2 Strain versus Time

Plots of volumetric strain (ϵ_{vol}) versus both logarithm of time ($\log t$) and square root of time ($t^{1/2}$) for each consolidation stage and each GCL specimen are shown in Fig. 5.4. Volumetric strains were used instead of vertical strains primarily because measurement of volumetric strains was easier and more reliable than was measurement of vertical strains (e.g., see Chapter 3). Also, because of the thinness of the GCL specimens relative to the width (diameter) of the GCL specimens, the volumetric strains were expected to be similar to the vertical strains, such that use of the volumetric strains for evaluation of consolidation properties instead of vertical strains should not result in significant differences in the results (e.g., Chapter 3).

A comparison of the plots in Fig. 5.4 for a given stress indicates that values of ϵ_{vol} increased with increasing effective consolidation stress, σ' , as expected the occurrence of somewhat significant volumetric strains at early elapsed times likely is due to compression of air bubbles, particularly since these early volumetric strains appear to increase with increasing effective consolidation stress.

5.3.3 Coefficients of Consolidation

Values for the coefficient of consolidation, c_v , based on the time-strain plots shown in Fig. 5.4 are summarized in Table 5.4, and plotted as a function of the average of σ' , σ'_{ave} , in Fig. 5.5 based on ϵ_{vol} . As previously noted (Chapter 3), σ'_{ave} is used here instead of the final σ' because values of c_v calculated in accordance with Casagrande's

method are based on the time to achieve 50 % consolidation of the applied loading increment, such that only half of the applied loading increment has been transferred to effective stress.

As indicated in Table 5.4, the value of c_v for GCL specimen at high effective stress conditions ($\sigma'_{ave} = 241$ kPa (35.0 psi)) tended to be greater than that of GCL specimen at low effective stress conditions ($\sigma'_{ave} = 103$ kPa (15.0 psi)), regardless of whether the Casagrande or Taylor method was used for the analysis. As shown in Fig. 5.5, values of c_v based on the Taylor method relative to those based on the Casagrande method, or $c_{v,Taylor}/c_{v,Casagrande}$, are practically the same for both GCL specimens regardless of the value of σ'_{ave} . For example, $c_{v,Taylor}/c_{v,Casagrande}$ ranges from 0.87 to 1.0 for at each effective stress conditions. These results suggest that method of analysis had a relatively minor effect on the determination of c_v for the GCL and test conditions evaluated in this study.

5.3.4 Electrical Conductivities

The values for the electrical conductivity (EC) measured in the circulation outflows from the top (EC_{top}) and bottom (EC_{bottom}) boundaries during the membrane testing stage are shown in Fig. 5.6. These measured EC values reflect the boundary conditions imposed in the tests. As previously mentioned (Chapter 4), the increasing magnitude of EC_{top} upon replacing the DIW with the KCl solutions directly reflects the progressively greater increase in ionic strength of the KCl solutions resulting from the circulation of solutions with progressively higher KCl concentrations. The lower values for EC_{top} relative to the EC values for the source solutions, EC_o (i.e., $EC_{top} < EC_o$), are

consistent with the loss of solute mass from the source solutions due to solute diffusion into the specimens, whereas the eventual increase in the values of EC_{bottom} with time is consistent with the gain of solute mass in the bottom circulation outflow due to solute diffusion through the specimen. Finally, leveling off of the values for both EC_{top} and EC_{bottom} during the 7-d periods applied for each stage of the test reflects the establishment of steady-state conditions with respect to EC in both the top and bottom boundaries. All of these observations are consistent with those previously reported for membrane tests involving rigid-wall cells (e.g., Malusis et al. 2001, Malusis and Shackelford 2002a,b, Shackelford and Lee 2003).

5.3.5 Boundary Pressures

The boundary water pressures occurring at the top (u_{top}) and bottom (u_{bottom}) of the specimens measured with in-line transducers T1 and T2 (see Fig. 4.1), respectively, during the membrane tests are presented in Figs. 5.7 through 5.10 for the GCL specimens. As diffusion of KCl occurs, both chloride (Cl^-) and potassium (K^+) ions exit the bottom boundary of the specimen into the circulating DIW, such that the concentration of KCl in the circulation outflow from the bottom, C_b , is greater than that for the circulation inflow for the bottom, C_{ob} ($= 0$), or $C_b > C_{\text{ob}}$ (e.g., see Fig. 4.1). This increasing salt concentration at the bottom boundary of the specimen tended to reduce the chemical potential of water (e.g., Mitchell and Soga 2005), such that the measured water pressure at the bottom of the specimen typically was slightly lower than the back pressure (i.e., $u_{\text{bottom}} < u_{\text{bp}}$).

The boundary water pressures for the GCL specimen consolidated to an initial

effective stress of 34.5 kPa (5.0 psi) indicate that the measured water pressure at the bottom of the specimen gradually increased to values greater than the back pressure in case of the solutions with relatively high (20 mM and 47 mM) KCl concentrations (e.g., Fig. 5.7a). The reasons for this somewhat anomalous behavior are not entirely clear, but the data suggest that the salt concentration in the lower circulating solution at these higher KCl concentrations is actually lower than that in the previous stages involving the solutions with the lower KCl concentrations (3.9 mM, 6.0 mM, and 8.7 mM).

The tendency of decreasing chemical potential for the water with increasing salt concentration also should hold true for the top circulation boundary, such that one might expect the chemical potential of the water in the top boundary to also have been lower than that for the bottom boundary (i.e., $u_{top} < u_{bottom}$), i.e., since the salt concentrations in the KCl solutions being circulated through the top boundary were greater than those occurring in the bottom boundary (e.g., Fig. 5.6). This expectation would be true in an open system, whereby water could readily flow from bottom to top via chemico-osmosis. However, since the system being evaluated is closed, such that chemico-osmotic flow is prevented, a chemico-osmotic pressure difference, $-\Delta P (> 0)$, builds up across the specimen to counteract the tendency for chemico-osmotic flow, such that the water pressure at the top boundary, $u_{top} [= u_{bottom} + (-\Delta P)]$, is greater than the back pressure, u_{bp} (i.e., $u_{top} > u_{bp} > u_{bottom}$).

Since the confining total stresses, σ_c , of 207, 276, 345, and 414 kPa (30.0, 40.0, 50.0, and 60.0 psi) at 172 kPa (25.0 psi) constant back pressure were maintained constant during the membrane tests for the GCL specimens at each effective stress condition, the variation in u_{top} and u_{bottom} with time also influenced the effective stresses at the top, σ'_{top}

($= \sigma_c - u_{top}$), and bottom, σ'_{bottom} ($= \sigma_c - u_{bottom}$), of the specimen, as shown in Figs. 5.7b through 5.10b. As a result, the average effective stresses in the specimens, σ'_{ave} [$= (\sigma'_{top} + \sigma'_{bottom})/2$], were not constant and also were not equal to each effective stress, σ' , of 34.5, 103, 172, and 241 kPa (5.0, 15.0, 25.0, and 35.0 psi), respectively, as typically would be assumed on the basis of the constant back pressure (Figs. 5.7c through 5.10c).

5.3.6 Induced Chemico-Osmotic Pressures

The measured induced chemico-osmotic pressure differences, $-\Delta P$ (> 0), measured by the differential pressure transducer (T3 in Fig. 4.1) as well as the differences between the pressures measured at the top and bottom of the specimen by the in-line transducers (T1 and T2 in Fig. 4.1), $-\Delta u$ ($= u_{top} - u_{bottom}$), are shown in Fig. 5.11 for GCL specimens. As shown, differences between $-\Delta u$ and $-\Delta P$ were virtually imperceptible for both GCL specimens (i.e., $-\Delta u \approx -\Delta P$). The results shown in Fig. 5.11 also indicate that, whereas virtually no membrane behavior was observed during circulation of DIW through both the top and bottom boundaries of the specimens, significant and sustained membrane behavior occurred in both specimens virtually immediately upon replacing the DIW circulating through the top boundary with KCl solutions. Finally, as shown in Fig. 5.11, close agreement between the values of $-\Delta P$ for the GCL specimens was achieved during DIW circulation, however the values of $-\Delta P$ during circulation through the top boundary with KCl solutions was achieved high values in the GCL specimen with high effective stress conditions (low void ratio).

5.3.7 Induced Membrane Efficiencies

The values of $-\Delta P$ for the GCL specimens shown in Fig. 5.12 correlate with close agreement between the values of the membrane efficiency coefficients, ω , for the each GCL specimen with effective stress conditions 34.5, 103, 172, and 241 kPa (5.0, 15.0, 25.0, and 35.0 psi), regardless of whether the ω values are based on $\Delta\pi$ values using Eq. 4.3 (Fig. 5.14a) or Eq. 4.5 (Fig. 5.14b). In calculating the values for ω shown in Figs. 5.14a and 5.14b, net or "effective" values of $-\Delta P$ (i.e., $-\Delta P_e$) were used corresponding to the measured values of $-\Delta P$ based on circulation with the KCl solutions minus the initial measured values of $-\Delta P$ based on circulation with DIW through both top and bottom boundaries (e.g., see Malusis et al 2001b).

As shown in Fig. 5.14, the values of ω tended to decrease with increasing KCl concentration, which is consistent with previous results based on rigid-wall cells that attributed decreasing ω with increasing salt concentration to a progressively greater collapse of the diffuse double layers (DDLs) surrounding individual clay particles, resulting in larger pores and correspondingly less restriction of solutes (e.g., Malusis et al. 2001a, Malusis and Shackelford 2002b, Shackelford et al. 2003). Also, the values of ω were relatively constant over any interval of time corresponding to a given KCl concentration, implying that steady-state conditions were achieved during the 7-d circulation periods.

This non-zero baseline pressure difference measured while $C_{ot} = C_{ob} = 0$ in the tests can be attributed to slight differences in the hydraulic resistance of the porous stones at the opposite ends of the specimen and, therefore, is not included in the chemico-osmotic efficiency evaluation (Malusis and Shackelford, 2002b). Introduction of KCl into

the top cap after the initial seven days resulted in an immediate and rapid increase in the pressure differences in each test. Values of effective or net pressure difference measured across specimen at steady state, $-\Delta P_e$, ranged from 2.3 kPa to 9.0 kPa (from 0.3 to 1.3 psi) in multiple-stage test No. 1 ($\sigma' = 34.5$ kPa (5.0 psi)), from 9.5 kPa to 11.2 kPa (from 1.4 to 1.6 psi) in multiple-stage test No. 2 ($\sigma' = 103$ kPa (15.0 psi)), from 12.6 kPa to 17.2 kPa (from 1.8 to 2.5 psi) in multiple-stage test No. 3 ($\sigma' = 172$ kPa (25.0 psi)), and from 12.9 kPa to 18.2 kPa (from 1.9 to 2.6 psi) in multiple-stage test No. 4 ($\sigma' = 241$ kPa (35.0 psi)). Measured membrane efficiency coefficients at steady-state, ω_{ss} , based on the data are shown in Table 5.6.

5.3.8 Volume Changes

Volume changes were recorded during the membrane testing stage via the cell-wall accumulator (CWA in Fig. 4.1) as a check on the assumption of undrained conditions. As shown in Fig. 5.15, some incremental volume changes, ΔV , of ± 0.36 mL, ± 0.33 mL, ± 0.24 mL, ± 0.47 mL) were recorded during the membrane testing stage, resulting in cumulative volume changes, $\Sigma(\Delta V)$, of -5.98 mL, -2.33 mL, -1.95 mL, and -5.12 mL for GCL specimens of 34.5, 103, 172, and 241 kPa (5.0, 15.0, 25.0, and 35.0 psi) average effective stress, respectively. As shown in Fig. 5.16, these volume changes corresponded to incremental volumetric strains ($\Delta V/V_0$) ranging from 0.4 % to 0.6 % and cumulative volumetric strains ($\Sigma(\Delta V)/V_0$) ranging from -2.9 % to -7.9 % for GCL specimens, respectively. As previously described, even though volume change was prevented from occurring during the actual measurement of the membrane efficiency of the GCL specimens (i.e., during KCl circulation between sampling/refilling periods),

some volume change did occur as a result of the sampling/refilling procedure and the desire to re-establish the reference (back) pressure before each daily circulation event. The resulting volume changes that did occur tended to be relatively low ($\leq -7.9\%$), although the magnitude of the impact of these volume changes on the measured membrane efficiencies cannot be quantified. In general, a decreasing specimen volume results in decreasing pore (void) space, which would be expected to increase solute restriction and, therefore, increase membrane efficiency coefficient (ω). The history of porosities and void ratios during consolidation and membrane testing for specimens of GCLs consolidated to an initial effective stress of 34.5, 103, 172, and 241 kPa (5.0, 15.0, 25.0 and 35.0 psi) tested in a flexible-wall cell is plotted in figs. 5.23 and 5.24 as a function of the elapsed time.

5.4 DISCUSSION

The final, or steady-state, values of ω for each KCl concentration, ω_{ss} , along with the values of $-\Delta P_e$, $-\Delta\pi_o$, and $-\Delta\pi_{ave}$ used to calculate ω_{ss} , are summarized in Table 5.6. The resulting values of ω_{ss} are plotted as a function of the average difference in the initial KCl concentrations, or $-\Delta C_{o,ave}$ [$= -\Delta C_o/2 = (C_{ot} - C_{ob})/2 = C_{ot}/2$], in Fig. 5.20a.

As expected, values of ω_{ss} based on $-\Delta\pi_o$, or $\omega_{ss,o}$, are more conservative (lower) than values of ω_{ss} based on $-\Delta\pi_{ave}$, or $\omega_{ss,ave}$, i.e., since $-\Delta\pi_o > -\Delta\pi_{ave}$. In fact, as shown in Fig. 5.20b, values of $\omega_{ss,ave}/\omega_{ss,o}$ increased virtually semi-log linearly with $-\Delta C_{o,ave}$. For example, $\omega_{ss,ave}/\omega_{ss,o}$ increased from 1.31 to 1.52 as $-\Delta C_{o,ave}$ increased from 1.95 mM to 23.5 mM, respectively, for the GCL specimen consolidated to 34.5 kPa (5.0 psi) effective stress, whereas $\omega_{ss,ave}/\omega_{ss,o}$ increased from 1.17 to 1.39 as $-\Delta C_{o,ave}$ increased from 1.95

mM to 23.5 mM, respectively, for specimen of 103 kPa (15.0 psi) effective stress, and $\omega_{ss,ave}/\omega_{ss,0}$ increased from 1.13 to 1.39 as $-\Delta C_{o,ave}$ increased from 1.95 mM to 23.5 mM, respectively, for specimen of 172 kPa (25.0 psi) effective stress, whereas $\omega_{ss,ave}/\omega_{ss,0}$ increased from 1.15 to 1.33 as $-\Delta C_{o,ave}$ increased from 1.95 mM to 23.5 mM, respectively, for specimen of 241 kPa (35.0 psi) effective stress.

Values of ω_{ss} measured in this study using the flexible-wall cell under closed-system boundary conditions are compared in Fig. 5.21 with values of ω_{ss} previously reported by Malusis and Shackelford (2002b) for the same GCL and same source KCl concentrations measured using a rigid-wall cell under closed-system boundary conditions. As expected and previously discussed, the membrane efficiencies decrease with increasing KCl concentration regardless of whether the flexible-wall or rigid-wall cell is used in the measurement. However, at least two distinct differences in the membrane efficiencies based on the flexible-wall cell versus those based on the rigid-wall cell are apparent. First, except for the values of $\omega_{ss,ave}$ at the lowest $\Delta C_{o,ave}$ concentration of 1.95 mM KCl (i.e., $C_{ot} = 3.9$ mM KCl), the membrane efficiencies based on the flexible-wall cell are lower than those based on the rigid-wall cell at any given value of $\Delta C_{o,ave}$ except $\Delta C_{o,ave}$ concentration of 1.95 mM and 3.0 mM KCl in the GCL specimen of 172 and 241 kPa (25.0 and 35.0 psi) effective stress. Second, whereas the membrane efficiency of the GCL based on the rigid-wall cell decreases essentially semi-log linearly with increasing $\Delta C_{o,ave}$, the decrease in the membrane efficiency of the GCL based on the flexible-wall cell with increasing logarithm of $\Delta C_{o,ave}$ is non-linear.

As shown in Fig. 5.23, these observed differences in the membrane efficiencies based on the flexible-wall cell versus those based on the rigid-wall cell cannot be

attributed entirely to differences in the void ratios of the specimens, since for any given concentration of KCl in the source solution (i.e., C_{ot}), the void ratios for the GCL specimens tested in the flexible-wall cell were at or lower than the lower range of void ratios for the same GCL tested in the rigid-wall cell.

5.5 SUMMARY AND CONCLUSIONS

The potential effect of the application of different consolidation effective stress on the observed membrane behavior of a GCL containing sodium bentonite using developed flexible-wall cell in a closed (no-flow) system that can be used to measure the membrane behavior of clays was evaluated. The GCL specimens were consolidated to a final effective stress, σ' , of 34.5, 103, 172, and 241 kPa (5.0, 15.0, 25.0, and 35.0 psi) prior to the start of membrane testing. Membrane testing consisted of multi-stage (MS) tests, whereby de-ionized water (DIW) was first circulated across both the bottom and the top of the specimens to establish a baseline pressure difference, $-\Delta P (> 0)$, of the specimen, followed by circulation of source KCl solutions across the top of the specimen (while maintaining DIW circulation across the bottom of the specimen) with sequentially higher source concentrations, C_{ot} , of KCl to establish the salt concentration differences, $-\Delta C (= C_{ot})$, required to evaluate the potential for membrane behavior.

The results indicated that the GCL behaved as a semi-permeable membrane, with measured membrane efficiencies at steady state, ω_{ss} , based on the difference in initial (source) concentrations, $\omega_{ss,o}$, ranging from 0.01 ($\sigma' = 34.5$ kPa (5.0 psi)) at C_{ot} of 47 mM KCl to 0.68 ($\sigma' = 241$ kPa (35.0 psi)) at C_{ot} of 3.9 mM KCl, and ω_{ss} values based on the average of the difference in boundary concentrations, $\omega_{ss,ave}$, ranging from 0.02 ($\sigma' = 34.5$

kPa (5.0 psi)) at C_{ot} of 47 mM KCl to 0.78 ($\sigma' = 241$ kPa (35.0 psi)) at C_{ot} of 3.9 mM KCl. Also, both $\omega_{ss,o}$ and $\omega_{ss,ave}$ decreased with increasing C_{ot} , which is consistent with previous findings based on the use of a rigid-wall cell and attributable to progressively greater collapse of the electrostatic diffuse double layers surrounding individual clay particles with increasing salt concentration in the pore water. Finally, $\omega_{ss,ave}$ was always greater than $\omega_{ss,o}$, with values for the ratio of $\omega_{ss,ave}$ to $\omega_{ss,o}$, or $\omega_{ss,ave}/\omega_{ss,o}$, increasing with increasing average difference in the initial KCl concentrations, or $-\Delta C_{o,ave} [=C_{ot}/2]$. For example, $\omega_{ss,ave}/\omega_{ss,o}$ increased from 1.31 to 1.52 as $-\Delta C_{o,ave}$ increased from 1.95 mM to 23.5 mM, respectively, for specimen of 34.5 kPa (5.0 psi) effective stress, whereas $\omega_{ss,ave}/\omega_{ss,o}$ increased from 1.17 to 1.39 as $-\Delta C_{o,ave}$ increased from 1.95 mM to 23.5 mM, respectively, for specimen of 103 kPa (15.0 psi) effective stress, and $\omega_{ss,ave}/\omega_{ss,o}$ increased from 1.13 to 1.39 as $-\Delta C_{o,ave}$ increased from 1.95 mM to 23.5 mM, respectively, for specimen of 172 kPa (25.0 psi) effective stress, whereas $\omega_{ss,ave}/\omega_{ss,o}$ increased from 1.15 to 1.33 as $-\Delta C_{o,ave}$ increased from 1.95 mM to 23.5 mM, respectively, for specimen of 241 kPa (35.0 psi) effective stress.

Values of ω_{ss} measured in this study using the developed flexible-wall cell under closed-system boundary conditions were compared with values of ω_{ss} for the same GCL previously measured using a rigid-wall cell under the same closed-system boundary conditions. As expected, the membrane efficiencies decrease with increasing KCl concentration regardless of whether the flexible-wall or rigid-wall cell was used in the measurement.

The results in measured membrane efficiencies based on average effective stress conditions in the flexible-wall cell indicate that increase in effective stress results in a

decrease in void ratio (e) whereas an increase of the membrane efficiency coefficient, ω . These trends among the effective stress (σ'), void ratio (e), and membrane efficiency coefficient (ω) are consistent with expected behavior in that lower void ratios in clays correlate to higher effective stress and greater membrane efficiency.

ACKNOWLEDGMENTS

Financial support for this study was provided by the U. S. National Science Foundation (NSF), Arlington, VA, under Grants CMS-0099430 entitled, "Membrane Behavior of Clay Soil Barrier Materials" and CMS-0624104 entitled, "Enhanced Clay Membrane Barriers for Sustainable Waste Containment". The opinions expressed in this paper are solely those of the writers and are not necessarily consistent with the policies or opinions of the NSF. The authors also express appreciation to Dr. Jae-Myung Lee of the California Department of Transportation for his assistance in the early stages of the development of the flexible-wall testing apparatus.

5.6 REFERENCES

- Barbour, S. L. and Fredlund, D. G. 1989. Mechanisms of osmotic flow and volume change in clay soils. *Canadian Geotechnical Journal*, Vol. 26, No. 4, 551-562.
- Daniel, D. E., Shan, H.-Y., and Anderson, J. D. 1993. Effects of partial wetting on the performance of the bentonite component of a geosynthetic clay liner. *Geosynthetics '93*, Industrial Fabrics Association International, St. Paul, Minnesota, USA, 3, 1483-1496.
- Daniel, D.E. 1994. State-of-the-art: Laboratory hydraulic conductivity test for saturated

- soils. *Hydraulic Conductivity and Waste Contaminant Transport in Soil*, ASTM STP 1142, D.E Daniel and S.J. Trautwein (Eds.), ASTM, West Conshohoken, PA, 30-78.
- Daniel, D. E., Shan, H.-Y., and Anderson, J. D. 1993. Effects of partial wetting on the performance of the bentonite component of a geosynthetic clay liner. *Geosynthetics '93*, Industrial Fabrics Association International, St. Paul, Minnesota, USA, 3, 1483-1496.
- Daniel, D.E., Anderson, D.C., and Boynton, S.S. 1985. Fixed-wall versus flexible-wall permeameters. *Hydraulic Barriers in Soil and Rock*, ASTM STP 874, A. I. Johnson, R. K. Frobels, N. J. Cavalli, and C. B. Pettersson (Eds.), ASTM, West Conshohoken, PA, 107-126.
- Daniel, D.E., Bowders, J.J., and Gilbert, R.B. 1997. Laboratory hydraulic conductivity testing of GCLs in flexible-wall permeameters. *Testing and Acceptance Criteria for Geosynthetic Clay Liners*, ASTM STP 1308, L. Well (Ed.), ASTM, West Conshohoken, PA, 208-226.
- Di Maio, C. 1996. Exposure of bentonite to salt solution: osmotic and mechanical effects. *Geotechnique*, Vol. 46, No. 4, 695-707.
- Estornell, P. and Daniel, D. 1992. Hydraulic conductivity of three geosynthetic clay liners. *Journal of Geotechnical Engineering*, 118(10), 1592-1606.
- Fritz, S.J. 1986. Ideality of clay membranes in osmotic process: A review. *Clays and Clay Minerals*, 34(2), 214-223.
- Fritz, S.J. and Marine, I.W. 1983. Experimental support for a predictive osmotic model of clay membranes. *Geochimica et Cosmochimica Acta*, 47(8), 1515-1522.

- Hanshaw, B.B. and Coplen, T.B. 1973. Ultrafiltration by a compacted clay membrane – II. Sodium ion exclusion at various ionic strengths. *Geochimica et Cosmochimica Acta*, 37(10), 2311-2327.
- Keijzer, Th.J.S., Kleingeld, P.J., and Loch, J.P.G. 1997. Chemical osmosis in compacted clayey material and the prediction of water transport. *Geoenvironmental Engineering, Contaminated Ground: Fate of Pollutants and Remediation*, R. N. Yong and H. R. Thomas (Eds.), University of Wales, Cardiff, U. K., Sept. 6-12, Thomas Telford Publ., London, 199-204.
- Kemper, W.D. and Rollins, J.B. 1966. Osmotic efficiency coefficients across compacted clays. *Soil Science Society of America Proceedings*, 30(5), 529-534.
- Koerner, R. M. and Daniel, D. E. 1995. A suggested methodology for assessing the technical equivalency of GCLs to CCLs. *Geosynthetic Clay Liners*, R. M Koerner, E. Gartung, and H. Zanzinger, eds., Balkema, Rotterdam, 73-98.
- Lee, J.-Y. and Shackelford, C. D. 2005a. Impact of bentonite quality on hydraulic conductivity of geosynthetic clay liners. *Journal of Geotechnical and Geoenvironmental Engineering*, 131(1), 64-77.
- McKelvey, J. G. and Milne, I. H. 1962. The flow of salt solutions through compacted clay. *The American Association of Petroleum Geologists Bulletin*, 60 (6), 973-980.
- Malusis, M.A. 2001. *Membrane Behavior and Coupled Solute Transport through a Geosynthetic Clay Liner*. PhD Dissertation, Colorado State University, Fort Collins, Colorado.
- Malusis, M.A. and Shackelford, C.D. 2002a. Coupling effects during steady-state solute

- diffusion through a semipermeable clay membrane. *Environmental Science and Technology*, 36(6), 1312-1319.
- Malusis, M.A. and Shackelford, C.D. 2002b. Chemico-osmotic efficiency of a geosynthetic clay liner. *Journal of Geotechnical and Geoenvironmental Engineering*, 128(2), 97-106.
- Malusis, M.A., Shackelford, C.D., and Olsen, H.W. 2001a. Flow and transport through clay membrane barriers. *Geoenvironmental Engineering: Geoenvironmental Impact Management*, R. N. Young and H. R. Thomas (Eds.), Thomas Telford Ltd., London, 334-341.
- Malusis, M.A., Shackelford, C.D., and Olsen, H.W. 2001b. A laboratory apparatus to measure chemico-osmotic efficiency coefficients for clay soils. *Geotechnical Testing Journal*, 24(3), 229-242.
- Malusis, M.A., Shackelford, C.D., and Olsen, H.W. 2003. Flow and transport through clay membrane barriers. *Engineering Geology*, 70(3), 235-248.
- Marine, I.W. and Fritz, S.J. 1981. Osmotic model to explain anomalous hydraulic heads. *Water Resources Research*, 17(1), 73-82.
- Mitchell, J. K., Greenberg, J. A., and Witherspoon, P. A. 1973. Chemico-osmotic effects in fine-grained soils. *Journal of the soil mechanics and foundations division*, Vol. 99, SM 4, 307-322.
- Mitchell, J.K. and Soga, K. 2005. *Fundamentals of Soil Behavior*, 3rd Ed. John Wiley and Sons, Inc., New York.
- Olsen, H.W. 1969. Simultaneous fluxes of liquid and charge in saturated kaolinite. *Soil Science Society of America Proceedings*, 33(3), 338-344.

- Olsen, H.W., Yearsley, E.N., and Nelson, K.R. 1990. Chemico-osmosis versus diffusion-osmosis. *Transportation Research Record No. 1288*, Transportation Research Board, Washington D.C., 15-22.
- Shackelford, C.D, Benson, C.H., Katsumi, T., Edil, T.B., and Lin, L. 2000. Evaluating the hydraulic conductivity of GCLs permeated with non-standard liquids. *Geotextiles and Geomembranes*, 18(2-4), 133-161.
- Shackelford, C.D. and Lee, J.-M. 2003. The destructive role of diffusion on clay membrane behavior. *Clays and Clay Minerals*, 51(2), 186-196.
- Shackelford, C. D., Malusis, M. A., and Olsen, H. W. 2003. Clay membrane behavior for geoenvironmental containment. *Soil and Rock America Conference 2003* (Proceedings of the joint 12th Panamerican Conference on Soil Mechanics and Geotechnical Engineering and the 39th U.S. Rock Mechanics Symposium), P. J. Culligan, H. H. Einstein, and A. J. Whittle, eds., Verlag Glückauf GMBH, Essen, Germany, Vol. 1, 767-774.
- Shackelford, C. D. 2005. Environmental issues in geotechnical engineering. *Proceedings, 16th International Conference on Soil Mechanics and Geotechnical Engineering*, Millpress, Rotterdam, The Netherlands, Vol. 5, 95-122.
- Yeo, S.-S. 2003. *Hydraulic Conductivity, Consolidation, and Membrane Behavior of Model Backfill-Slurry Mixtures for Vertical Cutoff Walls*. M. S. Thesis, Colorado State University, Fort Collins, Colorado.
- Yeo, S.-S., Shackelford, C.D., and Evans, J.C. 2005. Membrane behavior of model soil-bentonite backfills. *Journal of Geotechnical and Geoenvironmental Engineering*, 131(4), 418-429.

Table 5.1. Properties of bentonite in a geosynthetic clay liner.

Property	Standard	Value
Specific Gravity	ASTM D 854	2.43
Atterberg Limits (%):	ASTM D 4318	
Liquid Limit, LL		478
Plasticity Index, PI		439
Principal Minerals (%):	a	
Montmorillonite		71
Mixed-Layer Illite/Smectite		7
Quartz		15
Others		7
Cation Exchange Capacity, CEC (meq/100 g)	b	47.7
Exchangeable Metals (meq/100 g):	b	
Ca ²⁺		20.8
Mg ²⁺		6.4
Na ⁺		31.0
K ⁺		0.8
Sum		59.0
Soluble Metals (mg/kg):	b, c	
Ca ²⁺		443
Mg ²⁺		407
Na ⁺		4636
K ⁺		263
Saturated Soil Paste:		
pH	b, d	9.2
EC ^e (mS/m)	b, d	120

¹Notes:

^a Based on X-ray diffraction (XRD) analyses performed by Mineralogy Inc., Tulsa, OK and GeoServices Inc., Argyle, TX.

^b Based on procedures described in Shackelford and Redmond (1995).

^c Measured from a 1 g:20 mL clay-water extract.

^d Measured on a saturated soil paste.

^e Electrical conductivity at 25 °C.

Table 5.2 – Sequence of stress conditions imposed on test specimens.

Testing No.	Stage Conditions	Confining Stress, σ_c [kPa (psi)]	Applied Back Pressures, u_{bp} [kPa (psi)]		Effective Stress, $\sigma_r^{(a)}$ [kPa (psi)]
			Top, $u_{bp,top}$	Bottom, $u_{bp,bottom}$	
1	Flushing	207 (30.0)	155 (22.5)	189 (27.5)	34.5 (5.0)
	Consolidation	207 (30.0)	172 (25.0)	172 (25.0)	34.5 (5.0)
	Circulation	207 (30.0)	172 (25.0)	172 (25.0)	34.5 (5.0)
2	Flushing	207 (30.0)	155 (22.5)	189 (27.5)	34.5 (5.0)
	Consolidation	275 (40.0)	172 (25.0)	172 (25.0)	103 (15.0)
	Circulation	275 (40.0)	172 (25.0)	172 (25.0)	103 (15.0)
3	Flushing	207 (30.0)	155 (22.5)	189 (27.5)	34.5 (5.0)
	Consolidation	344 (50.0)	172 (25.0)	172 (25.0)	172 (25.0)
	Circulation	344 (50.0)	172 (25.0)	172 (25.0)	172 (25.0)
4	Flushing	207 (30.0)	155 (22.5)	189 (27.5)	34.5 (5.0)
	Consolidation	413 (60.0)	172 (25.0)	172 (25.0)	241 (35.0)
	Circulation	413 (60.0)	172 (25.0)	172 (25.0)	241 (35.0)

(a) Average effective stress during consolidation.

Table 5.3 Testing series for evaluating membrane efficiency of the GCL specimens.

Test No.	No. of Loading Increments ⁽¹⁾	Stress Increment,	Effective Stress,	Load Increment Ratio (LIR)
		$\Delta\sigma'$ [kPa (psi)]	σ' [kPa (psi)] ⁽²⁾	
1	0	0	34.5 (5.0)	N/A
2	1	69.0 (10.0)	103 (15.0)	2
3	1	69.0 (10.0)	172 (25.0)	4
4	1	69.0 (10.0)	241 (35.0)	6

⁽¹⁾ All test specimens were initially consolidated to 34.5 kPa (5.0 psi).

⁽²⁾ After consolidation, but before membrane testing.

Table 5.4. Summary of measured hydraulic conductivity and coefficient of consolidation values for the specimens of a geosynthetic clay liner (GCL).

Testing Stage	Effective Stress, σ' ^(a) [kPa (psi)]	Coefficient of Consolidation, c_v (10^{-9} m ² /s)	
		Casagrande Method	Taylor Method
Flushing	34.5 (5.0)	-----	-----
Consolidation	34.5 (5.0)	-----	-----
	103 (15.0)	6.1	5.3
	172 (25.0)	6.0	6.1
	241 (35.0)	7.3	7.4

(a) Final effective stress at the end of consolidation.

Table 5.5. Initial and final properties of 10-mm-thick specimens of the geosynthetic clay liner tested for membrane behavior in this study.

Test No.	Effective Stress, σ' kPa (psi)	Initial Properties			Final Properties		
		Water Content, w_i (%)	Void Ratio, e_i	Degree of Saturation, S_i (%)	Water Content, w_f (%)	Void Ratio, e_f	Degree of Saturation, S_f (%)
1	34 (5.0)	181.4	4.423	99.7	133.8	3.468	93.7
2	103 (15.0)	175.8	4.288	99.6	121.3	3.147	93.7
3	172 (25.0)	177.7	4.322	99.9	113.7	2.874	96.2
4	241 (35.0)	170.8	4.158	99.8	89.9	2.196	99.5

Table 5.6. Results of multi-stage membrane testing for specimens of the geosynthetic clay liner at each effective confining stress.

Effective Stress, σ' [kPa (psi)]	KCl Source Concentration, C_{oi} (mM)	Differences in Chemico-Osmotic Pressures ^(a) [kPa (psi)]			Membrane Efficiency Coefficients at Steady State, ω_{ss}	
		$-\Delta P_e$	$-\Delta\pi_0$	$-\Delta\pi_{ave}$	$\omega_{ss,o} (= \Delta P_e / \Delta\pi_0)$	$\omega_{ss,ave} (= \Delta P_e / \Delta\pi_{ave})$
34.5 (5.0)	3.9	8.117 (1.177)	19.011 (2.757)	14.472 (2.098)	0.427	0.561
	6.0	9.007 (1.306)	29.247 (4.242)	21.556 (3.126)	0.308	0.418
	8.7	8.572 (1.243)	42.408 (6.151)	29.978 (4.347)	0.202	0.286
	20.0	4.903 (0.711)	97.490 (14.140)	64.776 (9.392)	0.050	0.076
	47.0	2.290 (0.332)	229.101 (33.228)	151.017 (21.897)	0.010	0.015
103 (15.0)	3.9	9.476 (1.374)	19.011 (2.757)	16.214 (2.351)	0.498	0.584
	6.0	10.966 (1.590)	29.247 (4.242)	23.787 (3.449)	0.375	0.461
	8.7	11.034 (1.600)	42.408 (6.151)	33.678 (4.883)	0.260	0.328
	20.0	11.028 (1.599)	97.490 (14.140)	72.520 (10.515)	0.113	0.152
	47.0	11.159 (1.618)	229.101 (33.228)	164.448 (23.845)	0.049	0.068
172 (25.0)	3.9	12.062 (1.749)	19.011 (2.757)	16.781 (2.433)	0.634	0.719
	6.0	15.241 (2.210)	29.247 (4.242)	24.287 (3.522)	0.521	0.628
	8.7	16.552 (2.400)	42.408 (6.151)	34.202 (4.959)	0.390	0.484
	20.0	16.634 (2.412)	97.490 (14.140)	73.531 (10.662)	0.171	0.226
	47.0	16.131 (2.339)	229.101 (33.228)	164.990 (23.924)	0.070	0.098
241 (35.0)	3.9	12.931 (1.875)	19.011 (2.757)	16.492 (2.391)	0.680	0.784
	6.0	15.952 (2.313)	29.247 (4.242)	25.112 (3.641)	0.545	0.635
	8.7	16.234 (2.354)	42.408 (6.151)	35.375 (5.129)	0.383	0.459
	20.0	17.593 (2.551)	97.490 (14.140)	76.384 (11.076)	0.180	0.230
	47.0	18.200 (2.639)	229.101 (33.228)	172.085 (24.952)	0.079	0.106

(a) $-\Delta P_e$ = effective or net pressure difference measured across specimen at steady state; $-\Delta\pi_0$ = theoretical maximum pressure difference based on difference in initial (source) concentrations; $-\Delta\pi_{ave}$ = theoretical maximum pressure difference based on difference in average boundary concentrations at steady state.

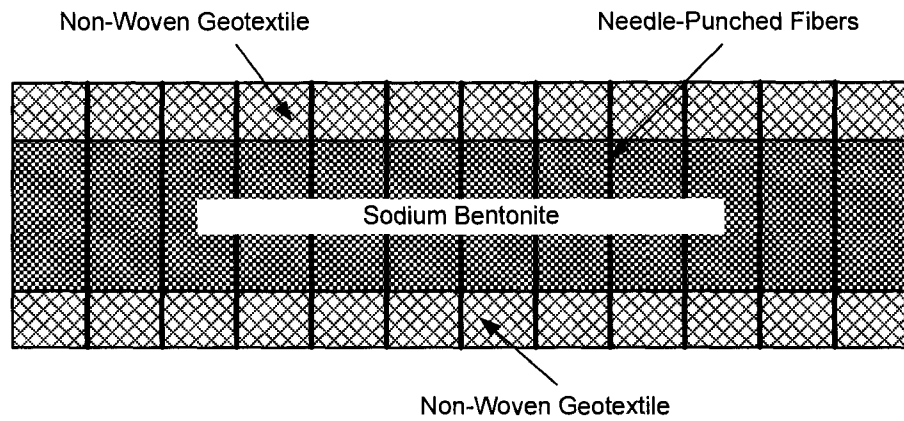


Fig. 5.1 – Schematic cross section of manufactured geosynthetic clay liner evaluated in this study (after Malusis et al. 2002)

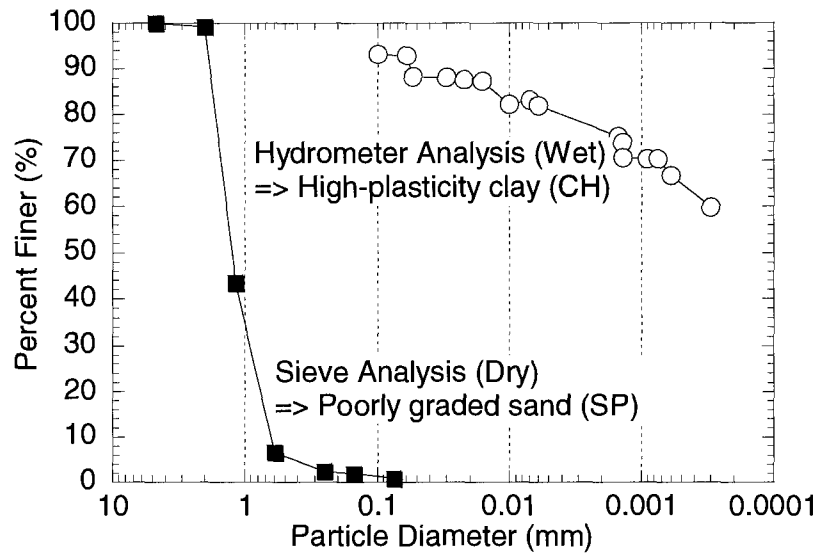


Fig. 5.2 – Wet (hydrometer) and dry (mechanical sieve) grain-size distributions for the bentonite in the geosynthetic clay liner evaluated in this study (after Malusis and Shackelford 2002)

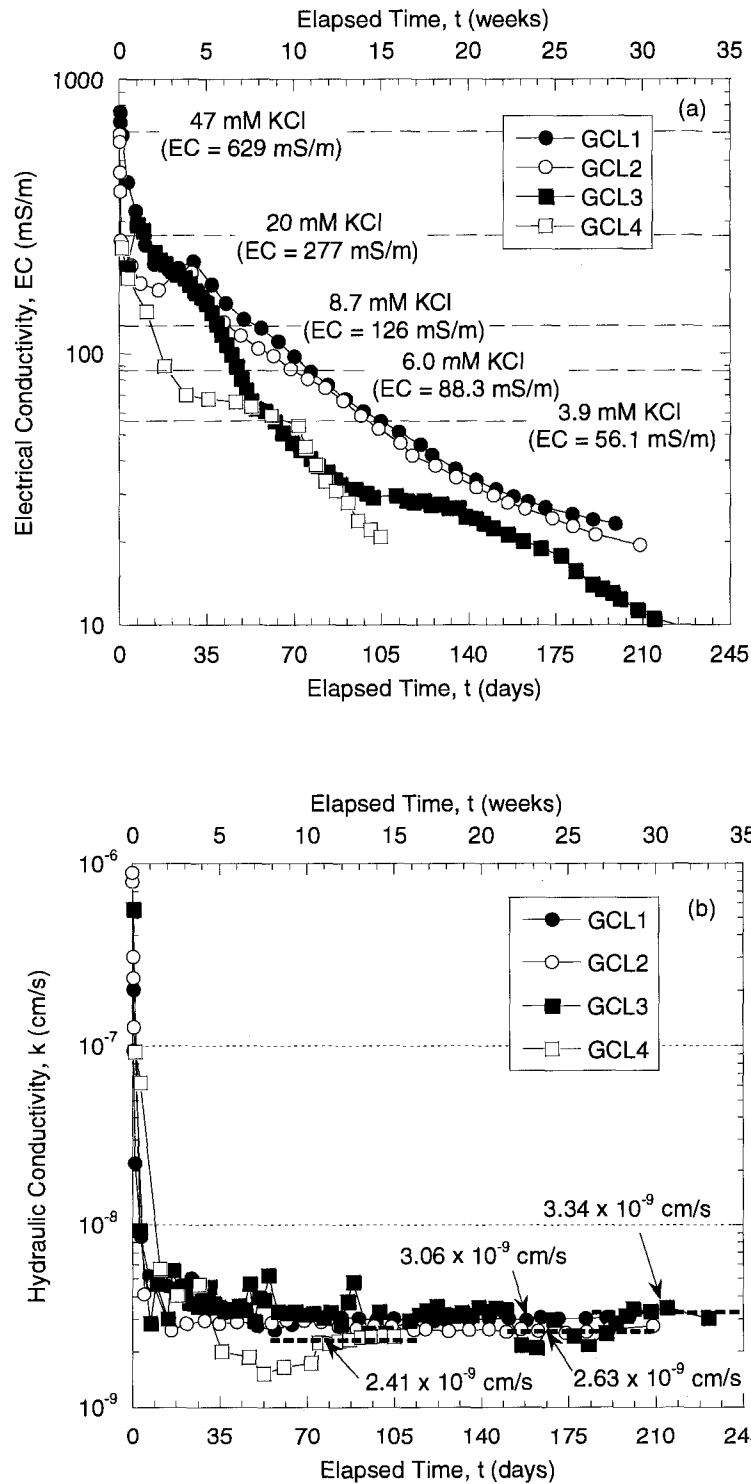


Fig. 5.3 – Electrical conductivity (a) and hydraulic conductivity (b) versus elapsed time for specimens of a geosynthetic clay liner permeated with de-ionized water during flushing stage of test prior to consolidation to initial effective stresses of 34.5, 103, 172, and 241 kPa (5.0, 15.0, 25.0, and 35.0 psi).

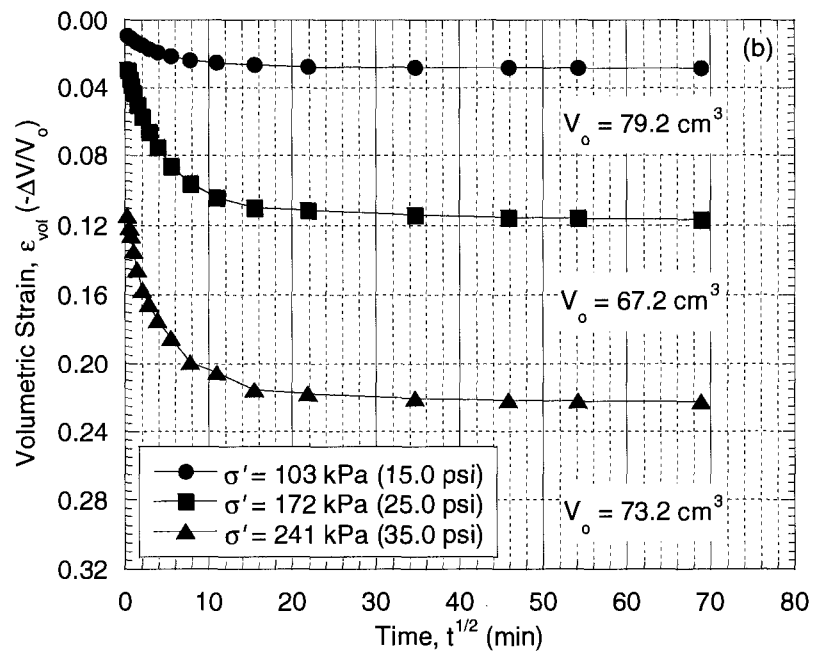
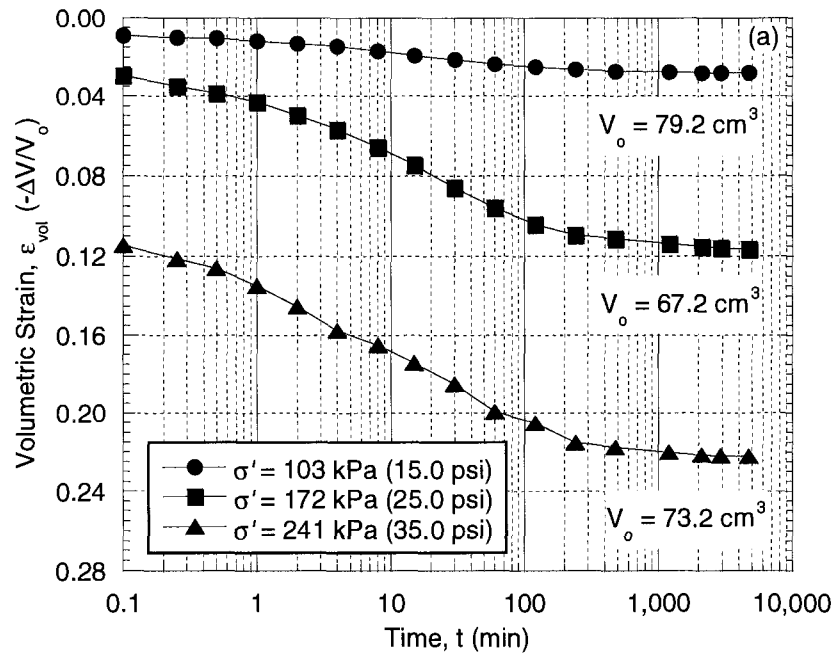


Fig. 5.4 – Volumetric strain versus (a) logarithm of time and (b) square root of time for specimens of a geosynthetic clay liner consolidated to initial effective stresses of 103, 172, and 241 kPa (15.0, 25.0, and 35.0 psi) prior to membrane testing in flexible-wall cell.

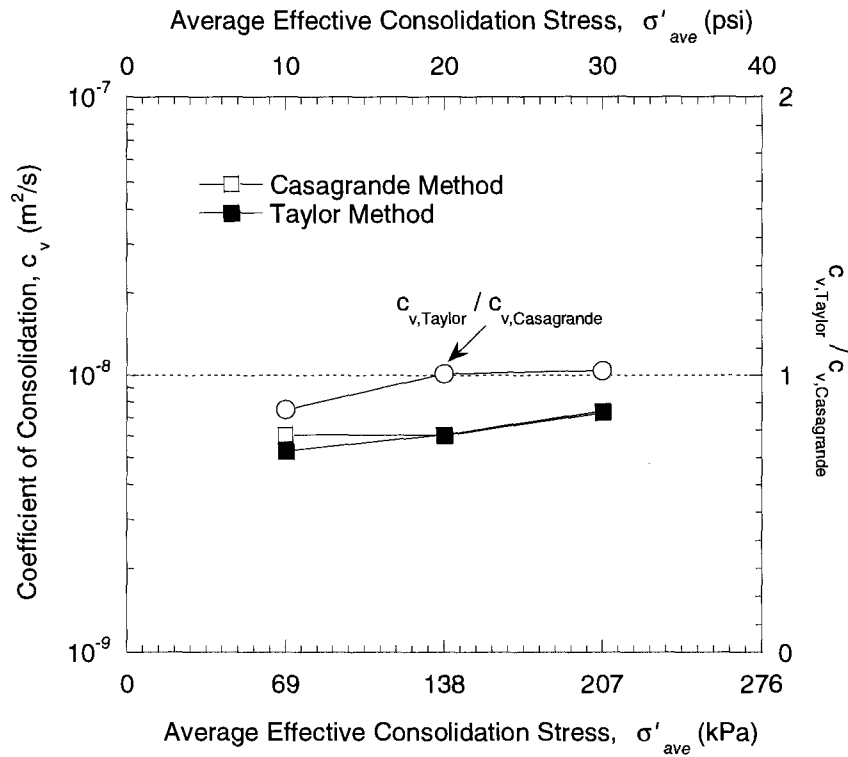


Fig. 5.5 – Effect of method of analysis on the coefficients of consolidation, c_v , based on volumetric strain for the specimens of a geosynthetic clay liner as function of average effective consolidation stress.

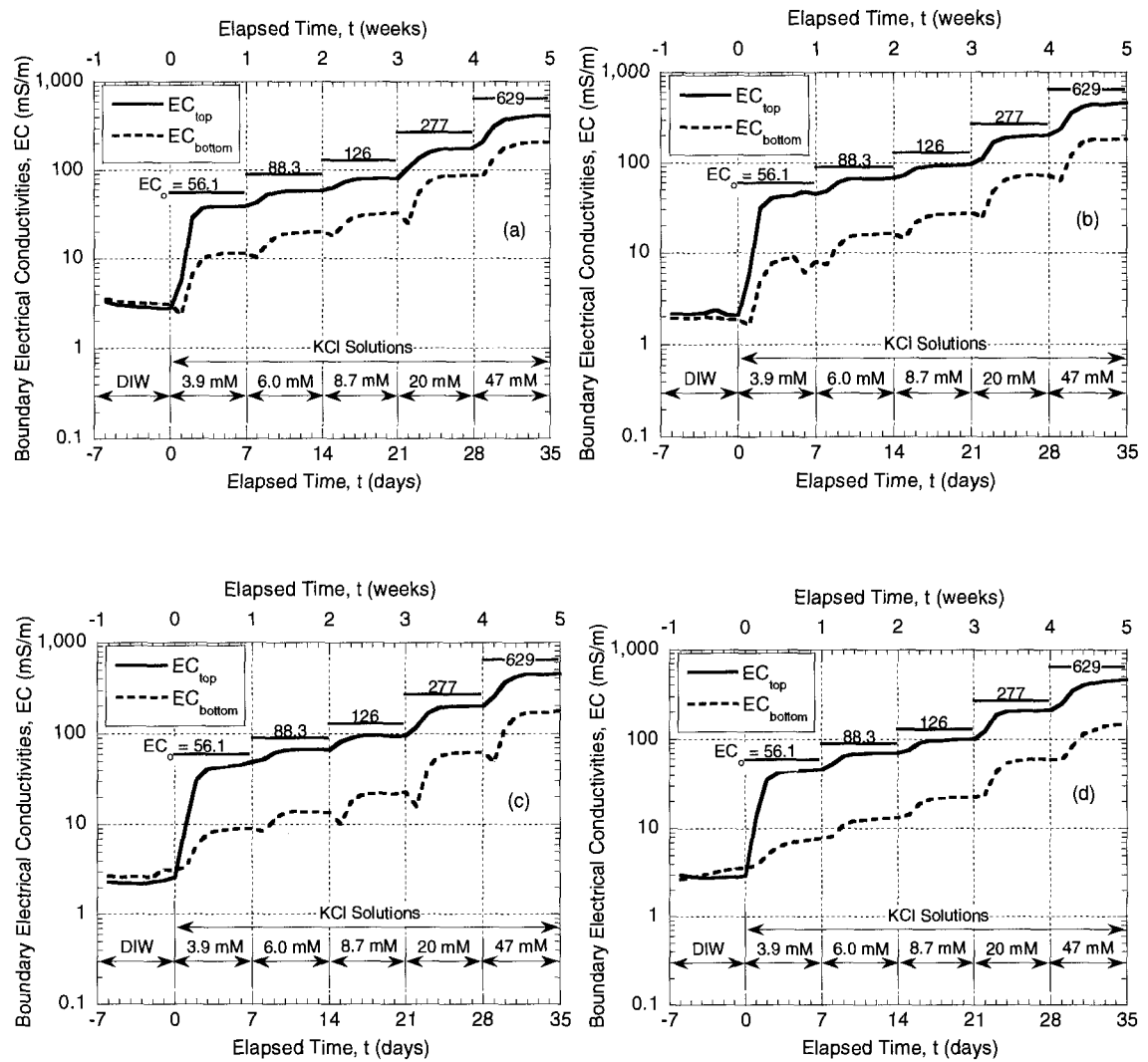


Fig. 5.6 – Electrical conductivity values in outflows from top and bottom boundaries of specimens of a geosynthetic clay liner consolidated to initial effective stresses of 103, 172, and 241 kPa (15.0, 25.0, and 35.0 psi) resulting from the chemico-osmotic stage in flexible-wall cell.

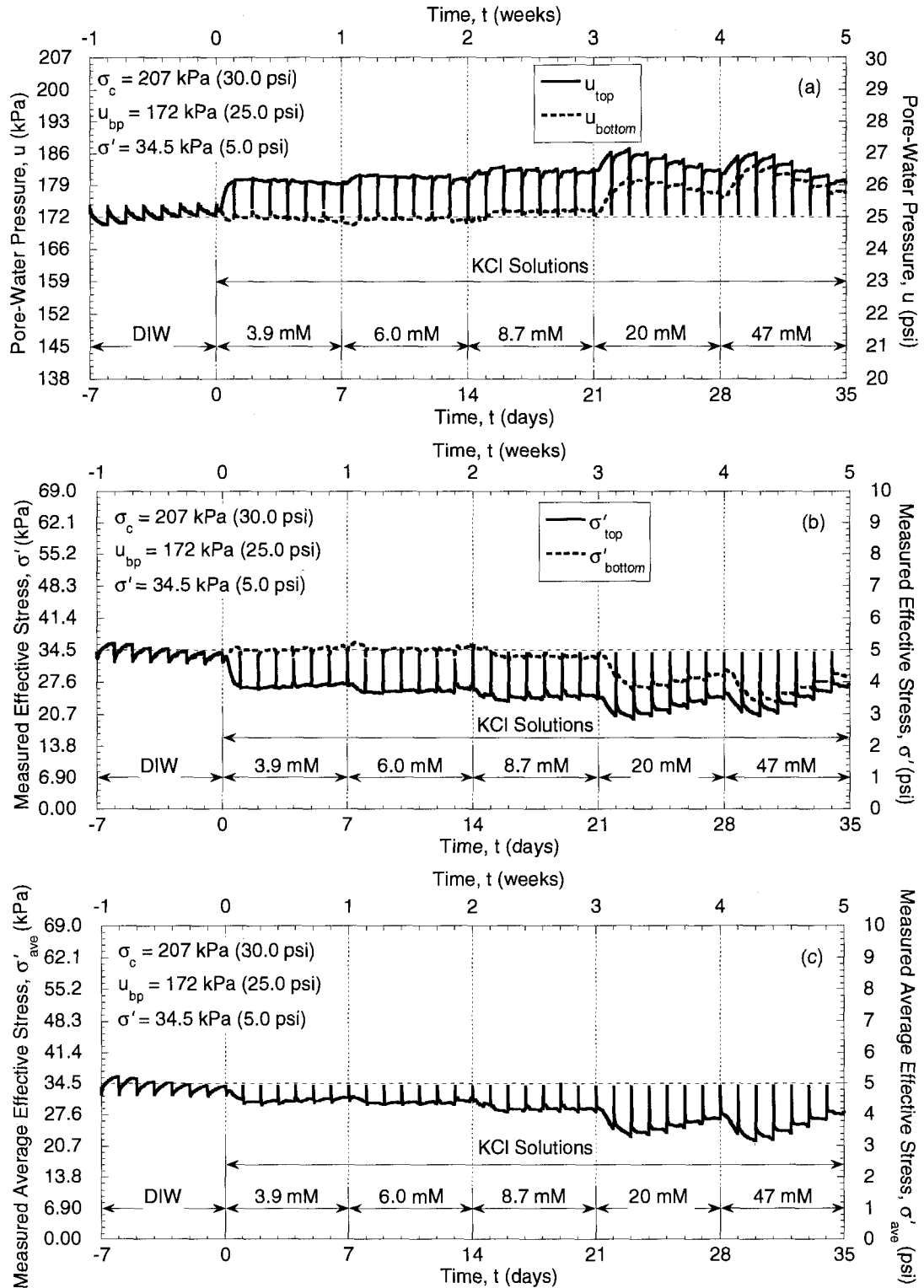


Fig. 5.7 – Boundary pressures and effective stresses for a specimen of a geosynthetic clay liner consolidated to an initial effective stress of 34.5 kPa (5.0 psi) during membrane testing in flexible-wall cell.

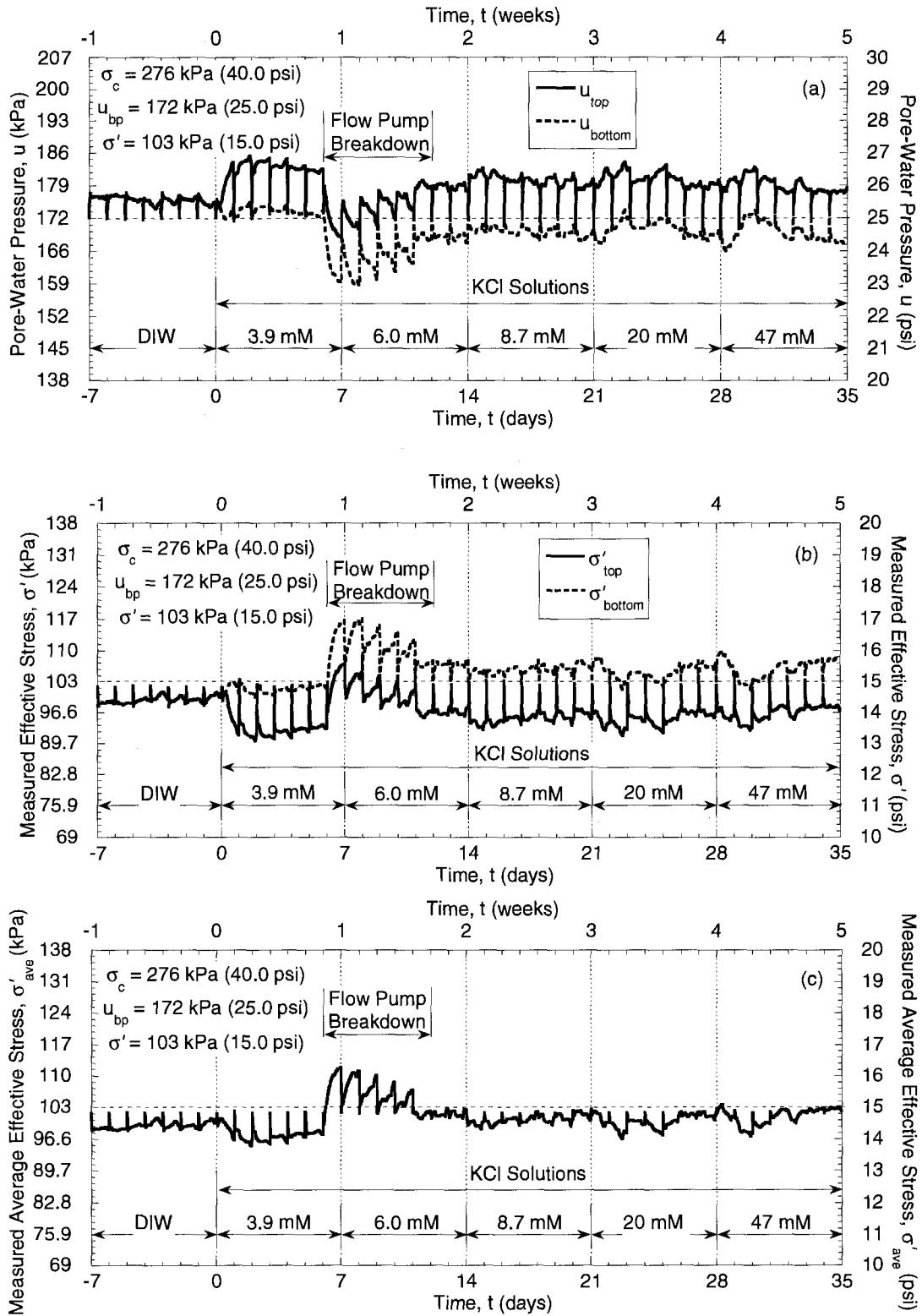


Fig. 5.8 – Boundary pressures and effective stresses for a specimen of GCL consolidated to an initial effective stress of 103 kPa (15.0 psi) during membrane testing in flexible-wall cell.

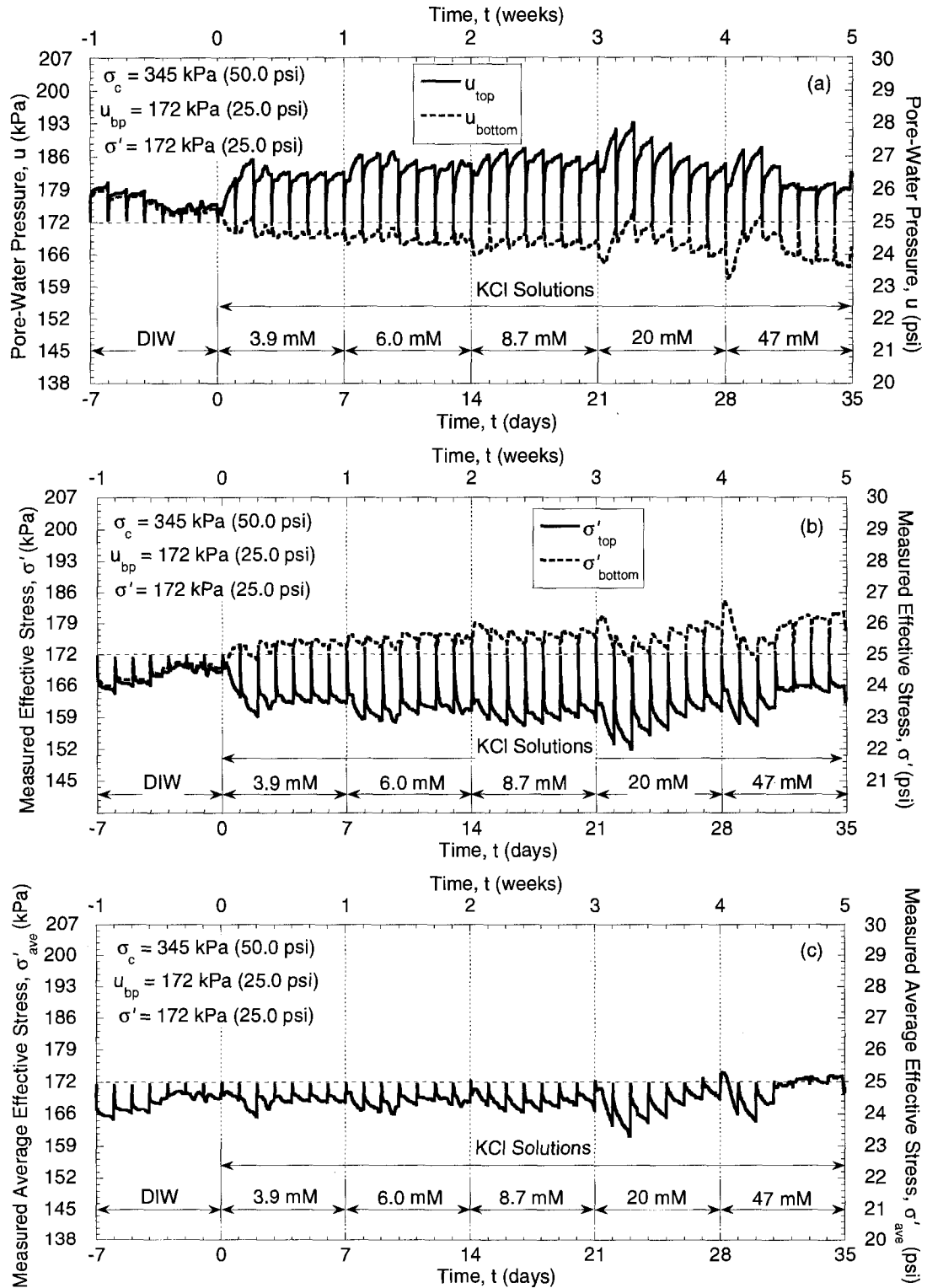


Fig. 5.9 – Boundary pressures and effective stresses for a specimen of a geosynthetic clay liner consolidated to an initial effective stress of 172 kPa (25.0 psi) during membrane testing in flexible-wall cell.

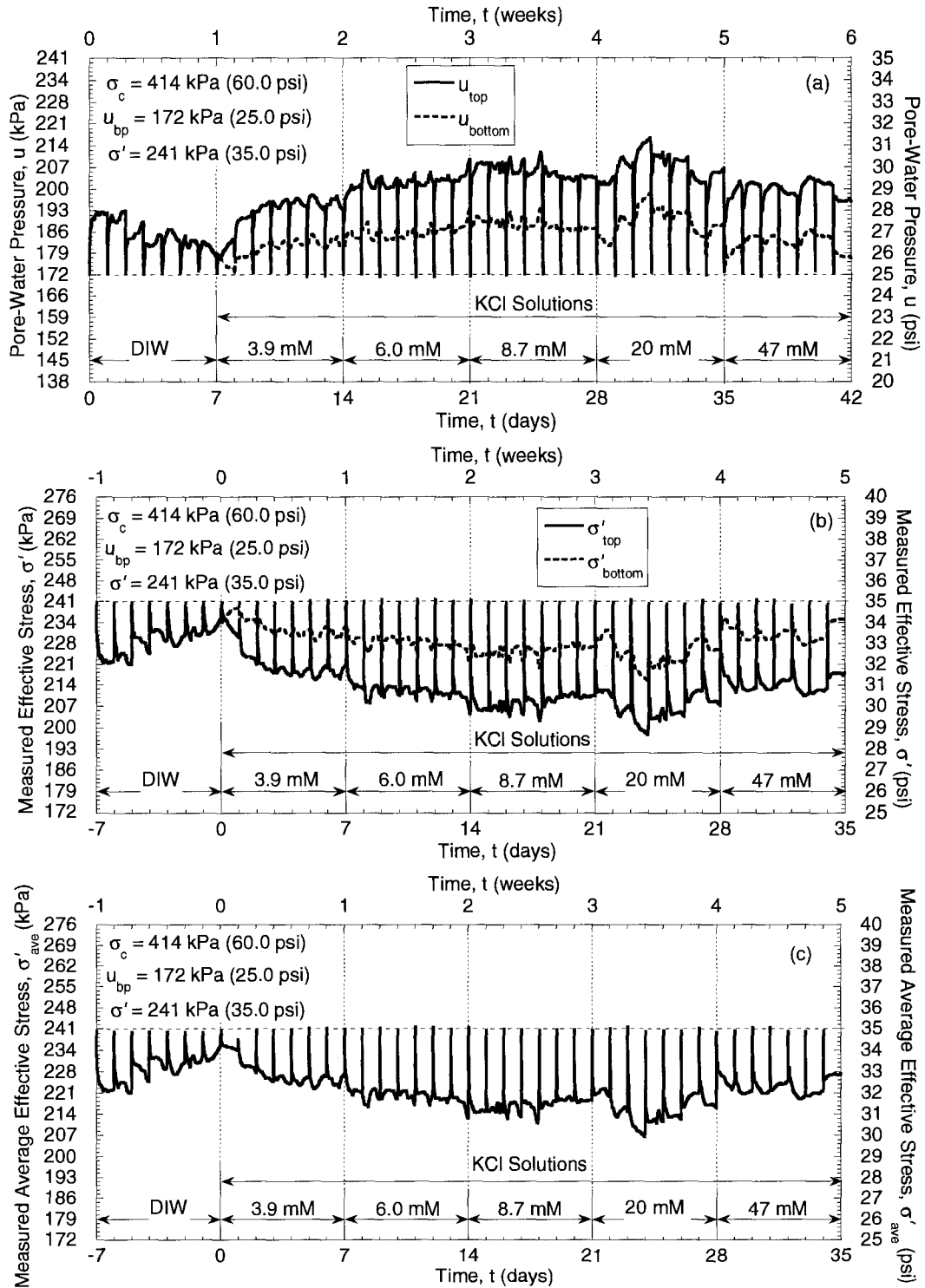


Fig. 5.10 – Boundary pressures and effective stresses for a specimen of a geosynthetic clay liner consolidated to an initial effective stress of 241 kPa (35.0 psi) during membrane testing in flexible-wall cell.

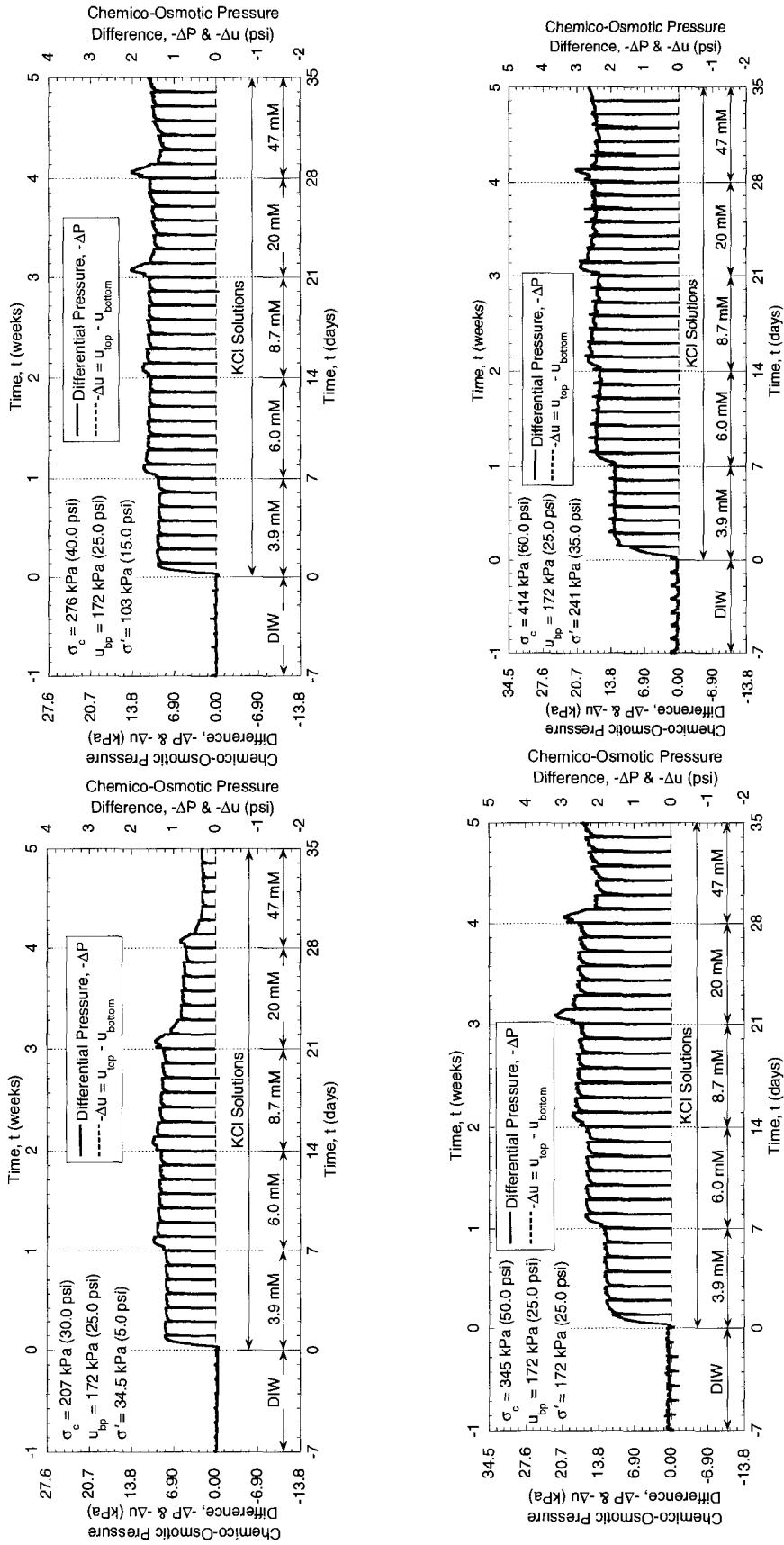


Fig. 5.11 – Measured chemico-osmotic pressure differences across for specimens of a geosynthetic clay liner consolidated to initial effective stresses of 34.5, 103, 172, and 241 kPa (5.0, 15.0, 25.0, and 35.0 psi) during membrane testing in flexible-wall cell.

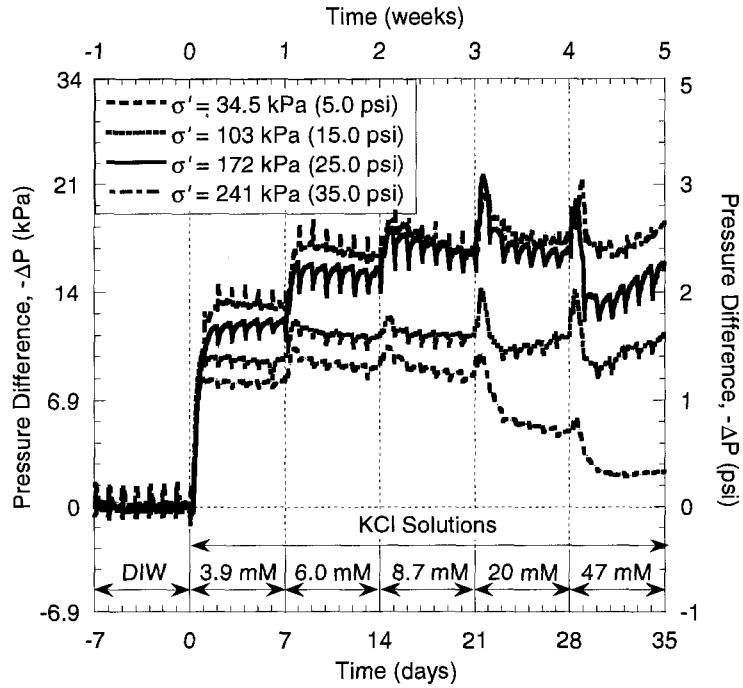


Fig. 5.12 – Induced differential pressure versus time for specimens of a geosynthetic clay liner as a function of effective stress, σ' , during multi-stage membrane testing in flexible-wall cell.

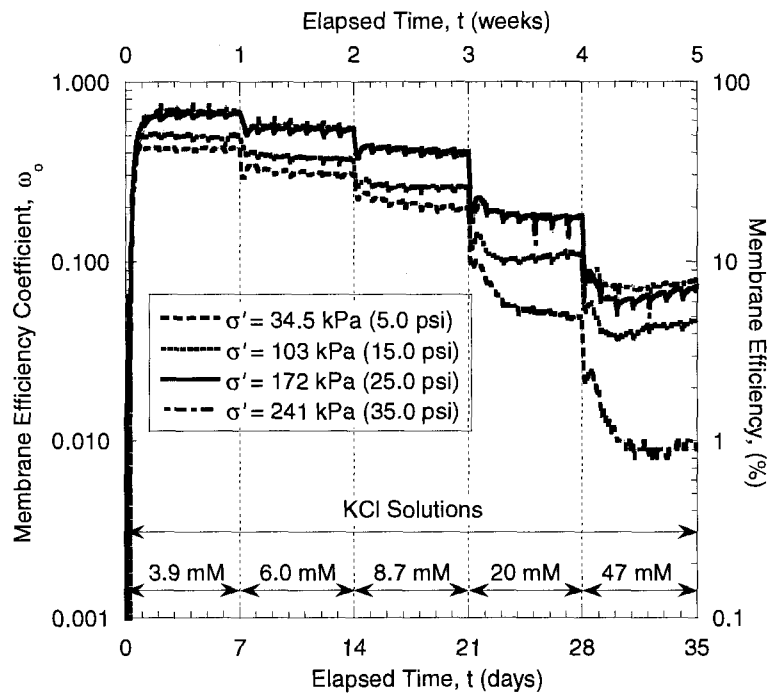


Fig. 5.13 – Elapsed time versus membrane efficiency coefficients for specimens of a geosynthetic clay liner as a function of effective stress, σ' , during multi-stage membrane testing in flexible-wall cell.

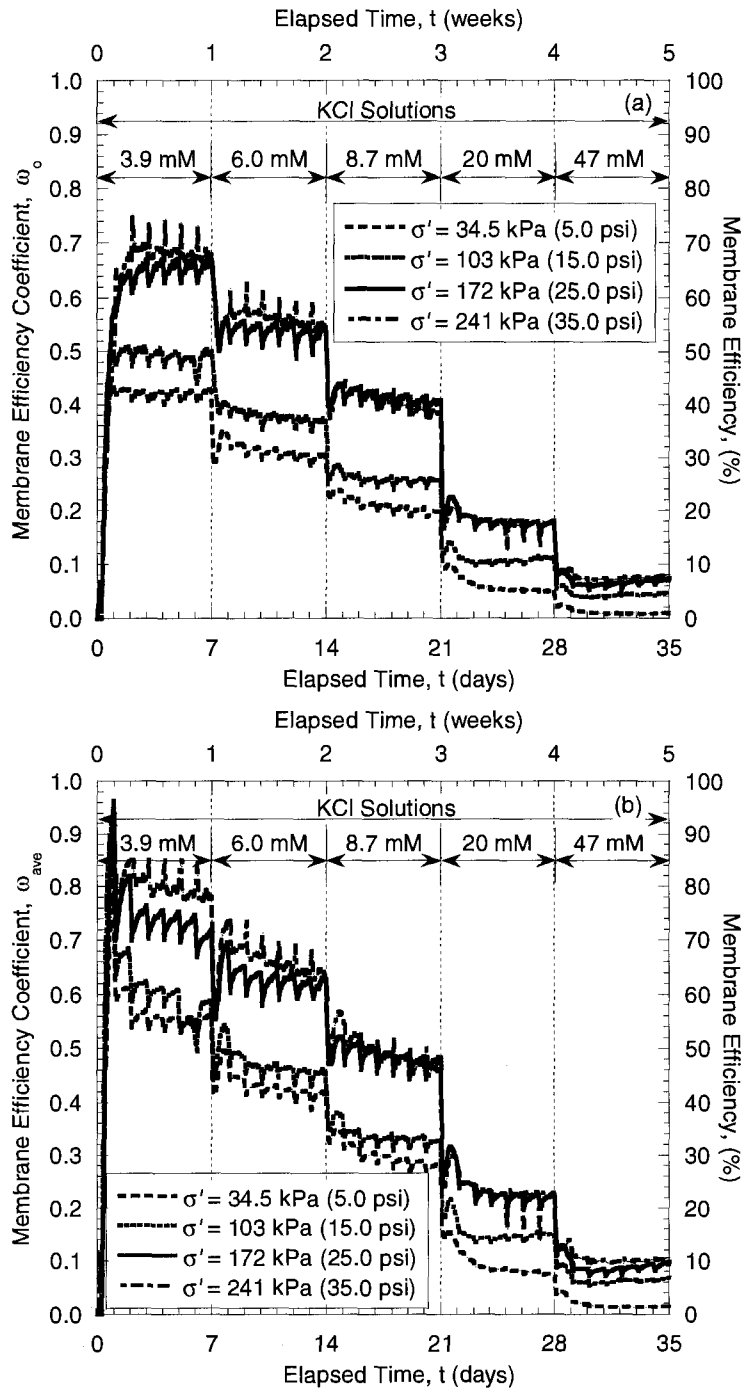


Fig. 5.14 – Comparison of measured membrane efficiencies versus elapsed time based on (a) initial concentration differences ($\Delta\pi_0$) and (b) average concentration differences ($\Delta\pi_{ave}$) for specimens of a geosynthetic clay liner as a function of effective stress, σ' , during multi-stage membrane testing in flexible-wall cell.

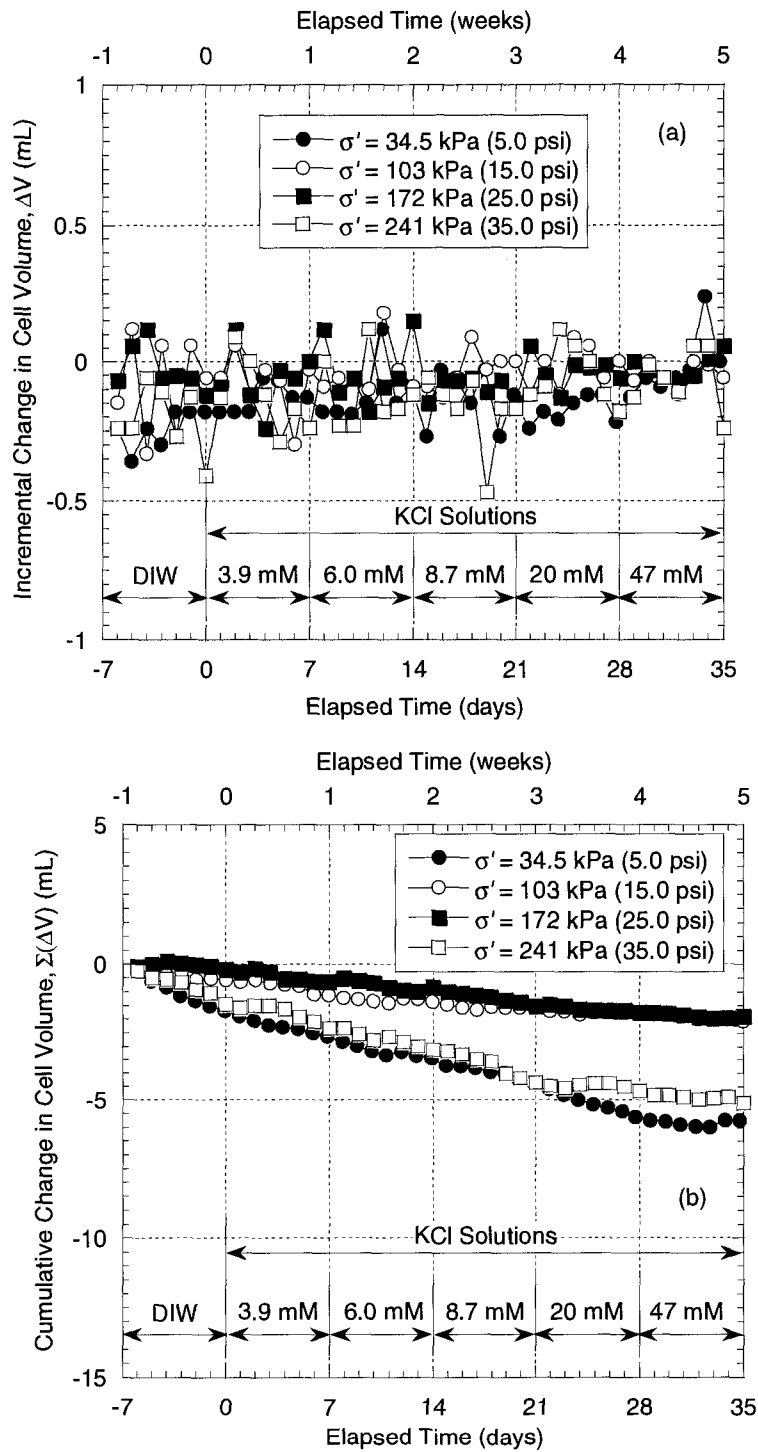


Fig. 5.15 – Incremental (a) and cumulative (b) changes in cell volume for specimens of a geosynthetic clay liner as a function of effective stress, σ' , during multi-stage membrane testing in flexible-wall cell.

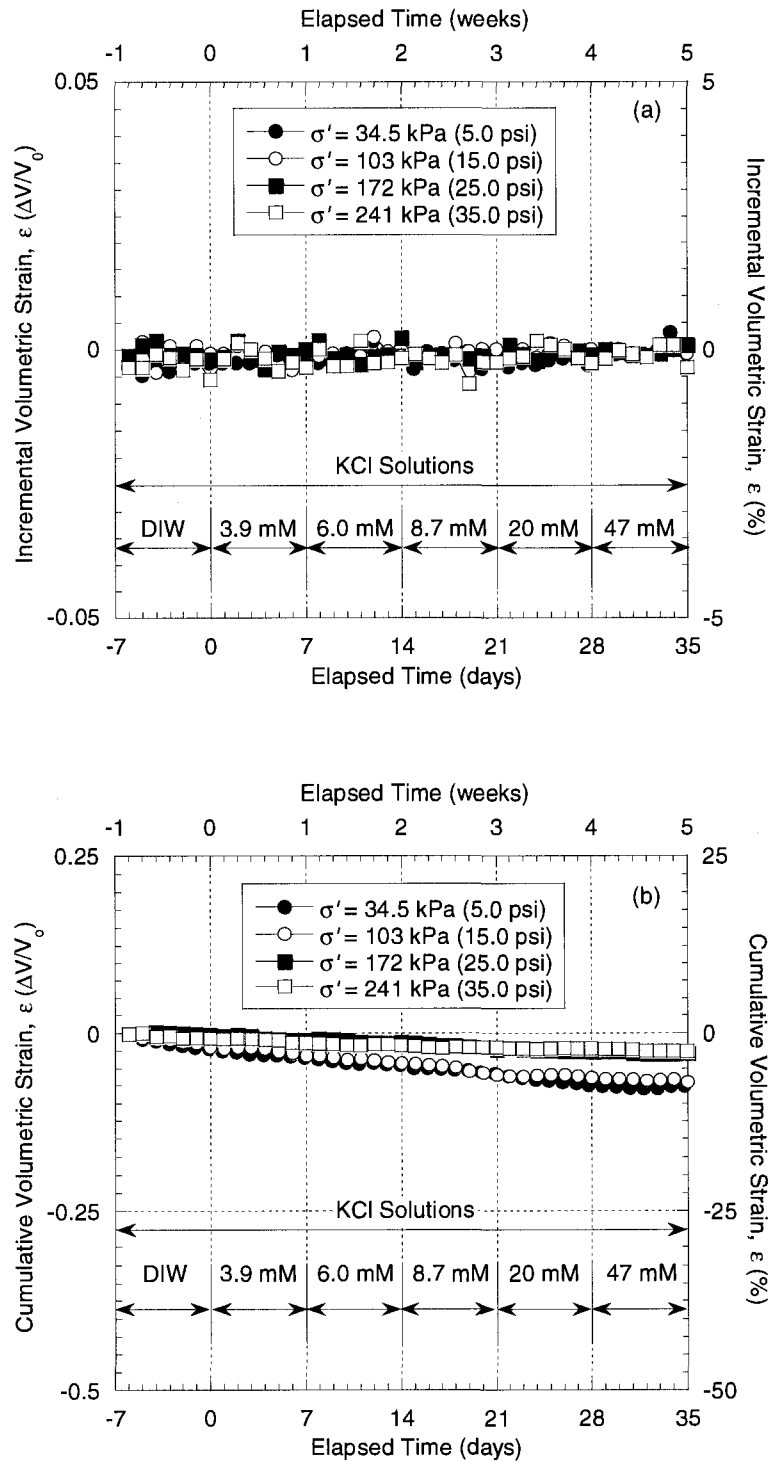


Fig. 5.16 – Incremental (a) and cumulative (b) volumetric strains for specimens of a geosynthetic clay liner as a function of effective stress, σ' , during multi-stage membrane testing in flexible-wall cell.

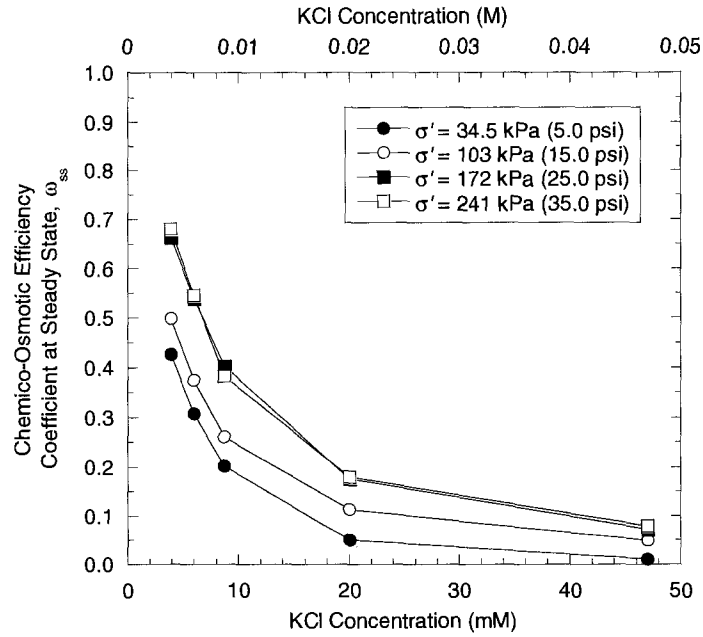


Fig. 5.17 – Effect of potassium chloride (KCl) source concentration on steady-state membrane efficiency coefficients for specimens of a geosynthetic clay liner as a function of effective stress, σ' , during multi-stage membrane testing in flexible-wall cell.

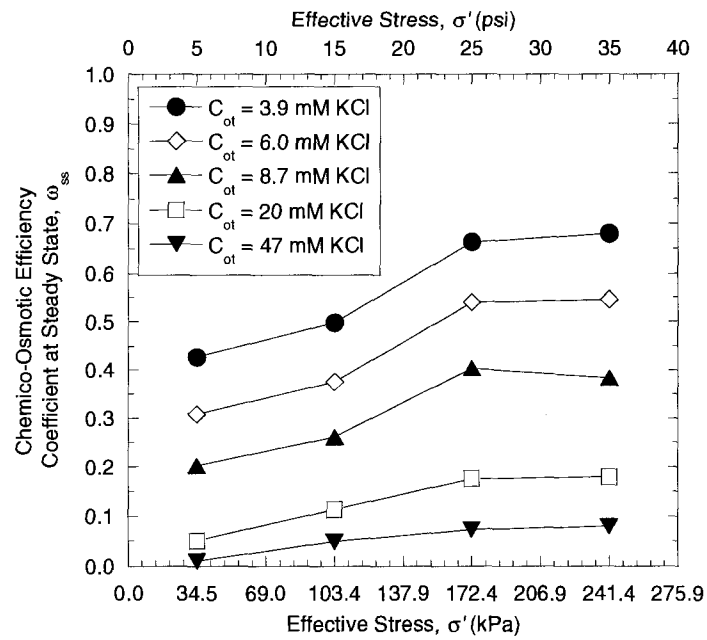


Fig. 5.18 – Effect of effective stress on steady-state membrane efficiency coefficients for specimens of a geosynthetic clay liner subjected to different source concentrations, C_{ot} , of potassium chloride (KCl).

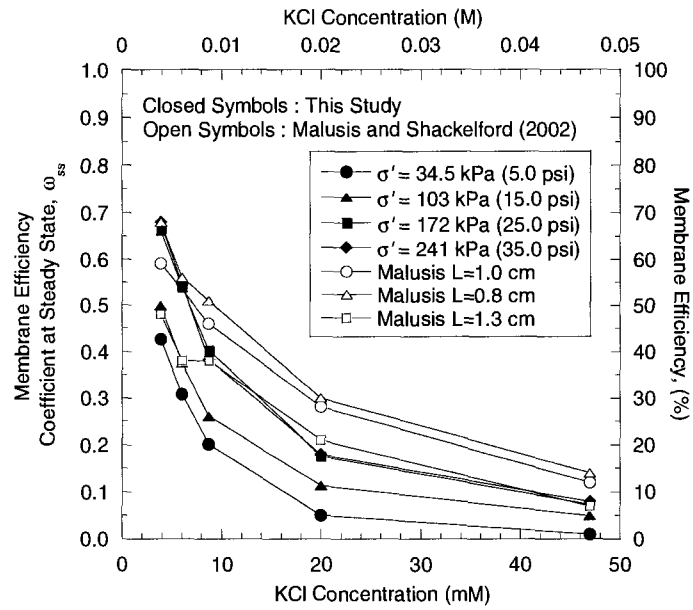


Fig. 5.19 – Comparison of steady-state membrane efficiency coefficients for specimens of a geosynthetic clay liner measured in this study using a flexible-wall cell as a function of effective stress, σ' , versus those reported by Malusis and Shackelford (2002b) using a rigid-wall cell with different specimen thicknesses, L.

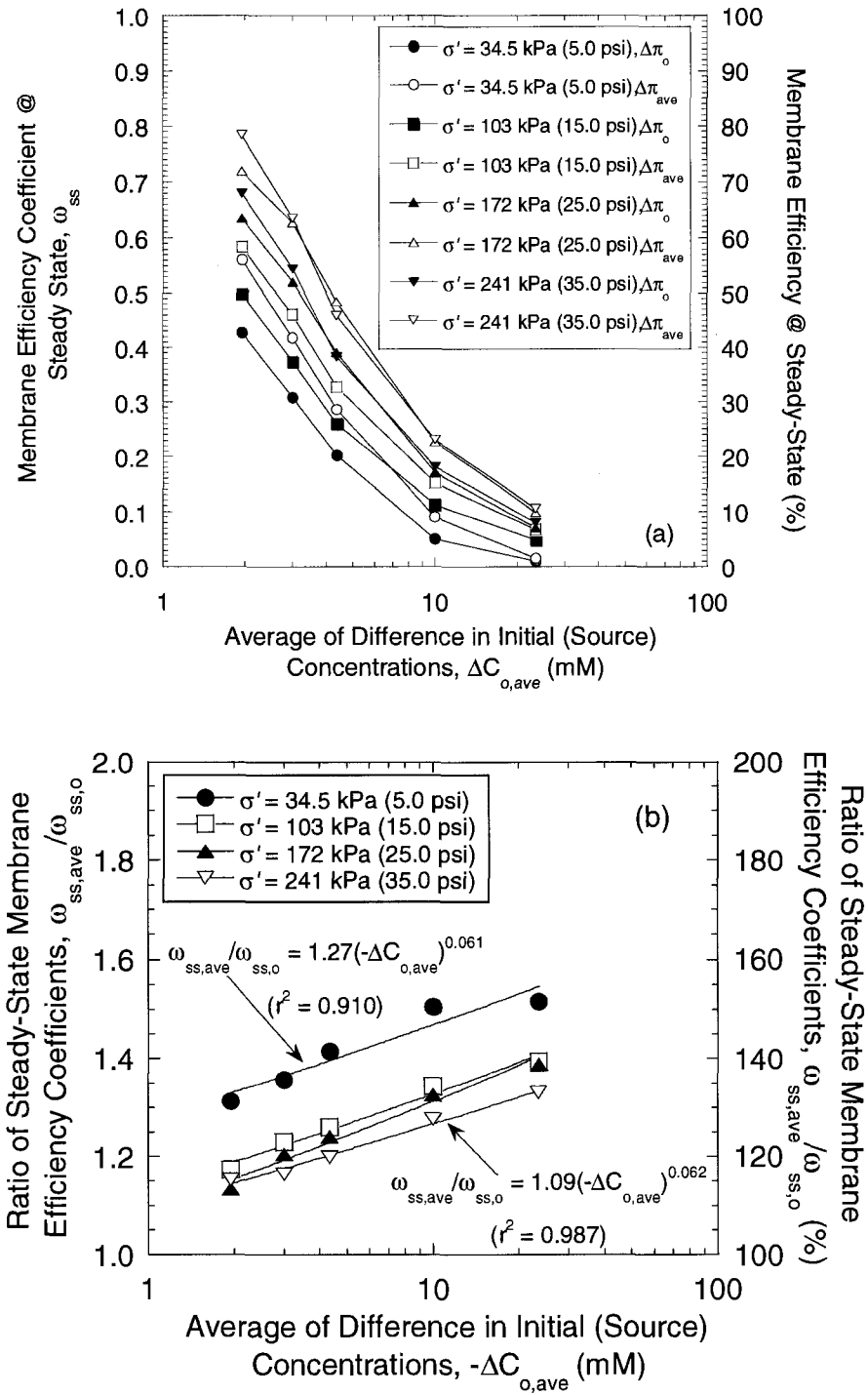


Fig. 5.20 – Steady-state membrane efficiency coefficients, ω_{ss} , versus average of difference in initial (source) KCl concentrations for specimens of a geosynthetic clay liner: (a) ω_{ss} values based initial concentration differences ($\Delta\pi_o$), $\omega_{ss,o}$, versus average concentration differences ($\Delta\pi_{ave}$), $\omega_{ss,ave}$; (b) ratio of ω_{ss} based on $\Delta\pi_{ave}$ relative to ω_{ss} based on $\Delta\pi_o$.

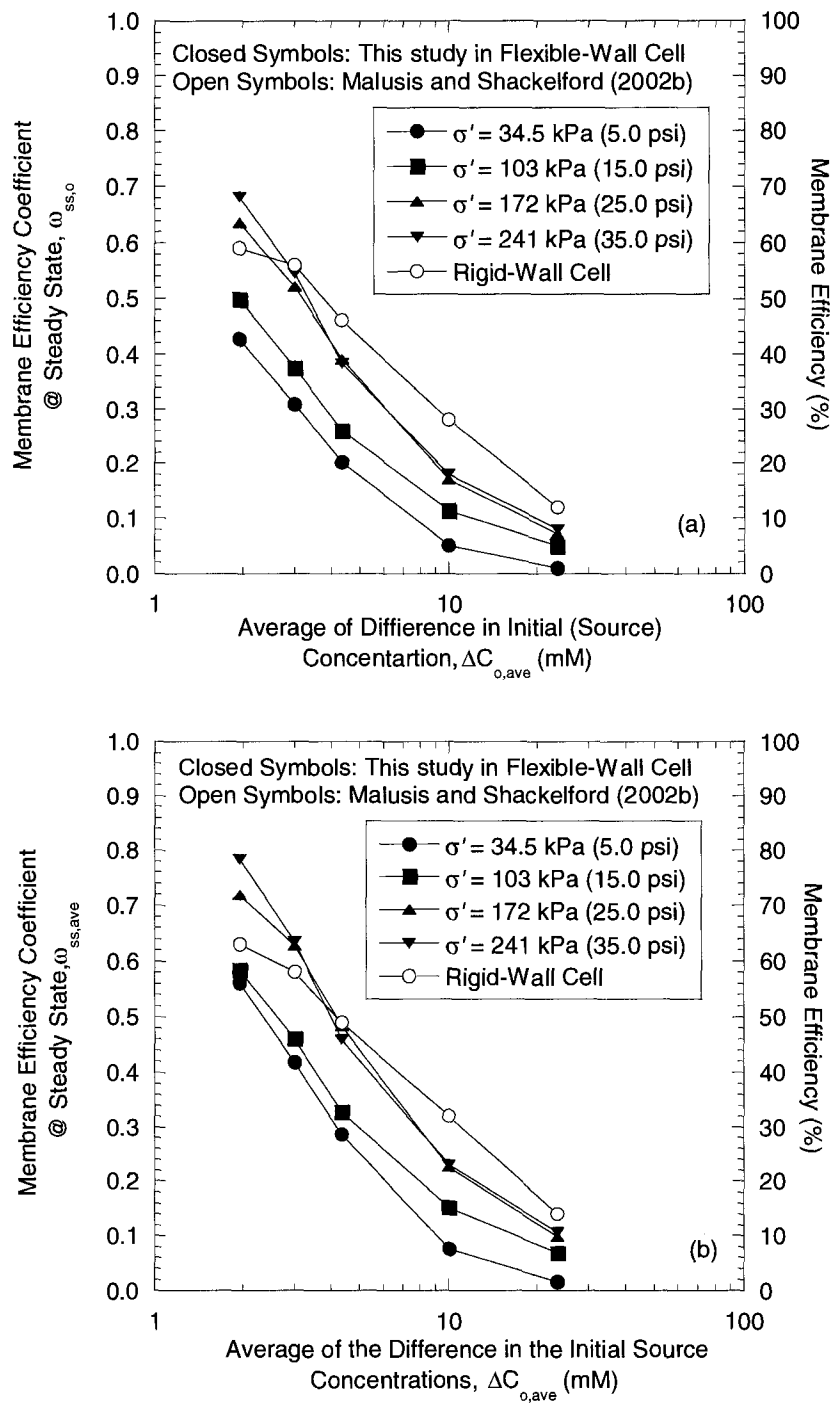


Fig. 5.21 – Comparison of membrane efficiency coefficients at steady state based on (a) initial concentration differences ($\Delta\pi_0$) and (b) average concentration differences ($\Delta\pi_{ave}$) measured in this study using a flexible-wall cell as a function of effective stress, σ' , versus those reported by Malusis and Shackelford (2002b) using a rigid-wall cell

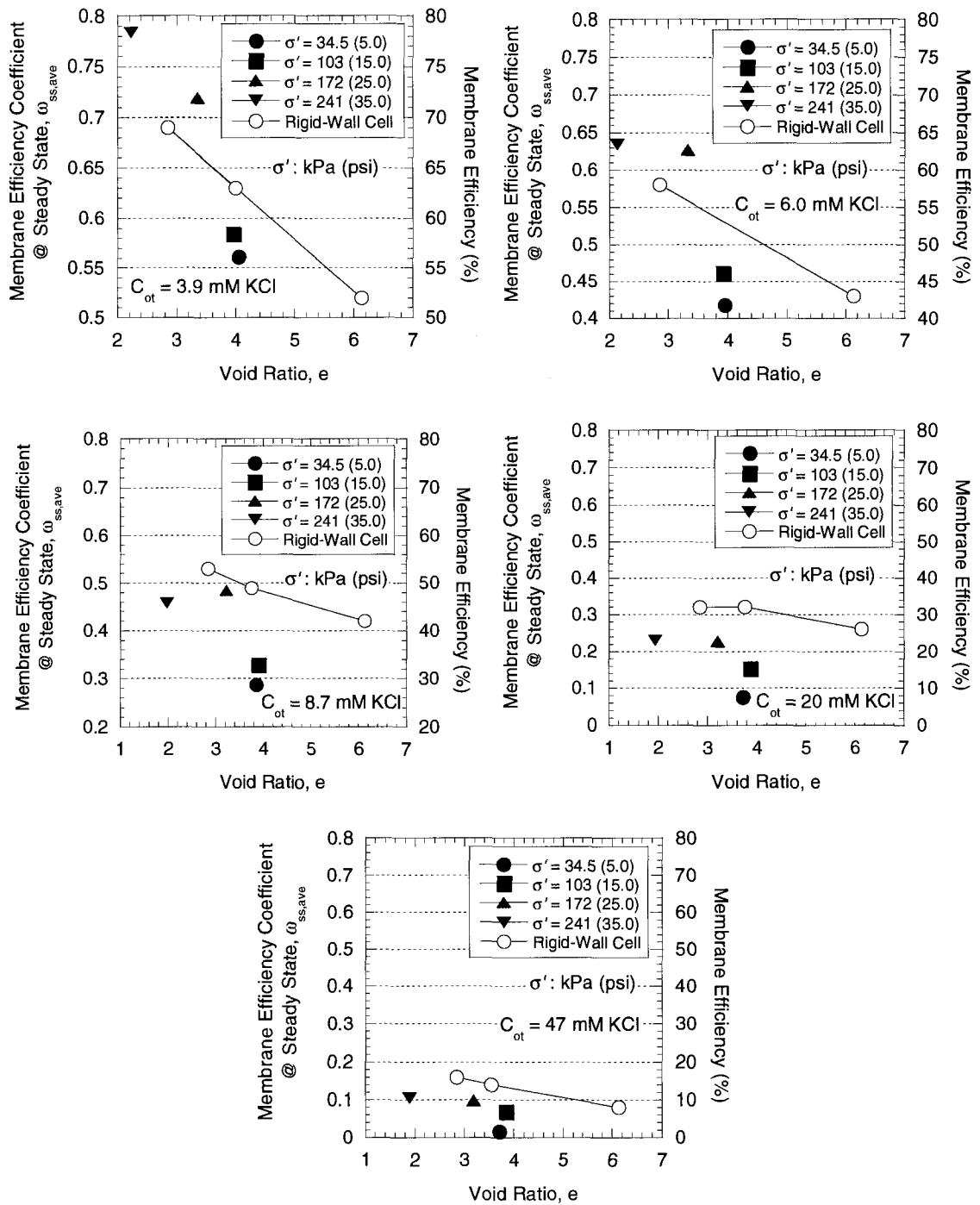


Fig. 5.22 – Comparison of membrane efficiency coefficients measured in this study using a flexible-wall cell as a function of effective stress, σ' , versus those previously measured in a rigid-wall cell reported by Malusis and Shackelford (2002b).

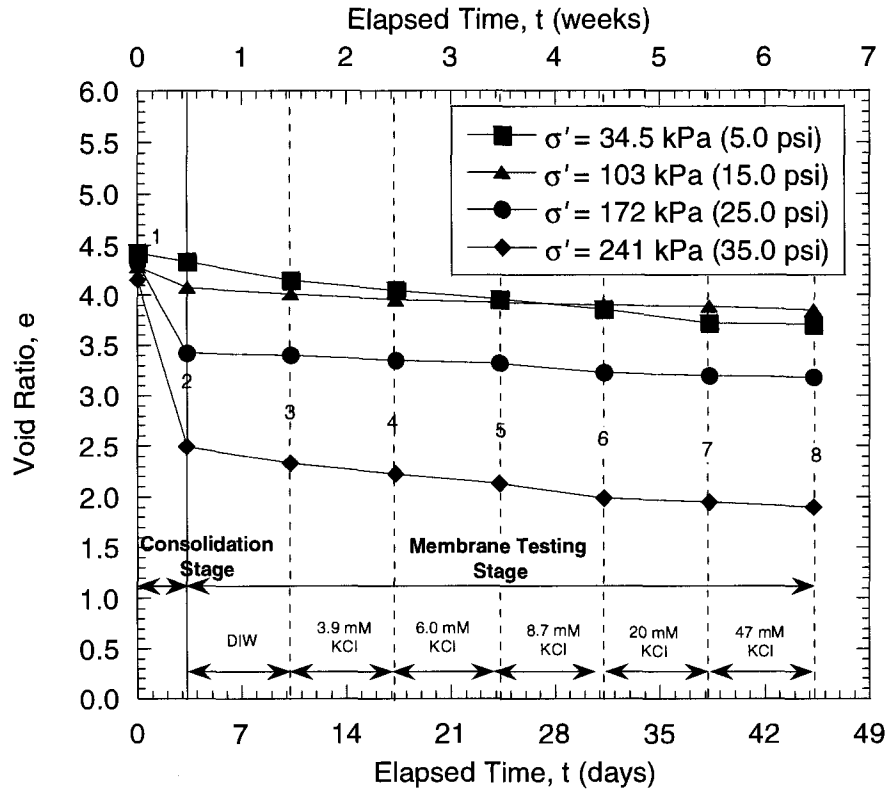


Fig. 5.23 – History of void ratios during consolidation and membrane testing for specimens of a geosynthetic clay liner consolidated to different effective stress, σ' .

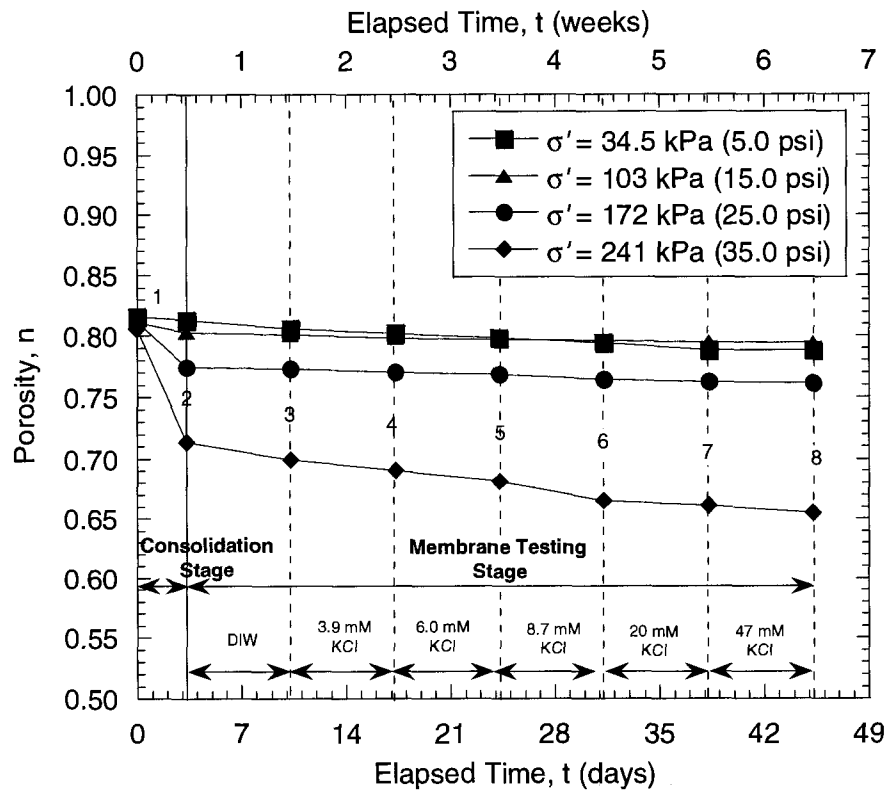


Fig. 5.24 – History of porosities during consolidation and membrane testing for specimens of a geosynthetic clay liner consolidated to different effective stress, σ' .

CHAPTER 6

MEMBRANE BEHAVIOR OF COMPACTED CLAY LINER MATERIALS

ABSTRACT: The goal of this study was to evaluate the potential existence of membrane behavior in compacted clay liner materials that are representative of those that could be considered for use in a waste containment applications. In this regard, a locally available natural clay soil referred to as Nelson Farm Clay (NFC) was evaluated both as a natural (unamended) soil and as a natural soil amended with 5 % (dry wt.) sodium bentonite to enhance the potential for membrane behavior. The membrane efficiency coefficients, ω , of specimens of both the natural and the bentonite amended NFC were measured by establishing steady salt (KCl) concentration differences of 3.9, 8.7, 20 and/or 47 mM across the specimens in a flexible-wall cell under closed-system boundary conditions. The results indicate that the compacted natural NFC exhibited essentially no membrane behavior (i.e., $\omega \approx 0$), even though the specimen was compacted at conditions that should have resulted in a suitably low value of hydraulic conductivity, k (i.e., $k < 10^{-7}$ cm/s). In contrast, compacted specimens of the bentonite amended NFC exhibited both lower k than those of the natural NFC as well as significant membrane behavior, with ω ranging from 0.762 (76.2 %) to 0.027 (2.7 %) as the KCl concentration ranged from 3.9 to 20 mM, respectively. The results suggest that natural clays typically suitable for use as compacted clay liners on the basis of low k in waste containment applications may not behave as semi-permeable membranes unless bentonite is added to the clay.

Key Words: bentonite, clay liner materials, chemico-osmosis, membrane efficiency coefficient, compacted clay, membrane efficiency, semi-permeable membrane

6.1 INTRODUCTION

Recent research involving the use of clays as liner materials for waste containment applications has focused on the potential of such materials to behave as semi-permeable membranes with improved solute (contaminant) restriction relative to that which would exist in the absence of such behavior (Malusis and Shackelford 2002a,b, Manassero and Dominijanni 2003, Shackelford et al. 2003, Henning 2004, Van Impe 2004, Lu et al. 2004, Dominijanni and Manassero 2005, Yeo et al. 2005). In this regard, research has focused on the determination of both the existence and magnitude of membrane behavior primarily in soils that are comprised either wholly or partially of high swelling smectite (montmorillonite) clay minerals, such as sodium bentonite, since such soils have long been recognized to possess the ability to behave as a semi-permeable membranes (Shackelford et al. 2003). Such materials have included geosynthetic clay liners, or GCLs (Malusis and Shackelford 2002a,b, Shackelford and Lee 2003), and soil-bentonite (SB) backfills for vertical cutoff walls (Yeo et al. 2005, Henning et al. 2006, Evans et al. 2008). Although the results of these studies have indicated the potential existence of membrane behavior in these materials, no information is available on the potential for membrane behavior in naturally occurring clays other than bentonite that would be suitable for use as compacted clay liners on the basis of the ability to achieve a suitably low hydraulic conductivity, k (e.g., $k < 10^{-7}$ cm/s).

Accordingly, the primary purpose of this study was to evaluate the potential

existence of membrane behavior in a compacted, naturally occurring clay that would be representative of clays that could be used as liners in waste containment applications. The study included evaluation of both a naturally occurring local clay, known as Nelson Farm Clay (NFC), and the NFC amended with 5 % (dry wt.) sodium bentonite to enhance the potential for membrane behavior. The results of this study are believed to be the first results pertaining to the evaluation of the potential for membrane behavior in compacted clay liner materials that are suitable for waste containment applications.

6.2 MATERIALS AND EXPERIMENTAL METHODS

6.2.1 Materials

Two different constituent soils were used in this study: a natural clay and a powdered sodium bentonite. Compacted specimens of both the natural clay and the natural clay amended with 5 % (dry wt.) of the sodium bentonite were evaluated in this study.

The natural clay soil is referred to as Nelson Farm Clay (NFC) because the soil comes from the Nelson Farm area of Fort Collins, CO. The powdered sodium bentonite, sold commercially under the trade name NATURALGEL[®] [Wyo-Ben, Inc., Billings, MT], is commonly specified for use in slurry trenching, diaphragm walls, and as a soil mixture additive. The physical and chemical properties and the mineralogical compositions of the constituent soils are provided in Table 6.1.

Based on the grain-size distribution (ASTM D 422) shown in Fig. 6.3, the NFC contains 89 percent fines (i.e., % < 0.075 mm) and 11 percent sand, and the sodium bentonite is comprised of 100 percent fines. However, a comparison of the results from the dry and wet mechanical sieve analyses for the NFC shows that the dry NFC actually

consists of assemblages or granules (i.e., clods) of individual clay particles. The NFC is classified as a low plasticity clay (CL) according to the USCS (ASTM D 2487), whereas the sodium bentonite is a high plasticity clay (CH).

6.2.2 Permeant Liquids

The permeant liquids used in this study consist of de-ionized water (DIW) and solutions of DIW and potassium chloride (KCl) (certified A.C.S.; Fisher Scientific, Fair Lawn, NJ) dissolved in DIW at measured concentrations ranging from 3.9, 8.7, 20, and 47 mM. These particular salt solutions were used to allow comparison of the results from this study with those of previous studies by Malusis and Shackelford (2002a,b) and Yeo et al. (2005) that used the same or similar salt solutions, but with different soil specimens. Each solution was mixed in a 20-L carboy, and EC values of the permeant liquids were monitored with time using the EC probe (Accumet[®] AB30 meter, Fisher Scientific Co., Pittsburgh, PA). The measured values of electrical conductivity (EC) of the DIW and KCl solutions are given in Appendix A.1.

6.2.3 Compacted Specimen of NFC

The Nelson Farm Clay (NFC) and NFC plus 5 % (dry wt.) bentonite were compacted in one lift into a mold with a diameter of 10.28 cm and a height of 2.91 cm, for a compaction volume of 241 cm³. Molds that are generally used in the compaction tests based on ASTM are much higher (e.g., cm³) and the soil is compacted in either three (ASTM D 698) or five lifts (ASTM D 1557). However, in this study, the smaller volume molds were used to reduce the time required to measure the steady-state membrane

behavior, which is affected by diffusion of invading solutes, such that the shorter the distance for diffusion, the shorter the testing duration.

The clay was compacted using three different compaction energies as recommended by Daniel and Benson (1990) for development of an acceptable compaction protocol for compacted clay liners. The three compaction energies included the modified compaction energy (ASTM D 1557), the standard compaction energy (ASTM D 698), and a reduced compaction energy (Eng. Manual EM-1110-2-1906) which represents 60 % of the standard compaction energy (15 drops per lift versus 25 drops per lift). However, because of the smaller mold volumes, the actual compaction energies were slightly different than those specified by the standards, with the high energy corresponding to 100.02 % of that specified in ASTM D 1557, the medium energy corresponding to 98.98 % of that specified in ASTM D 698, and the low energy corresponding to 104.19 % of that specified in Eng. Manual EM-1110-2-1906. The optimum water content for the compaction curves was determined using a 3rd-order polynomial equation as recommended by Howell et al. (1997). The results of three compaction curves for each soil are shown in Figs. 6.4 through 6.6, and the maximum dry unit weights and optimum water contents for each compaction curve are summarized in Table 6.3. As indicated in Tble 6.3, the maximum dry unit weights for each of the two compacted soils increase with increasing compaction energy, whereas the optimum water contents decrease with increasing compaction energy, as expected.

6.2.4 Development of Acceptable Zones

Hydraulic conductivity tests for specimens of the NFC and NFC plus 5 % (dry

weight) bentonite were performed in flexible-wall permeameters (Daniel 1994, Shackelford 1994). The purpose for performing the hydraulic conductivity tests was to develop an acceptable zone (AZ) that provides a range of dry unit weights (γ_d) and gravimetric water contents (w) that correspond to compacted specimens with values of hydraulic conductivity, k , less than 10^{-7} cm/s, in accordance with standard procedure for compacted clay liners (Daniel and Benson 1990). This AZ then was used as a basis for compacting specimens for membrane testing.

After establishing the compaction curves, five specimens (e.g., two specimens on the dry side, two specimens on the wet side and one specimen at the water optimum) were chosen for the hydraulic conductivity test based on each compaction curves. After the compaction, the compacted specimen was extruded from the compaction mold using a hydraulic jack and placed into a flexible-wall permeameter. The assembled specimens then were back-pressured maintaining an effective stress of 34.5 kPa (5.0 psi) until a minimum B value of 0.95 was established in accordance with ASTM D 5084. At the end of back pressure saturation, the cell (confining) pressure was 414 kPa (60.0 psi), and the back pressure was 379 kPa (55.0 psi).

Following the back-pressure saturation stage, specimens were permeated with tap water as a permanent fluid. The falling headwater-rising tailwater method was used for permeation (ASTM D 5084). Flow was induced from bottom to top of the specimen by changing the headwater pressure to 348 kPa (50.5 psi) and the tailwater pressure to 341 kPa (49.5 psi), resulting in a pressure difference 6.9 kPa (1.0 psi), an average effective stress of 34.5 kPa (5.0 psi) of the specimen, and hydraulic gradients ranging from 24.1 to 24.2.

The tests were not terminated before all of the following criteria had been achieved (see Daniel 1994, Shackelford et al. 2000, ASTM D 5084): (1) at least four consecutive volumetric flow ratios of outflow relative to inflow were within 1.00 ± 0.25 (e.g., ASTM D 5084); (2) at least four consecutive k values were within $\pm 25\%$ of the mean value for $k \geq 1 \times 10^{-8}$ cm/s or within $\pm 50\%$ for $k < 1 \times 10^{-8}$ cm/s (e.g., ASTM D 5084); and (3) a minimum of two pore volumes of flow (PVF) had passed through the specimen.

The results of the hydraulic conductivity testing are summarized in Table 6.5 and illustrated in Fig. 6.6, and the developed acceptable zones are showed in Figs. 6.7 and 6.8 for the compacted NFC and compacted NFC amended with bentonite, respectively. In general, the k values for the compacted NFC range from 1.45×10^{-8} cm/s to 3.82×10^{-5} cm/s, whereas those for the compacted specimens of NFC amended with bentonite range from 3.24×10^{-9} cm/s to 4.12×10^{-7} cm/s. Thus, the bentonite addition reduced the k of the NFC by approximately 0.01 to 0.1 orders of magnitude. In addition, the highest measured k value was 3.82×10^{-5} cm/s corresponding to a specimen of NFC compacted using the reduced compaction energy, whereas the lowest k value was 3.24×10^{-9} cm/s corresponding to a specimen of NFC plus 5 % bentonite compacted using the maximum compaction energy.

6.2.5 Specimen Preparation and Assembly

For the compacted NFC and NFC plus 5 % bentonite specimens tested for membrane behavior, the specimen preparation consisted of two stages, a compaction stage and a flushing stage. The purpose of the compaction stage was to compact the

specimens with the acceptable zone (AZ) for the respective soil such that the compacted specimen would be expected to be representative of those suitable as a compacted clay liner. The purpose of the flushing stage was to reduce the amount of the soluble ions from the specimens of NFC and NFC plus 5 % bentonite to enhance the potential for membrane behavior, to saturate the test specimens prior to membrane tests, and to measure the initial hydraulic conductivity for each specimen (e.g., Shackelford et al. 2003).

For the flushing stage, circular specimens of the compacted NFC and NFC plus 5 % bentonite with a diameter of 102.8 mm and a thickness 29.1 mm were permeated by using modified rigid-wall permeameter in Fig. 6.1. The modified rigid-wall permeameter from commercial double-ring compaction mold consists of a clear plastic (acrylic) and a stainless steel cylindrical cell that is held together between top and bottom plates by three threaded tie rods at 120-degree spacings. O-rings contained within grooved cavities machined into the top and bottom plates together with vacuum grease provide water tight seals between the top, stainless steel porous disk, and bottom plates and the cylindrical cell. This stainless steel porous disk (1/8-in thick, 316 SS material, 10 μ m pore size, Mott Corp., Farmington, CT) was applied to the top of the specimen in order to minimize the volume change due to saturation during flushing stage.

The specimens compacted in the cylindrical mold were assembled directly within the rigid-wall permeameters, i.e., without extruding the compacted specimens. The specimens for membrane testing were compacted using the standard compaction energy (ASTM D 698) to values for w and γ_d that were within the AZ for that specific soil type, such that the resulting specimens should be able to achieve suitably the low hydraulic

conductivity ($k < 10^{-7}$ cm/s) consistent with that of compacted clay liners. The compacted specimen with a diameter of 102.8 mm and a thickness of 29.1 mm was placed on top of Whatman No. 2 filter paper resting on a porous stone situated within the based pedestal, the top of the specimen was covered by filter paper and the stainless steel porous disk. And the entire system was assembled together. The chamber then was filled with de-aired water via the cell-water accumulator (CWA). The permeation with DIW continued until the electrical conductivity, EC, of the effluent from the specimen was $\sim 63.8\%$ of the measured EC of 56.1 mS/m for the lowest salt concentration (3.9 mM KCl) that was used in the subsequent membrane testing.

After completion of the flushing stage, the specimens of NFC and NFC plus 5 % bentonite were transferred to the flexible-wall cell specifically developed for membrane testing (see Chapter 4) for membrane testing. After re-assembling the specimens in the flexible-wall membrane cell, the specimens were back-pressure saturated at an effective stress 34.5 kPa (5.0 psi) until a final confining stress of 207.0 kPa (30.0 psi) and a final back pressure of 172 kPa (25.0 psi). After equilibrium had been established, the drainage valves were closed to start the membrane testing stage. Volume changes (ΔV) were monitored versus time via measuring changes in the air-water interface within the cell-water accumulator attached to the flexible-wall membrane cell.

6.2.6 Testing Program

Both multiple-stage (MS) and single-stage (SS) membrane tests were conducted to evaluate the potential existence and magnitude of membrane behavior for compacted specimens of both NFC and NFC plus 5 % bentonite. The primary difference between SS

and MS tests is that the SS tests involve establishing only one concentration gradient across the test specimen, whereas the MS tests involve establishing several concentration gradients across a test specimen through sequential circulation of KCl solutions with increasingly higher concentrations. Thus, more than one ω value can be determined for a single specimen within a relatively short testing duration (< 40 d) in an MS test. The complete testing program is summarized in Table 6.4. Only one membrane test was conducted for the unamended NFC because the results of this test indicated virtually no membrane behavior (see subsequent Results).

6.3 RESULTS

6.3.1 Flushing Stage of Specimens

The results from flushing the compacted test specimens by permeation with DIW prior to membrane testing are shown in Fig. 6.9a. Both All specimens were permeated with DIW until the electrical conductivity, EC, in the effluent from the specimens was only a fraction of the EC of 56.1 mS/m for the 3.9 mM KCl solution, i.e., in order to enhance the potential for membrane behavior. The compacted NFC specimen was flushed for 99 d resulting in an effluent EC of 20.6 mS/m, or 36.7 % of that for the 3.9 mM KCl solution, whereas the compacted specimens of the bentonite amended NFC were flushed for 193, 244, 220, and 239 d resulting in an effluent EC of 35.8, 34.1, 28.5, and 27.1 mS/m, or 63.8, 60.8, 50.8, and 48.3 % of the EC associated with a 3.9 mM KCl solution, respectively. The significantly longer flushing durations for the bentonite amended NFC is attributable to the lower k values for these specimens relative to that for the unamended NFC specimen.

The k values for the compacted specimens also were measured during the flushing stage. As shown in Fig. 6.9b, in spite of somewhat erratic behavior in the measured k values, permeation with DIW resulted in measured steady-state k values of 1.46×10^{-8} cm/s for the single compacted NFC specimen and 5.22×10^{-9} cm/s, 7.14×10^{-9} cm/s, 8.64×10^{-9} cm/s, and 9.61×10^{-9} cm/s for the four compacted specimens of NFC amended with 5 % sodium bentonite. Thus, the measured k values for the specimens compacted within the AZs for the respective soils were all lower than 10^{-7} cm/s prior to membrane testing, and the measured k values for the bentonite amended NFC were from 1.52 to 2.80 times lower than that for the unamended NFC specimen.

6.3.2 Electrical Conductivities

The values for the electrical conductivity (EC) measured in the circulation outflows from the top (EC_{top}) and bottom (EC_{bottom}) boundaries during the membrane testing stage are shown in Fig. 6.10. These measured EC values reflect the boundary conditions imposed in the tests. The lower values for EC_{top} relative to the EC values for the source solutions, EC_o (i.e., $EC_{top} < EC_o$), are consistent with the loss of solute mass from the source solutions due to solute diffusion into the specimens, whereas the eventual increase in the values of EC_{bottom} with time is consistent with the gain of solute mass in the bottom circulation outflow due to solute diffusion through the specimen. The values for both EC_{top} and EC_{bottom} indicate that the establishment of steady-state conditions with respect to EC at both the top and bottom boundaries takes longer time than 7-d period typical for the tests conducted using the thinner GCL specimens reported in Chapters 4 and 5.

6.3.3 Boundary Pressures

The water pressures occurring at the top (u_{top}) and bottom (u_{bottom}) of the boundaries of the specimens measured with in-line transducers T1 and T2 (see Fig. 4.1), respectively, during the membrane tests are presented in Figs. 6.12 through 6.16.. In the case of the compacted NFC specimen (Fig. 6.12), there are relatively small differences in the pore-water pressure build-up at the top and bottom boundaries of the specimen, which indicates that the unamended NFC soil does not possess and significant ability to restrict the migration of solutes (KCl). In contrast, all of the compacted specimens of the bentonite amended NFC indicate noticeable differences between the boundary water pressures during KCl circulation (Figs. 6.13-6.16), indicating that the addition of the sodium bentonite to the NFC imparted relatively significant solute restriction and associated potential for membrane behavior.

6.3.4 Induced Membrane Efficiencies

The measured chemico-osmotic pressure differences, $-\Delta P (> 0)$, induced across the compacted specimens of NFC and NFC plus 5 % bentonite are presented in Figs. 6.11 through 6.15. Introduction of KCl into the top cap after the initial circulation with DIW resulted in a more gradual increase in the pressure differences than have been previously reported for tests involving geosynthetic clay liners (GCLs), and the durations of the established KCl concentration differences required to achieve equilibrium in the stage were also greater than the typical 7-d periods required for GCL specimens. (see Chapters 4 and 5). The differences in differential pressure responses observed in this study involving the compacted specimens of the NFC and bentonite amended NFC versus those

of GCLs likely is due, in part, to the fact the soil portion of the GCL is comprised on 100 % sodium bentonite, such that the soil component of the GCL is more homogeneous relative to the NFC and NFC amended with 5 % bentonite. Thus, the pore structure in the bentonite in the GCL is likely to be more consistent than that in either the compacted NFC or the compacted NFC amended with bentonite. The longer time required to establish equilibrium for the tests involving compacted NFC and compacted NFC amended with bentonite again can be attributed to the much greater thickness of the compacted specimens relative to that of the GCLs.

Values of effective or net pressure difference measured across specimen at steady state, $-\Delta P_e$, ranged from 0.2 kPa to 0.8 kPa for the compacted NFC specimen, and from 2.6 kPa to 15.0 kPa for the specimens of NFC plus 5 % bentonite. Measured membrane efficiency coefficients at steady-state, ω_{ss} , based on the data are summarized in Table 6.5. These measured values of ω_{ss} range from 0.003 to 0.013 for the compacted specimen of NFC, and from 0.027 to 0.762 for the compacted specimens of the NFC amended with bentonite, depending on the KCl concentration difference.

6.3.5 Volume Changes

Volume changes were recorded during the membrane testing stage via the cell-wall accumulator (CWA in Fig. 4.1) as a check on the assumption of undrained conditions. As shown in Fig. 6.22, some incremental volume changes, ΔV ($\leq \pm 1.26$ mL), were recorded during the membrane testing stage, resulting in cumulative volume changes, $\Sigma(\Delta V)$, ranging from -3.98 mL and -25.78 mL for specimens of NFC soils and NFC plus 5 % bentonite soils. The vast majority of these volume changes were negative,

corresponding to decreases in the specimen volumes (i.e., compression), and occurred primarily during the circulation of the KCl solutions as opposed to during circulation of only DIW. As shown in Fig. 6.23, these volume changes corresponded to incremental volumetric strains ($\Delta V/V_o$) of $\leq \pm 1\%$ and cumulative volumetric strains ($\Sigma(\Delta V)/V_o$) of $\leq -2.0\%$ and $\leq -11.0\%$ for specimens of NFC soils and NFC plus 5% bentonite soils. As explained in Chapter 4, these volume changes likely occurred during the refilling and sampling stages of the tests, during which drainage lines were opened briefly (< 10 s) to equilibrate the back pressure prior to each circulation event, as opposed to during the membrane measurement periods of the tests (24 h), and the drainage likely occurred due to physico-chemical interactions in the effective stress in the specimens resulting from the variation on salt concentrations in the pore water during the testing.

6.4 DISCUSSION

The values of ω_{ss} summarized in Table 6.5 are plotted as a function of the average difference in the initial KCl concentrations, or $-\Delta C_{o,ave}$ [$= -\Delta C_o/2 = (C_{ot} - C_{ob})/2 = C_{ot}/2$], in Fig. 6.25. As expected, values of ω_{ss} based on $-\Delta\pi_o$, or $\omega_{ss,o}$, are more conservative (lower) than values of ω_{ss} based on $-\Delta\pi_{ave}$, or $\omega_{ss,ave}$, i.e., since $-\Delta\pi_o > -\Delta\pi_{ave}$. For example, $\omega_{ss,ave}/\omega_{ss,o}$ increased from 1.11 to 1.12 as $-\Delta C_{o,ave}$ increased from 1.95 mM to 23.5 mM, respectively, for the compacted specimen of NFC, whereas $\omega_{ss,ave}/\omega_{ss,o}$ decreased from 1.28 to 1.10 as $-\Delta C_{o,ave}$ increased from 1.95 mM to 10 mM, respectively, for the compacted specimens of NFC amended with bentonite.

The measured values of ω_{ss} were somewhat lower in the MS tests versus the SS tests. One possible reason for this difference is that sequentially establishing several

concentration gradients across a test specimen sequentially compresses the DDL with increasingly higher concentrations to a greater extent than that compression that occurs from establishing a single concentration difference across the specimen. Thus, even though MS tests can be used to determine several different ω_{ss} values on a single specimen in a relatively short time (< 40 d), the measured ω_{ss} value at for a given KCl concentration difference may be as much as 103 % lower than that obtained in a SS test using the same KCl concentration difference and soil. This relative difference between the ω_{ss} values measured in MS versus SS tests also has been indicated in the results of tests conducted with GCLs (e.g., Malusis and Shackelford 2002a or b).

Testing duration is directly correlated with the thickness of the specimens since thicker specimens require longer elapsed time to establish equilibrium due to greater extent of diffusion. As a result, the testing durations for the compacted specimens of NFC and NFC amended with bentonite in this study were on the order of 6 to 15 times greater than those previously reported for tests involving GCLs (see Chapter 4 and 5), since the thicknesses of the specimens tested in this study were on the order of about three times greater than those for the GCLs previously tested (i.e., 29.1 mm vs. 10 mm).

The results indicate that membrane behavior was evident in the compacted specimen of the Nelson Farm Clay, although the magnitude of h=this membrane behavior was relatively insignificant in that the values for ω_{ss} ranged from only 0.003 to 0.013. This range of ω_{ss} values is significantly lower than that previously reported for GCL specimens, where ω_{ss} ranged from 0.680 to 0.010 as the KCl concentration ranged from 3.9 to 47 mM, respectively (Chapter 5). However, the addition of only 5 % of sodium bentonite to the NFC imparted significant membrane behavior to the NFC, with ω_{ss}

values ranging from 0.762 to 0.027 as the KCl concentration ranged from 3.9 to 20 mM, respectively. The differences in the measured membrane behaviors can be attributed, in part, to the difference in the bentonite contents of the materials (Shackelford et al. 2003). Overall, the results of this study suggest that the membrane behavior in compacted natural clays not comprised of significant percentages of high swelling smectite clay minerals likely will not be significant even if the hydraulic conductivity, k , is relatively low ($k < 10^{-7}$ cm/s), unless such clays are amended with sodium bentonite.

6.5 SUMMARY AND CONCLUSIONS

The results indicated that compacted NFC does not exhibit significant semi-permeable membrane behavior, with measured membrane efficiencies at steady state, ω_{ss} , based on the difference in initial (source) concentrations, $\omega_{ss,o}$, ranging from 0.003 (one specimen) at C_{ot} of 47 mM KCl to 0.013 (one specimen) at C_{ot} of 3.9 mM KCl, and ω_{ss} values based on the average of the difference in boundary concentrations, $\omega_{ss,ave}$, ranging from 0.004 (one specimen) at C_{ot} of 47 mM KCl to 0.014 (one specimen) at C_{ot} of 3.9 mM KCl. However, specimens of compacted NFC amended with 5 % sodium bentonite did behave as a semi-permeable membranes, with measured values of $\omega_{ss,o}$ ranging from 0.027 (one specimen) at C_{ot} of 20 mM KCl to 0.728 ± 0.034 (two specimens) at C_{ot} of 3.9 mM KCl, and measured values of $\omega_{ss,ave}$, ranging from 0.030 (one specimen) at C_{ot} of 20 mM KCl to 0.934 ± 0.039 (two specimens) at C_{ot} of 3.9 mM KCl. Thus, compacted NFC, although suitable for use as a compacted clay liner based on k , does not possess significant membrane behavior, whereas compacted NFC amended with only 5 % sodium bentonite not only results in lower k than compacted NFC, but also exhibits significant

membrane behavior. Thus, the results of this study show that the membrane behavior of compacted NFC can be enhanced by up to 52 times based on the addition of only 5 % of sodium bentonite.

The measured membrane efficiency coefficients, ω , for the compacted NFC amended with 5 % bentonite specimens were relatively high (e.g., 0.728 and 0.762) at the low concentration difference of 3.9 mM KCl, but decreased significantly with increasing KCl concentration difference, unlike GCL specimens with 100 % sodium bentonite. Thus, higher salt concentrations tend to adversely affect the membrane behavior of the compacted NFC amended with sodium bentonite to a greater extent than previously observed for specimens of a GCL subjected to the same testing conditions. This difference in effect likely is due, in part, to the differences in the amount of bentonite contained in the two cases and the resulting differences in the pore structures of the two soils.

ACKNOWLEDGMENTS

Financial support for this study was provided by the U. S. National Science Foundation (NSF), Arlington, VA, under Grants CMS-0099430 entitled, "Membrane Behavior of Clay Soil Barrier Materials" and CMS-0624104 entitled, "Enhanced Clay Membrane Barriers for Sustainable Waste Containment". The opinions expressed in this paper are solely those of the writers and are not necessarily consistent with the policies or opinions of the NSF. The authors also express appreciation to Dr. Jae-Myung Lee of the California Department of Transportation for his assistance in the early stages of the development of the flexible-wall testing apparatus.

6.6 REFERENCES

- Daniel, D.E. 1994. State-of-the-art: Laboratory hydraulic conductivity test for saturated soils." *Hydraulic Conductivity and Waste Contaminant Transport in Soil*, ASTM STP 1142, D.E Daniel and S.J. Trautwein (Eds.), ASTM, West Conshohoken, PA, 30-78.
- Daniel, D. E., and Benson, C. H. 1990. Water content-density criteria for compacted soil liners. *Journal of Geotechnical Engineering*, 116(12), 1811-1830.
- Dominijanni, A. and Manassero, M. 2005. Modelling osmosis and solute transport through clay membrane barriers. *Geo-Frontiers 2005*, Austin, TX, Jan. 24-26, 2005, ASCE, Reston, VA.
- Evans, J.C., Shackelford, C.D., Yeo, S.-S., and Henning, J. 2008. Membrane behavior of soil-bentonite slurry-trench cutoff walls. *Soil and Sediment Contamination*, 17(4), 316-322.
- Gleason, M. H., Daniel, D. E., and Eykholt, G. R. 1997. Calcium and sodium bentonite for hydraulic containment applications. *Journal of Geotechnical and Geoenvironmental Engineering*, 123(5), 438-445.
- Henning, J. T. 2004. *Chemico-Osmotic Efficiency of Two Real World SB Slurry Trench Cutoff Wall Backfills*. MS Thesis, Bucknell University, Lewisburg, Pennsylvania, USA.
- Henning, J.T., Evans, J.C., and Shackelford, C.D. 2006. Membrane behavior of two backfills from field-constructed soil-bentonite cutoff walls. *Journal of Geotechnical and Geoenvironmental Engineering*, 132(10), 1243-1249.

- Jo, H. Y., Katsumi, T., Benson, C. H., and Edil, T. B. 2001. Hydraulic conductivity and swelling on nonprehydrated GCLs permeated with single-species salt solutions. *Journal of Geotechnical and Geoenvironmental Engineering*, 127(7), 557-567.
- Kolstad, D. C. 2000. *Compatibility of Geosynthetic Clay Liners (GCLs) with Multispecies Inorganic Solutions*. MS Thesis, University of Wisconsin, Madison, Wisconsin, USA.
- Lee, J.-Y. and Shackelford, C. D. 2005a. Impact of bentonite quality on hydraulic conductivity of geosynthetic clay liners. *Journal of Geotechnical and Geoenvironmental Engineering*, 131(1), 64-77.
- Malusis, M.A., Shackelford, C.D., and Olsen, H.W. 2001b. A laboratory apparatus to measure chemico-osmotic efficiency coefficients for clay soils. *Geotechnical Testing Journal*, 24(3), 229-242.
- Malusis, M. A. and Shackelford, C. D. 2002a. Chemico-osmotic efficiency of a geosynthetic clay liner. *Journal of Geotechnical and Geoenvironmental Engineering*, 128(2), 97-106.
- Malusis, M.A. and Shackelford, C.D., 2002b. Coupling effects during steady-state solute diffusion through a semipermeable clay membrane. *Environmental Science and Technology*, 36(6), 1312-1319.
- Malusis, M.A., Shackelford, C.D., and Olsen, H.W. 2003. Flow and transport through clay membrane barriers. *Engineering Geology*, 70(3), 235-248.
- Manassero, M. and Dominijanni, A. 2003. Modelling the osmosis effect on solute migration through porous media. *Geotechnique*, 53(5), 481-492.
- Mitchell, J.K. and Soga, K. 2005. *Fundamentals of Soil Behavior*, 3rd Ed. John Wiley and

Sons, Inc., New York.

- Olsen, H.W., Yearsley, E.N., and Nelson, K.R. 1990. Chemico-osmosis versus diffusion-osmosis. *Transportation Research Record No. 1288*, Transportation Research Board, Washington D.C., 15-22.
- Shackelford, C.D, Benson, C.H., Katsumi, T., Edil, T.B., and Lin, L. 2000. Evaluating the hydraulic conductivity of GCLs permeated with non-standard liquids. *Geotextiles and Geomembranes*, 18(2-4), 133-161.
- Shackelford, C. D. 1994. Waste-soil interactions that alter hydraulic conductivity. *Hydraulic Conductivity and Waste Contaminant Transport in Soil*, ASTM STP 1142, D. E. Daniel and S. J. Trautwein, eds., ASTM, West Conshohoken, Pennsylvania, USA, 111-168.
- Shackelford, C.D. and Lee, J.-M. 2003. The destructive role of diffusion on clay membrane behavior. *Clays and Clay Minerals*, 51(2), 186-196.
- Shackelford, C.D., Malusis, M.A., and Olsen, H.W. 2003. Clay membrane behavior for geoenvironmental containment. *Soil and Rock America Conference 2003*, P. J. Culligan, H. H. Einstein, and A. J. Whittle (Eds.), Verlag Glückauf GMBH, Essen, Germany, Vol. 1, 767-774.
- Stern, R. T. and Shackelford, C. D. 1998. Permeation of sand-processed clay mixtures with calcium chloride solutions. *Journal of Geotechnical and Geoenvironmental Engineering*, 124(3), 231-241.
- VanGulck, J. F. and Rowe, R. K. 2004. Evolution of clog formation with time in columns permeated with synthetic landfill leachate. *Journal of Contaminant Hydrology*, 75(1-2), 115-139.

Yeo, S.-S. 2003. *Hydraulic Conductivity, Consolidation, and Membrane Behavior of Model Backfill-Slurry Mixtures for Vertical Cutoff Walls*. M. S. Thesis, Colorado State University, Fort Collins, Colorado.

Yeo, S.-S., Shackelford, C.D., and Evans, J.C. 2005. Membrane behavior of model soil-bentonite backfills. *Journal of Geotechnical and Geoenvironmental Engineering*, 131(4), 418-429.

Table 6.1. Physical and chemical properties and mineralogical compositions of constituent soils used for model backfill mixtures.

Property	Standard	Soil Type	
		NFC	Bentonite
Specific Gravity, <i>G_s</i>	ASTM D 854	2.70	2.72
Liquid Limit, LL (%)	ASTM D 4318	32.3	497
Plastic Index, PI (%)	ASTM D 4318	14.5	454
Principal Minerals (%)			
Montmorillonite		-	65
Cristobalite		-	18
Mixed-Layer Illite/Smectite	a	22	-
Quartz		40	6
Plagioclase Feldspar		13	5
Calcite		13	2
Other		12	4
Cation Exchange Capacity (meq/100g)	b	10.1	86.1
Exchangeable Metals (meq/100g):			
Ca		4.2	4.4
Mg	b	3.1	8.1
Na		0.3	77.5
K		0.3	0.99
Sum		7.9	90.99
Soluble Salts (mg/kg):			
Ca		35.3	47.0
Mg		8.30	14.1
Na		22.7	2097
K	b	3.40	61.2
CO ₃		< 0.4	< 0.4
HCO ₃		78.7	674
SO ₄		37.5	3610
Cl		20.9	238
NO ₃		53.3	217
Soil pH	ASTM D 4972	8.30	7.9
Soil Electrical Conductance, EC (mS/m) at 25°C	c	36.0	193

Notes:

NFC: Nelson Farm Clay.

^a Based on x-ray diffraction analyses performed by Mineralogy Inc., Tulsa, OK.

^b Procedures described in Shackelford and Redmond (1995).

^c Measured using saturated soil paste.

Table 6.2 Testing series for membrane efficiency of Nelson Farm Clay (NFC) and NFC plus 5 % bentonite specimens.

Test No.	Constituent soils ⁽¹⁾	Type of test ⁽²⁾	KCl Source Concentration, C _{ot} (mM)
1	NFC	MS	3.9, 8.7, 47.0
2	NFC plus 5 % bentonite	MS	3.9, 8.7
3	NFC plus 5 % bentonite	SS	3.9
4	NFC plus 5 % bentonite	SS	8.7
5	NFC plus 5 % bentonite	SS	20.0

⁽¹⁾ All test specimens at 34.5 kPa (5.0 psi) initial effective stress.

⁽²⁾ MS = multiple-stage test, SS = single-stage test.

Table 6.3. Results of compaction

Constituents soils	Compaction energy ^(a)	Maximum dry unit weight ^(b) γ_d [kN/m ³ (lb/ft ³)]	Optimum water content ^(b) w_{opt} (%)
Nelson Farm Clay (NFC)	Modified	18.7 (119.1)	12.2
	Standard	17.2 (109.5)	16.6
	Reduced	16.9 (107.6)	18.1
NFC plus 5 % bentonite	Modified	18.2 (115.9)	11.5
	Standard	16.5 (105.0)	16.0
	Reduced	15.4 (98.0)	21.2

^(a) Modified = ASTM D 1557; Standard = ASTM D 698; Reduced = Eng. Manual EM-1110-2-1906.

^(b) Based on third-order polynomial regression as per Howell et al. (1997).

Table 6.4. Range of measured hydraulic conductivities for each compacted soil

Constituents soils	Compaction energy ^(a)	Hydraulic conductivity, k (cm/s)
Nelson Farm Clay	Modified	$1.45 \times 10^{-8} \leq k \leq 1.74 \times 10^{-6}$
	Standard	$3.75 \times 10^{-8} \leq k \leq 1.38 \times 10^{-6}$
	Reduced	$3.24 \times 10^{-8} \leq k \leq 3.82 \times 10^{-5}$
NFC plus 5 % bentonite	Modified	$3.24 \times 10^{-9} \leq k \leq 1.69 \times 10^{-7}$
	Standard	$1.07 \times 10^{-8} \leq k \leq 4.12 \times 10^{-7}$
	Reduced	$9.19 \times 10^{-9} \leq k \leq 2.10 \times 10^{-7}$

^(a) Modified = ASTM D 1557; Standard = ASTM D 698; Reduced = Eng. Manual EM-1110-2-1906.

Table 6.5. Results of multi-stage membrane testing using flexible-wall cell for compacted specimens of Nelson Farm Clay (NFC) and NFC plus 5 % bentonite.

Constituents soils	Test Type ^(a)	KCL Source Concentration, C_{ot} (mM)	Differences in Chemo-Osmotic Pressures ^(b) [kPa (psi)]		Membrane Efficiencies at Steady State, ω_{ss}		
			$-\Delta P_e$	$-\Delta\pi_0$	$-\Delta\pi_{ave}$	$\omega_{ss,0}$ ($=\Delta P_e/\Delta\pi_0$)	$\omega_{ss,ave}$ ($=\Delta P_e/\Delta\pi_{ave}$)
NFC	MS	3.9	0.248 (0.036)	19.011 (2.757)	17.178 (2.491)	0.013	0.014
		8.7	0.434 (0.063)	42.408 (6.149)	38.878 (5.637)	0.010	0.011
		47.0	0.779 (0.113)	229.101 (33.220)	204.255 (29.617)	0.003	0.004
NFC plus 5 % bentonite	MS	3.9	13.841 (2.007)	19.011 (2.757)	14.820 (2.149)	0.728	0.934
		8.7	7.317 (1.061)	42.408 (6.149)	37.325 (5.412)	0.173	0.196
		3.9	14.483 (2.100)	19.011 (2.757)	14.885 (2.158)	0.762	0.973
	SS	8.7	14.959 (2.169)	42.408 (6.149)	38.571 (5.593)	0.353	0.388
		20.0	2.603 (0.377)	97.490 (14.136)	88.019 (12.763)	0.027	0.030

^(a) MS = multiple-stage test, SS = single-stage test

^(b) $-\Delta P_e$ = effective or net pressure difference measured across specimen at steady state; $-\Delta\pi_0$ = theoretical maximum pressure difference based on difference in initial (source) concentrations; $-\Delta\pi_{ave}$ = theoretical maximum pressure difference based on difference in average boundary concentrations at steady state.

Table 6.6. Comparison for evaluation of factors affecting membrane efficiency according to soil types and specimen thicknesses used in previous research.

Material Type	Type of test ⁽¹⁾	Thickness of specimen (mm)	Testing Duration (day)	Initial void ratio (e)	Source KCl Concentration, C_{ot} (mM)	Membrane efficiency coefficient at steady-state (ω_{ss})	Reference
Bentomat @ GCL	MS	8	40	2.846	3.9, 6.0, 9.7, 20, 47	0.14 – 0.51	Malusis and Shackelford (2002)
Bentomat @ GCL	SS	10	15 – 20	3.545 – 4.000	3.9, 6.0, 9.7, 20, 47	0.12 – 0.68	
Bentomat @ GCL	MS	13	36	6.143	3.9, 6.0, 9.7, 20, 47	0.07 – 0.38	
Nelson Farm Clay backfill	SS	8, 9, 10	18	0.605 – 1.008	3.9	0.018 – 0.024	Yeo et al. (2005)
Sand-bentonite backfill	SS	9, 10, 11	18	0.812 – 1.212	3.9	0.118 – 0.166	
Bentomat @ GCL	MS	10	35	1.896 – 4.049	3.9, 6.0, 9.7, 20, 47	0.010 – 0.680	This study (2008)
Nelson Farm Clay (NFC)	MS	29.1	42	0.524	3.9, 8.7, 47	0.003 – 0.013	
NFC plus 5 % bentonite	MS	29.1	105	0.527	3.9, 8.7	0.173 – 0.728	
NFC plus 5 % bentonite	SS	29.1	42 – 49	0.538 – 0.576	3.9, 8.7, 20	0.027 – 0.762	

⁽¹⁾ MS = multiple-stage test, SS = single-stage test.

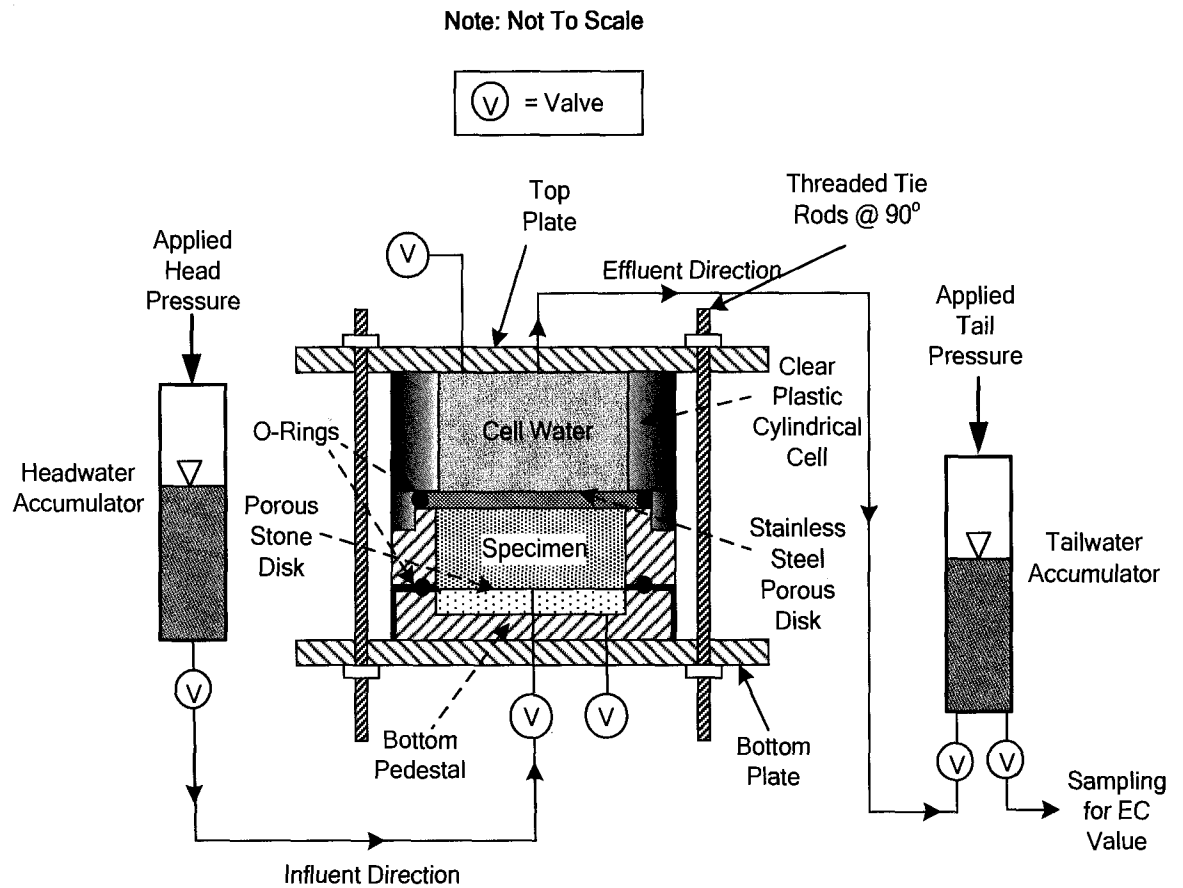


Fig. 6.1 – A schematic diagram for the flushing and hydraulic conductivity test for compacted specimens of Nelson Farm Clay (NFC) and NFC plus 5 % bentonite.

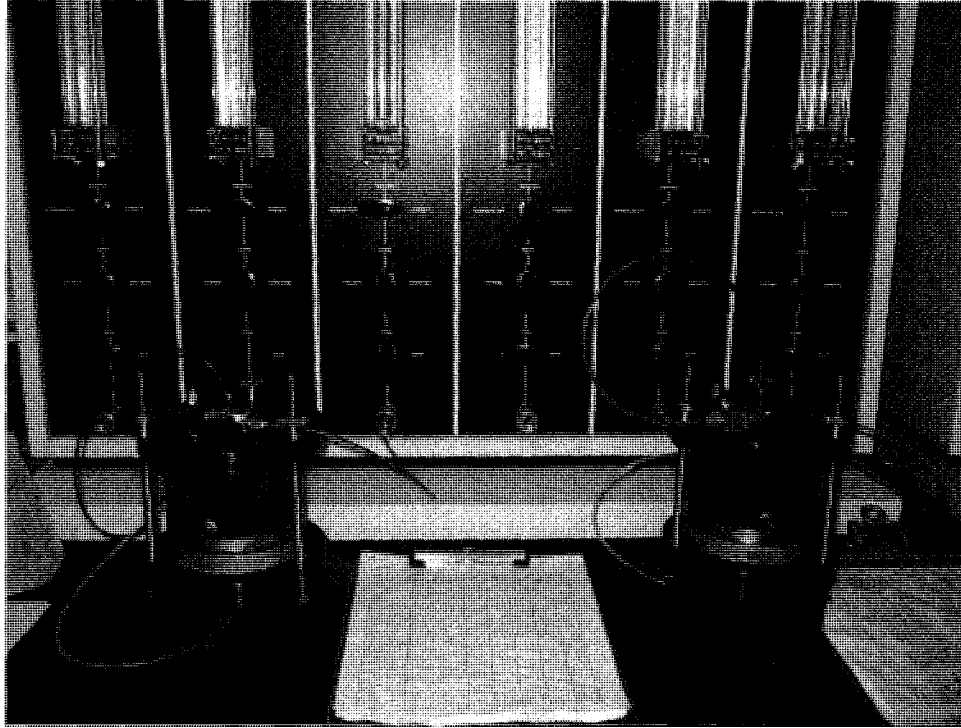


Fig. 6.2 – Pictorial view of permeating compacted specimens of Nelson Farm Clay (NFC) and NFC plus 5 % bentonite.

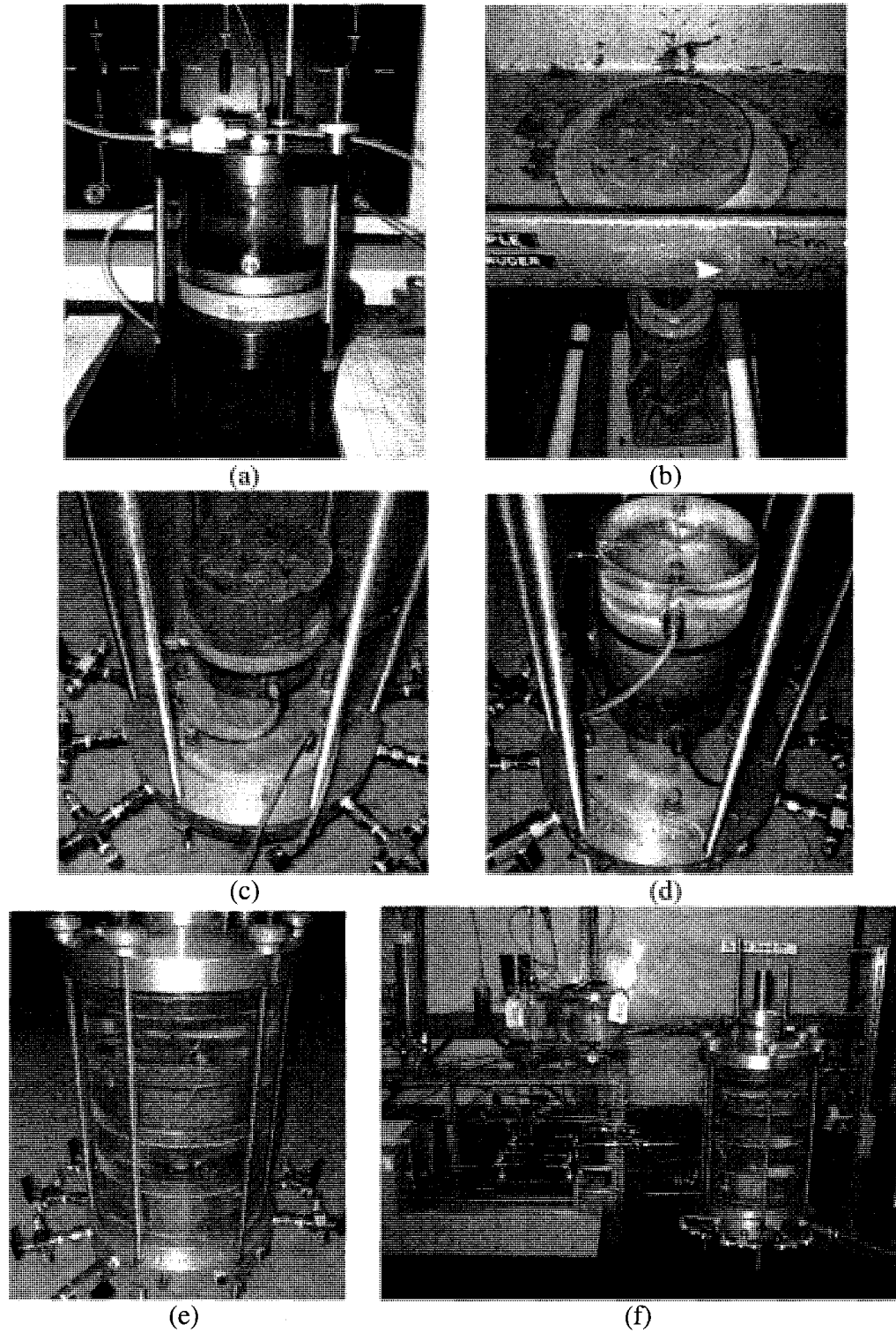


Fig. 6.3 – Pictorial views for different stage for setting up compacted specimens of Nelson Farm Clay (NFC) and NFC plus 5 % bentonite in flexible-wall cell for membrane testing (clockwise from top left): (a) permeating; (b) extruding; (c) specimen setup; (d) membrane and top cap; (e) flexible-wall cell; and (f) membrane testing system.

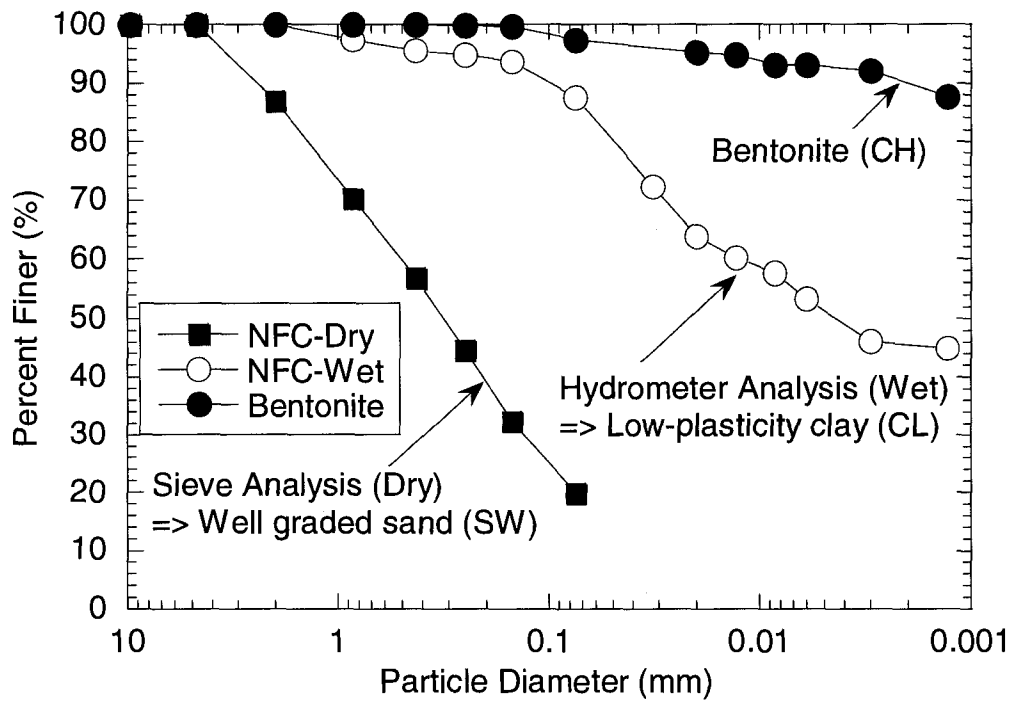


Fig. 6.4 – Grain-size distributions for Nelson Farm Clay (NFC) and bentonite used in this study (after Yeo et al. 2005)

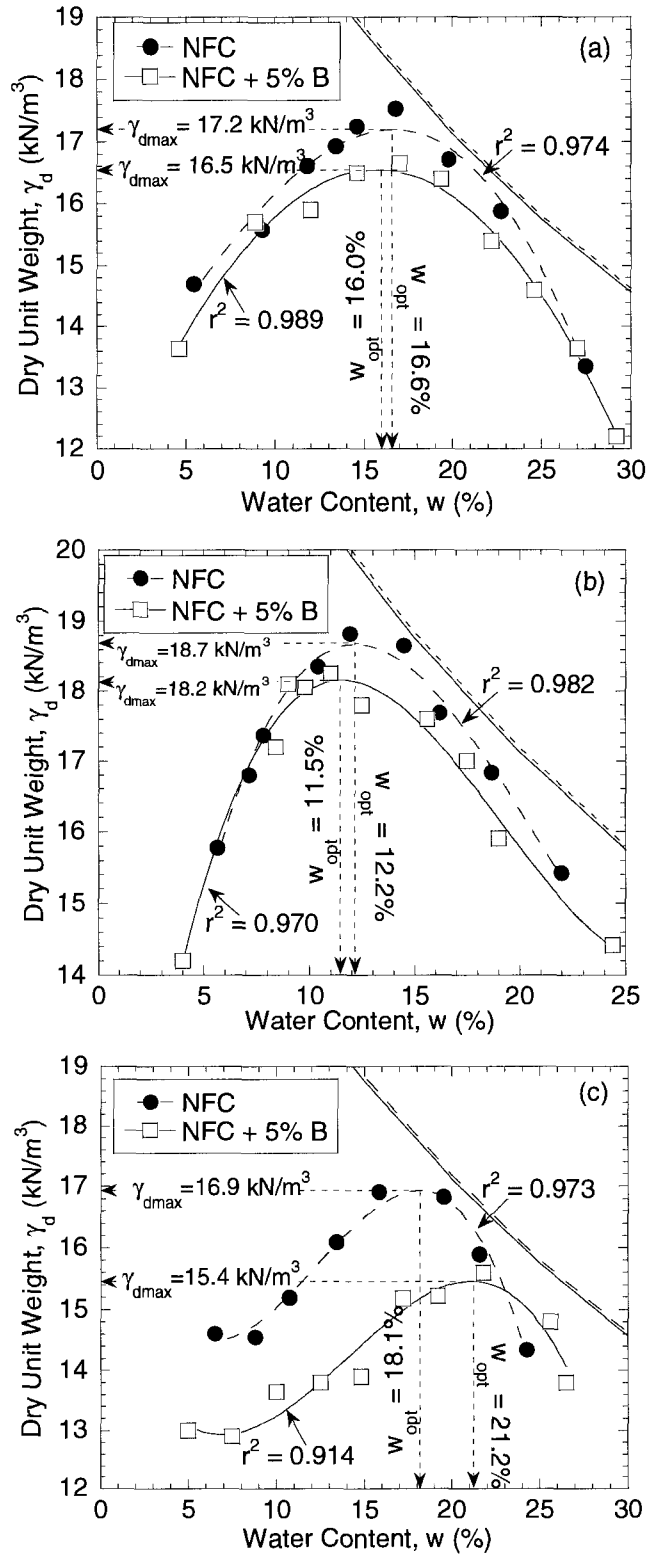


Fig. 6.5 – Compaction curves for Nelson Farm Clay (NFC) and NFC plus 5% (dry weight) bentonite (B): (a) standard compaction curve (ASTM D 698) (b) modified compaction curve (ASTM D 1557); (c) reduced compaction curve (Eng. Manual EM-1110-2-1906).

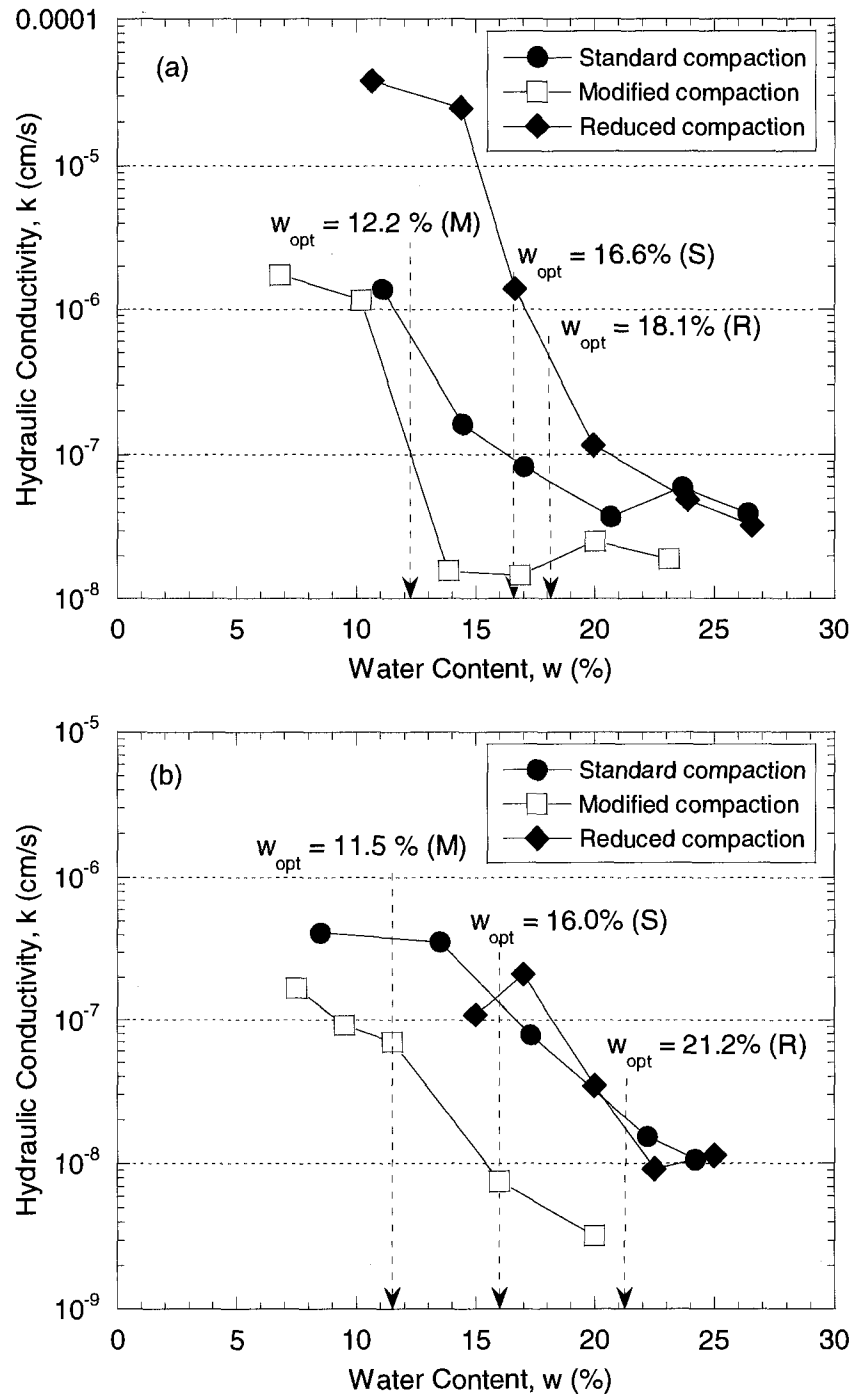


Fig. 6.6 – Initial water contents versus hydraulic conductivity of compacted specimens of (a) Nelson Farm Clay (NFC) (b) NFC plus 5 % bentonite compacted by standard compaction (ASTM D 698), modified compaction (ASTM D 1557), and reduced compaction (Eng. Manual EM-1110-2-1906).

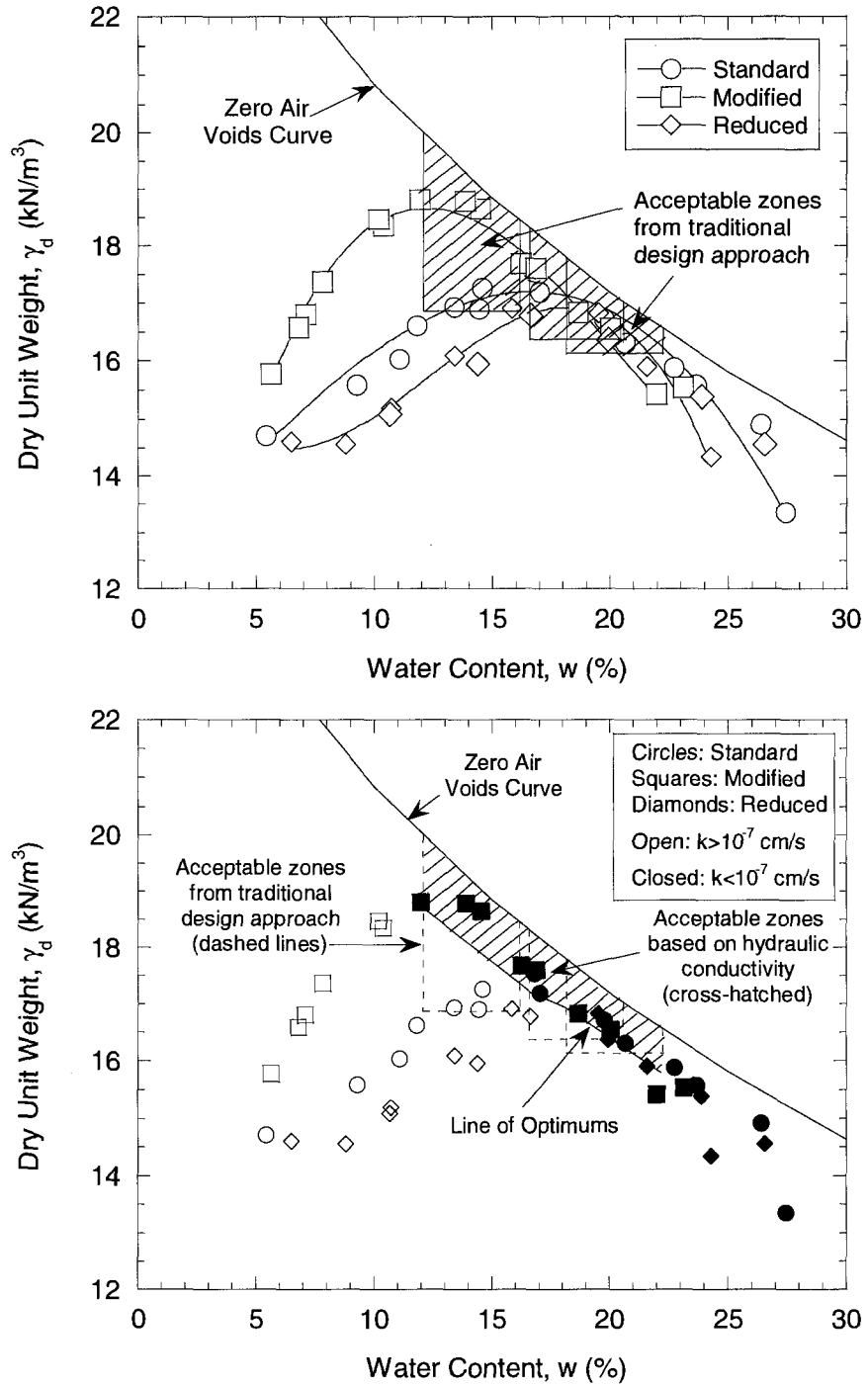


Fig. 6.7 – Acceptable zones for Nelson Farm Clay (NFC) based on (a) the traditional design approach (b) the hydraulic conductivity approach proposed by Daniel and Benson (1990).

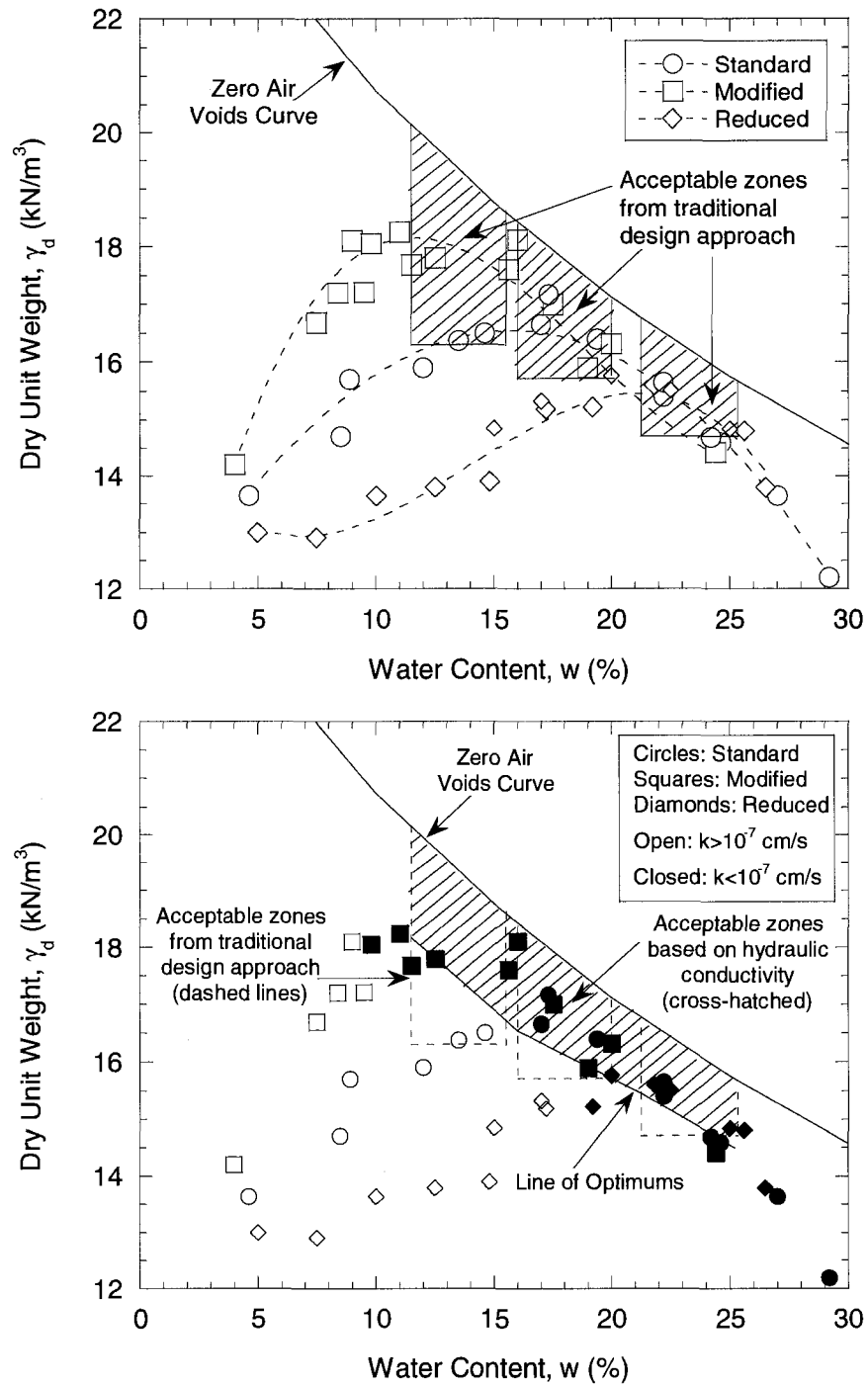


Fig. 6.8 – Acceptable zones for Nelson Farm Clay (NFC) plus 5 % bentonite based on (a) the traditional design approach (b) the hydraulic conductivity approach proposed by Daniel and Benson (1990).

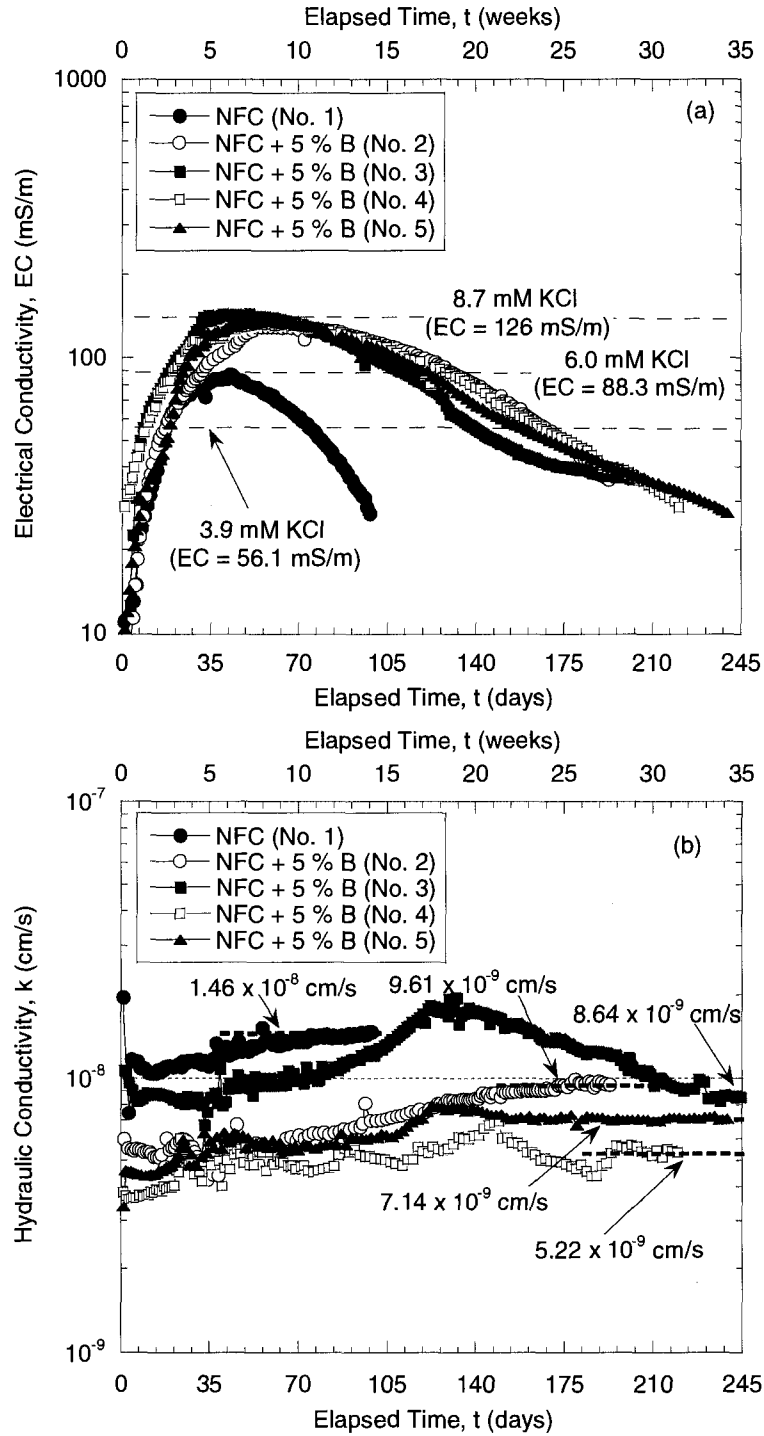


Fig. 6.9 – Electrical conductivity (a) and hydraulic conductivity (b) versus elapsed time for compacted specimens of Nelson Farm Clay (NFC) and NFC plus 5 % bentonite (B) permeated with de-ionized water during flushing stage of test prior to membrane testing.

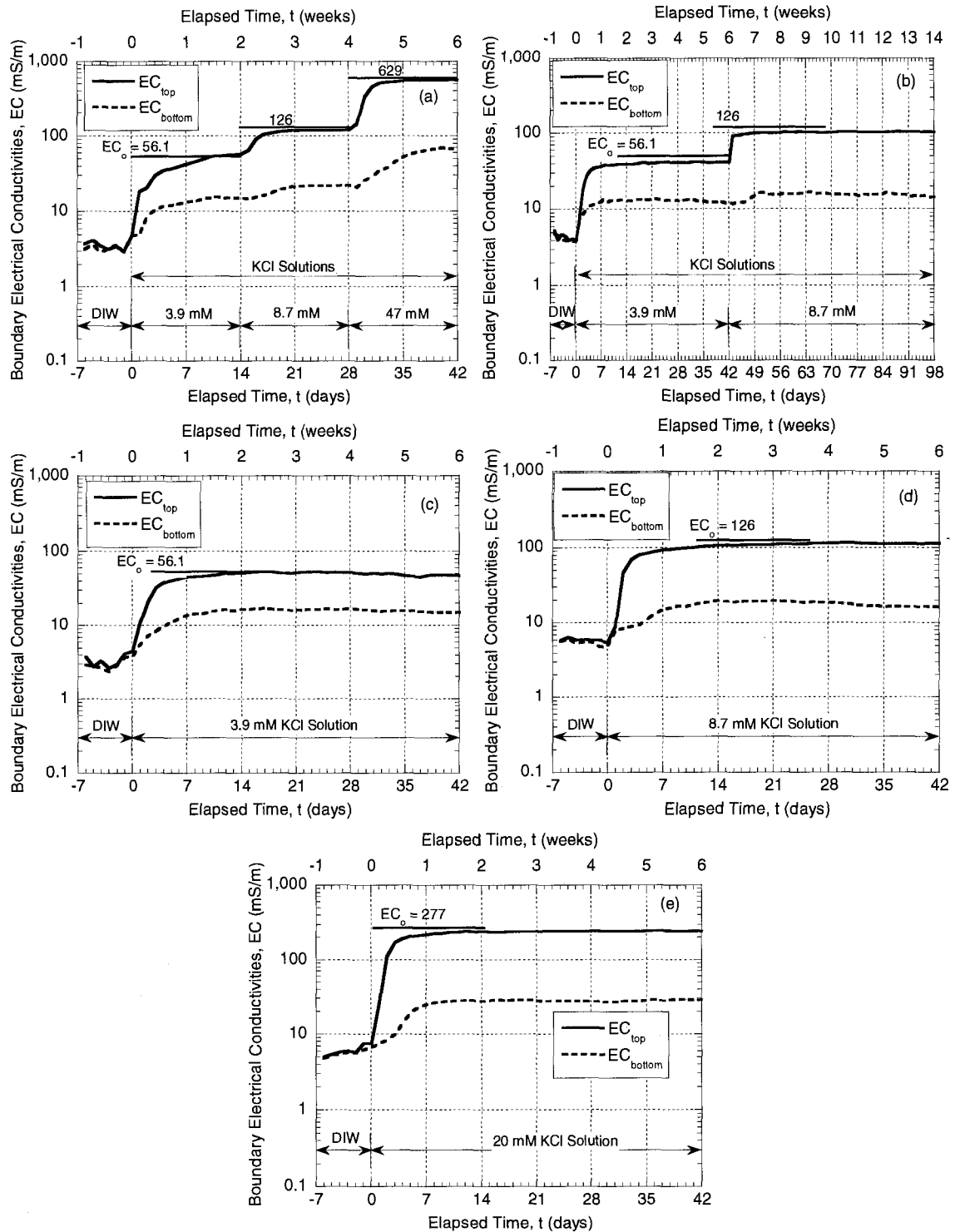


Fig. 6.10 – Electrical conductivity (EC) in circulation outflows from top and bottom boundaries of flexible-wall cell during membrane testing for compacted specimens of Nelson Farm Clay (NFC) and NFC plus 5 % bentonite (B) [$EC_o = EC$ of KCl source solution]: (a) NFC multi-stage; (b) NFC plus 5 % B multi-stage; and NFC plus 5 % B single-stage at (c) 3.9 mM KCl (d) 8.7 mM KCl, and (e) 20 mM KCl concentration differences.

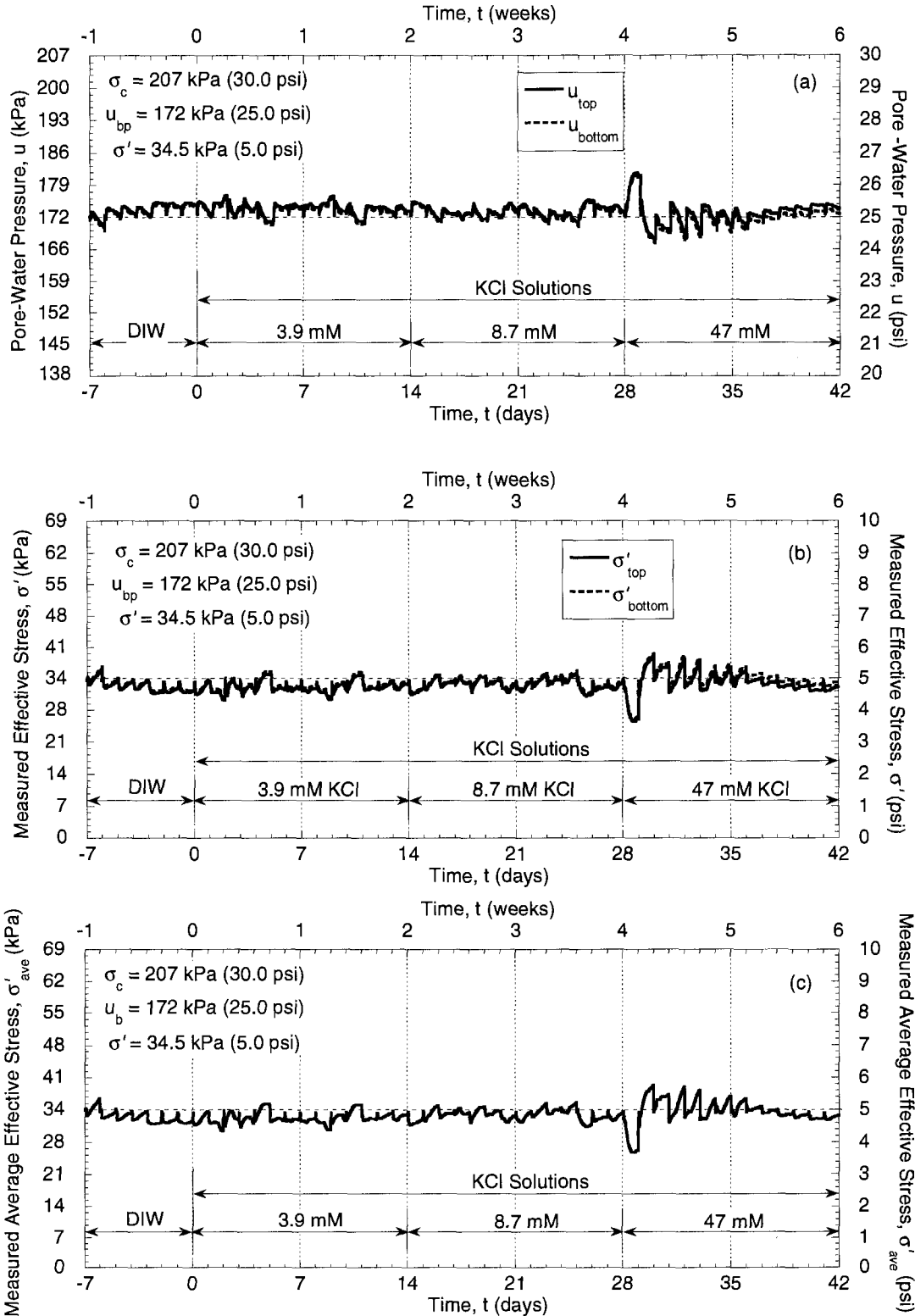


Fig. 6.11 – Boundary pressures and effective stresses for a compacted specimen of Nelson Farm Clay (No.1) at an initial effective stress of 34.5 kPa (5.0 psi) during membrane testing in flexible-wall cell.

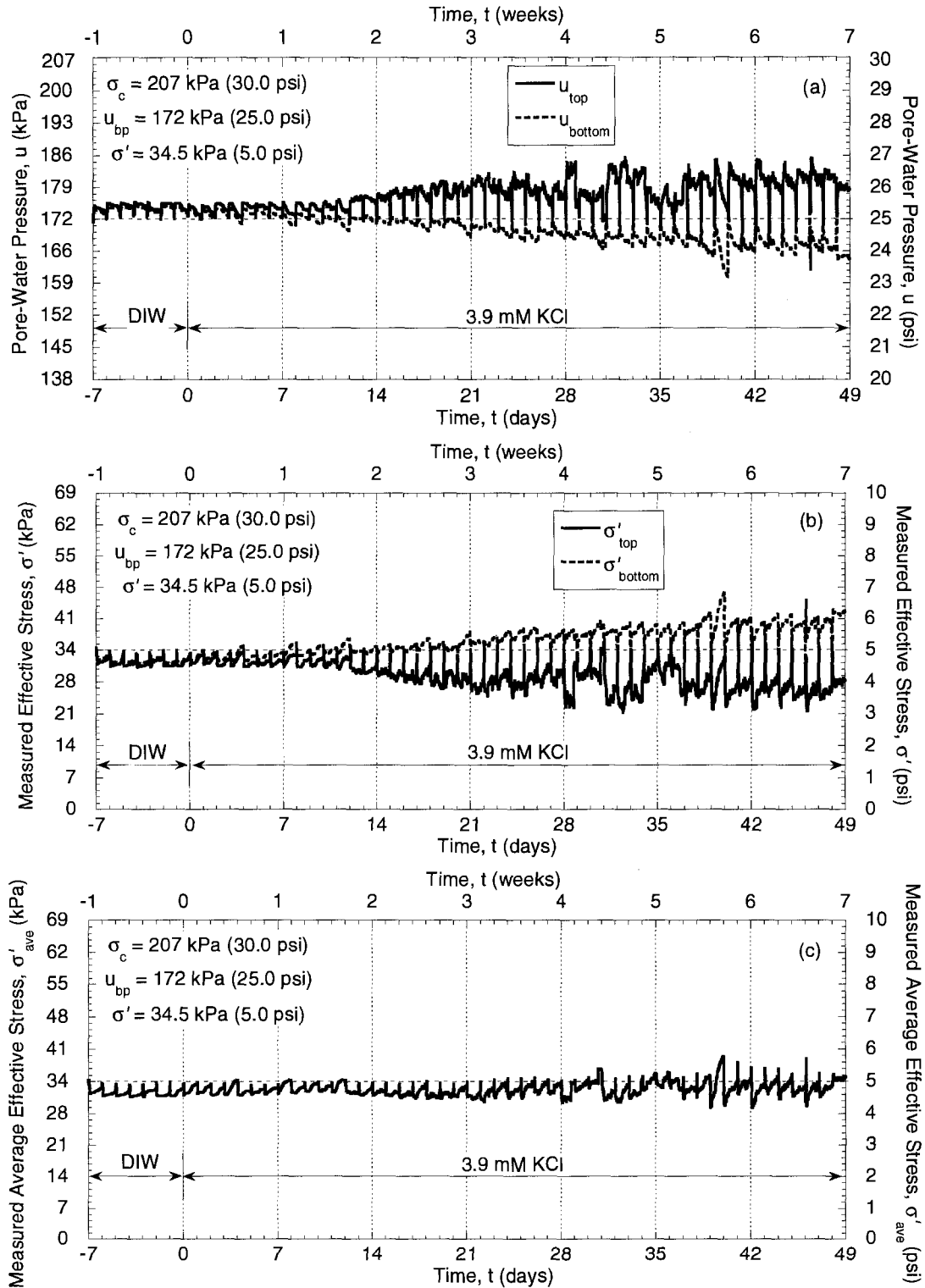


Fig. 6.12 – Boundary pressures and effective stresses for a compacted specimen of Nelson Farm Clay (NFC) plus 5% bentonite (No. 2) at an initial effective stress of 34.5 kPa (5.0 psi) during membrane testing in flexible-wall cell.

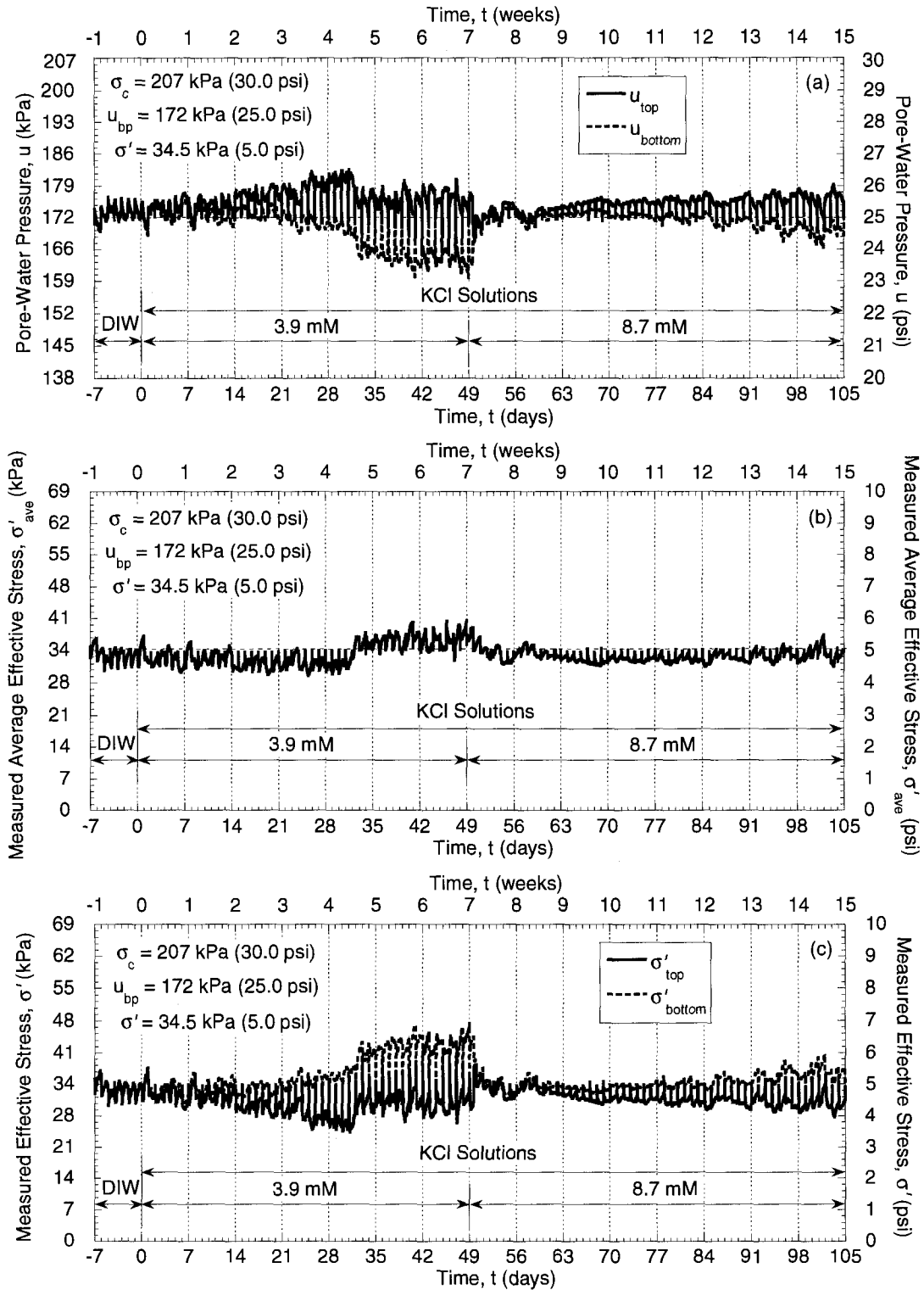


Fig. 6.13 – Boundary pressures and effective stresses for a compacted specimen of Nelson Farm Clay (NFC) plus 5 % bentonite (No. 3) at an initial effective stress of 34.5 kPa (5.0 psi) during membrane testing in flexible-wall cell.

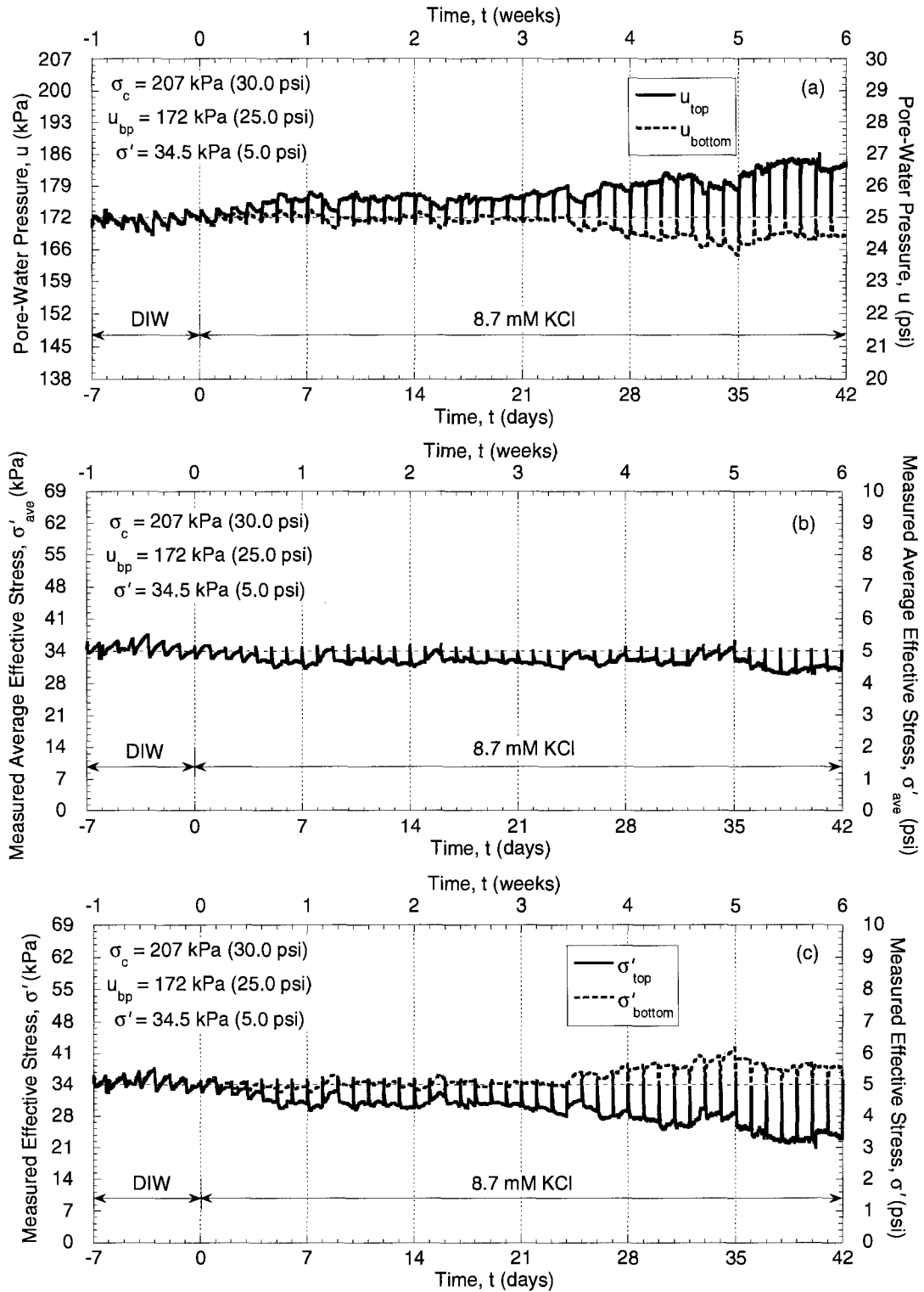


Fig. 6.14 – Boundary pressures and effective stresses for a compacted specimen of Nelson Farm Clay (NFC) plus 5 % bentonite (No. 4) to an initial effective stress of 34.5 kPa (5.0 psi) during membrane testing in flexible-wall cell.

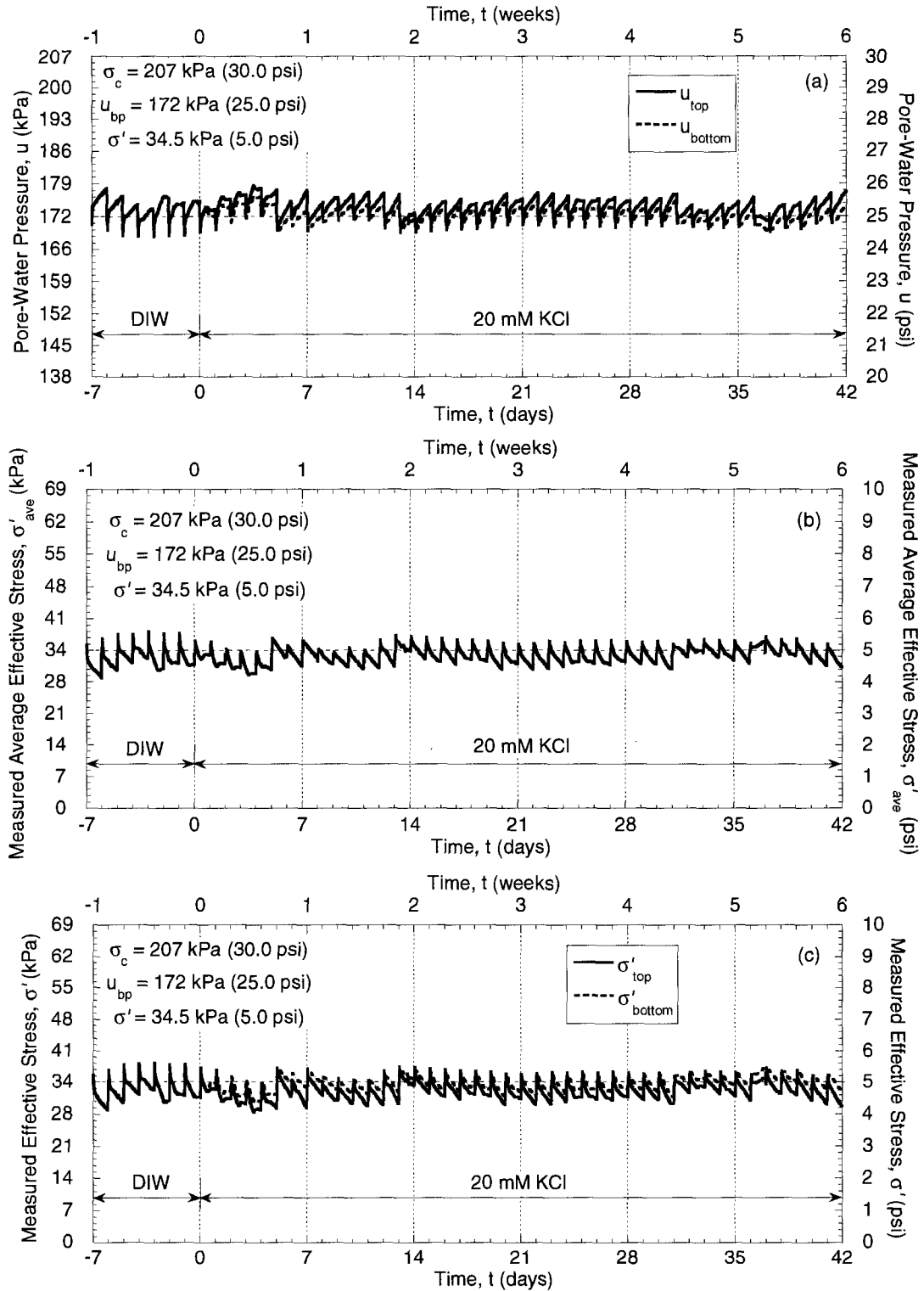


Fig. 6.15 – Boundary pressures and effective stresses for a compacted specimen of Nelson Farm Clay (NFC) plus 5 % bentonite (No. 5) at an initial effective stress of 34.5 kPa (5.0 psi) during membrane testing in flexible-wall cell.

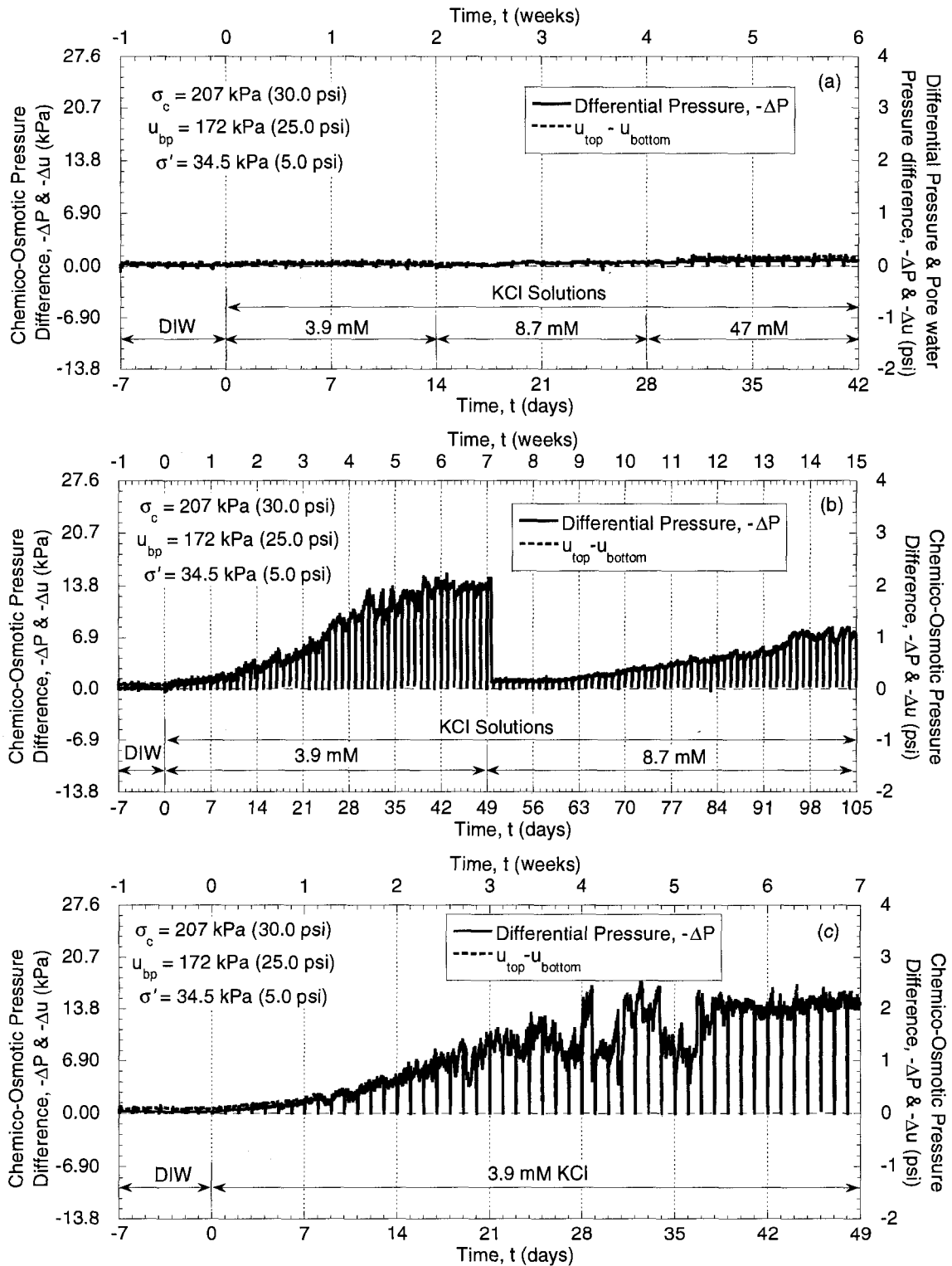


Fig. 6.16 – Measured chemico-osmotic pressure differences across compacted specimens of (a) Nelson Farm Clay (NFC; No. 1) and (b) and (c) NFC plus 5 % bentonite (Nos. 2 and 3) at an initial effective stress of 34.5 kPa (5.0 psi) during membrane testing in flexible-wall cell.

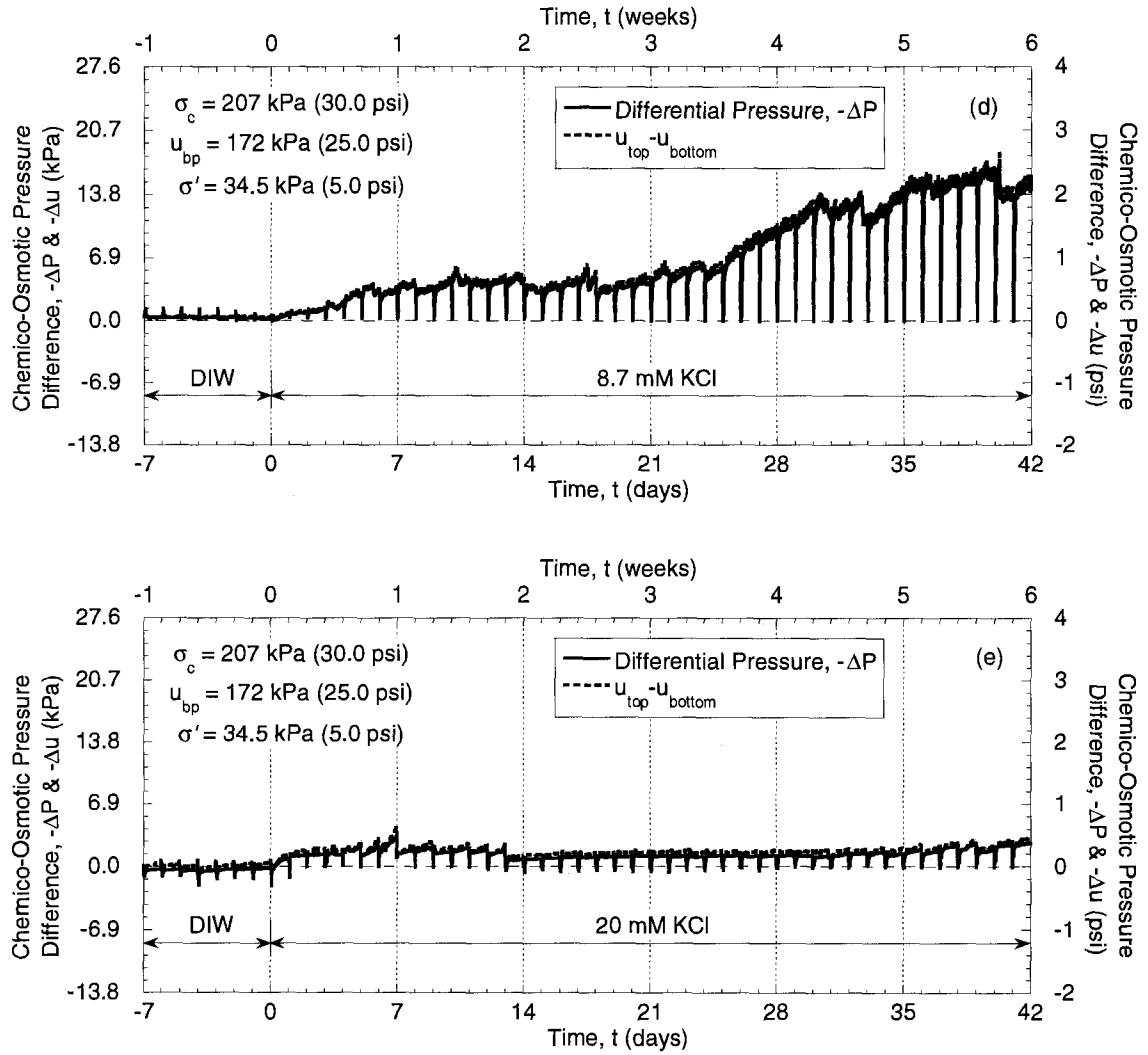


Fig. 6.17 – Measured chemico-osmotic pressure differences across compacted specimens of (d) and (e) NFC plus 5 % bentonite (Nos. 4 and 5) at an initial effective stress of 34.5 kPa (5.0 psi) during membrane testing in flexible-wall cell.

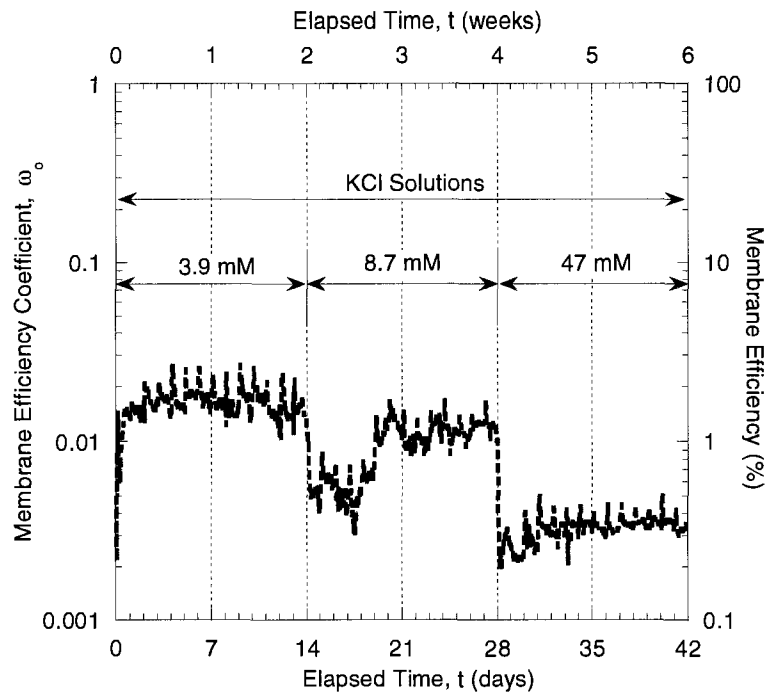


Fig. 6.18 – Elapsed time versus membrane efficiency coefficients for compacted specimens of Nelson Farm Clay (NFC) during multi-stage membrane testing in flexible-wall cell.

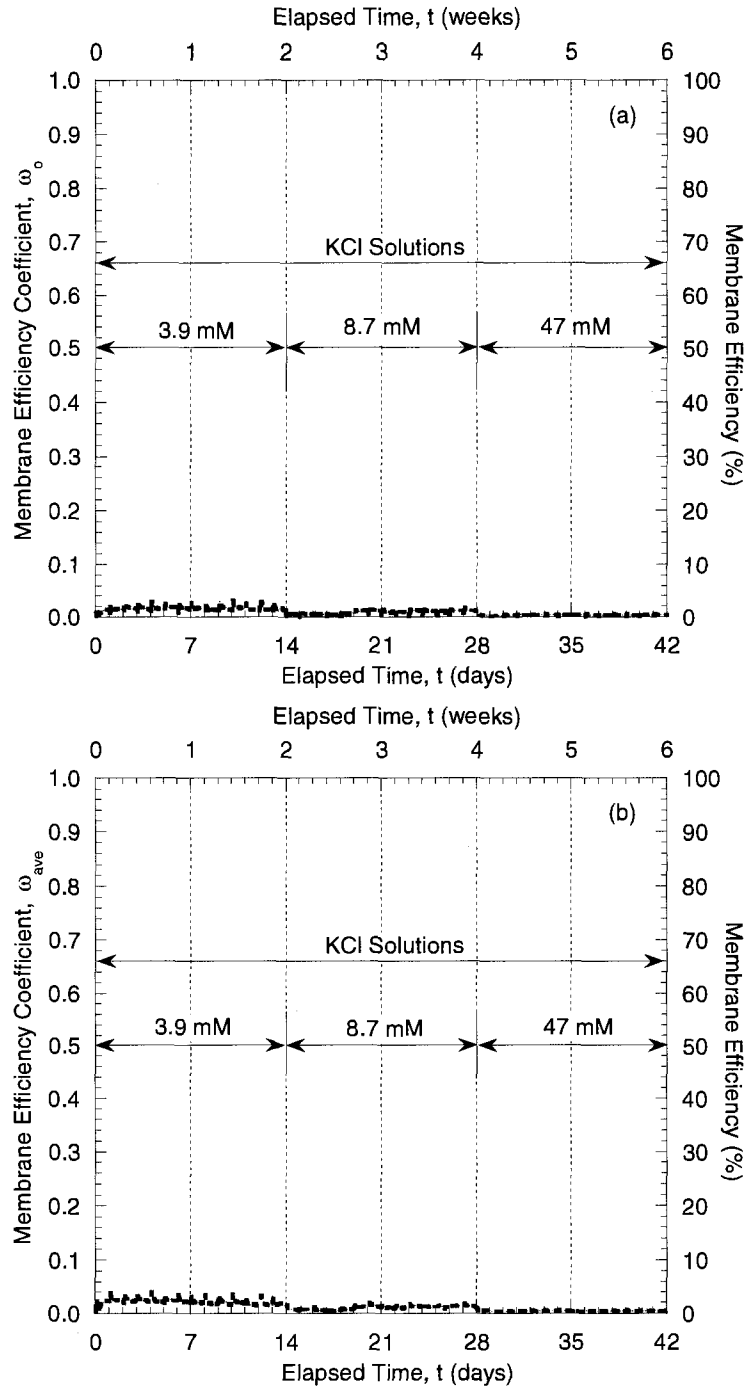


Fig. 6.19 – Comparison of measured membrane efficiencies versus elapsed time based on (a) initial concentration differences ($\Delta\pi_0$) and (b) average concentration differences ($\Delta\pi_{ave}$) for a compacted specimen of Nelson Farm Clay (NFC) during multi-stage membrane testing in flexible-wall cell.

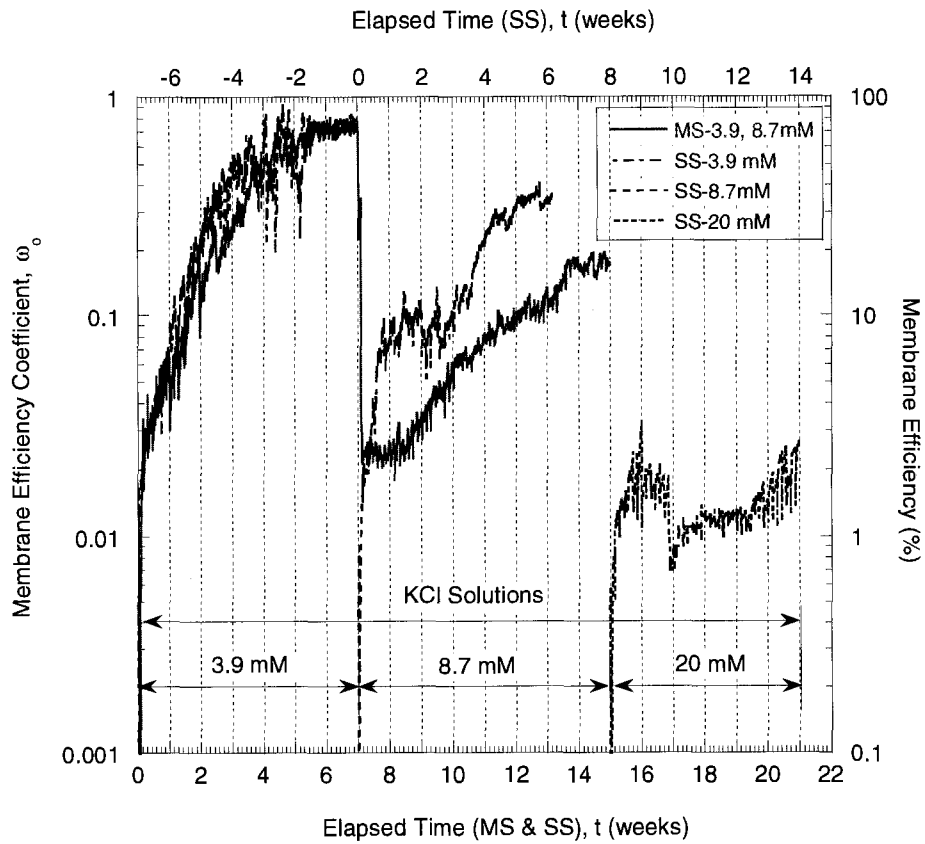


Fig. 6.20 – Elapsed time versus membrane efficiency coefficients for compacted specimens of Nelson Farm Clay (NFC) plus 5 % bentonite soils during multi-stage membrane testing in flexible-wall cell.

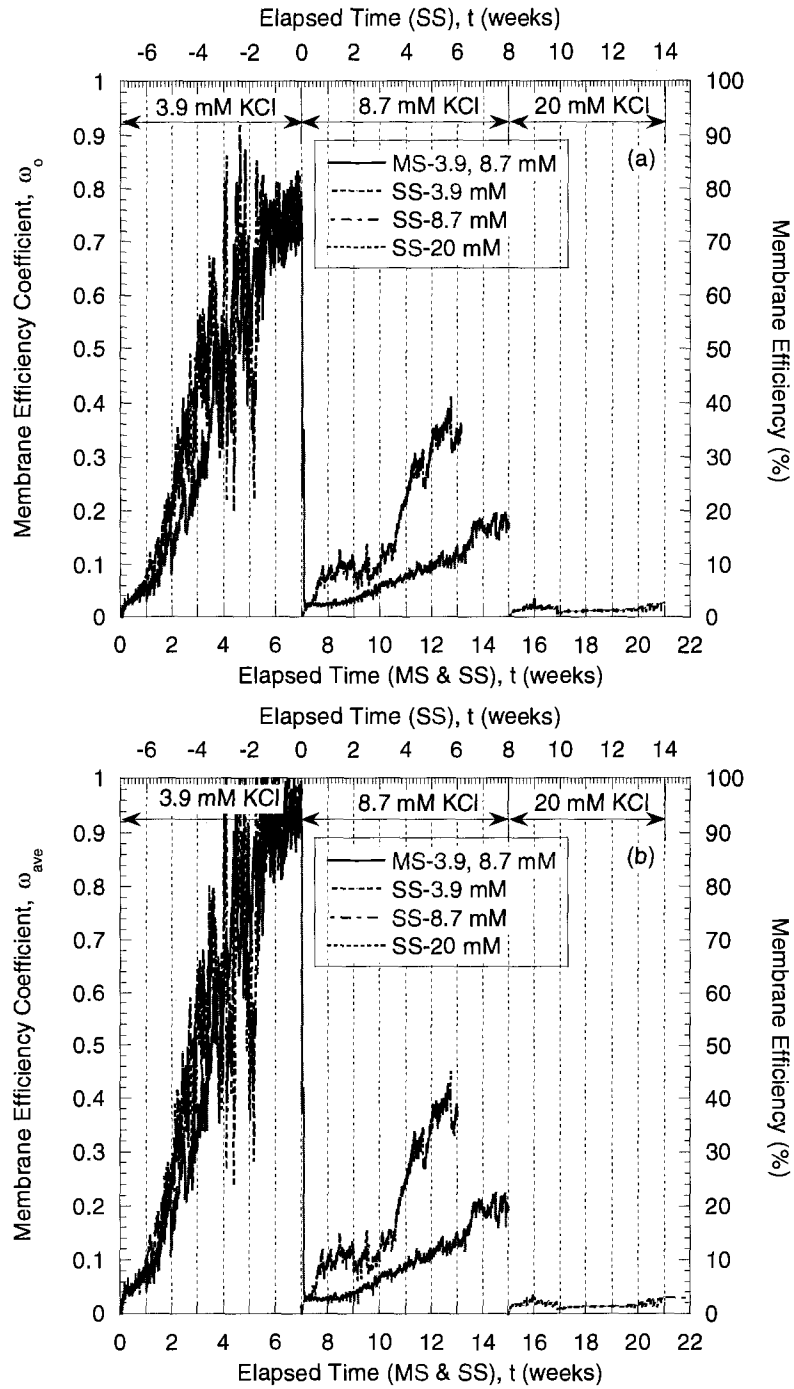


Fig. 6.21 – Comparison of measured membrane efficiencies versus elapsed time based on (a) initial concentration differences ($\Delta\pi_0$) and (b) average concentration differences ($\Delta\pi_{ave}$) for compacted specimens of Nelson Farm Clay (NFC) plus 5 % bentonite soils during multi-stage membrane testing in flexible-wall cell.

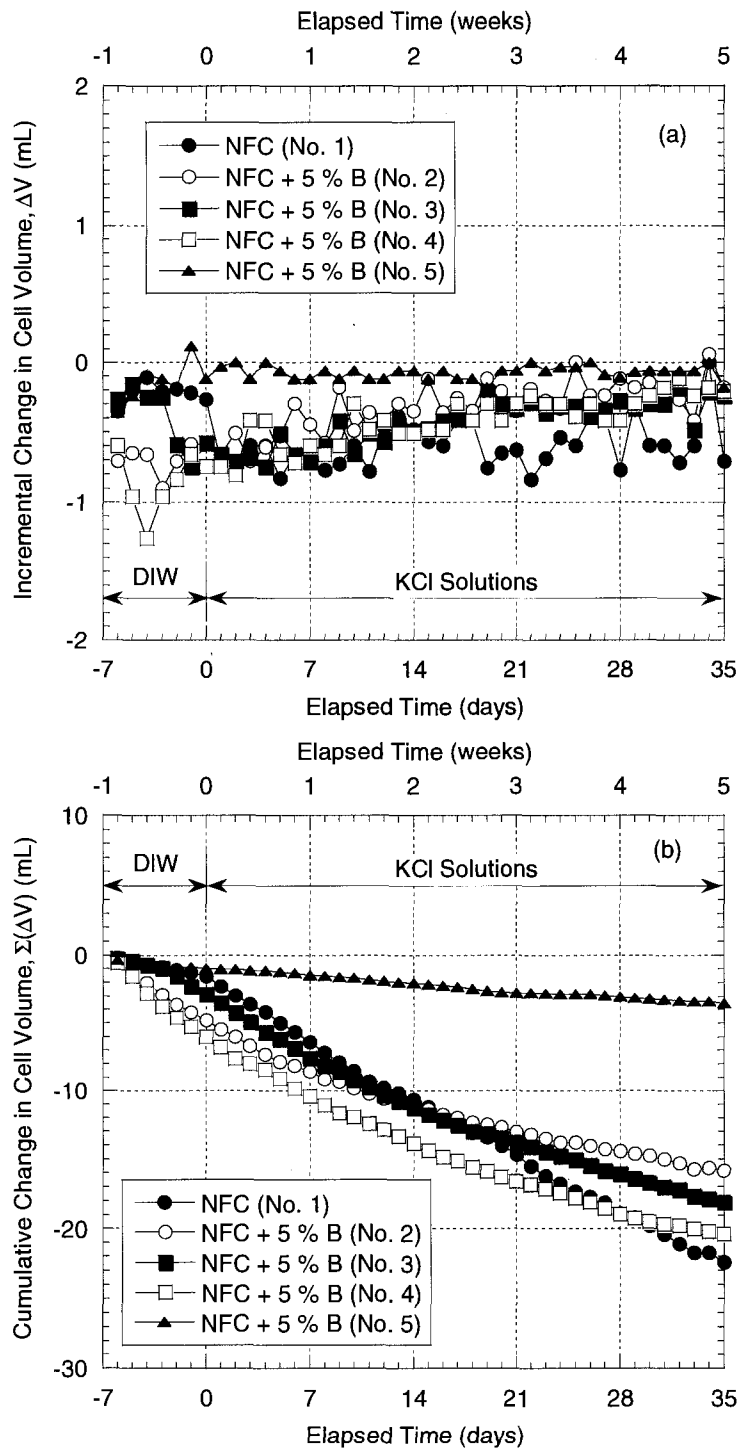


Fig. 6.22 – Incremental (a) and cumulative (b) changes in cell volume for compacted specimens of Nelson Farm Clay (NFC) and NFC plus 5 % bentonite (B) during membrane testing in a flexible-wall cell.

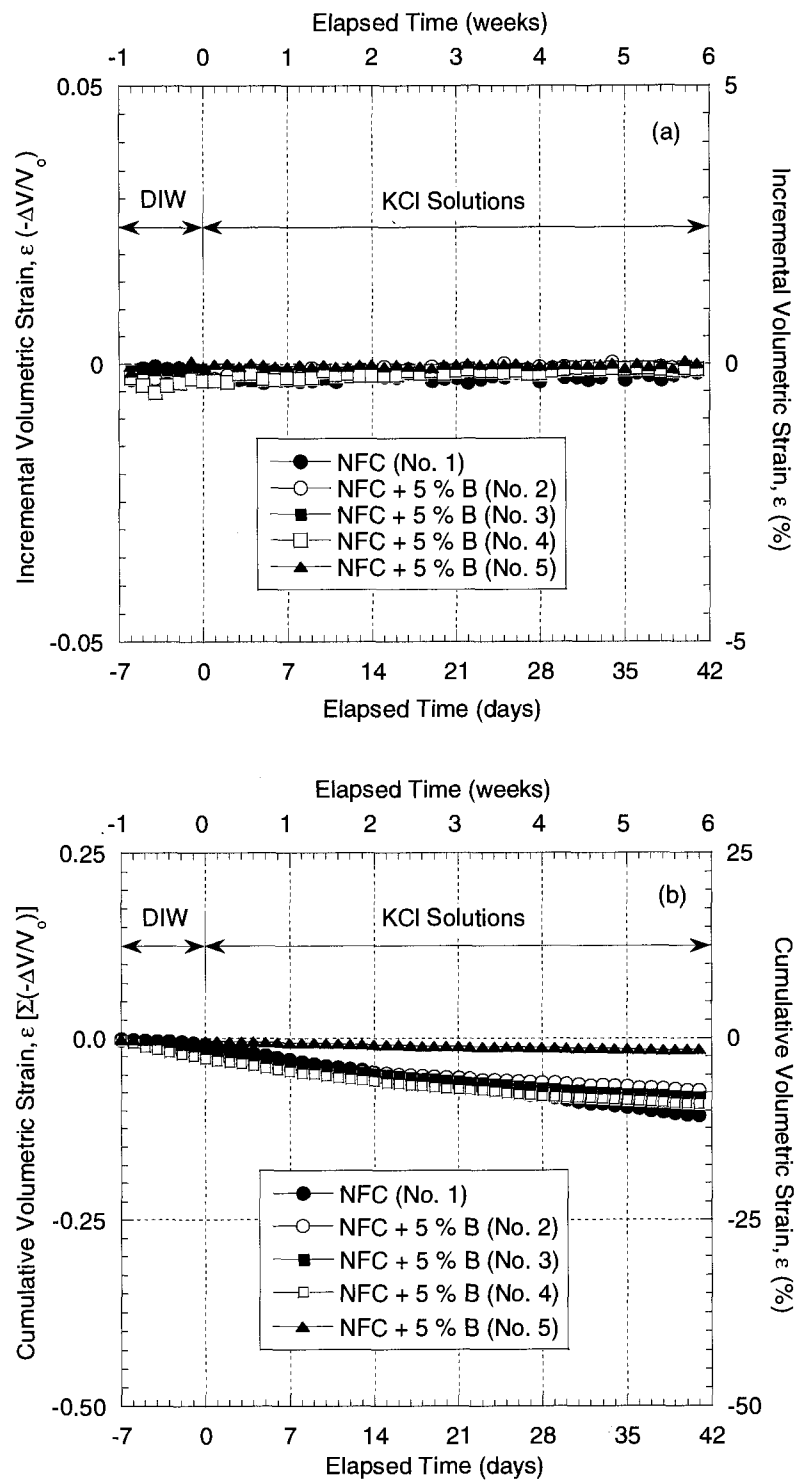


Fig. 6.23 – Incremental (a) and cumulative (b) volumetric strains for compacted specimens of Nelson Farm Clay, NFC (No. 1), and NFC plus 5 % bentonite (Nos. 2, 3, 4, and 5) during membrane testing in a flexible-wall cell.

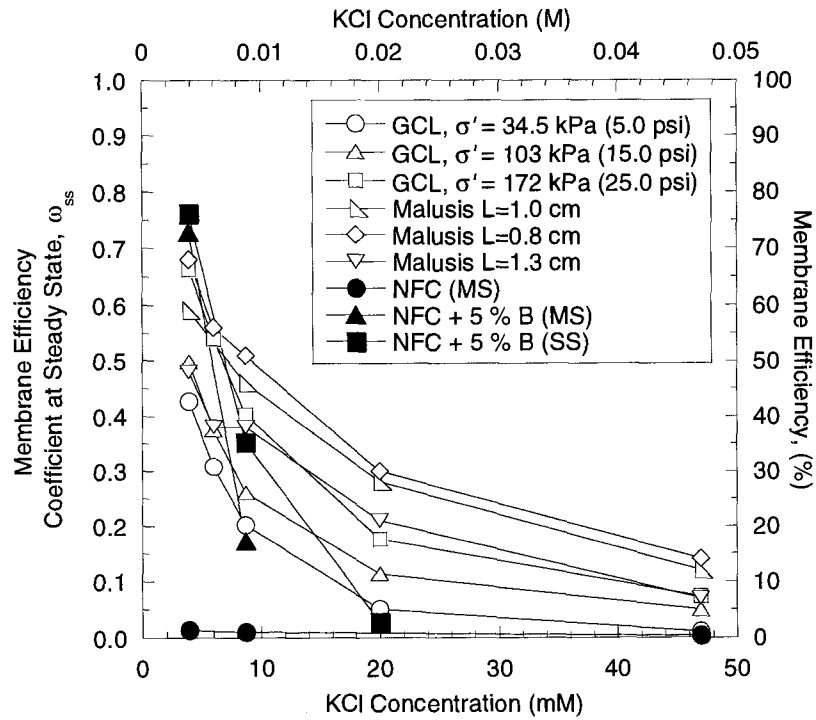


Fig. 6.24 – Comparison of steady-state membrane efficiency coefficients for compacted specimens of Nelson Farm Clay (NFC) and NFC plus 5 % bentonite (B) measured in this study using a flexible-wall cell as a function of effective stress, σ' , versus those reported by Malusis and Shackelford (2002b) using a rigid-wall cell with different specimen thicknesses, L.

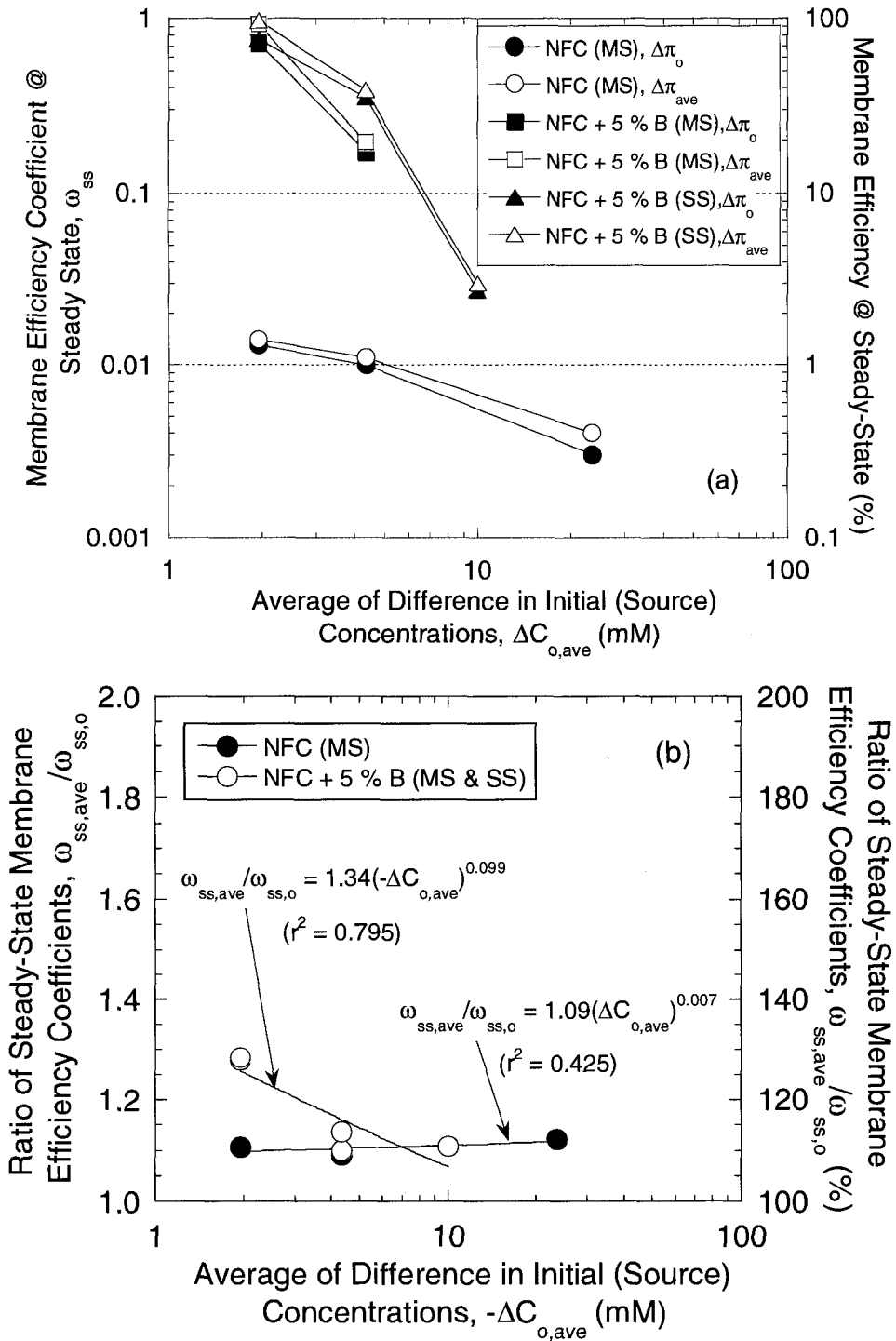


Fig. 6.25 – Steady-state membrane efficiencies, ω_{ss} , versus average of difference in initial (source) KCl concentrations for compacted specimens of Nelson Farm Clay (NFC) and NFC plus 5 % sodium bentonite (B): (a) ω_{ss} values based initial concentration differences ($\Delta\pi_o$), $\omega_{ss,o}$, versus average concentration differences ($\Delta\pi_{ave}$), $\omega_{ss,ave}$; (b) ratio of ω_{ss} based on $\Delta\pi_{ave}$ relative to ω_{ss} based on $\Delta\pi_o$.

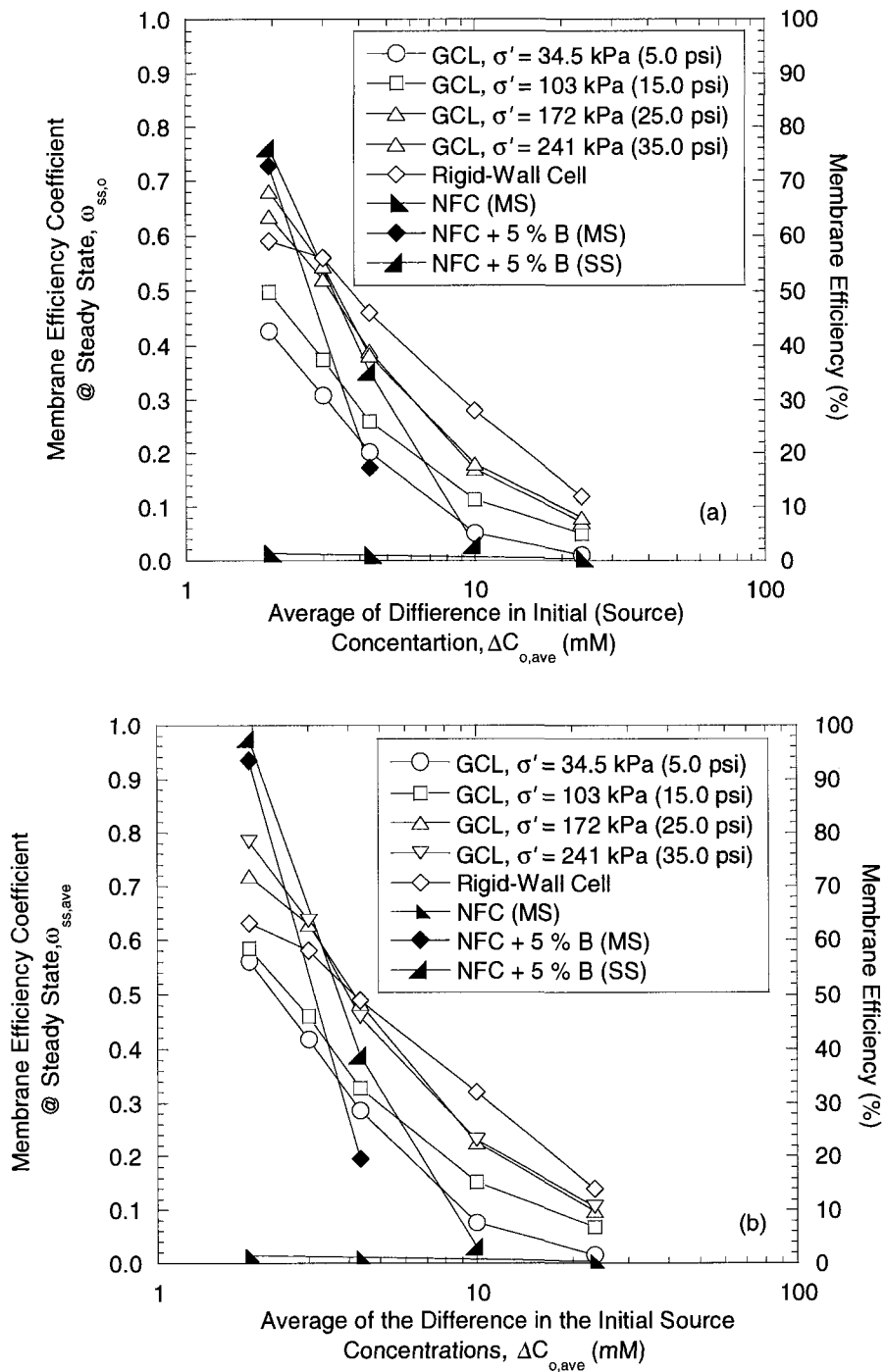


Fig. 6.26 – Comparison of membrane efficiency coefficients at steady state based on (a) initial concentration differences ($\Delta\pi_0$) and (b) average concentration differences ($\Delta\pi_{ave}$) measured in this study using a flexible-wall cell as a function of effective stress, σ' , versus those reported by Malusis and Shackelford (2002b) using a rigid-wall cell

CHAPTER 7

SUMMARY AND CONCLUSIONS

7.1 SUMMARY

Membrane behavior has previously been shown to exist in geological formations that contain appreciable amounts of highly swelling clay minerals, such as the sodium smectites (e.g., sodium montmorillonite), as well as in clay pastes comprised entirely of pure montmorillonite and bentonite based barriers, such as geosynthetic clay liners (GCLs) and soil-bentonite backfills from vertical cutoff walls, used in waste containment applications (refs.). Also, membrane behavior has been evaluated in compacted clay specimens consisting of pure bentonite (Bader and Heister 2006). However, the existence of membrane behavior in compacted natural clay soils commonly used as compacted clay liners (CCLs) in waste containment applications has heretofore not been evaluated. Thus, the primary original contribution from this study is the evaluation of the potential existence of membrane behavior in a compacted natural clay soil that is similar to those used as compacted clay liners in waste containment applications.

A second original contribution of this study pertains to the development of the flexible-wall apparatus for testing the existence of membrane behavior. Although various flexible-wall apparatuses have been developed and used in the past to measure membrane behavior of fine-grained porous media, such as clays, dredged soils and shales, (e.g., Keijzer et al. 1997, 1999, Keijzer and Loch 2001, Rahman et al. 2005), the system either has been developed as an open systems that allows hydraulic and chemico-osmotic flow

(Keijzer et al. 1997, 1999, Keijzer and Loch 2001,), as opposed to the closed-system developed herein, or the control on the hydraulic boundary conditions for the system is poorly defined (Rahman et al. 2005). Thus, development of a closed system, flexible-wall apparatus with well-defined boundary conditions represents a novel contribution to the open literature pertaining to equipment used to measure membrane behavior of clay soils.

The third original contribution pertains to the evaluation of the influence of an isotropic state-of-stress (SOS) on the membrane behavior of a GCL. Although the effect of SOS has been evaluated for a specially prepared kaolin clay using a rigid-wall apparatus (Olsen 1972) as well as a naturally occurring shale using a flexible-wall apparatus (Rahman et al. 2005), the evaluation of the potential influence of an isotropic SOS on the membrane behavior of a GCL has not heretofore been evaluated.

Finally, values of membrane efficiency coefficients at steady state, ω_{ss} for compacted specimens of both the natural and the bentonite amended NFC were evaluated by establishing steady KCl concentration differences of 3.9, 8.7, 20 and/or 47 mM across the specimens in the flexible-wall cell under closed-system boundary conditions.

7.2 CONCLUSIONS

7.2.1 Consolidation Behavior of a Geosynthetic Clay Liner

Duplicate specimens of a geosynthetic clay liner (GCL) were consolidated under isotropic states of stress in a flexible-wall cell after permeation at an effective stress, σ' , of 34.5 kPa (5.0 psi) to flush soluble salts from the soil pores in preparation to be tested for semi-permeable membrane behavior. The specimens were consolidated using a constant loading increment of 69.0 kPa (10.0 psi) to final effective stresses of 103 kPa

(15.0 psi), 172 kPa (25.0 psi), and 241 kPa (35.0 psi). The hydraulic conductivity, k , also was measured at the end of each loading increment. The strain-versus-time data were analyzed in terms of both vertical strain (ϵ_{vert}) and volumetric strain (ϵ_{vol}) using both the Casagrande ($\log t$) and Taylor ($t^{1/2}$) methods to determine values for the coefficient of consolidation (c_v), the coefficients of volume compressibility (m_v) and compressibility (a_v), the theoretical hydraulic conductivity (k_{theory}), and the secondary compression ratio (R_α) and index (C_α). The results of the stress-strain curves were analyzed in terms of both ϵ_{vert} and ϵ_{vol} and void ratios to determine values for the compression ratio (R_c) and compression index (C_c), respectively. The study is believed to represent the first comprehensive attempt to quantify the consolidation behavior of a GCL subjected to an isotropic state of stress, and the results are among the few available, if any, pertaining to the consolidation behavior of a GCL.

The stress-versus-strain curves for both GCL specimens were semi-log linear, such that the GCL specimens were considered to be normally consolidated with a maximum previous effective consolidation stress, σ'_{max} , of 34.5 kPa (5.0 psi). This observation is consistent with limited published results based on conventional, one-dimensional (oedometer) consolidation testing of four different GCLs indicating values for σ'_{max} of ≤ 38.3 kPa (5.6 psi) for all four GCLs and ≤ 34.5 kPa (5.0 psi) for three of the four GCLs.

The coefficients of consolidation, c_v , for the two GCL specimens ranged from 5.2×10^{-10} m²/s to 2.1×10^{-9} m²/s, which is among the lowest range of c_v values reported in the literature for clays. In addition, c_v for a given GCL specimen decreased with increasing effective consolidation stress, σ' , albeit only slightly. Both of these

observations were attributed primarily to the dominance of the relatively low magnitudes of k measured for the two specimens (i.e., $k_{\text{measured}} \leq 5.0 \times 10^{-9}$ cm/s). Finally, values of c_v calculated using different types of strain (ϵ_{vert} vs. ϵ_{vol}) or different methods of analysis (Casagrande vs. Taylor) varied by at most a factor of about two, such that type of strain or method of analysis had a relatively minor effect on determining c_v .

Values of the hydraulic conductivity measured as the end of each loading increment, k_{measured} , as well as those calculated on the basis of consolidation theory, k_{theory} , were found to generally decrease with increasing σ' , which is consistent with decreases in void ratio with increasing σ' . In addition, the range of values for k_{measured} was similar to that for k_{theory} (i.e., 5.0×10^{-10} cm/s $\leq k_{\text{measured}} \leq 5.0 \times 10^{-9}$ cm/s vs. 2.1×10^{-10} cm/s $\leq k_{\text{theory}} \leq 4.1 \times 10^{-9}$ cm/s). The overall good agreement between k_{theory} and k_{measured} for the GCL and testing conditions imposed in this study (e.g., isotropic stress conditions, DIW as the permeant liquid, etc.) suggests that reasonably good approximations of k (i.e., within a factor of about two) can be obtained from the results of consolidation testing, i.e., without the need for direct measurement of k .

The values for the compression ratios, R_c , and compression indexes, C_c , for both GCL specimens were reasonably close, with better agreement between the R_c values of the two GCL specimens being obtained when ϵ_{vol} versus ϵ_{vert} was considered in the analysis. Also, the measured values for C_c for the two GCL specimens of 1.31 and 1.57 were significantly lower by factors of 3.2 and 2.7, respectively, relative to those based solely on empirical correlation with the liquid limit, LL , of the bentonite in the GCL ($LL = 478$). Thus, estimates of C_c for the GCL based solely on the liquid limit of the bentonite in accordance with the empirical correlation are likely to be not only inaccurate but also

conservative (high).

Values of the secondary compression ratio, R_{α} , based on both ϵ_{vert} ($R_{\alpha,\text{vert}}$) and ϵ_{vol} ($R_{\alpha,\text{vol}}$), and the associated secondary compression index, C_{α} , were found to decrease essentially linearly as σ' increased from 103 kPa (15.0 psi) to 241 kPa (35.0 psi). Values of $R_{\alpha,\text{vert}}/R_{\alpha,\text{vol}}$ ($= C_{\alpha,\text{vert}}/C_{\alpha,\text{vol}}$) also tended to decrease approximately linearly with increasing σ' .

7.2.2 Development and Evaluation of Flexible-Wall Cell for Membrane Behavior

The development of a flexible-wall testing apparatus consisting of a flexible-wall cell and a hydraulic control system that imposes closed-system boundary conditions for measurement of the membrane behavior of clay soils was described. The advantages of a flexible-wall cell include complete control over the state of stress existing within the test specimen and the ability to back-pressure saturate and consolidate the specimen prior to membrane testing. Use of the developed flexible-wall cell was illustrated via tests conducted to measure the membrane behavior of a geosynthetic clay liner (GCL). The GCL specimens were consolidated to a final effective stress, σ' , of 241 kPa (35.0 psi) prior to the start of membrane testing. Membrane testing consisted of multi-stage tests, whereby de-ionized water (DIW) was first circulated across both the bottom and the top of the specimens to establish a baseline pressure difference, $-\Delta P (> 0)$, of the specimen, followed by circulation of source KCl solutions across the top of the specimen (while maintaining DIW circulation across the bottom of the specimen) with sequentially higher source concentrations, C_{ot} , of KCl to establish the salt concentration differences, $-\Delta C (= C_{ot})$, required to evaluate the potential for membrane behavior.

The results indicated that the GCL behaved as a semi-permeable membrane, with measured membrane efficiencies at steady state, ω_{ss} , based on the difference in initial (source) concentrations, $\omega_{ss,o}$, ranging from 0.068 (one specimen) at C_{ot} of 47 mM KCl to 0.539 ± 0.015 (two specimens) at C_{ot} of 3.9 mM KCl, and ω_{ss} values based on the average of the difference in boundary concentrations, $\omega_{ss,ave}$, ranging from 0.091 (one specimen) at C_{ot} of 47 mM KCl to 0.636 ± 0.025 (two specimens) at C_{ot} of 3.9 mM KCl. Also, both $\omega_{ss,o}$ and $\omega_{ss,ave}$ decreased with increasing C_{ot} , which is consistent with previous findings based on the use of a rigid-wall cell and attributable to progressively greater collapse of the electrostatic diffuse double layers surrounding individual clay particles with increasing salt concentration in the pore water. Finally, $\omega_{ss,ave}$ was always greater than $\omega_{ss,o}$, with values for the ratio of $\omega_{ss,ave}$ to $\omega_{ss,o}$, or $\omega_{ss,ave}/\omega_{ss,o}$, increasing with increasing average difference in the initial KCl concentrations, or $-\Delta C_{o,ave}$ [$=C_{ot}/2$]. For example, $\omega_{ss,ave}/\omega_{ss,o}$ for specimen GCL1 increased from 1.16 to 1.28 as $-\Delta C_{o,ave}$ increased from 1.95 mM to 10 mM, respectively, whereas $\omega_{ss,ave}/\omega_{ss,o}$ for specimen GCL2 increased from 1.19 to 1.33 as $-\Delta C_{o,ave}$ increased from 1.95 mM to 23.5 mM, respectively.

Although the membrane efficiencies of the GCL specimens were measured under closed (no-flow) conditions, some volume changes were recorded during the tests. These volume changes resulted in cumulative volumetric strains of $\leq -4.9\%$ and $\leq -9.5\%$ for specimens GCL1 and GCL2, respectively, and were attributed to drainage that occurred during the brief (≤ 2 min), daily sampling and refilling procedures for the syringes as opposed to during the circulation periods for measurement of membrane behavior, which lasted ~ 24 h.

Values of ω_{ss} measured in this study using the flexible-wall cell under closed-

system boundary conditions were compared with values of ω_{ss} for the same GCL previously measured using a rigid-wall cell under the same closed-system boundary conditions. As expected, the membrane efficiencies decrease with increasing KCl concentration regardless of whether the flexible-wall or rigid-wall cell was used in the measurement. Except for the values of $\omega_{ss,ave}$ at the lowest $-\Delta C_{o,ave}$ concentration of 1.95 mM KCl (i.e., $C_{ot} = 3.9$ mM KCl), all of the membrane efficiencies based on the flexible-wall cell were lower than those based on the rigid-wall cell at any given value of $\Delta C_{o,ave}$. Also, whereas the membrane efficiency of the GCL based on the rigid-wall cell decreased essentially semi-log linearly with increasing $\Delta C_{o,ave}$, the decrease in the membrane efficiency of the GCL with increasing logarithm of $\Delta C_{o,ave}$ was non linear in the case of the flexible-wall cell. These differences in measured membrane efficiencies based on the flexible-wall cell versus the rigid wall cell can be attributed, in part, to the difference in the stress conditions induced in the specimens in the two types of cells, as well as the difference in specimen preparation procedures. Despite these differences, the membrane efficiencies measured with the flexible-wall cell evaluated in this study were both reproducible and similar to, albeit somewhat less than, those measured previously with a rigid-wall cell.

7.2.3 Influence of Effective Consolidation Stress on GCL Membrane Behavior

The potential effect of the application of effective stress on the observed membrane behavior of a GCL containing sodium bentonite using developed flexible-wall cell in a closed (no-flow) system that can be used to measure the membrane behavior of clays was evaluated. The GCL specimens were consolidated to a final effective stress, σ' ,

of 103, 172, and 241 kPa (15, 25, and 35 psi) in developed flexible-wall cell prior to the start of membrane testing. Membrane testing consisted of multi-stage tests, whereby de-ionized water (DIW) was first circulated across both the bottom and the top of the specimens to establish a baseline pressure difference, $-\Delta P (> 0)$, of the specimen, followed by circulation of source KCl solutions across the top of the specimen (while maintaining DIW circulation across the bottom of the specimen) with sequentially higher source concentrations, C_{ot} , of KCl to establish the salt concentration differences, $-\Delta C (= C_{ot})$, required to evaluate the potential for membrane behavior.

The results indicated that the GCL behaved as a semi-permeable membrane, with measured membrane efficiencies at steady state, ω_{ss} , based on the difference in initial (source) concentrations, $\omega_{ss,o}$, ranging from 0.01 ($\sigma' = 34.5$ kPa) at C_{ot} of 47 mM KCl to 0.68 ($\sigma' = 241$ kPa) at C_{ot} of 3.9 mM KCl, and ω_{ss} values based on the average of the difference in boundary concentrations, $\omega_{ss,ave}$, ranging from 0.02 ($\sigma' = 34.5$ kPa) at C_{ot} of 47 mM KCl to 0.78 ($\sigma' = 241$ kPa) at C_{ot} of 3.9 mM KCl. Also, both $\omega_{ss,o}$ and $\omega_{ss,ave}$ decreased with increasing C_{ot} , which is consistent with previous findings based on the use of a rigid-wall cell and attributable to progressively greater collapse of the electrostatic diffuse double layers surrounding individual clay particles with increasing salt concentration in the pore water. Finally, $\omega_{ss,ave}$ was always greater than $\omega_{ss,o}$, with values for the ratio of $\omega_{ss,ave}$ to $\omega_{ss,o}$, or $\omega_{ss,ave}/\omega_{ss,o}$, increasing with increasing average difference in the initial KCl concentrations, or $-\Delta C_{o,ave} [=C_{ot}/2]$. For example, $\omega_{ss,ave}/\omega_{ss,o}$ increased from 1.31 to 1.52 as $-\Delta C_{o,ave}$ increased from 1.95 mM to 23.5 mM, respectively, for specimen of 34.5 kPa (5 psi) effective stress, whereas $\omega_{ss,ave}/\omega_{ss,o}$ increased from 1.17 to 1.39 as $-\Delta C_{o,ave}$ increased from 1.95 mM to 23.5 mM, respectively, for specimen of 103

kPa (15 psi) effective stress, and $\omega_{ss,ave}/\omega_{ss,o}$ increased from 1.13 to 1.39 as $-\Delta C_{o,ave}$ increased from 1.95 mM to 23.5 mM, respectively, for specimen of 172 kPa (25 psi) effective stress, whereas $\omega_{ss,ave}/\omega_{ss,o}$ increased from 1.15 to 1.33 as $-\Delta C_{o,ave}$ increased from 1.95 mM to 23.5 mM, respectively, for specimen of 241 kPa (35 psi) effective stress.

Values of ω_{ss} measured in this study using the developed flexible-wall cell under closed-system boundary conditions were compared with values of ω_{ss} for the same GCL previously measured using a rigid-wall cell under the same closed-system boundary conditions. As expected, the membrane efficiencies decrease with increasing KCl concentration regardless of whether the flexible-wall or rigid-wall cell was used in the measurement.

The results in measured membrane efficiencies based on average effective stress conditions in the flexible-wall cell indicate that increase in effective stress results in a decrease in void ratio (e) whereas an increase of the membrane efficiency coefficient, ω . These trends among the effective stress (σ'), void ratio (e), and membrane efficiency coefficient (ω) are consistent with expected behavior in that lower void ratios in clays correlate to higher effective stress and greater membrane efficiency.

7.2.4 Membrane Efficiency of Compacted Clay Liner Materials

The potential existence of membrane behavior in compacted clay liner materials that are representative of those that could be considered for use in a waste containment applications was evaluated. A locally available natural clay soil referred to as Nelson Farm Clay (NFC) was evaluated both as a natural (unamended) soil and as a natural soil amended with 5 % (dry wt.) sodium bentonite to enhance the potential for membrane

behavior. The membrane efficiencies, ω , of specimens of both the natural and the bentonite amended NFC were measured by establishing steady salt (KCl) concentration differences of 3.9, 8.7, 20 and/or 47 mM across the specimens in a flexible-wall cell under closed-system boundary conditions.

The results indicate that the compacted natural NFC exhibited essentially no membrane behavior (i.e., $\omega \approx 0$), even though the specimen was compacted at conditions that should have resulted in a suitably low value of hydraulic conductivity, k (i.e., $k < 10^{-7}$ cm/s). In contrast, compacted specimens of the bentonite amended NFC exhibited both lower k than those of the natural NFC as well as significant membrane behavior, with ω ranging from 0.762 (76.2 %) to 0.027 (2.7 %) as the KCl concentration ranged from 3.9 to 20 mM, respectively. The results suggest that natural clays typically suitable for use as compacted clay liners on the basis of low k in waste containment applications may not behave as semi-permeable membranes unless bentonite is added to the clay.

APPENDIX A

**CALIBRATION BETWEEN KCl CONCENTRATIONS AND ELECTRICAL
CONDUCTIVITY**

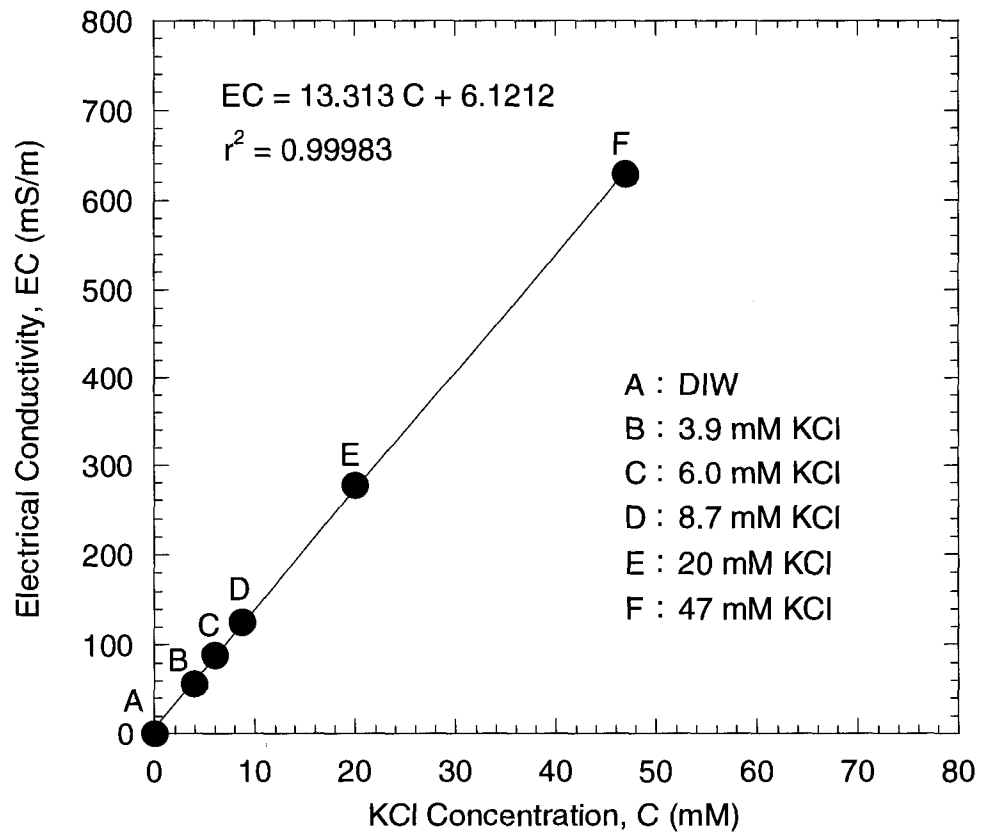


Fig. A.1 – Calibration between KCl concentrations and electrical conductivity.

Table A.1 – Measured chemical properties of liquids used in study.

Liquid	KCl Concentration		pH	EC@25°C ^a
	(mM)	(mg/L)		(mS/m)
De-ionized Water (DIW)	0	0	4.52	0.09
KCl Solutions	3.9	290	4.68	56.1
	6.0	450	4.84	88.3
	8.7	650	5.06	125.8
	20	1500	5.33	277.0
	47	3500	5.60	629.0

^aEC: electrical conductivity

APPENDIX B

VARIATION IN LABORATORY TEMPERATURE DURING MEMBRANE TESTING

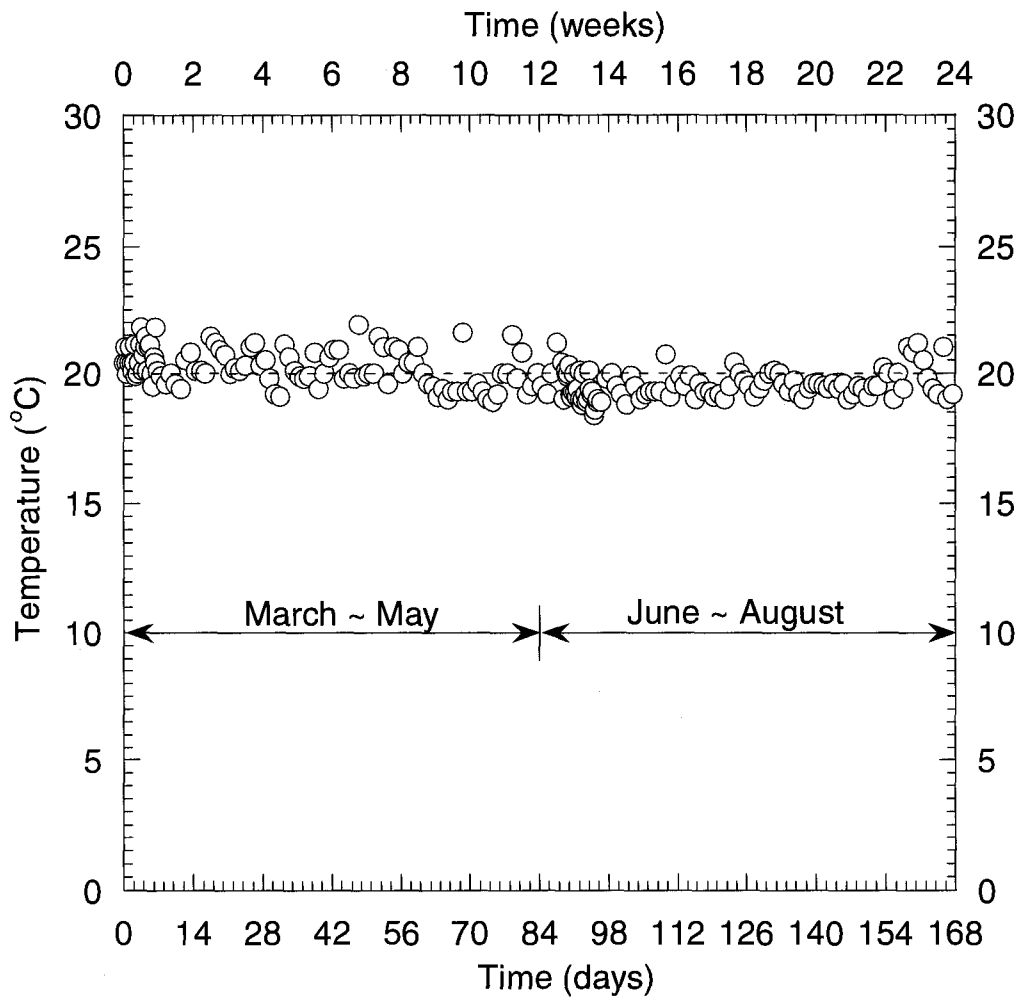


Fig. B.1 – Variation of laboratory temperature during multi-stage membrane testing.

APPENDIX C

FLUSHING, CONSOLIDATION, AND VOLUME CHANGE DATA

DURING MEMBRANE TESTING

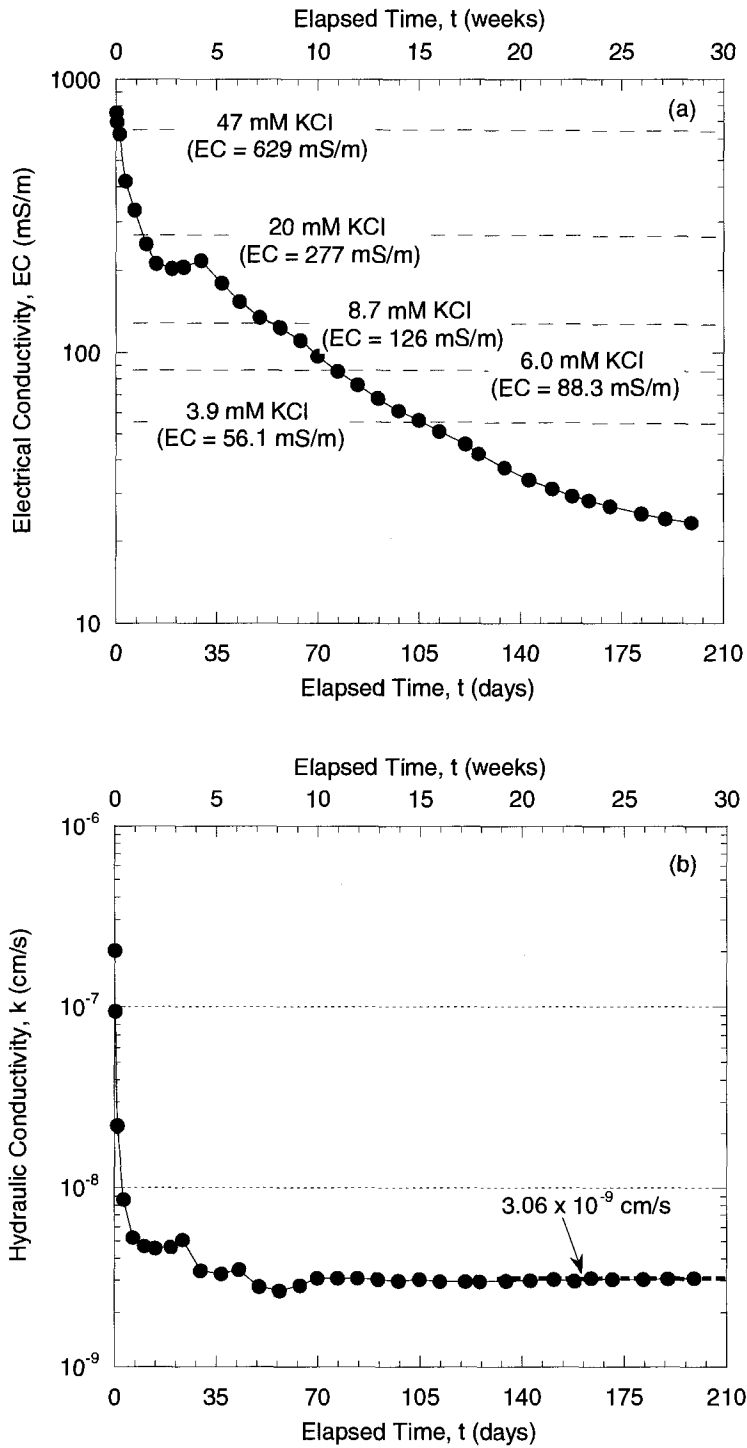


Fig. C.1 – Electrical conductivity (a) and hydraulic conductivity (b) versus elapsed time for a specimen of a GCL consolidated to an initial effective stress of 34.5 kPa (5.0 psi) and permeated with de-ionized water during flushing stage of test.

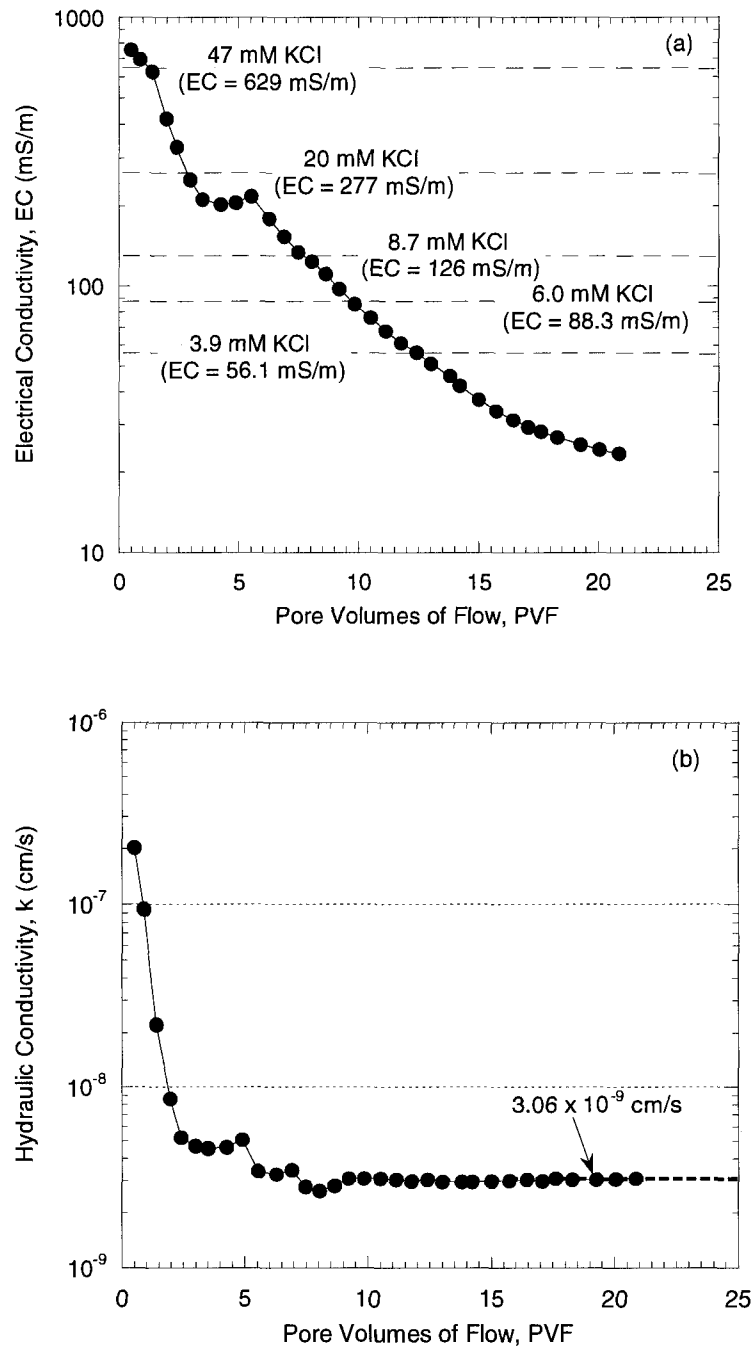


Fig. C.2 – Electrical conductivity (a) and hydraulic conductivity (b) versus pore volumes of flow for a specimen of a GCL consolidated to an initial effective stress of 34.5 kPa (5.0 psi) and permeated with de-ionized water during flushing stage of test.

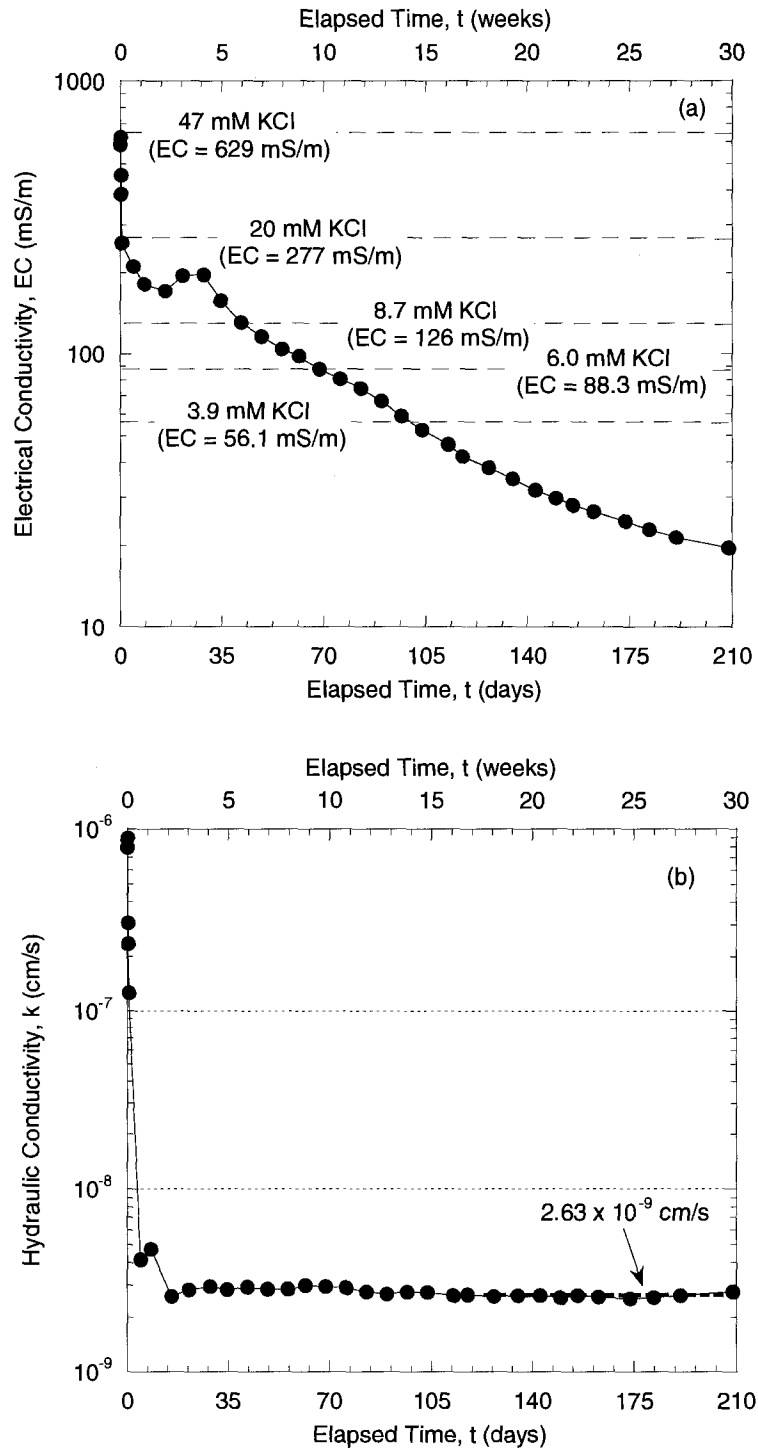


Fig. C.3 – Electrical conductivity (a) and hydraulic conductivity (b) versus elapsed time for a specimen of a GCL consolidated to an initial effective stress of 103 kPa (15.0 psi) and permeated with de-ionized water during flushing stage of test.

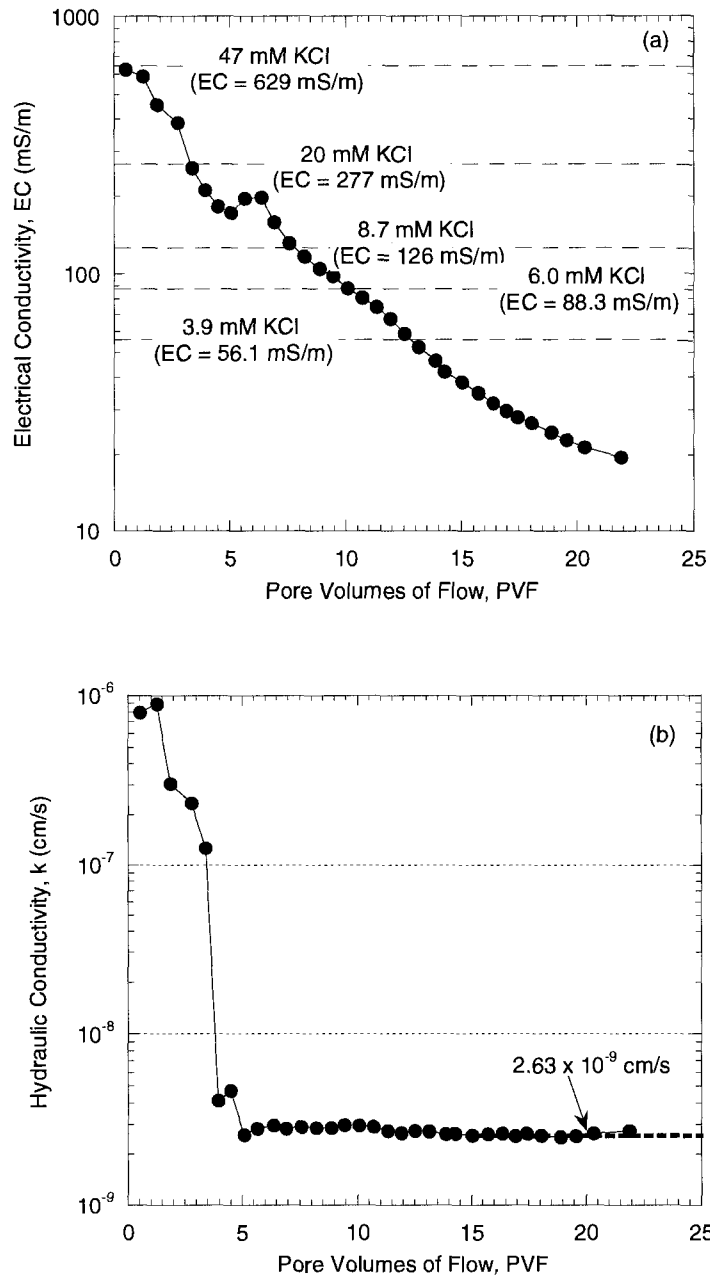


Fig. C.4 – Electrical conductivity (a) and hydraulic conductivity (b) versus pore volumes of flow for a specimen of a GCL consolidated to an initial effective stress of 103 kPa (15.0 psi) and permeated with de-ionized water during flushing stage of test.

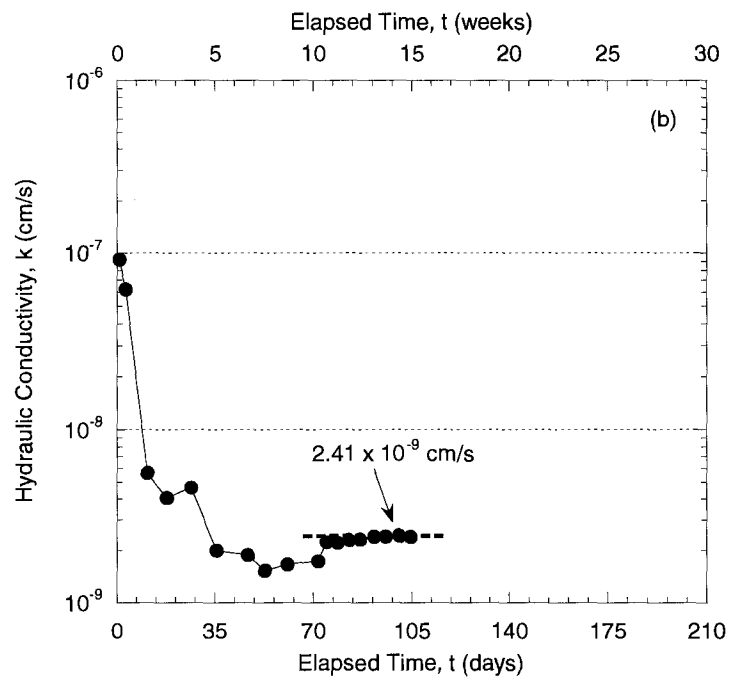
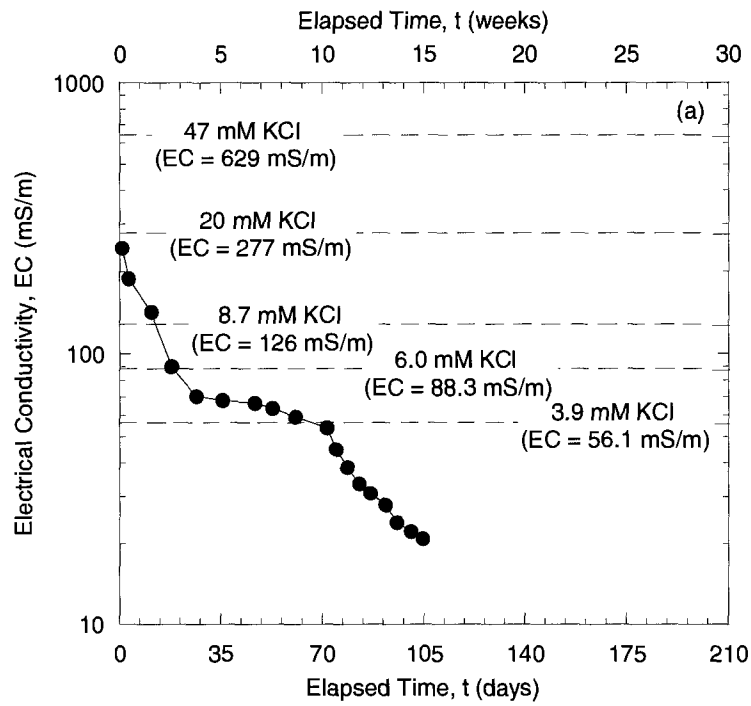


Fig. C.5 – Electrical conductivity (a) and hydraulic conductivity (b) versus elapsed time for a specimen of a GCL consolidated to an initial effective stress of 172 kPa (25.0 psi) and permeated with de-ionized water during flushing stage of test.

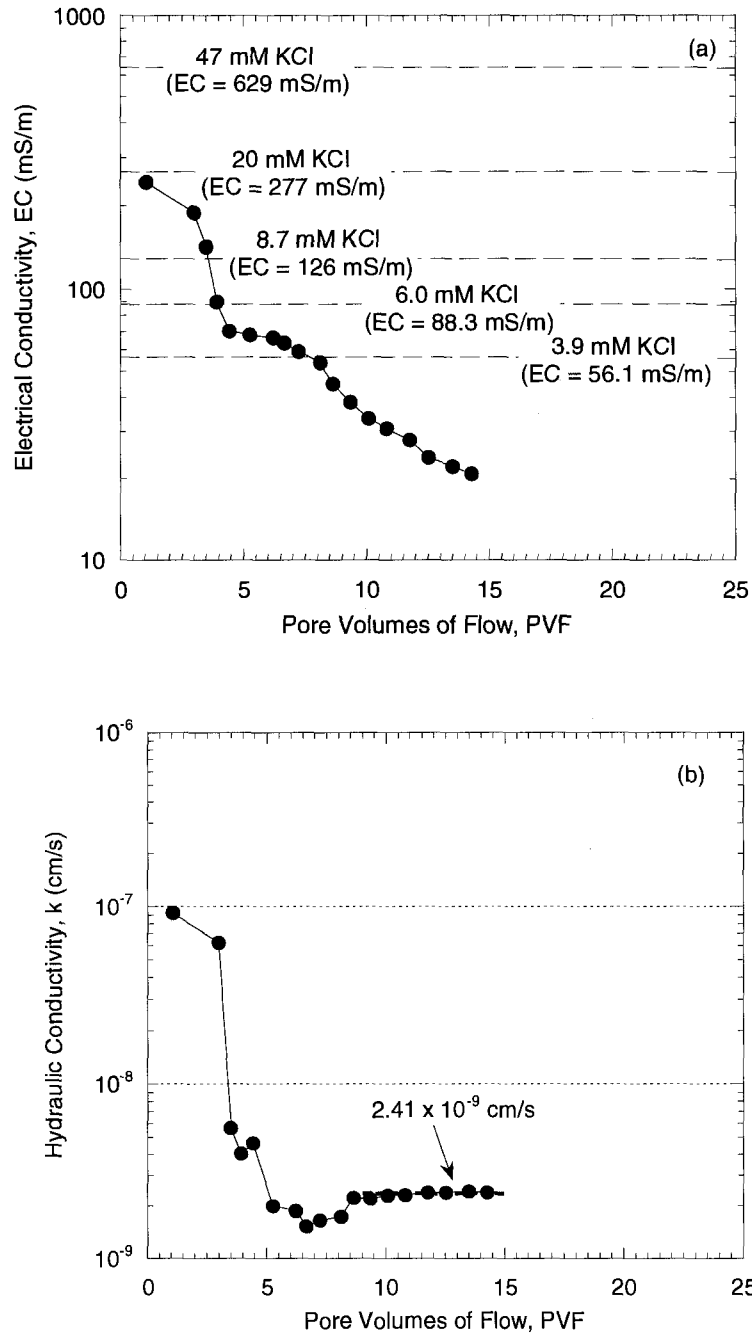


Fig. C.6 – Electrical conductivity (a) and hydraulic conductivity (b) versus pore volumes of flow for a specimen of a GCL consolidated to an initial effective stress of 172 kPa (25.0 psi) and permeated with de-ionized water during flushing stage of test.

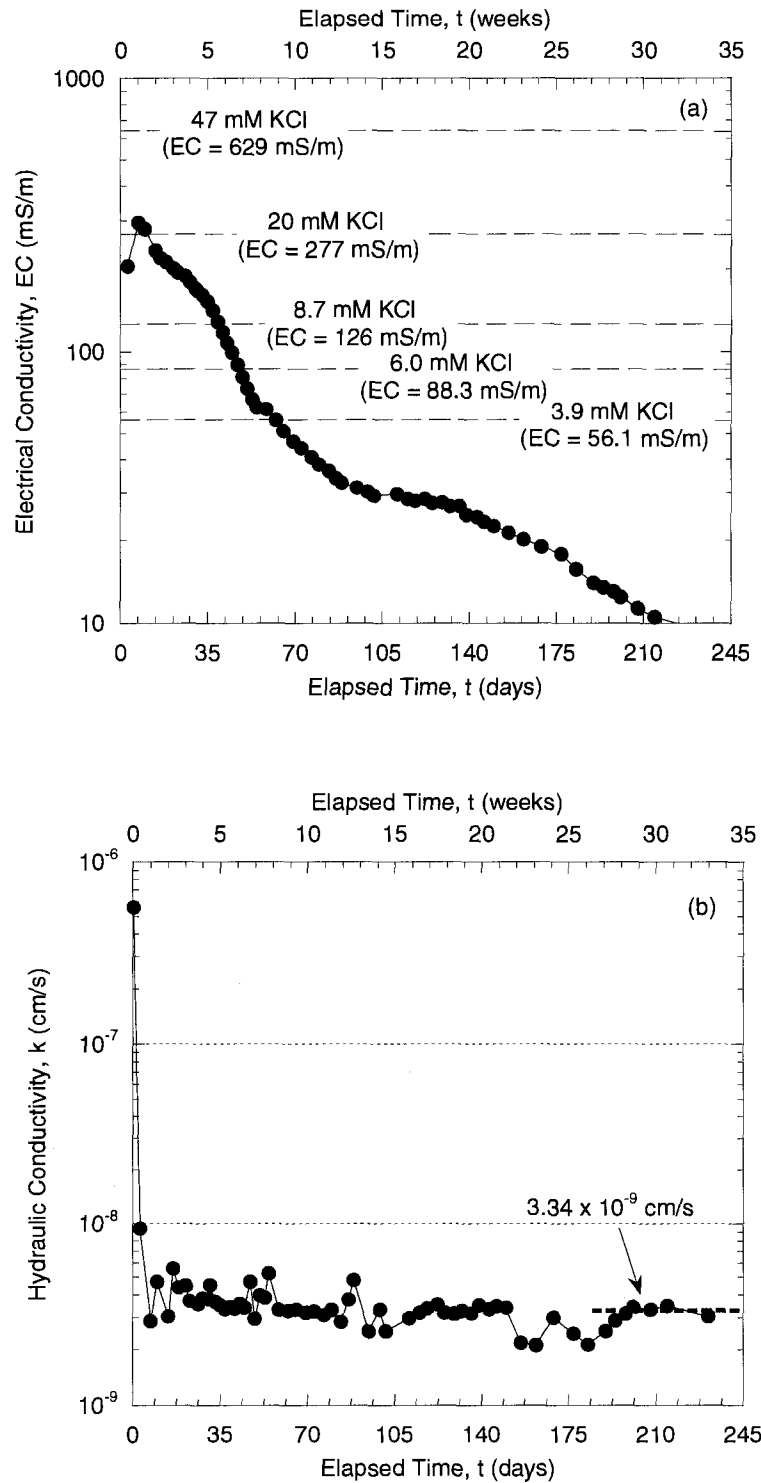


Fig. C.7 – Electrical conductivity (a) and hydraulic conductivity (b) versus elapsed time for a specimen of a GCL consolidated to an initial effective stress of 241 kPa (35.0 psi) and permeated with de-ionized water during flushing stage of test.

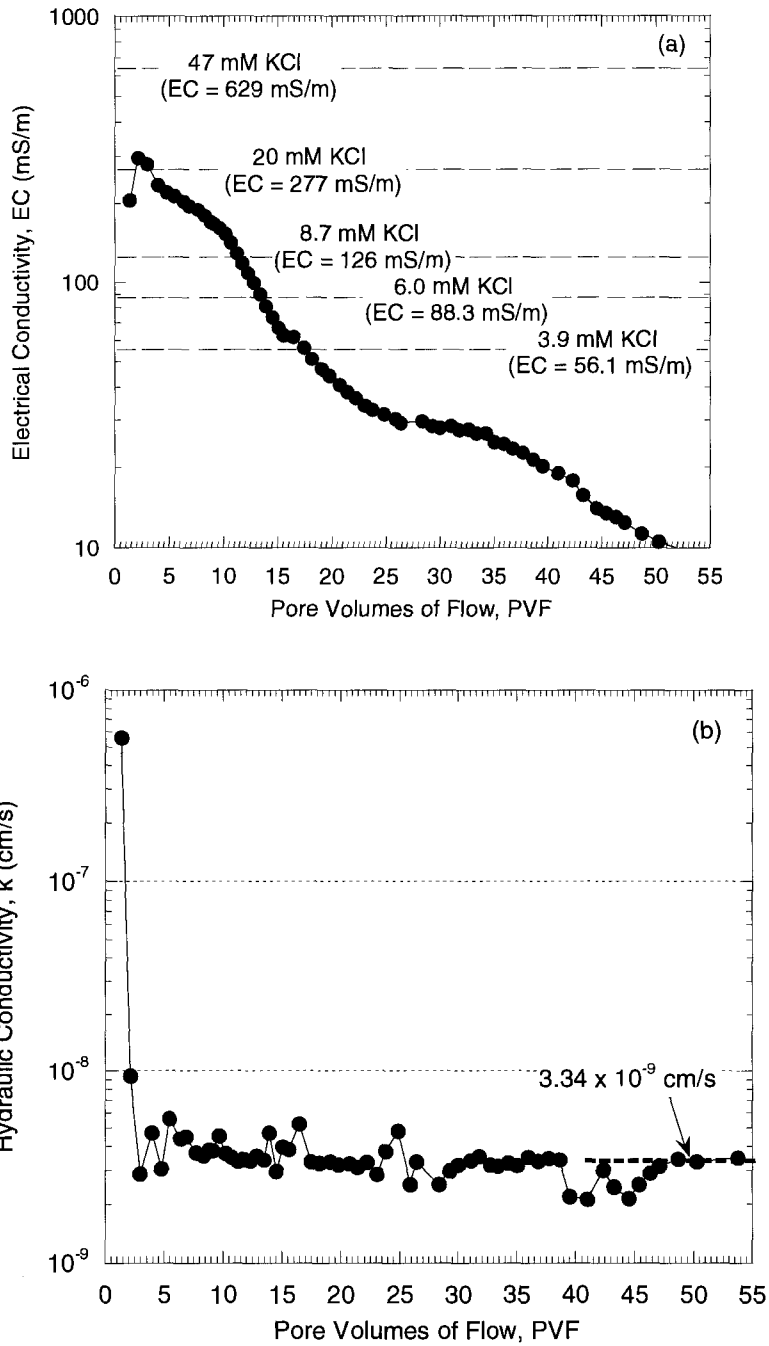


Fig. C.8 – Electrical conductivity (a) and hydraulic conductivity (b) versus pore volumes of flow for a specimen of a GCL consolidated to an initial effective stress of 241 kPa (35.0 psi) and permeated with de-ionized water during flushing stage of test.

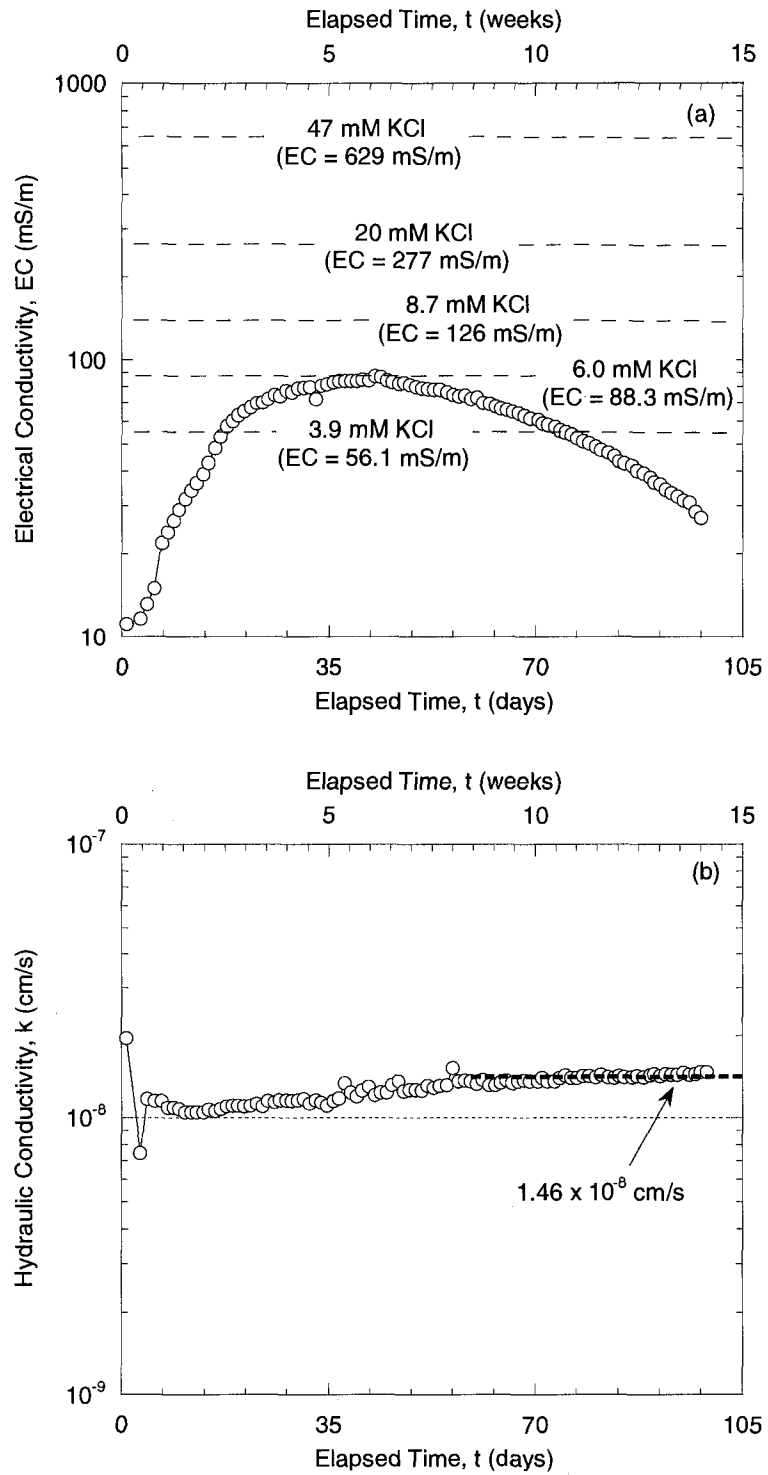


Fig. C.9 – Electrical conductivity (a) and hydraulic conductivity (b) versus elapsed time for a specimen of NFC No.1 permeated with de-ionized water during flushing stage of test prior to membrane testing.

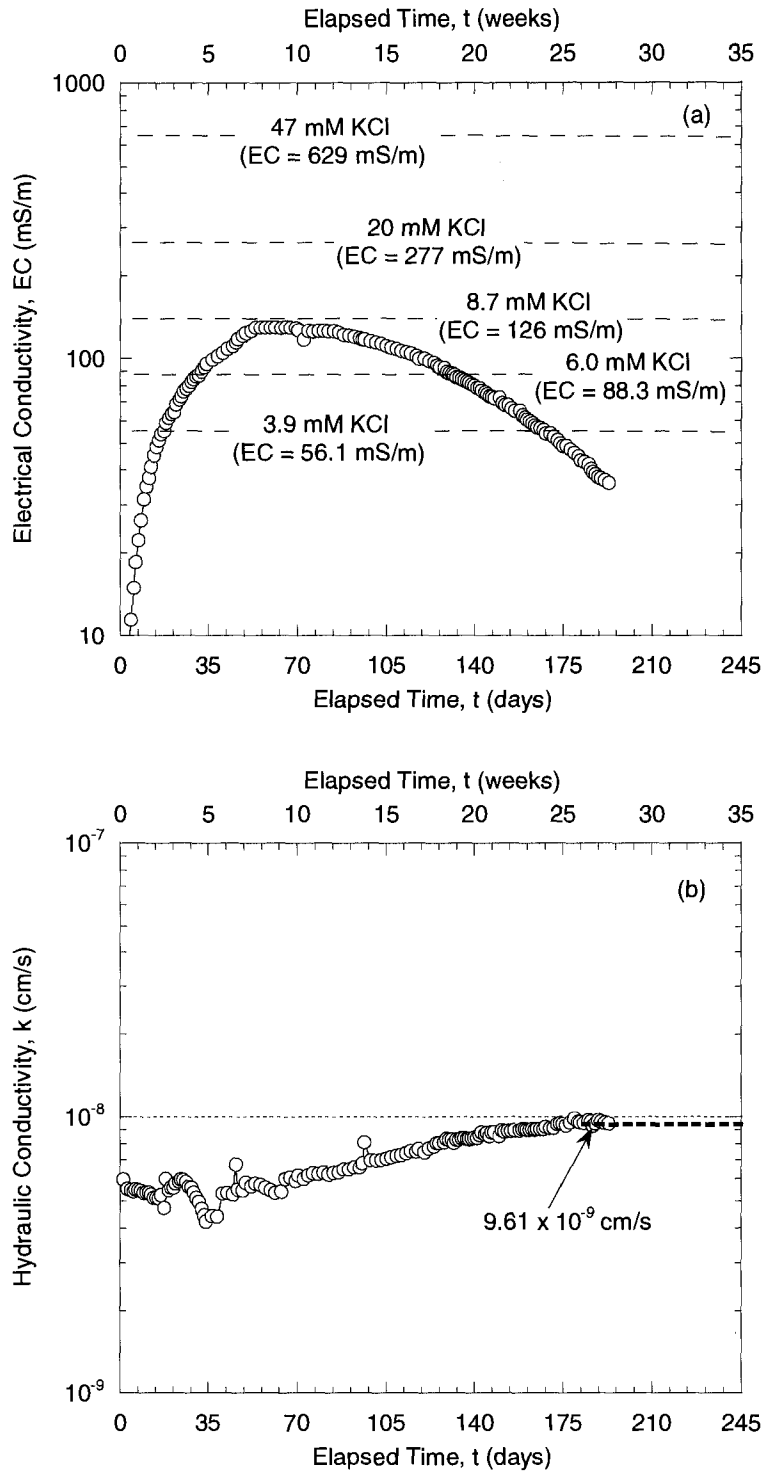


Fig. C.10 – Electrical conductivity (a) and hydraulic conductivity (b) versus elapsed time for a specimen of NFC plus 5 % bentonite No.2 permeated with de-ionized water during flushing stage of test prior to membrane testing.

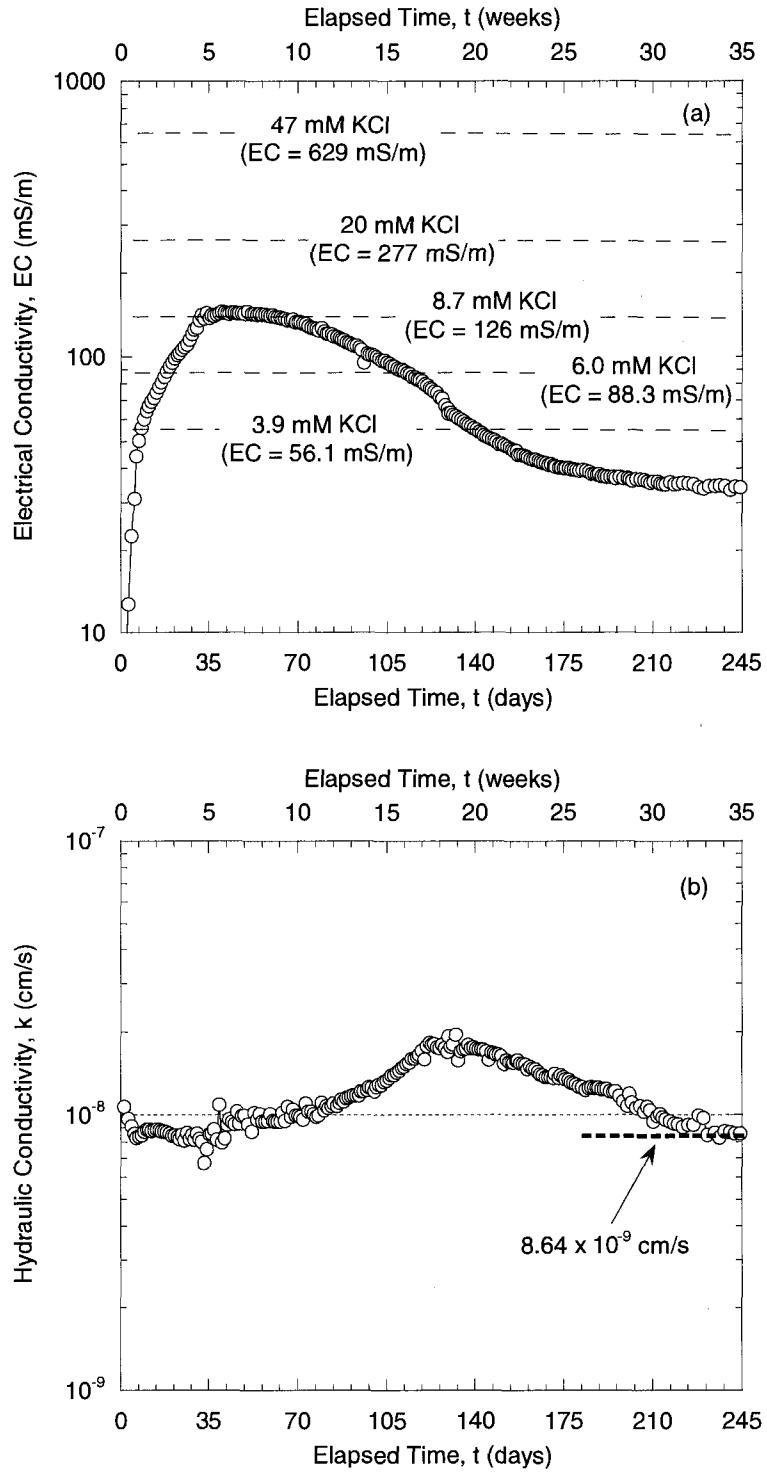


Fig. C.11 – Electrical conductivity (a) and hydraulic conductivity (b) versus elapsed time for a specimen of NFC plus 5% bentonite No.3 permeated with de-ionized water during flushing stage of test prior to membrane testing.

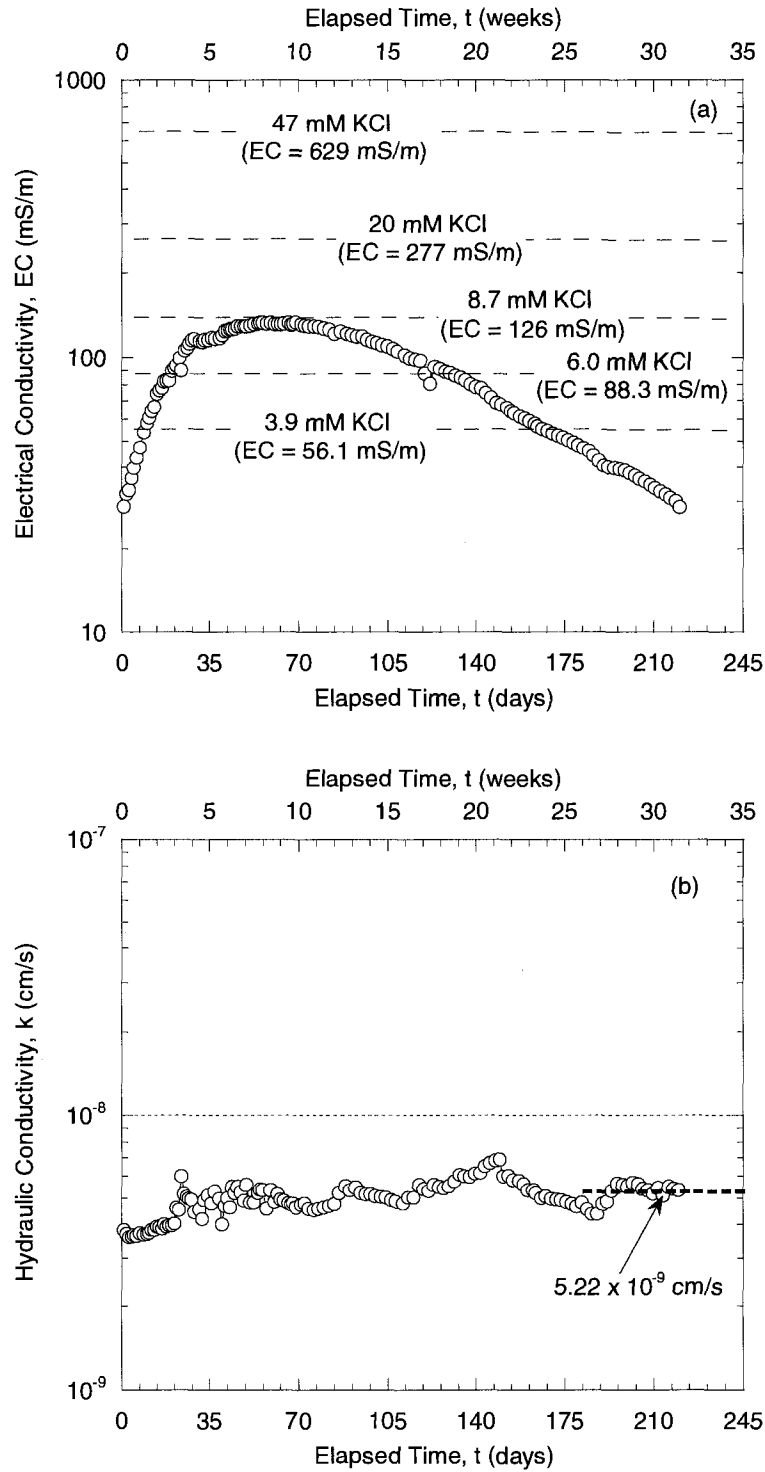


Fig. C.12 – Electrical conductivity (a) and hydraulic conductivity (b) versus elapsed time for a specimen of NFC plus 5 % bentonite No.4 permeated with de-ionized water during flushing stage of test prior to membrane testing.

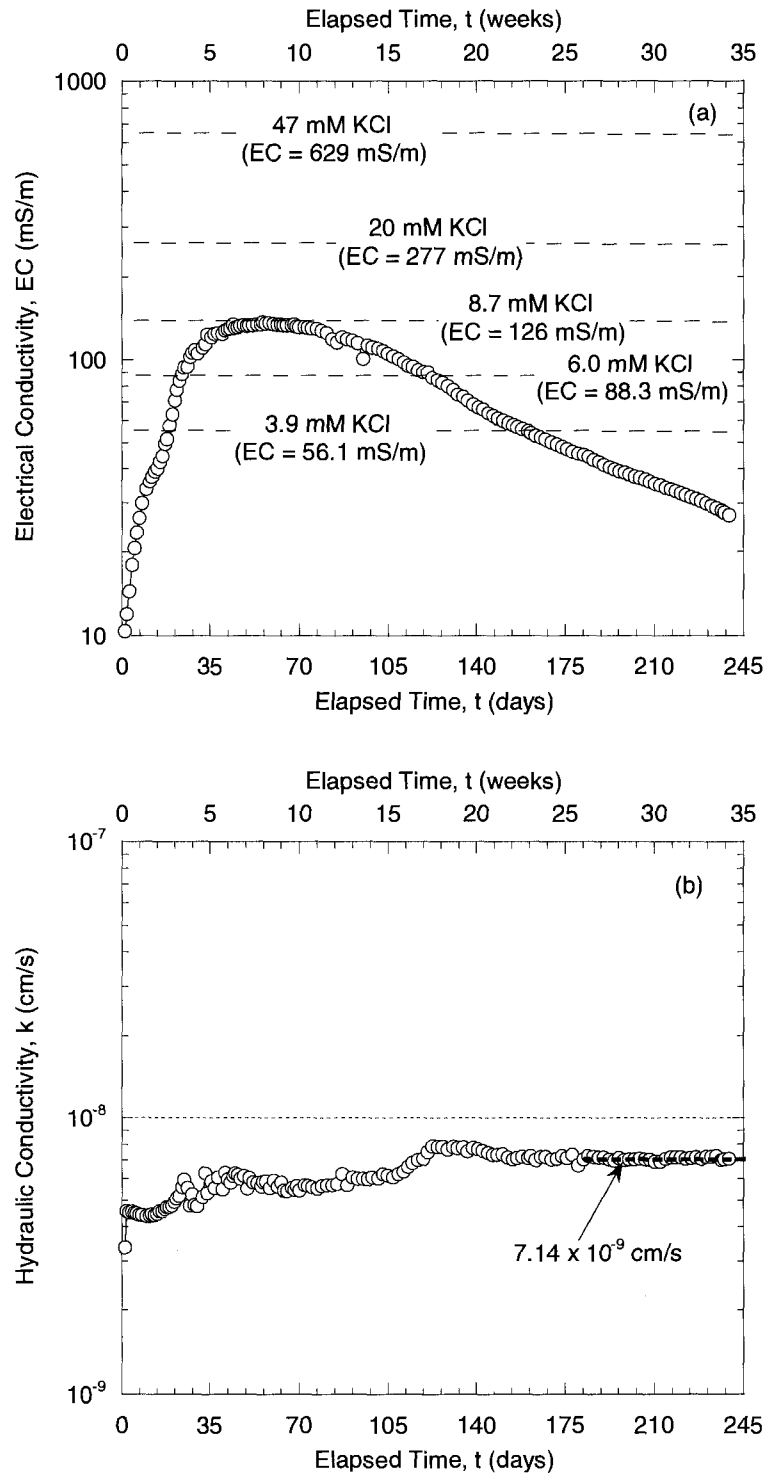


Fig. C.13 – Electrical conductivity (a) and hydraulic conductivity (b) versus elapsed time for a specimen of NFC plus 5 % bentonite No. 5 permeated with de-ionized water during flushing stage of test prior to membrane testing.

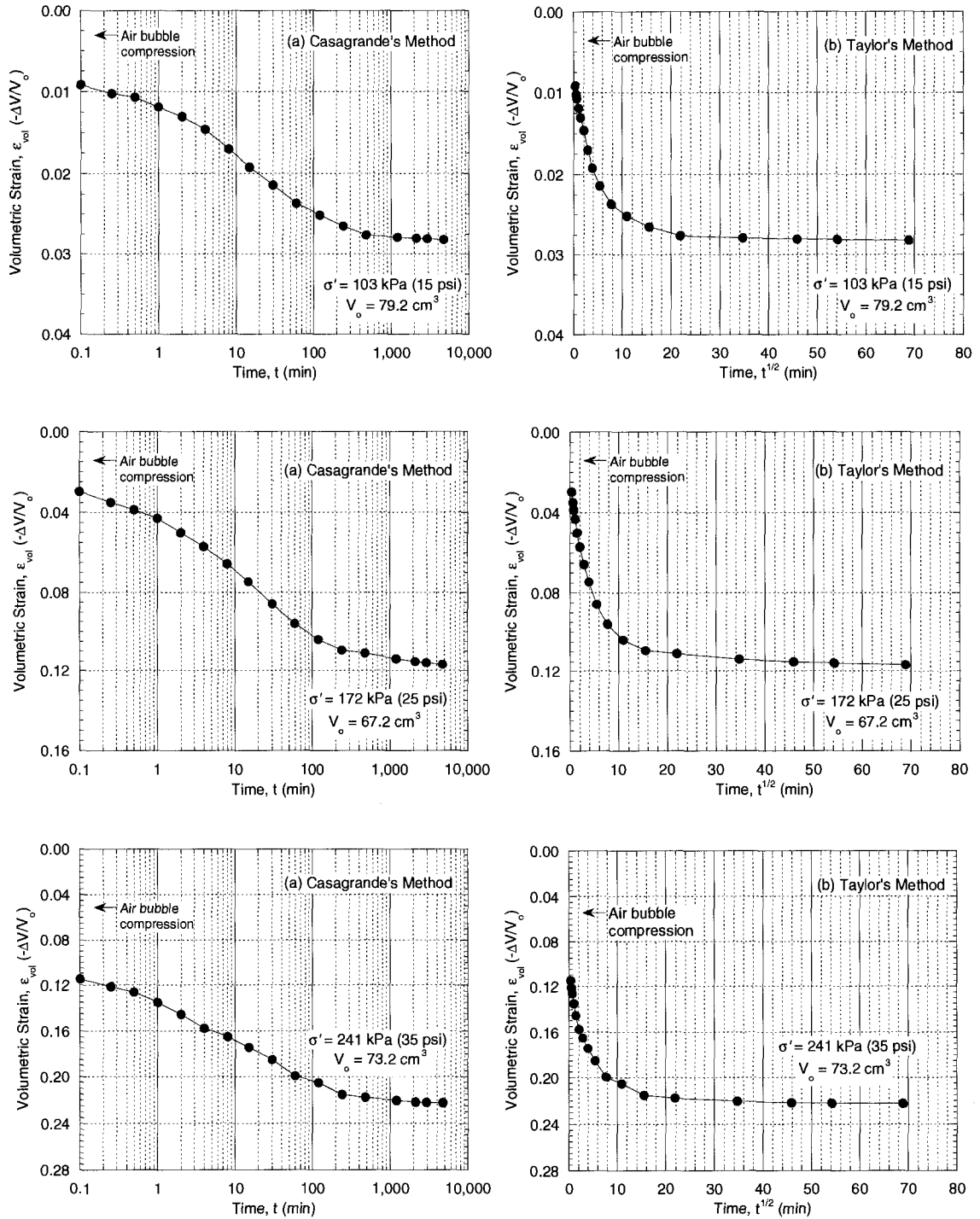


Fig. C.14 – Volumetric strain versus (a) logarithm of time and (b) square root of time for Bentomat GCL specimens consolidated to 103, 172, and 241 kPa (15.0, 25.0, and 35.0 psi) effective stress prior to membrane testing in flexible-wall cell.

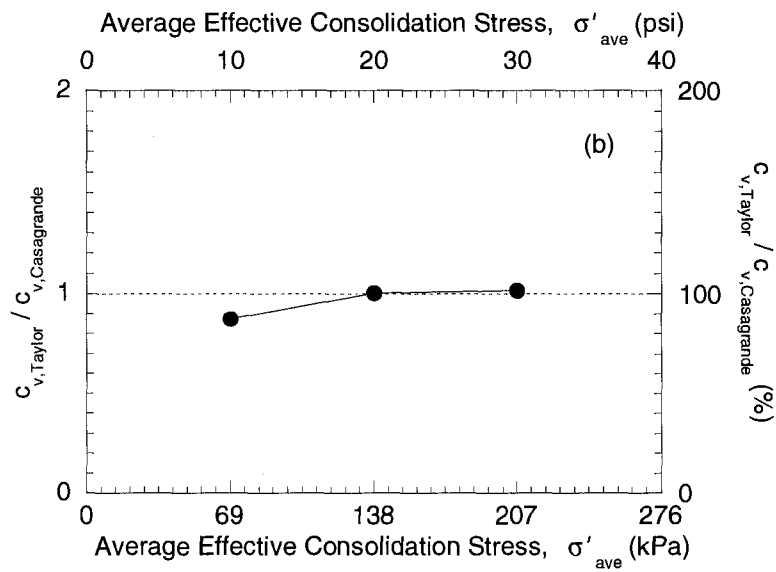
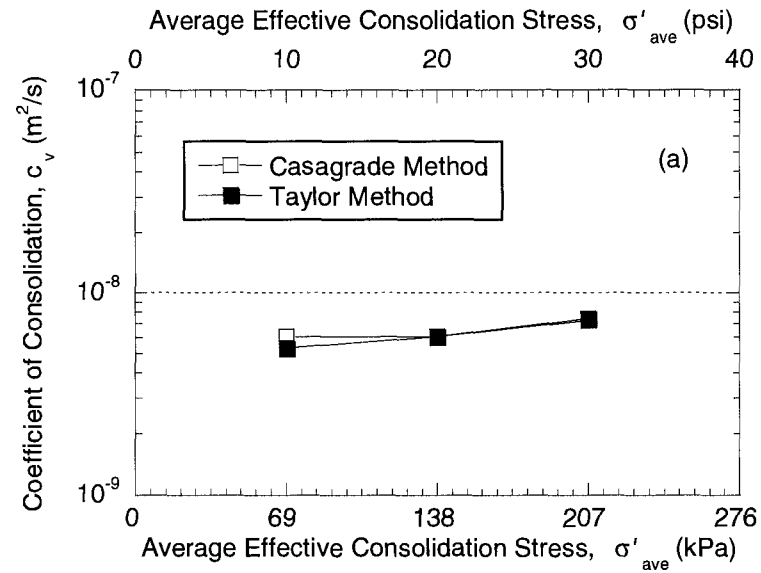


Fig. C.15 – Effect of method of analysis on the coefficients of consolidation, c_v , based on volumetric strain for the GCL specimens as function of average effective consolidation stress: (a) individual values; (b) ratio of values.

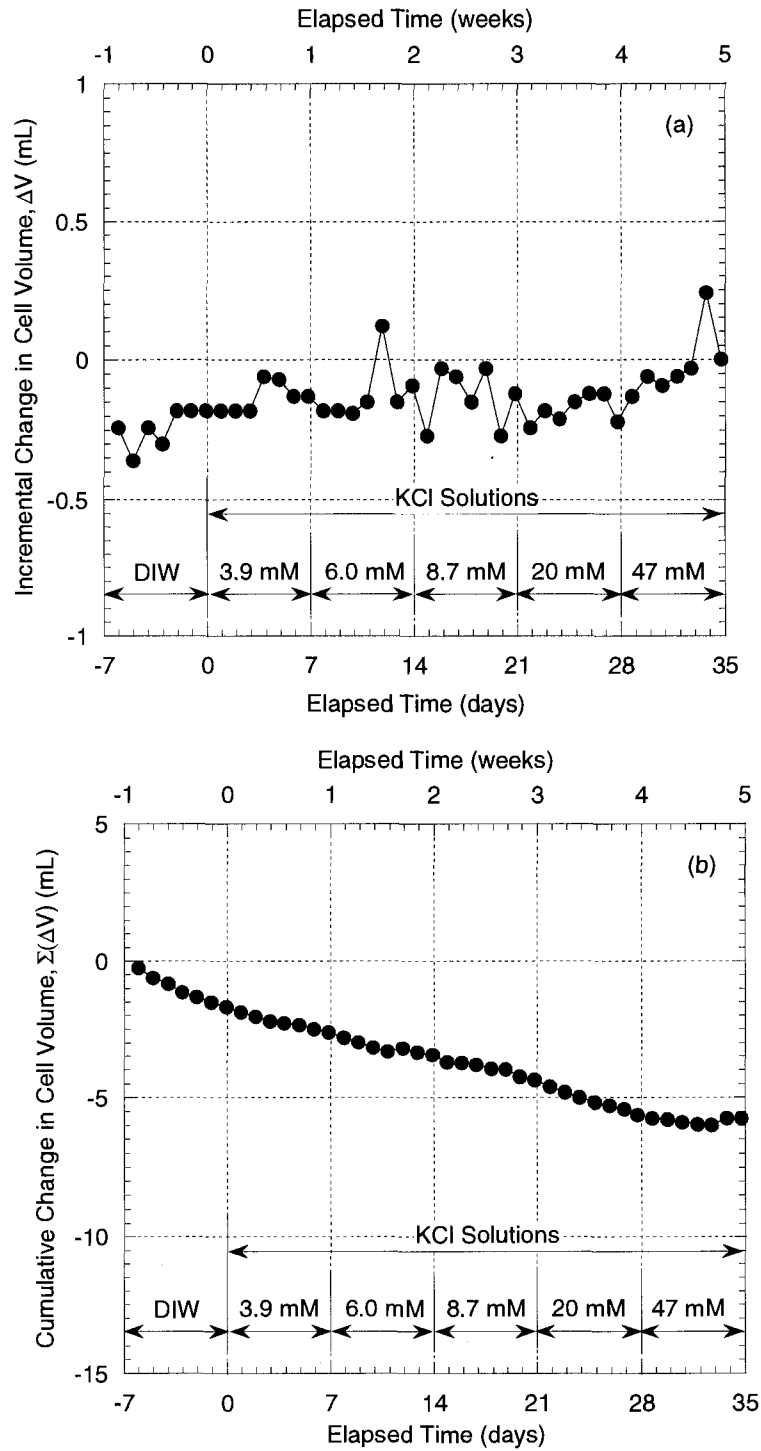


Fig. C.16 – Incremental (a) and cumulative (b) changes in cell volume for a specimen of GCL consolidated to an initial effective stress of 34.5 kPa (5.0 psi) during membrane testing in flexible-wall cell.

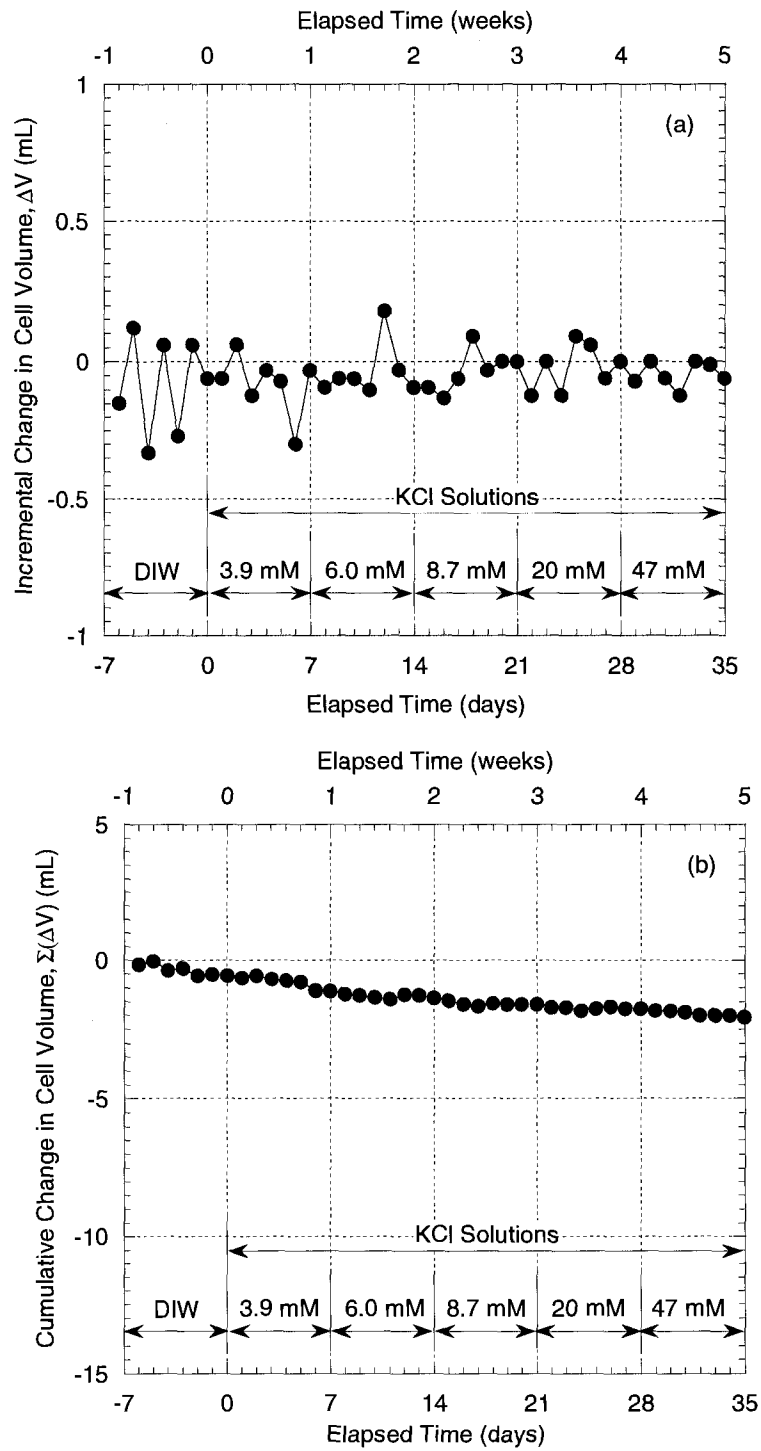


Fig. C.17 – Incremental (a) and cumulative (b) changes in cell volume for a specimen of GCL consolidated to an initial effective stress of 103 kPa (15.0 psi) during membrane testing in flexible-wall cell.

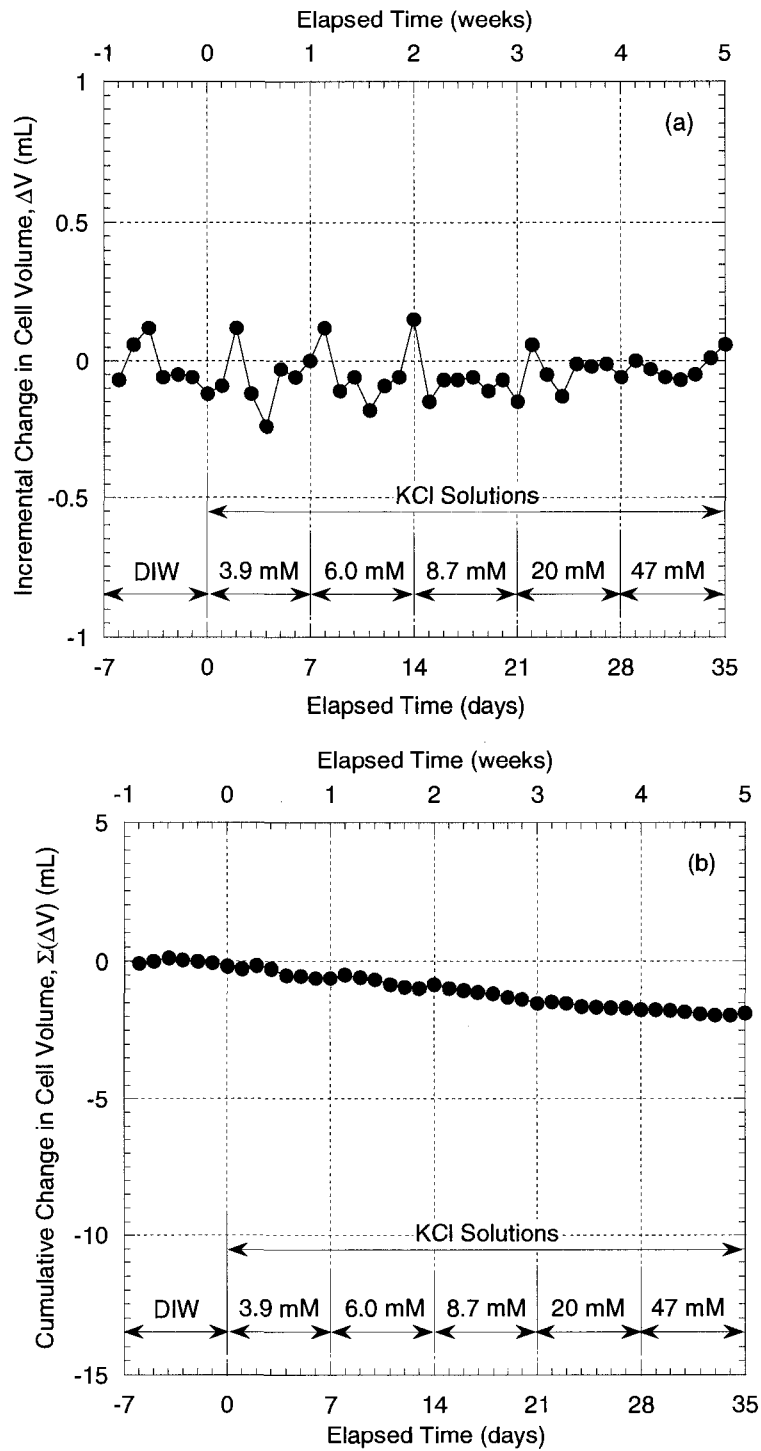


Fig. C.18 – Incremental (a) and cumulative (b) changes in cell volume for a specimen of GCL consolidated to an initial effective stress of 172 kPa (25.0 psi) during membrane testing in flexible-wall cell.

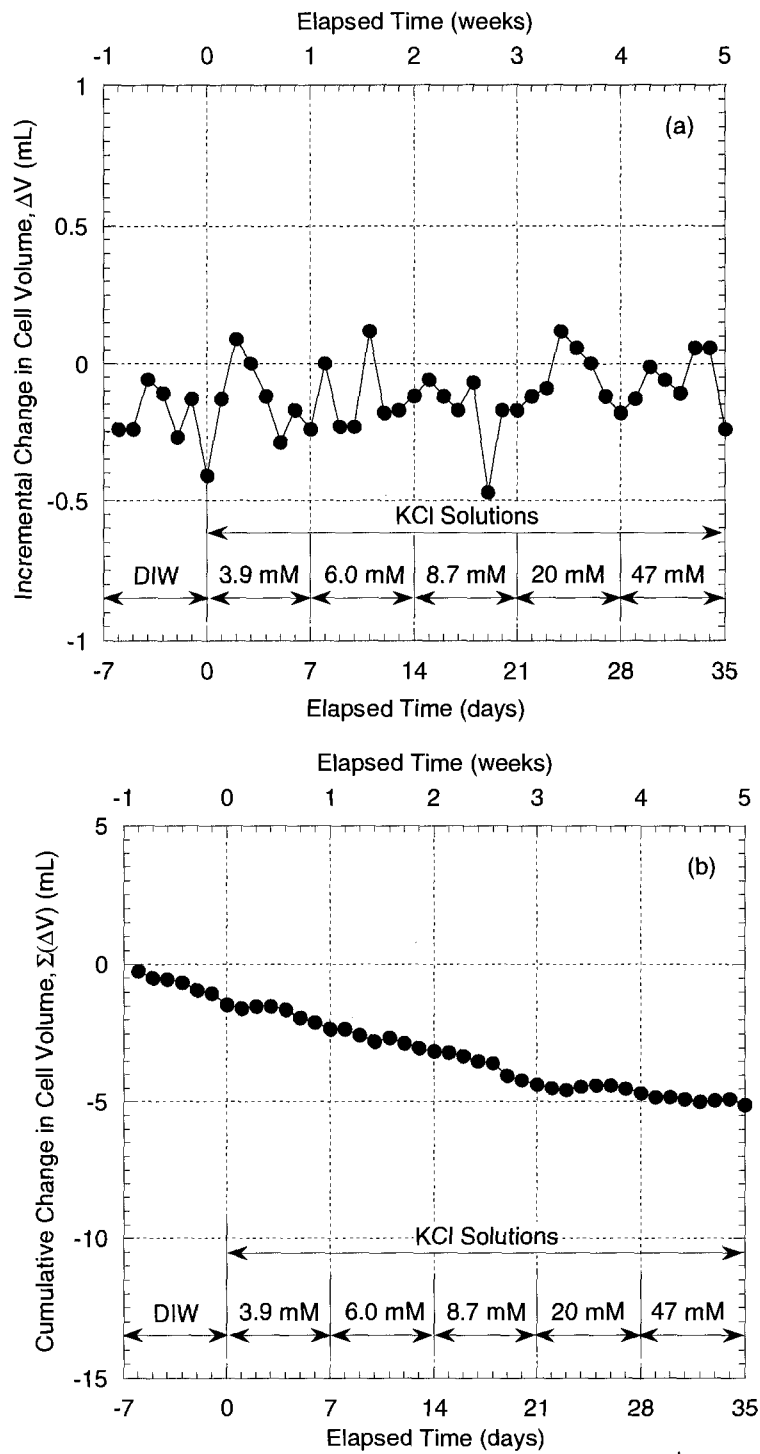


Fig. C.19 – Incremental (a) and cumulative (b) changes in cell volume for a specimen of GCL consolidated to an initial effective stress of 241 kPa (35.0 psi) during membrane testing in flexible-wall cell.

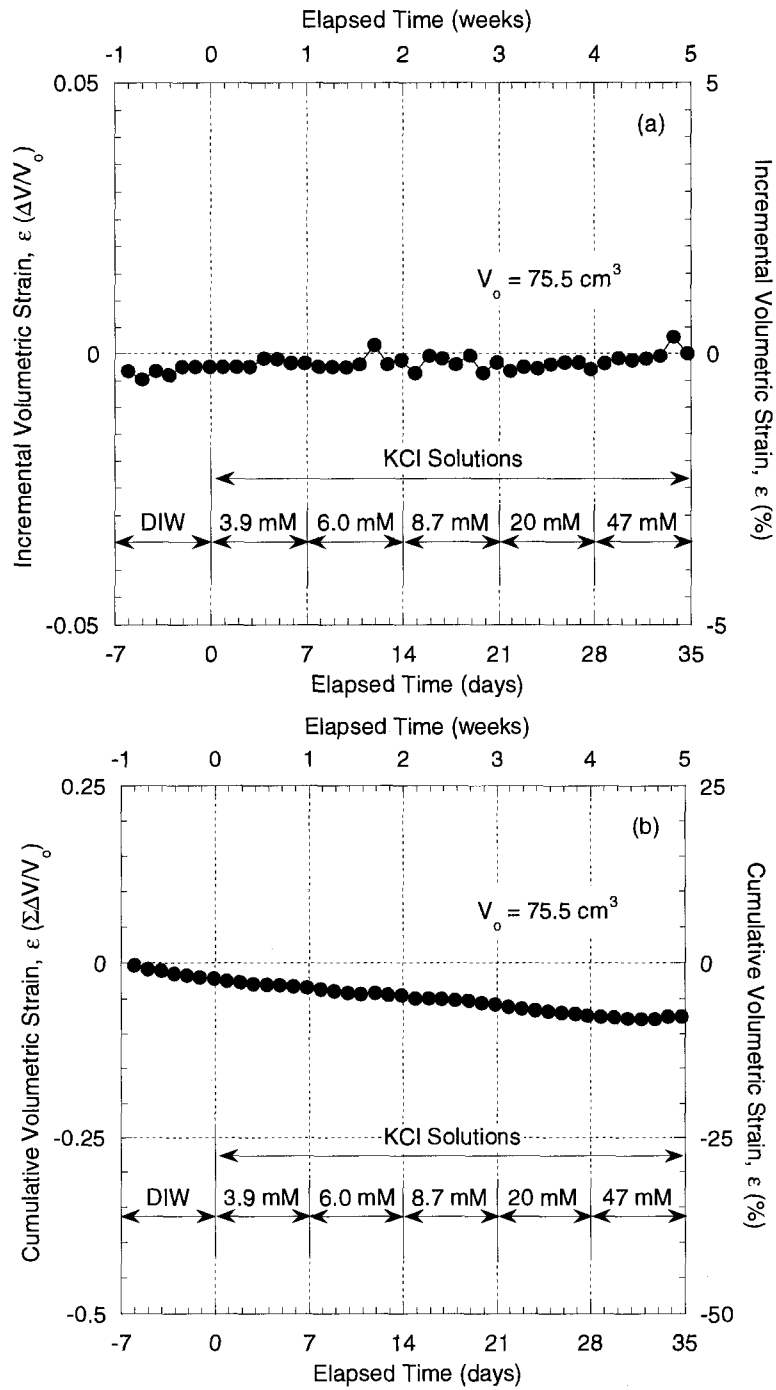


Fig. C.20 – Incremental (a) and cumulative (b) volumetric strains for a specimen of GCL consolidated to an initial effective stress of 34.5 kPa (5.0 psi) during membrane testing in a flexible-wall cell.

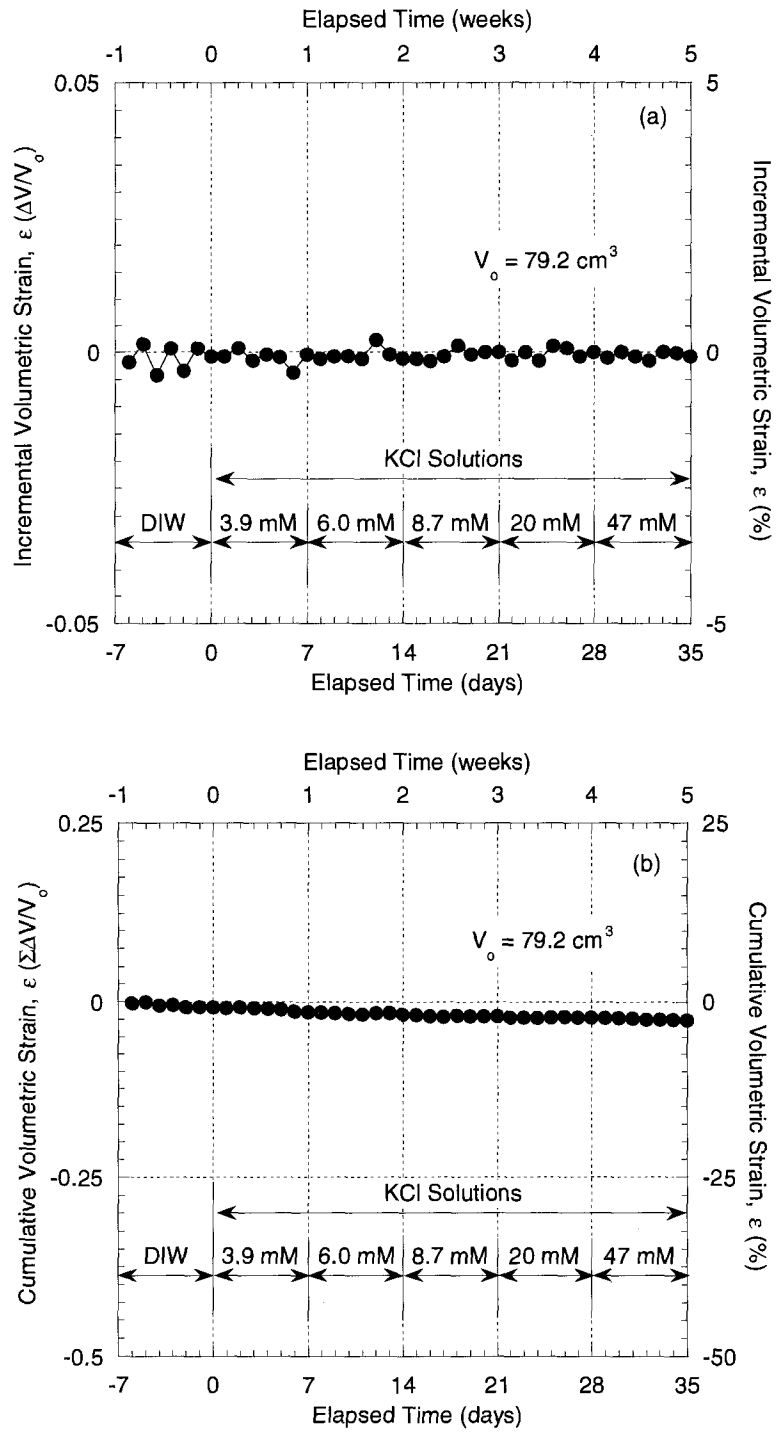


Fig. C.21 – Incremental (a) and cumulative (b) volumetric strains for a specimen of GCL consolidated to an initial effective stress of 103 kPa (15.0 psi) during membrane testing in a flexible-wall cell.

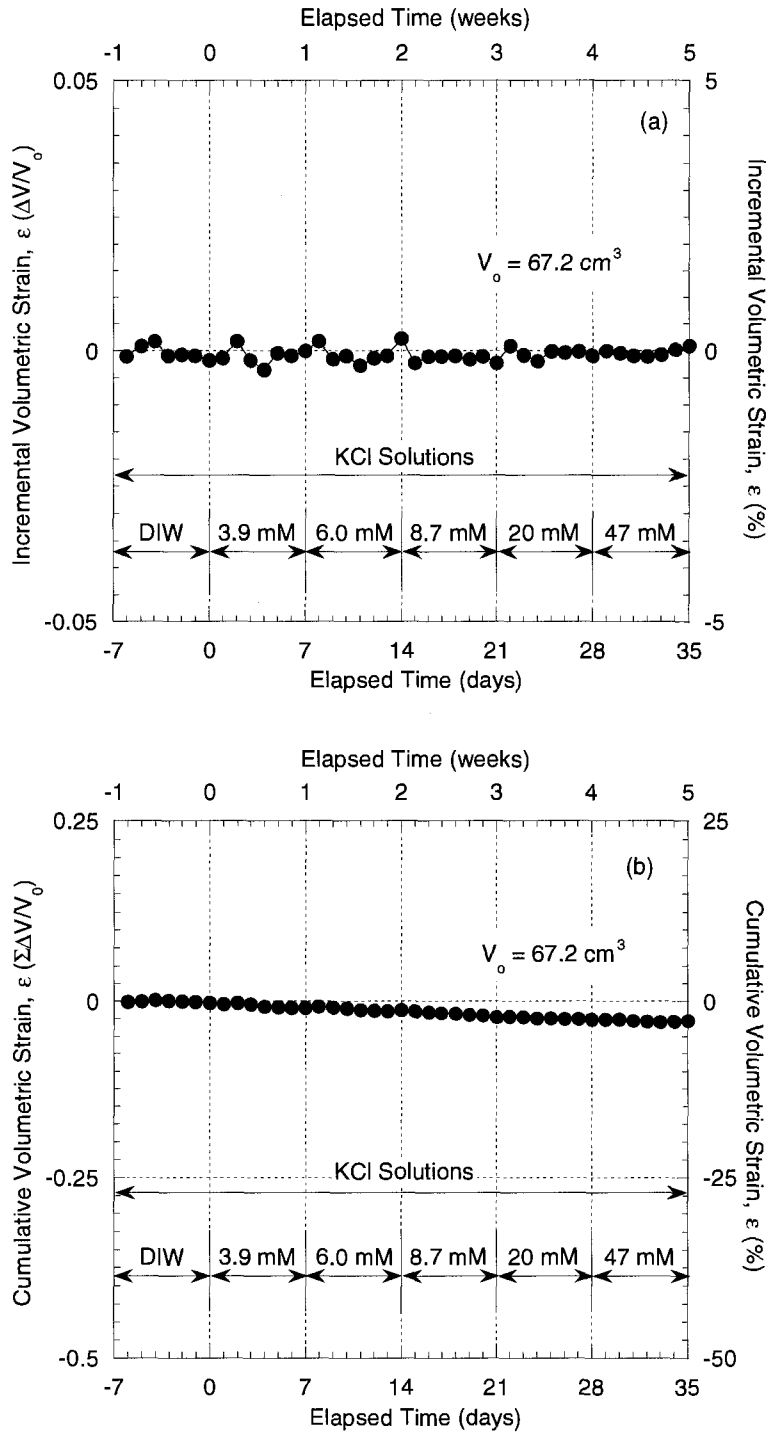


Fig. C.22 – Incremental (a) and cumulative (b) volumetric strains for a specimen of GCL consolidated to an initial effective stress of 172 kPa (25.0 psi) during membrane testing in a flexible-wall cell.

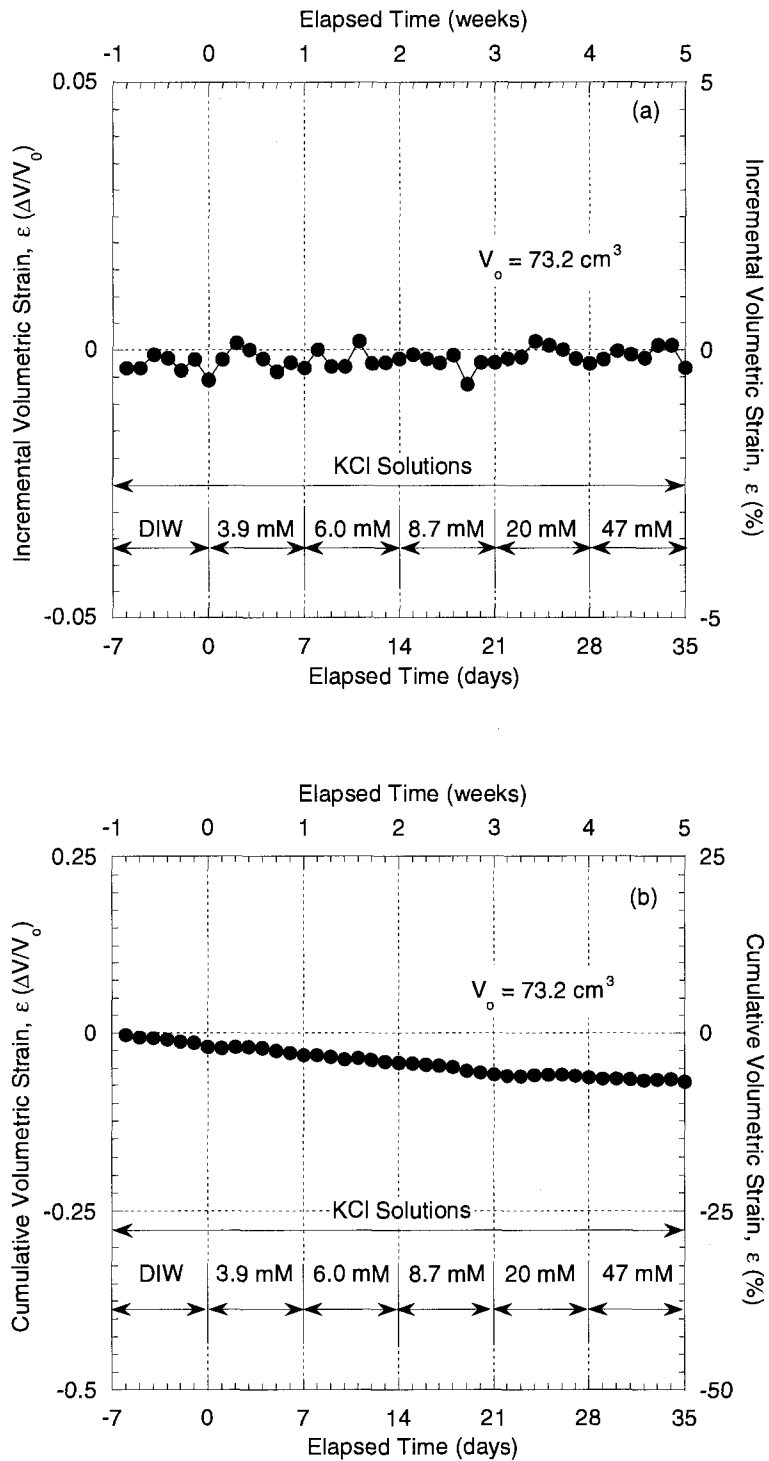


Fig. C.23 – Incremental (a) and cumulative (b) volumetric strains for a specimen of GCL consolidated to an initial effective stress of 241 kPa (35.0 psi) during membrane testing in a flexible-wall cell.

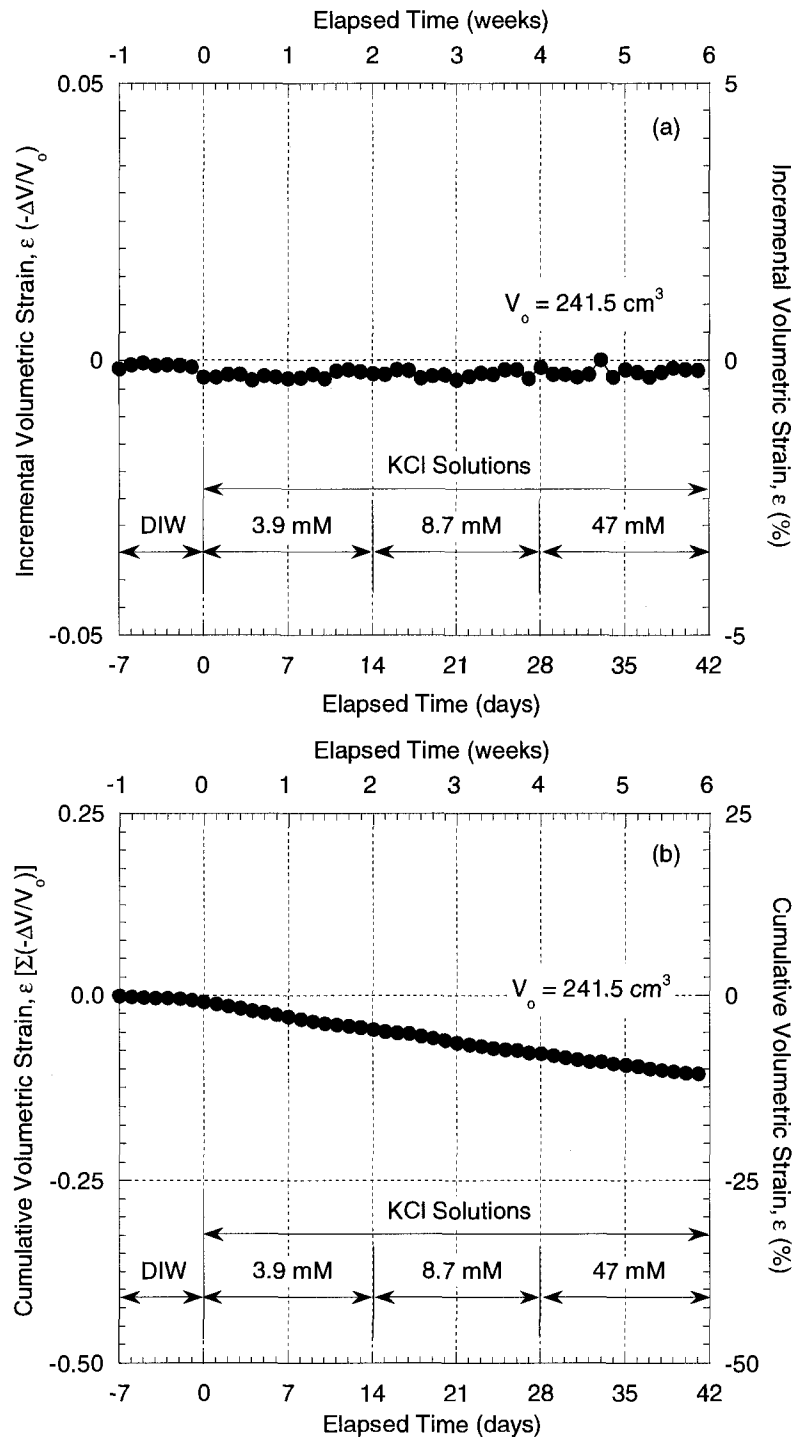


Fig. C.24 – Incremental (a) and cumulative (b) volumetric strains for a specimen of NFC No.1 during membrane testing in a flexible-wall cell.

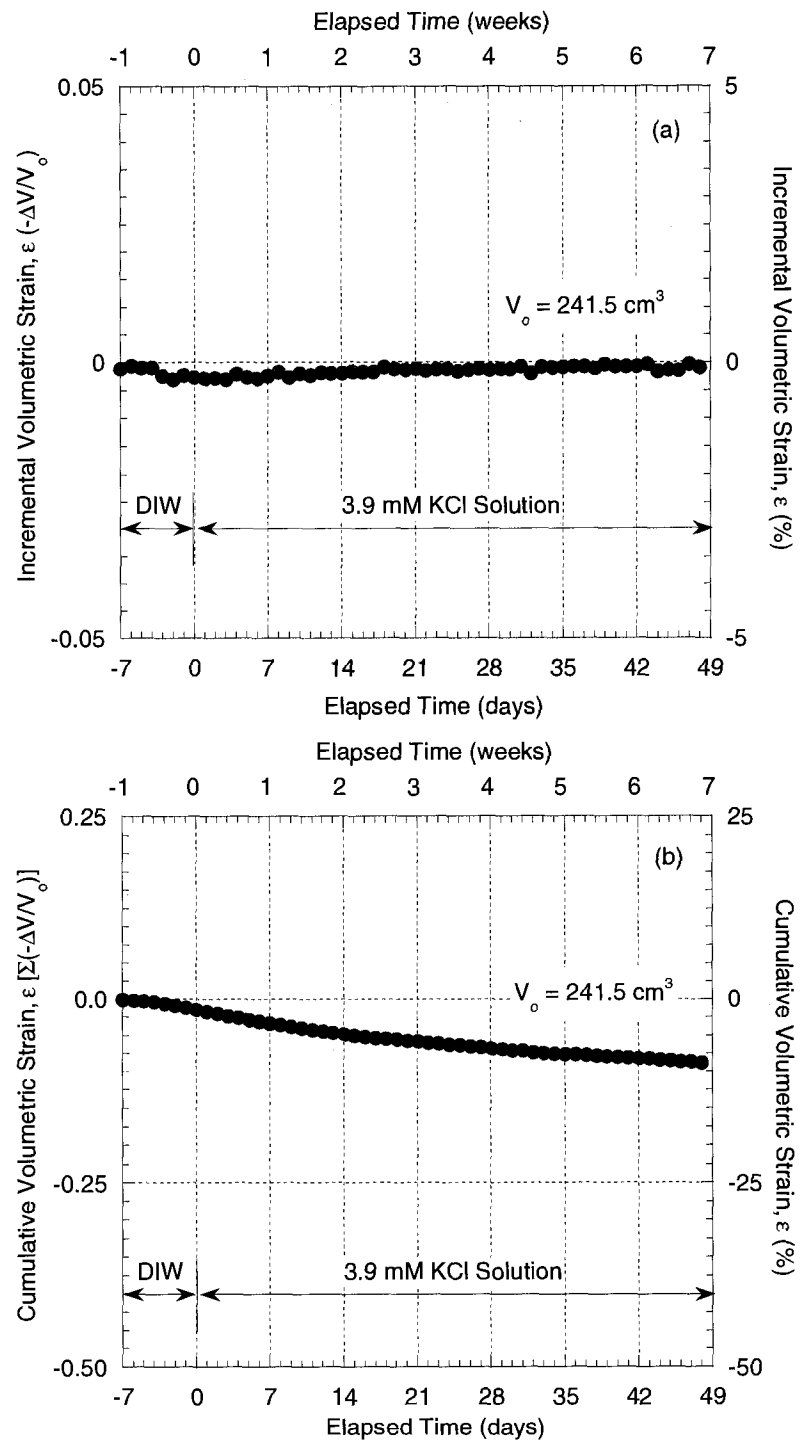


Fig. C.25 – Incremental (a) and cumulative (b) volumetric strains for a specimen of NFC plus 5 % bentonite No.2 during membrane testing in a flexible-wall cell.

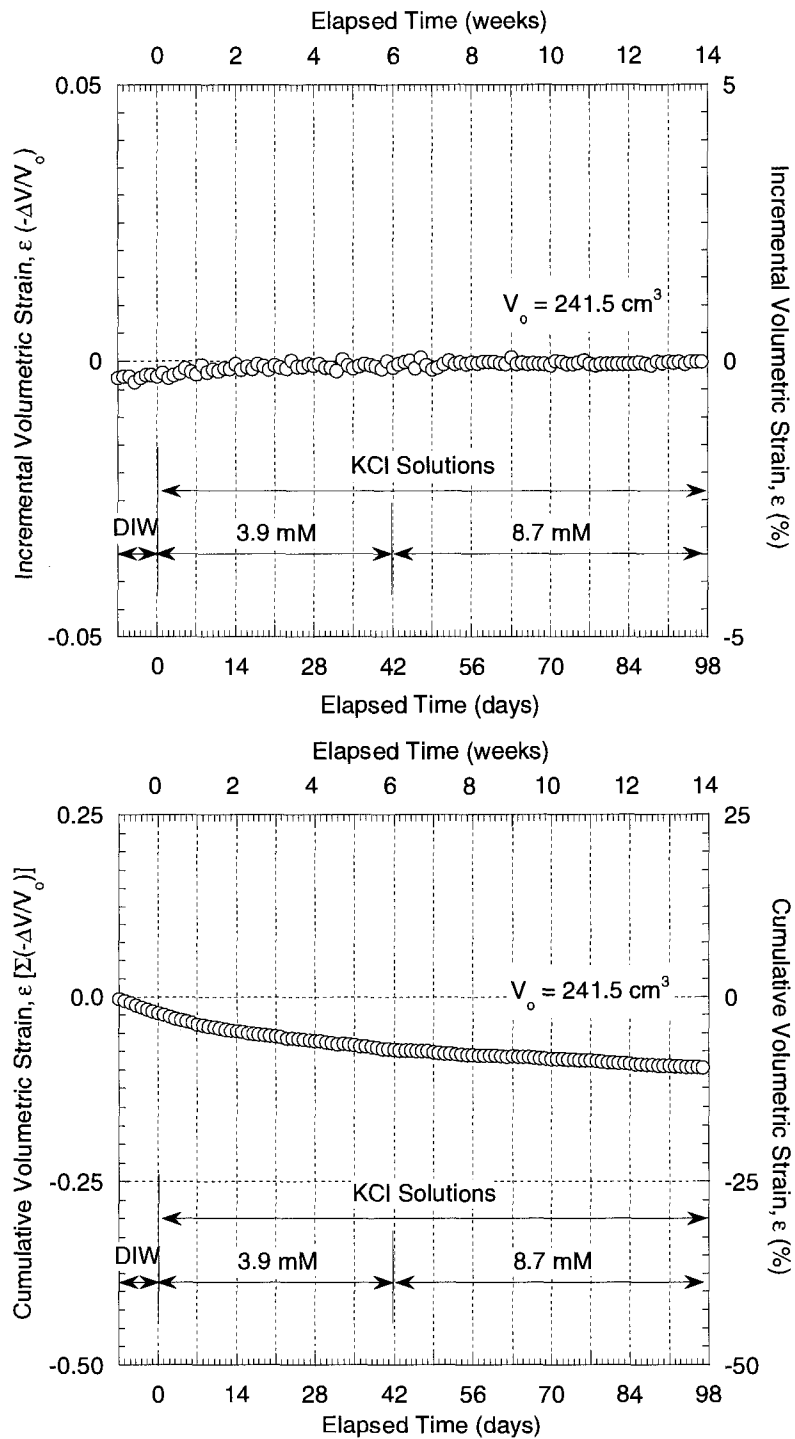


Fig. C.26 – Incremental (a) and cumulative (b) volumetric strains for a specimen of NFC plus 5 % bentonite No.3 during membrane testing in a flexible-wall cell.

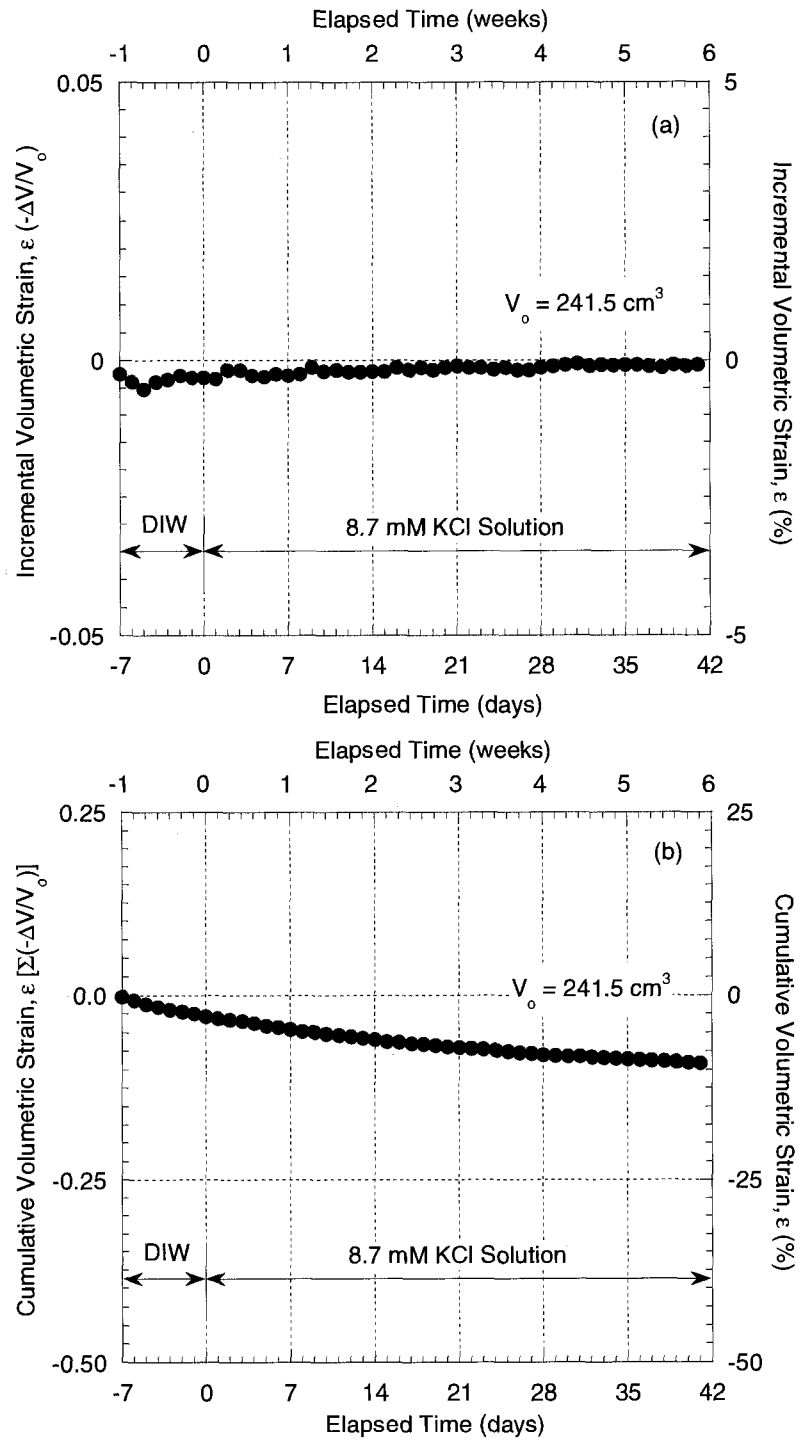


Fig. C.27 – Incremental (a) and cumulative (b) volumetric strains for a specimen of NFC plus 5 % bentonite No.4 during membrane testing in a flexible-wall cell.

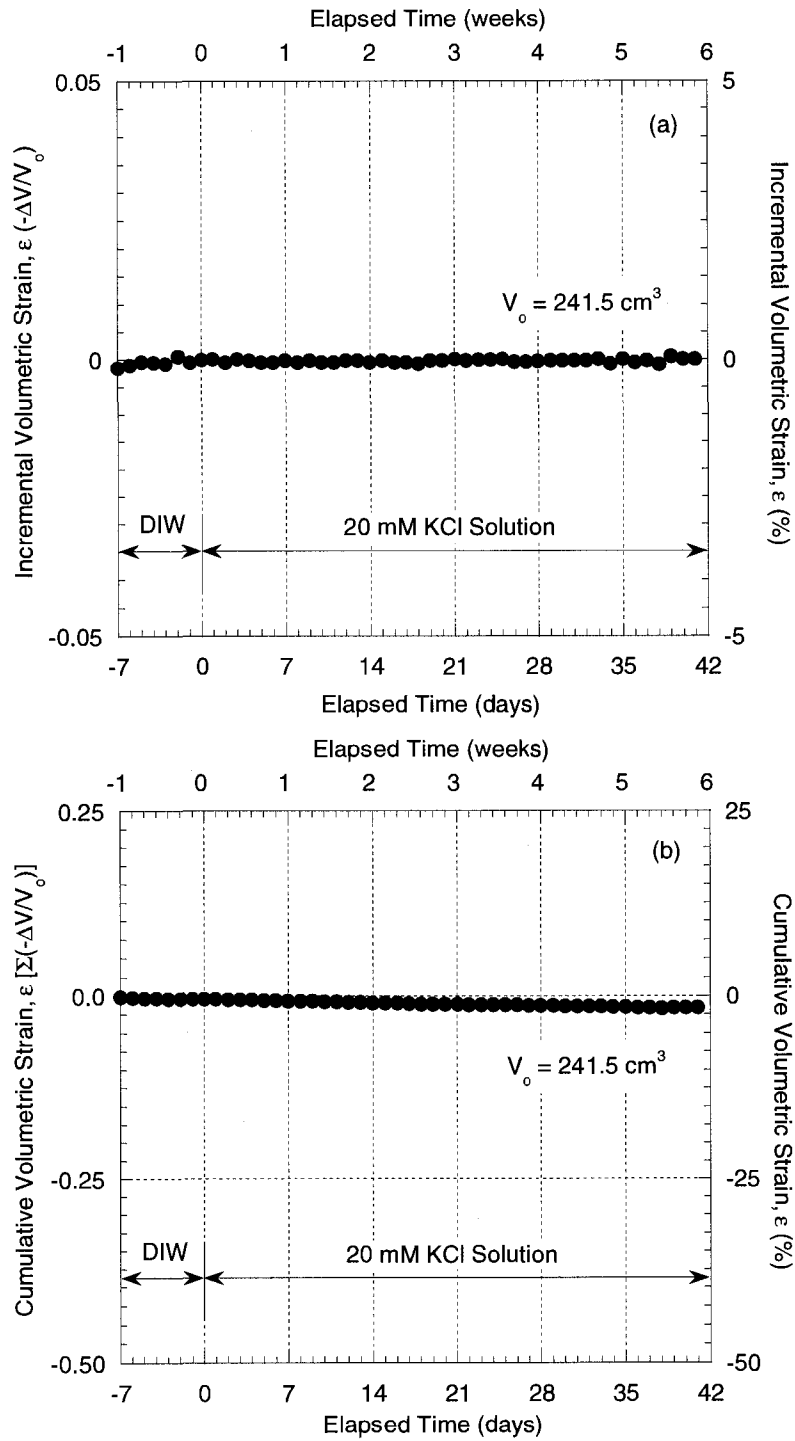


Fig. C.28 – Incremental (a) and cumulative (b) volumetric strains for a specimen of NFC plus 5 % bentonite No.5 during membrane testing in a flexible-wall cell.

APPENDIX D

HYDRAULIC CONDUCTIVITY TEST DATA FOR COMPACTED CLAY MATERIALS

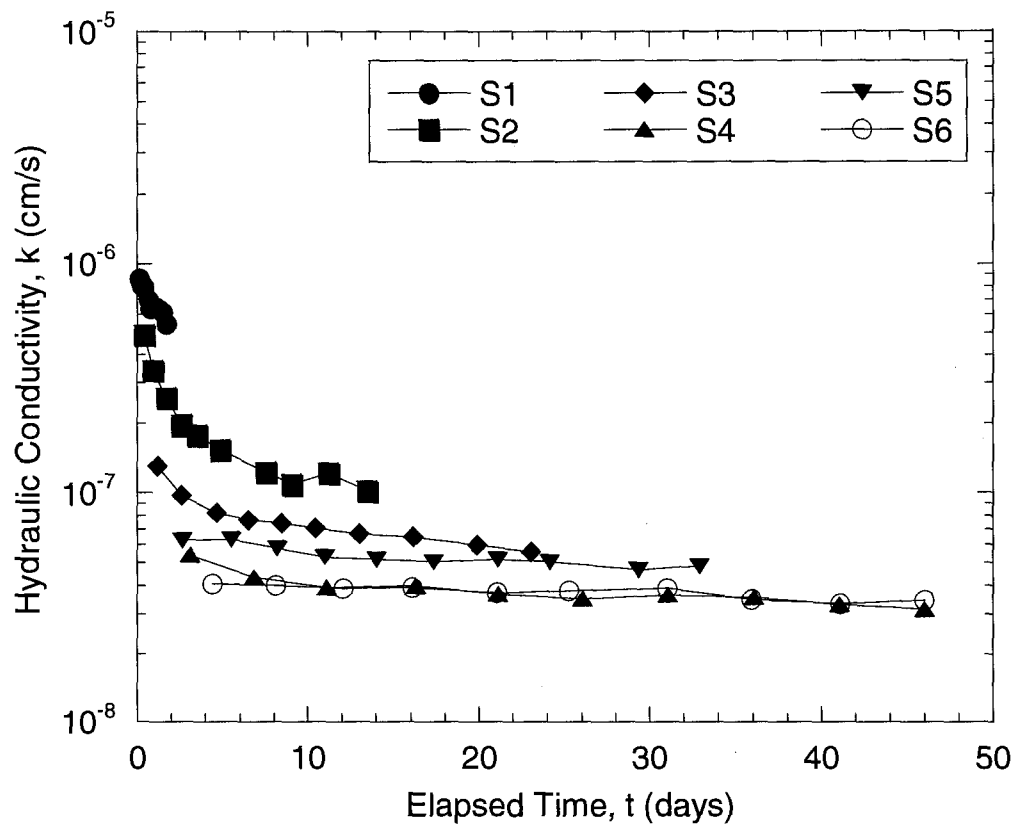


Fig. D.1 – Elapsed time versus hydraulic conductivity for specimens of Nelson Farm Clay compacted by standard compaction (ASTM D 698).

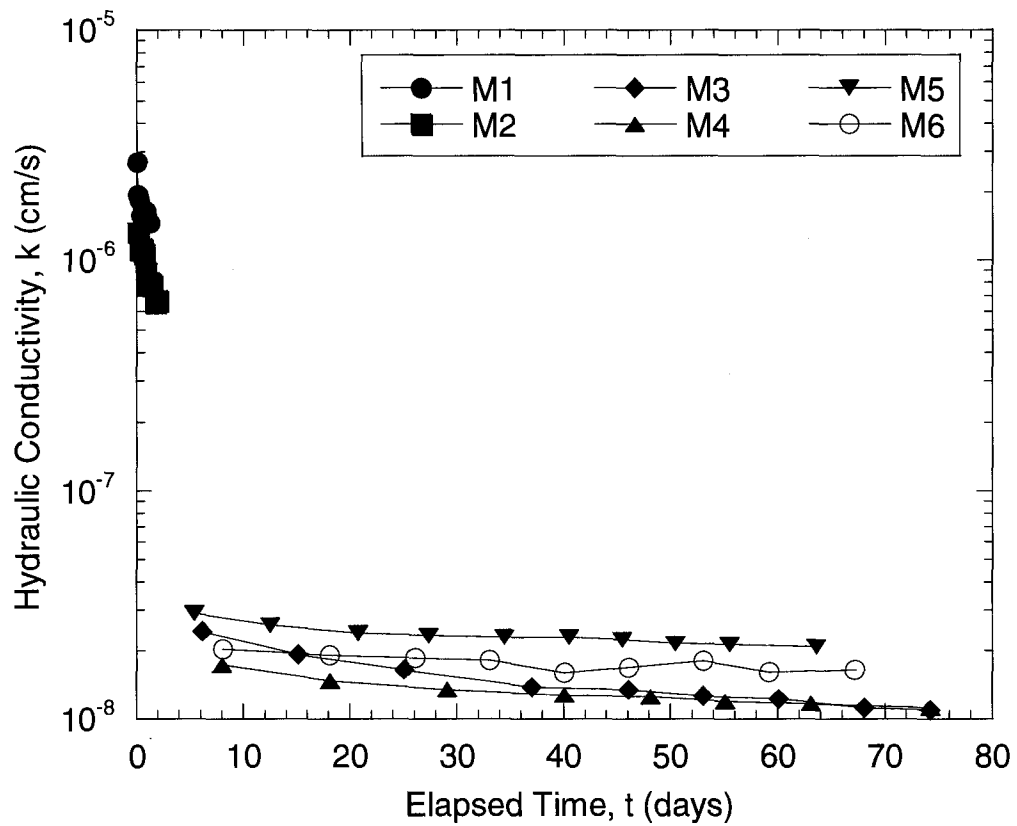


Fig. D.2 – Elapsed time versus hydraulic conductivity for specimens of Nelson Farm Clay compacted by modified compaction (ASTM D 1557).

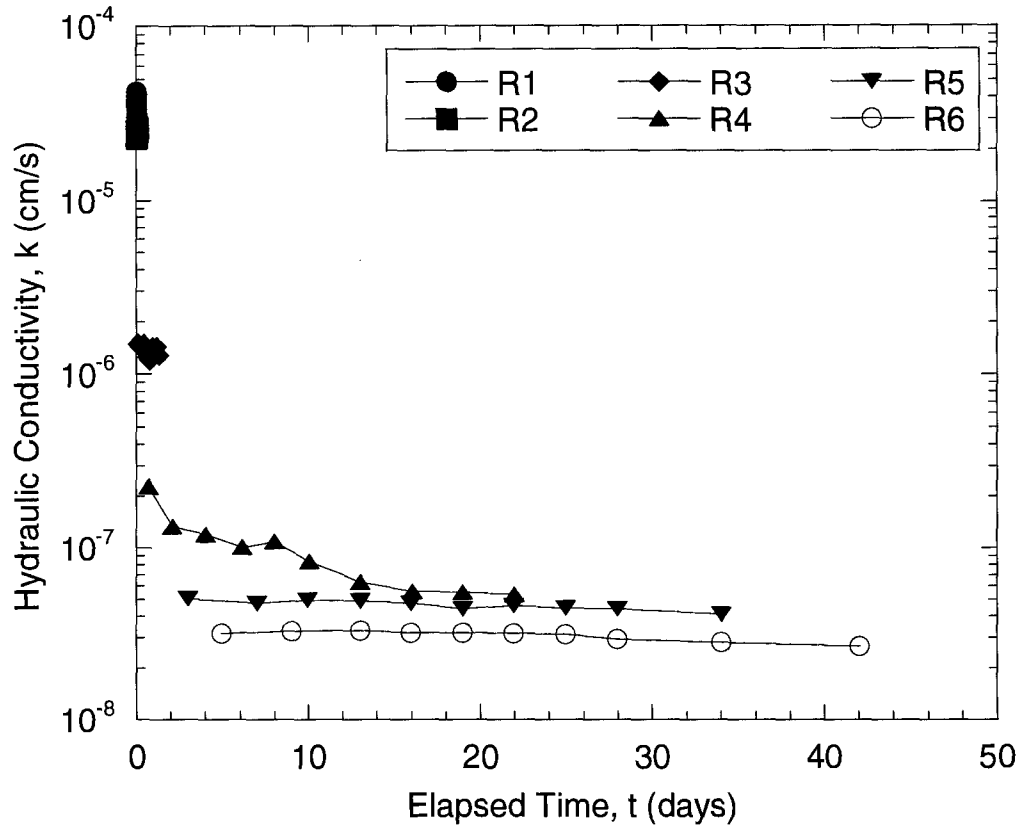


Fig. D.3 – Elapsed time versus hydraulic conductivity for specimens of Nelson Farm Clay compacted by reduced compaction (Eng. Manual EM-1110-2-1906).

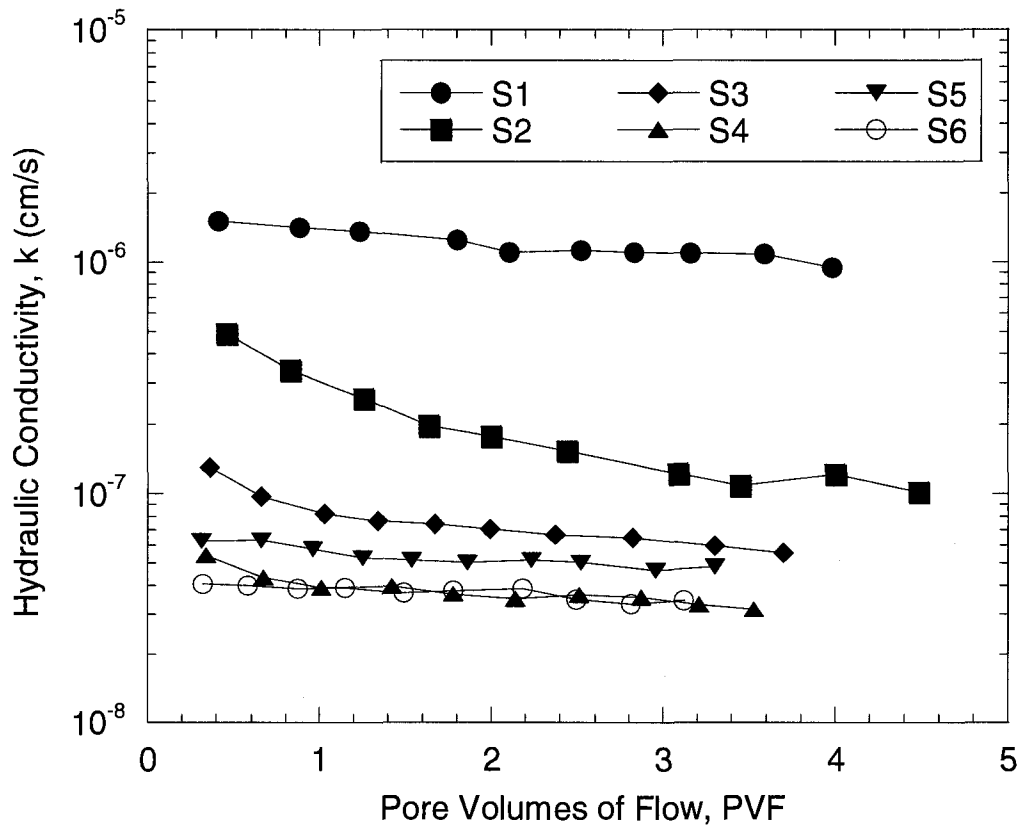


Fig. D.4 – Pore volumes of flow versus hydraulic conductivity for specimens of Nelson Farm Clay compacted by standard compaction (ASTM D 698).

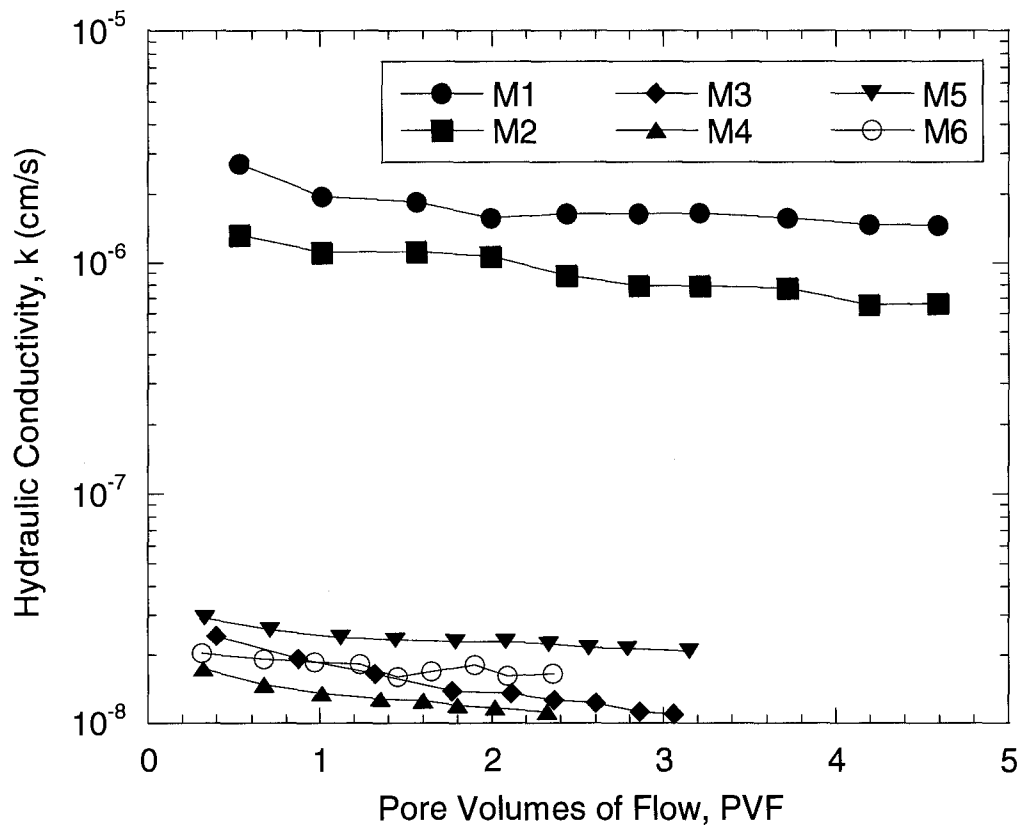


Fig. D.5 – Pore volumes of flow versus hydraulic conductivity for specimens of Nelson Farm Clay compacted by modified compaction (ASTM D 1557).

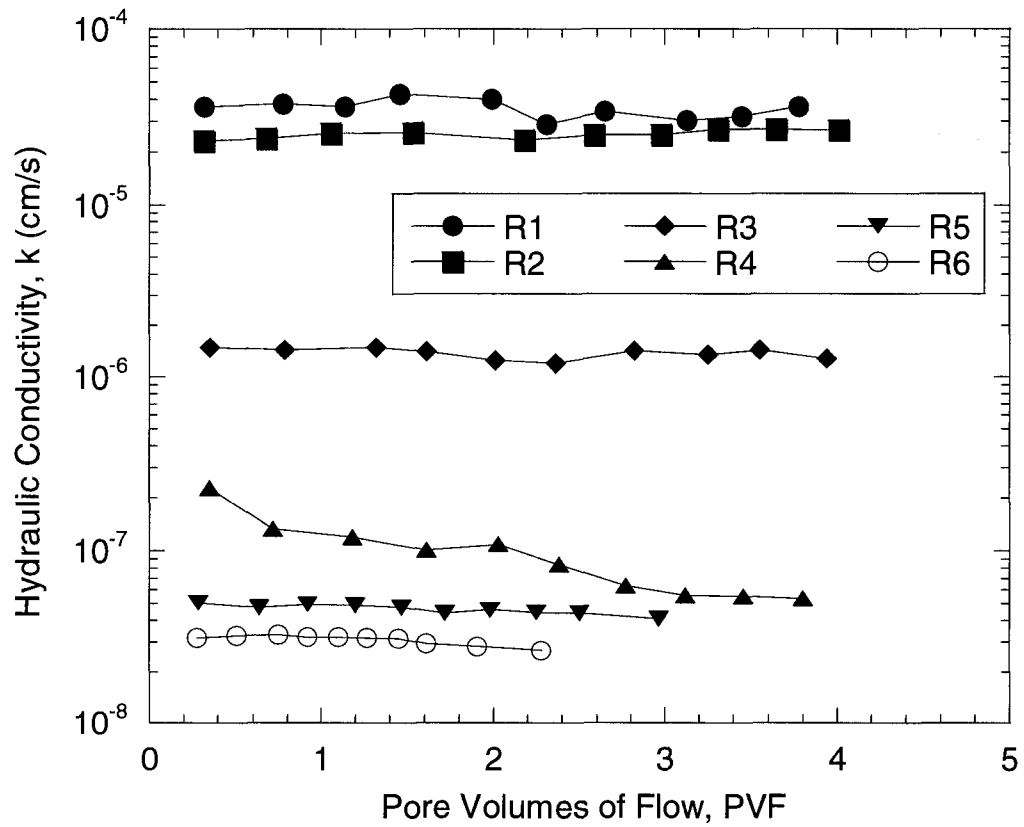


Fig. D.6 – Pore volumes of flow versus hydraulic conductivity for specimens of Nelson Farm Clay compacted by reduced compaction (Eng. Manual EM-1110-2-1906).

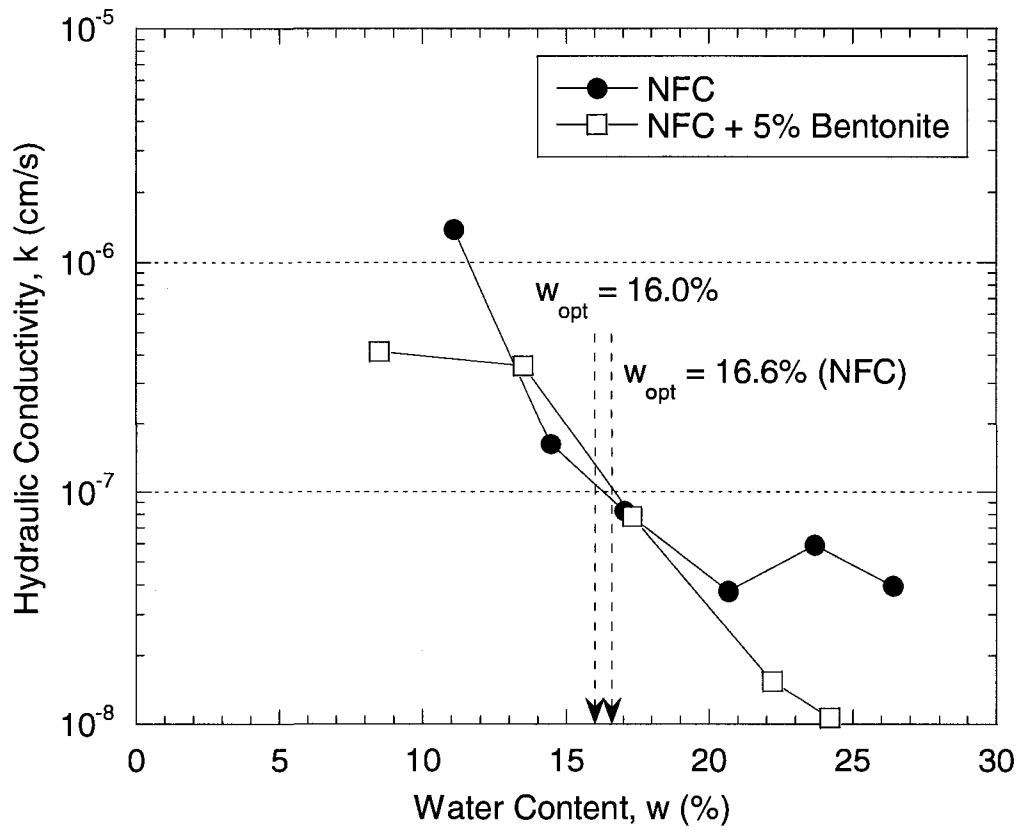


Fig. D.7 – Initial water contents versus hydraulic conductivity for specimens of Nelson Farm Clay (NFC) and NFC plus 5 % bentonite compacted by standard compaction (ASTM D 698).

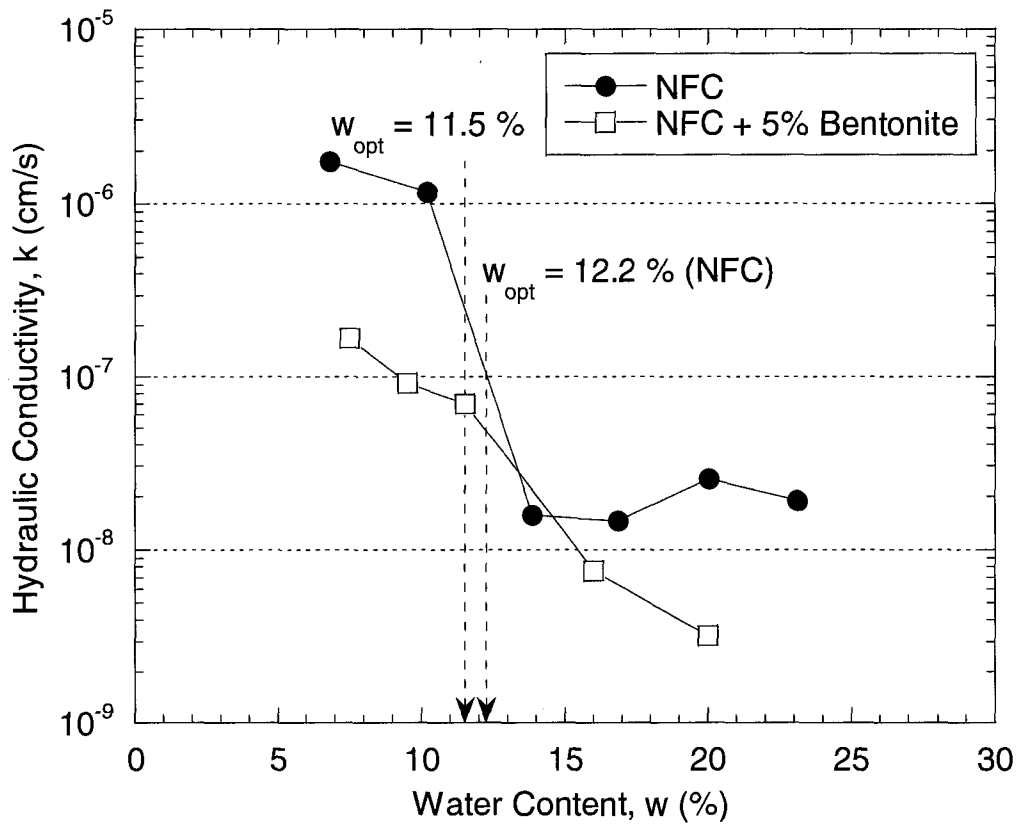


Fig. D.8 – Initial water contents versus hydraulic conductivity for specimens of Nelson Farm Clay (NFC) and NFC plus 5 % bentonite compacted by modified compaction (ASTM D 1557).

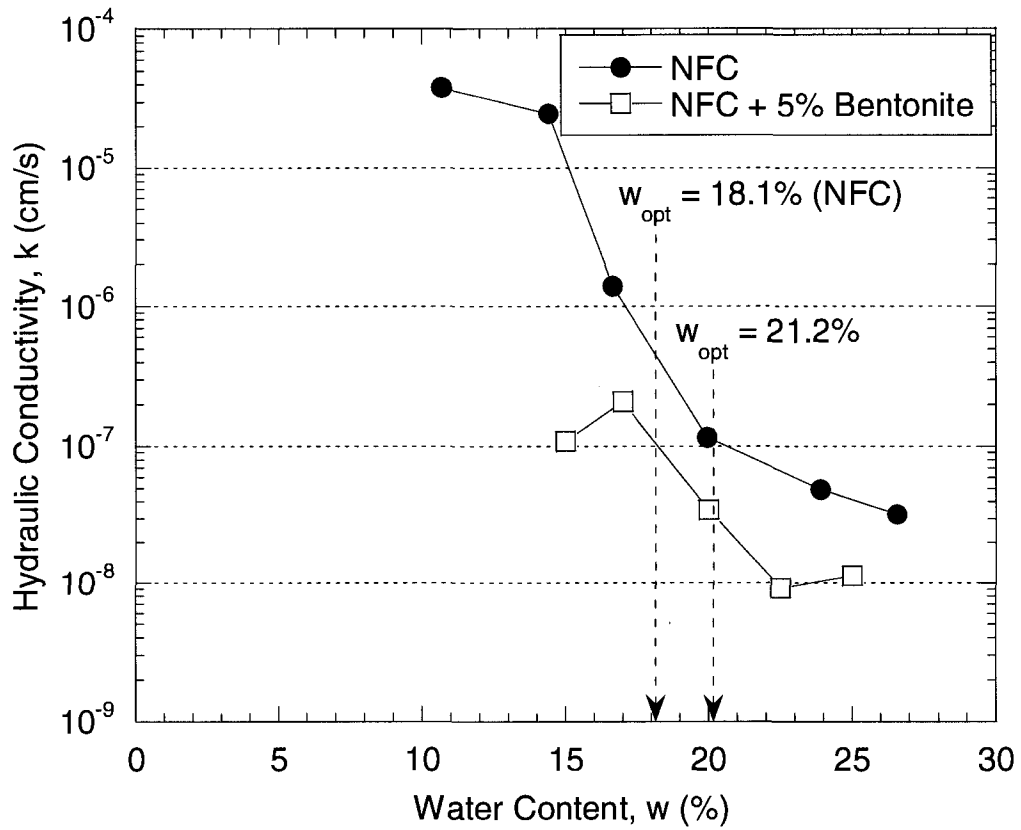


Fig. D.9 – Initial water contents versus hydraulic conductivity for specimens of Nelson Farm Clay (NFC) and NFC plus 5 % bentonite compacted by reduced compaction (Eng. Manual EM-1110-2-1906).

Table D.1 – Results of hydraulic conductivity tests for compacted specimens of Nelson Farm Clay.

Test No.	Parameter Values for Specimens							
	w_o (%)	S_i (%)	γ_d (kN/m ³)	PV (cm ³)	e	w_f (%)	S_f (%)	k (cm/s)
S1	11.09	45.98	16.03	95.27	0.65	22.25	96.47	1.38 x 10 ⁻⁶
S2	14.46	68.93	16.90	87.35	0.57	22.29	97.92	1.62 x 10 ⁻⁷
S3	17.02	84.98	17.18	84.76	0.54	19.60	98.49	8.26 x 10 ⁻⁸
S4	20.68	89.62	16.31	92.71	0.62	23.64	98.51	3.75 x 10 ⁻⁸
S5	23.68	91.46	15.58	99.38	0.70	23.37	97.74	5.91 x 10 ⁻⁸
S6	26.40	91.85	14.90	105.55	0.78	23.81	96.61	3.96 x 10 ⁻⁸
M1	6.82	30.89	16.59	90.18	0.60	21.93	96.70	1.74 x 10 ⁻⁶
M2	10.19	63.57	18.47	72.97	0.43	19.07	95.85	1.16 x 10 ⁻⁶
M3	13.86	91.71	18.80	70.00	0.41	16.84	95.95	1.57 x 10 ⁻⁸
M4	16.86	90.33	17.60	80.93	0.50	18.73	93.44	1.45 x 10 ⁻⁸
M5	20.04	90.35	16.56	90.47	0.60	20.79	98.35	2.54 x 10 ⁻⁸
M6	23.11	88.75	15.54	99.71	0.70	22.90	94.09	1.90 x 10 ⁻⁸
R1	10.66	38.13	15.08	103.91	0.76	26.79	99.94	3.82 x 10 ⁻⁵
R2	14.38	58.91	15.96	95.95	0.66	23.72	98.62	2.47 x 10 ⁻⁵
R3	16.63	77.76	16.78	88.40	0.58	21.36	97.60	1.39 x 10 ⁻⁶
R4	19.96	87.25	16.36	92.22	0.62	22.47	95.44	1.16 x 10 ⁻⁷
R5	23.90	89.50	15.38	101.18	0.72	23.77	93.76	4.92 x 10 ⁻⁸
R6	26.55	87.71	14.56	108.63	0.82	24.35	90.94	3.24 x 10 ⁻⁸

Notes:

w_o : Initial water contents

w_f : Final water contents

γ_d : Initial dry unit weight

PV : Pore void volume

S_i : Initial degree of saturation

S_f : Final degree of saturation

e : Void ratio

k : Hydraulic conductivity

Table D.2 – Results of hydraulic conductivity tests for specimens of compacted Nelson Farm Clay with five percent (dry weight) sodium bentonite.

Test No.	Parameter Values for Specimens						
	w_o (%)	S_i (%)	γ_d (kN/m ³)	PV (cm ³)	e	w_f (%)	k (cm/s)
S1	9.0	58.0	14.71	108.66	0.82	26.0	4.12×10^{-7}
S2	14.0	64.0	16.38	93.68	0.64	24.7	3.57×10^{-7}
S3	17.5	60.0	17.17	86.60	0.56	21.4	7.84×10^{-8}
S4	22.5	60.0	15.65	100.25	0.71	24.9	1.54×10^{-8}
S5	25.0	58.0	14.69	108.86	0.83	26.4	1.07×10^{-8}
M1	7.5	71.0	16.69	90.96	0.61	26.7	1.69×10^{-7}
M2	9.5	69.0	17.21	86.29	0.56	24.9	9.19×10^{-8}
M3	11.5	64.0	17.69	81.99	0.52	21.9	7.01×10^{-8}
M4	16.0	64.0	18.11	78.20	0.48	20.7	7.62×10^{-9}
M5	20.0	75.0	16.32	94.27	0.64	29.6	3.24×10^{-9}
R1	15.0	58.0	14.85	107.42	0.81	26.0	1.09×10^{-7}
R2	17.0	61.0	15.33	103.16	0.75	26.1	2.10×10^{-7}
R3	20.0	61.0	15.76	99.31	0.70	25.2	3.46×10^{-8}
R4	22.5	56.0	15.51	101.53	0.73	23.7	9.19×10^{-9}
R5	25.0	63.0	14.84	107.56	0.81	28.2	1.14×10^{-8}

Notes:

w_o : Initial water contents

w_f : Final water contents

γ_d : Initial dry unit weight

PV : Pore void volume

S_i : Initial degree of saturation

S_f : Final degree of saturation

e : Void ratio

k : Hydraulic conductivity

APPENDIX E

MEMBRANE TEST DATA IN FLEXIBLE-WALL CELL

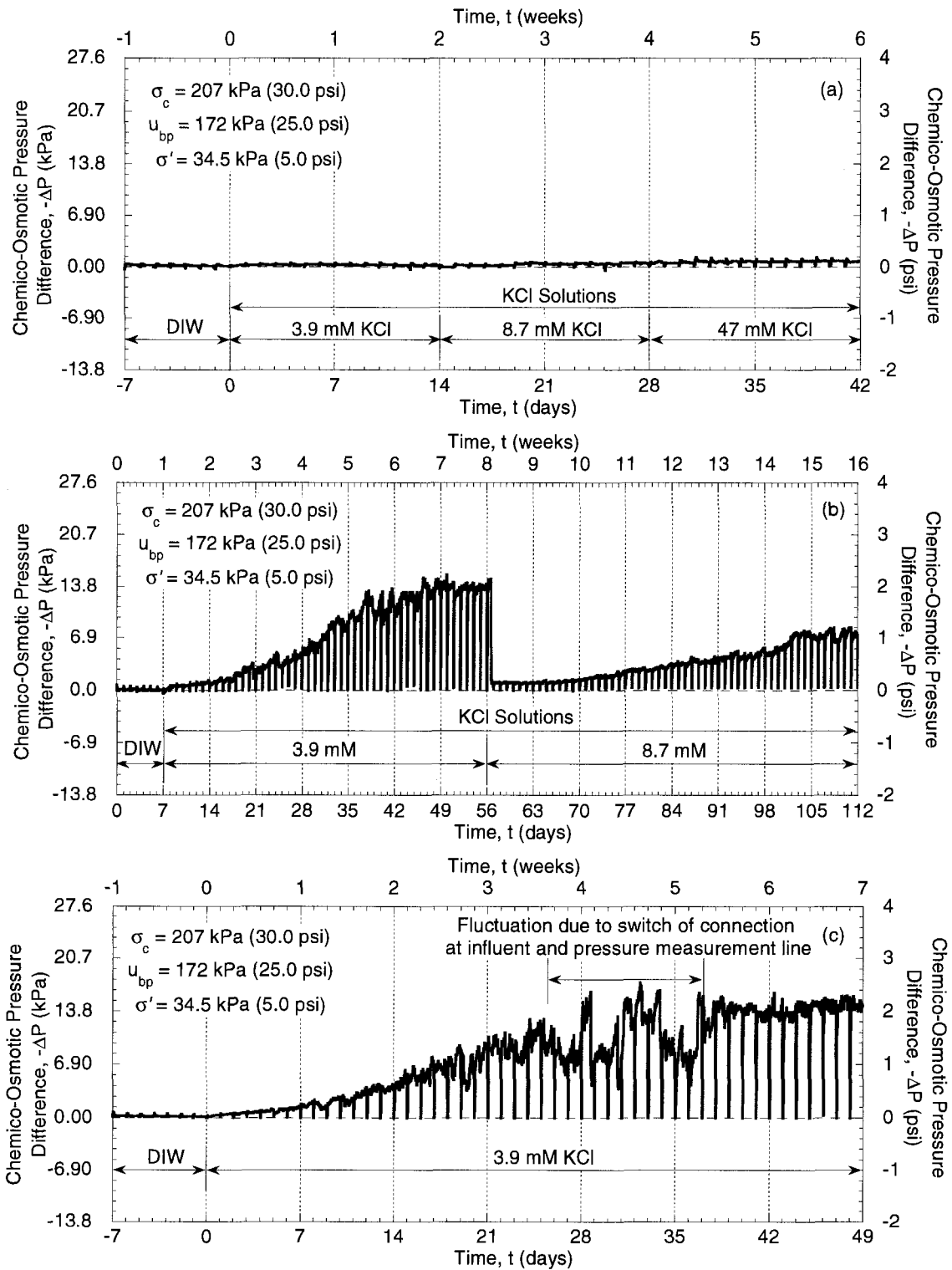


Fig. E.1 – Measured chemico-osmotic pressure differences across compacted specimens of (a) Nelson Farm Clay (NFC; No.1) and (b) and (c) NFC plus 5 % bentonite (Nos. 2 and 3) at an initial effective stress of 35.5 kPa (5.0 psi) during membrane testing in flexible-wall cell.

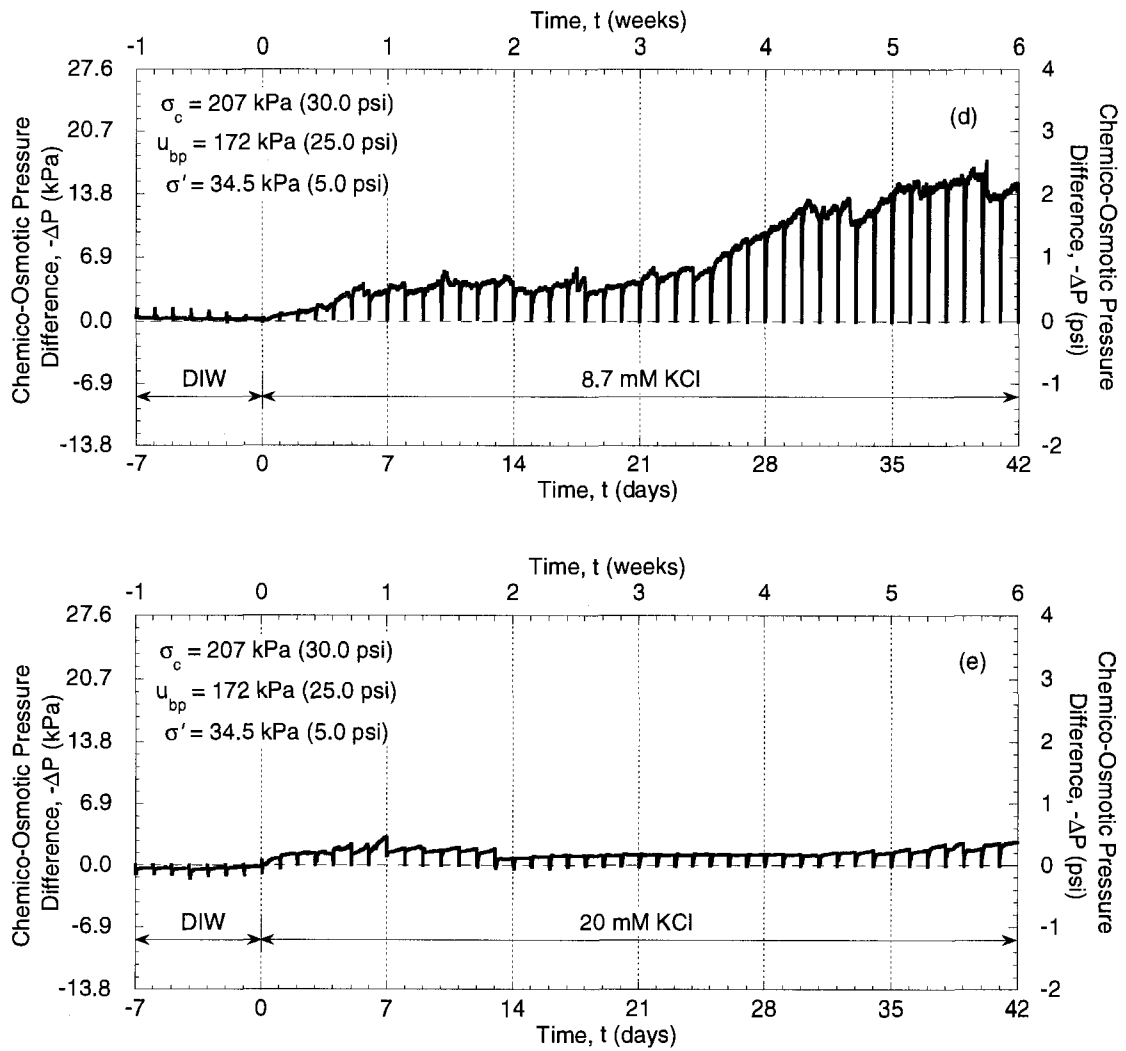


Fig. E.2 – Measured chemico-osmotic pressure differences across compacted specimens of NFC plus 5 % bentonite (d) No. 4 and (e) No. 5 at an initial effective stress of 35.5 kPa (5.0 psi) during membrane testing in flexible-wall cell.

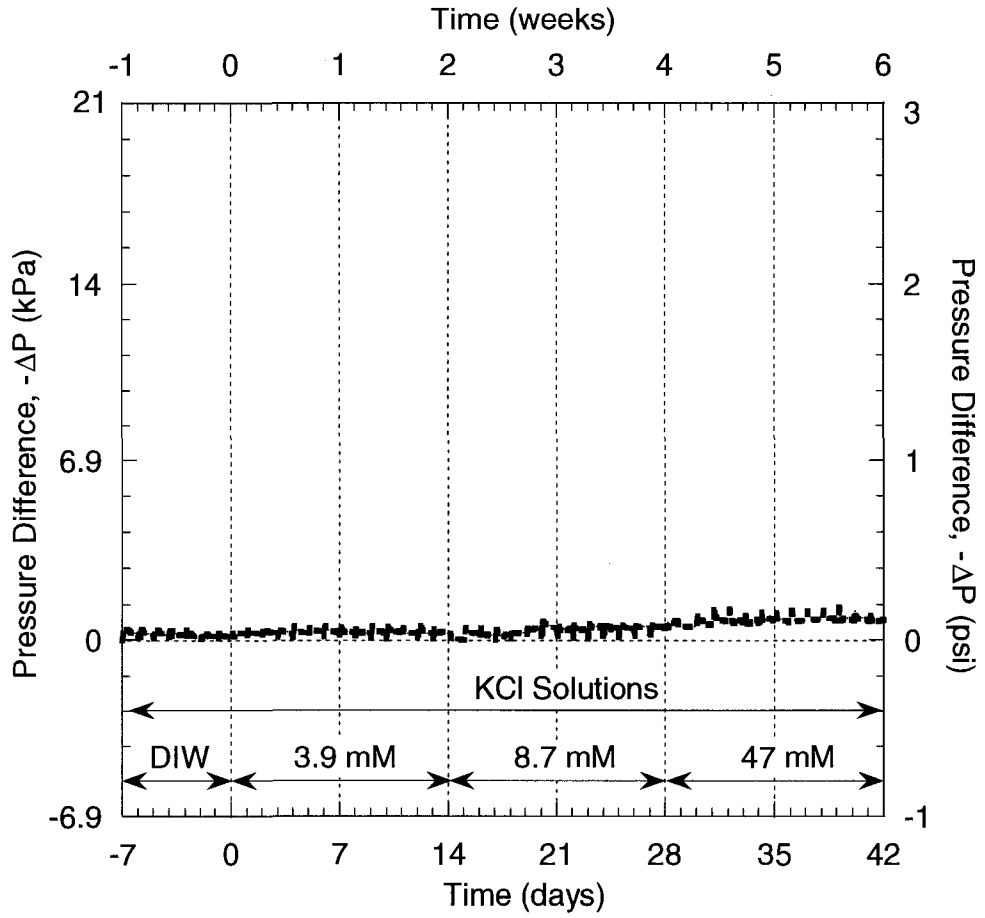


Fig. E.3 – Induced pressure difference versus time for a NFC specimen (1) during multi-stage membrane testing in flexible-wall cell.

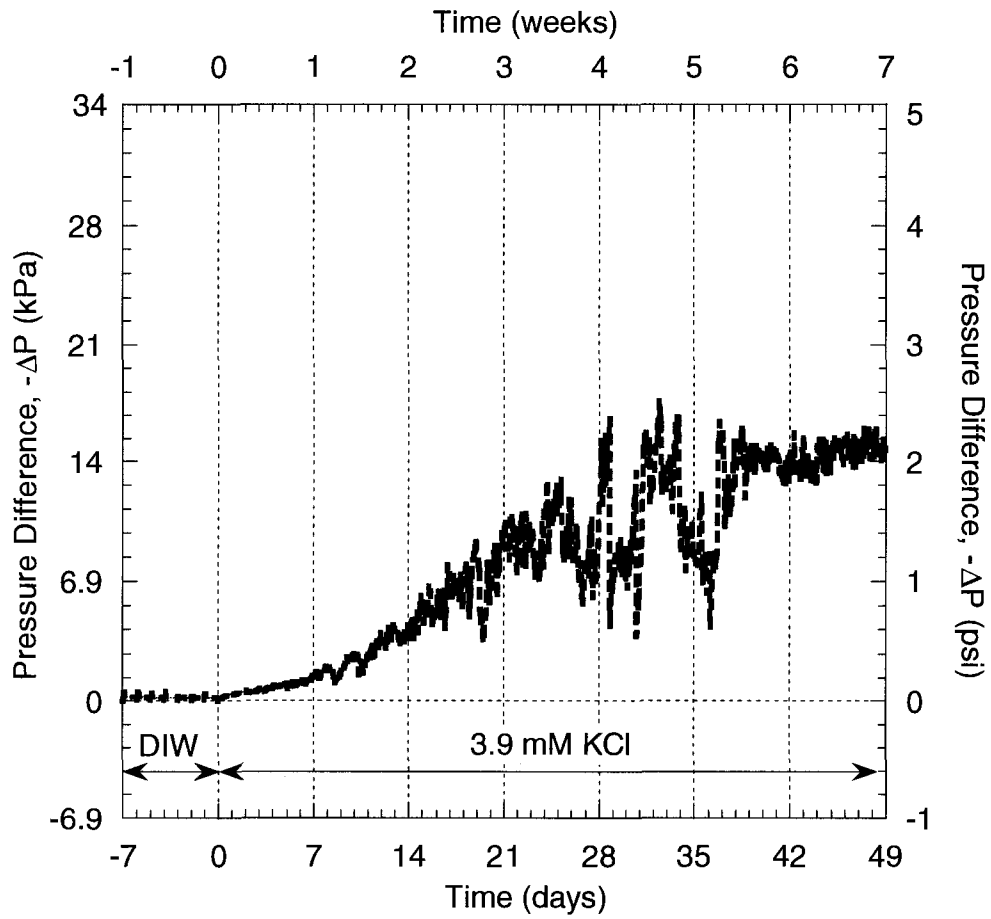


Fig. E.4 – Induced pressure difference versus time for a NFC plus 5 % bentonite specimen (2) due to effective stress condition 34.5 kPa (5.0 psi) during single-stage membrane testing in flexible-wall cell.

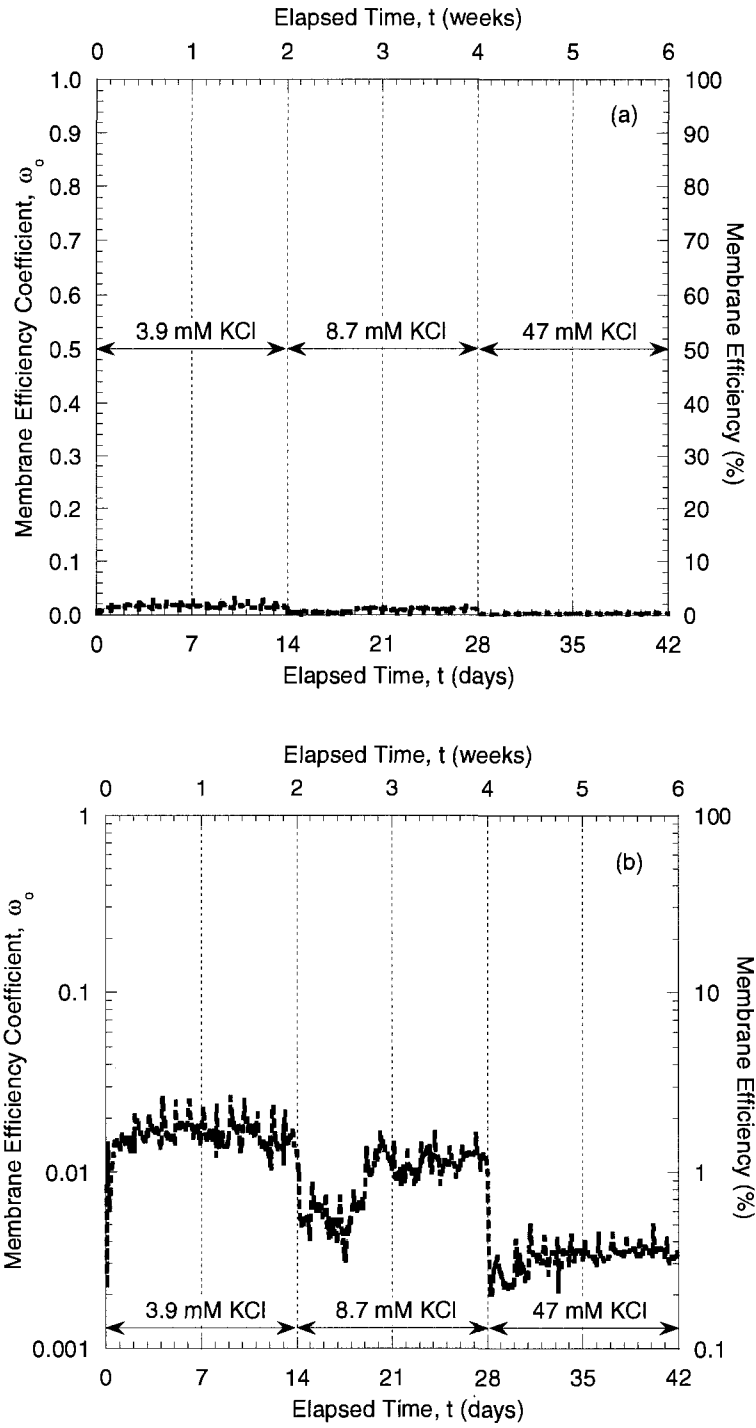


Fig. E.5 – Measured membrane efficiencies versus time as a function of (a) arithmetic and (b) logarithmic axis for a specimen of NFC No.1 during membrane testing in flexible-wall cell.

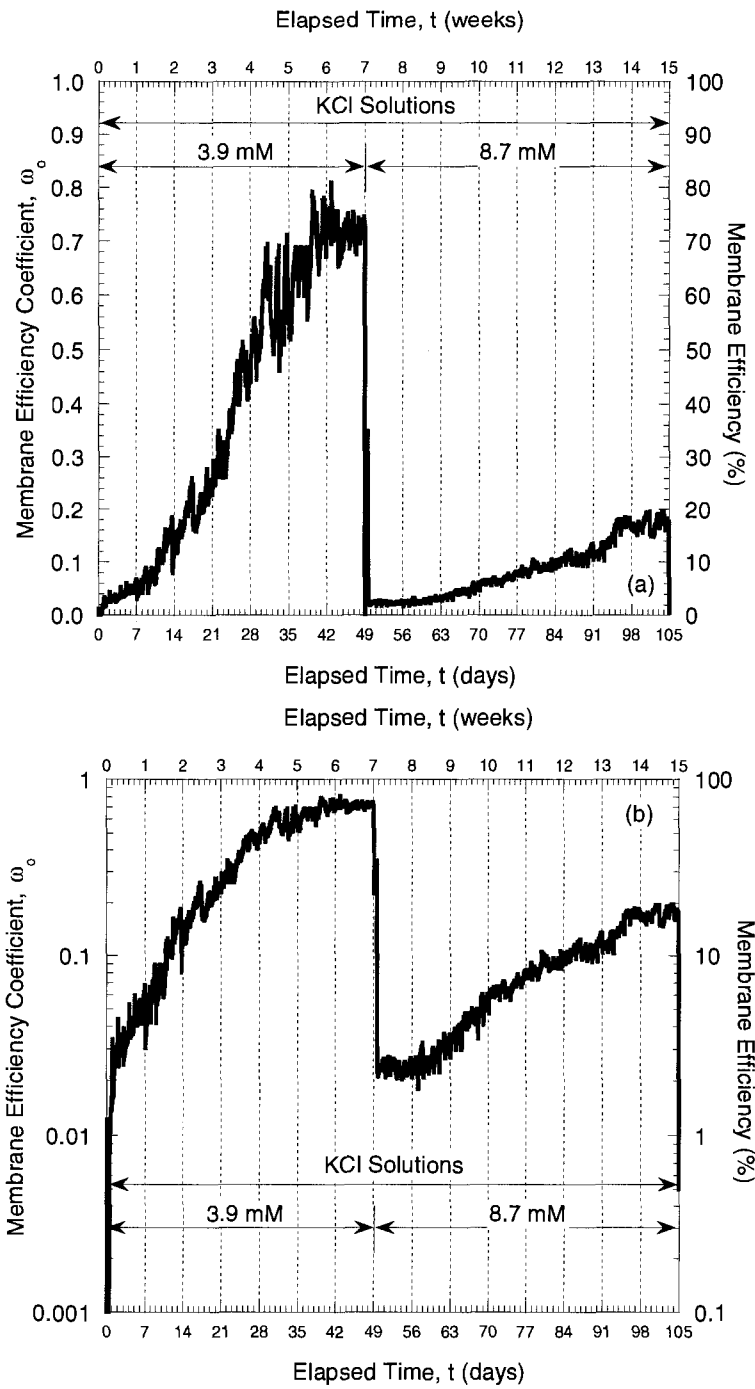


Fig. E.6 – Measured membrane efficiencies versus time as a function of (a) arithmetic and (b) logarithmic axis for a specimen of NFC plus 5 % bentonite No.2 during membrane testing in flexible-wall cell.

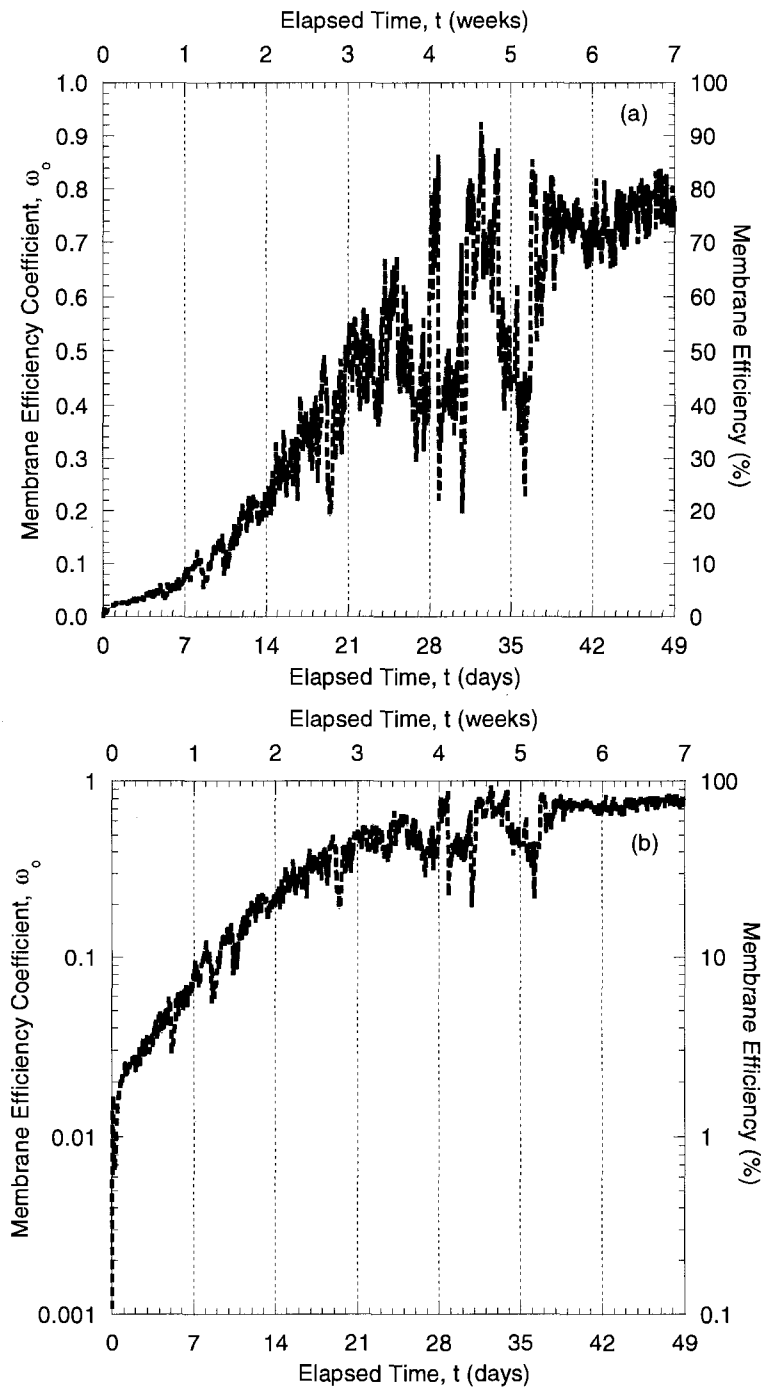


Fig. E.7 – Measured membrane efficiencies versus time as a function of (a) arithmetic and (b) logarithmic axis for a specimen of NFC plus 5 % bentonite No.3 during membrane testing in flexible-wall cell.

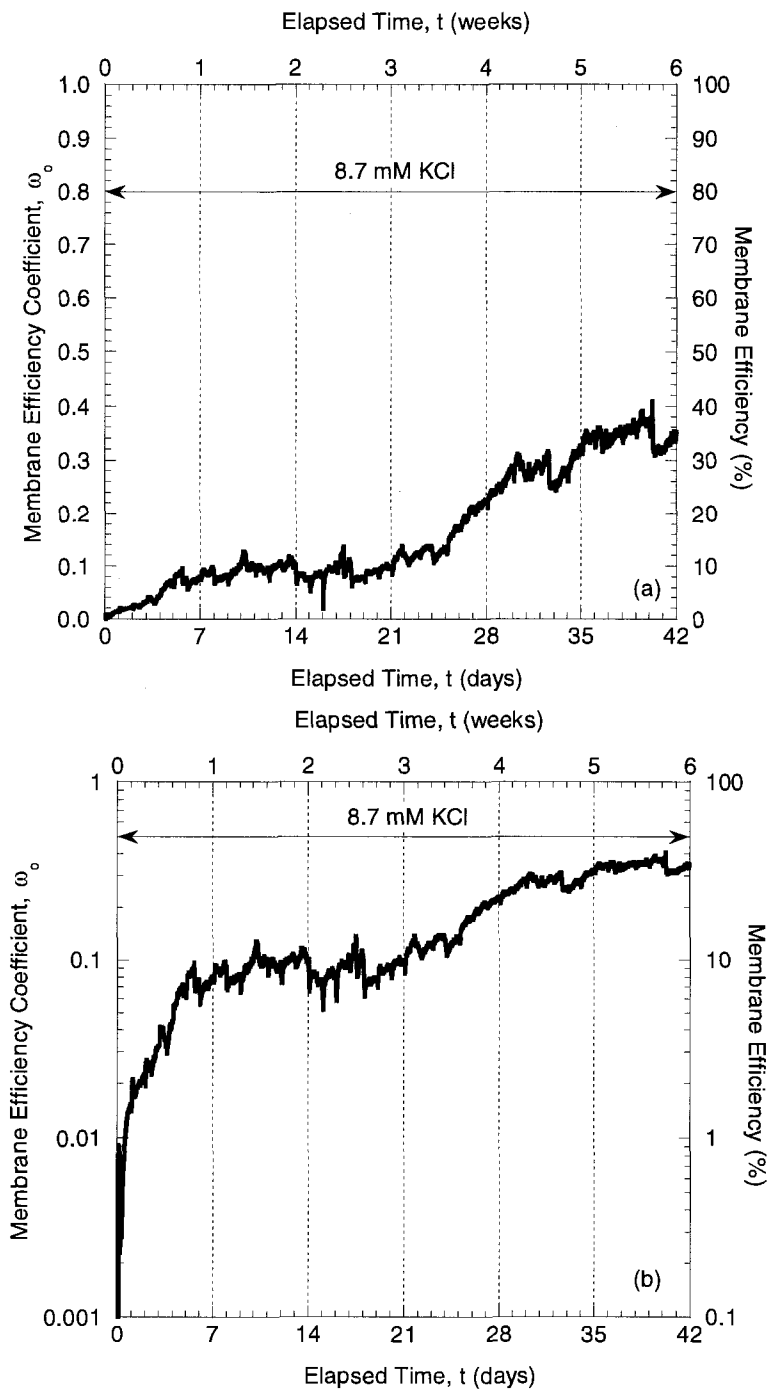


Fig. E.8 – Measured membrane efficiencies versus time as a function of (a) arithmetic and (b) logarithmic axis for a specimen of NFC plus 5 % bentonite No.4 during membrane testing in flexible-wall cell.

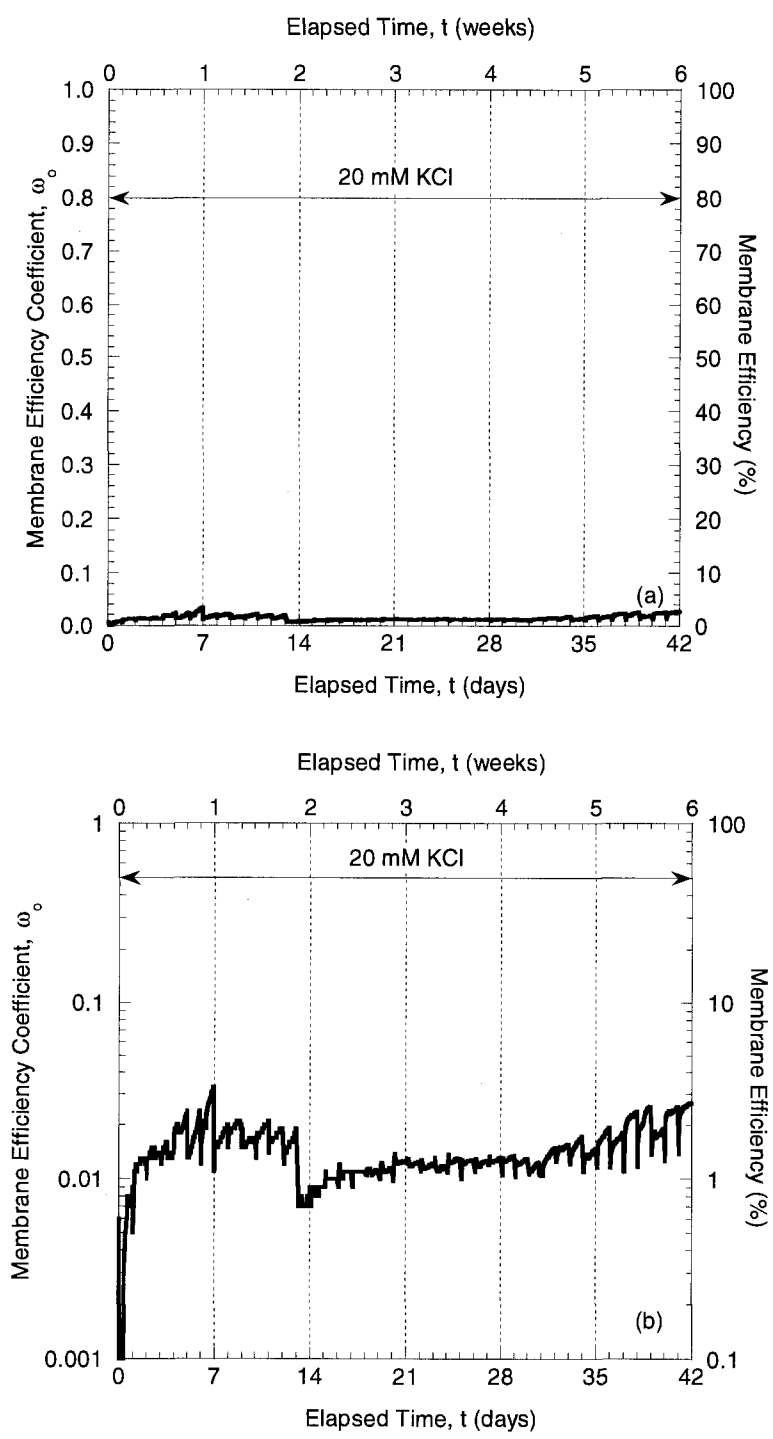


Fig. E.9 – Measured membrane efficiencies versus time as a function of (a) arithmetic and (b) logarithmic axis for a specimen of NFC plus 5 % bentonite No.5 during membrane testing in flexible-wall cell.

APPENDIX F

HYDRAULIC CONDUCTIVITY TEST DATA FOR POROUS STAINLESS STEEL DISK

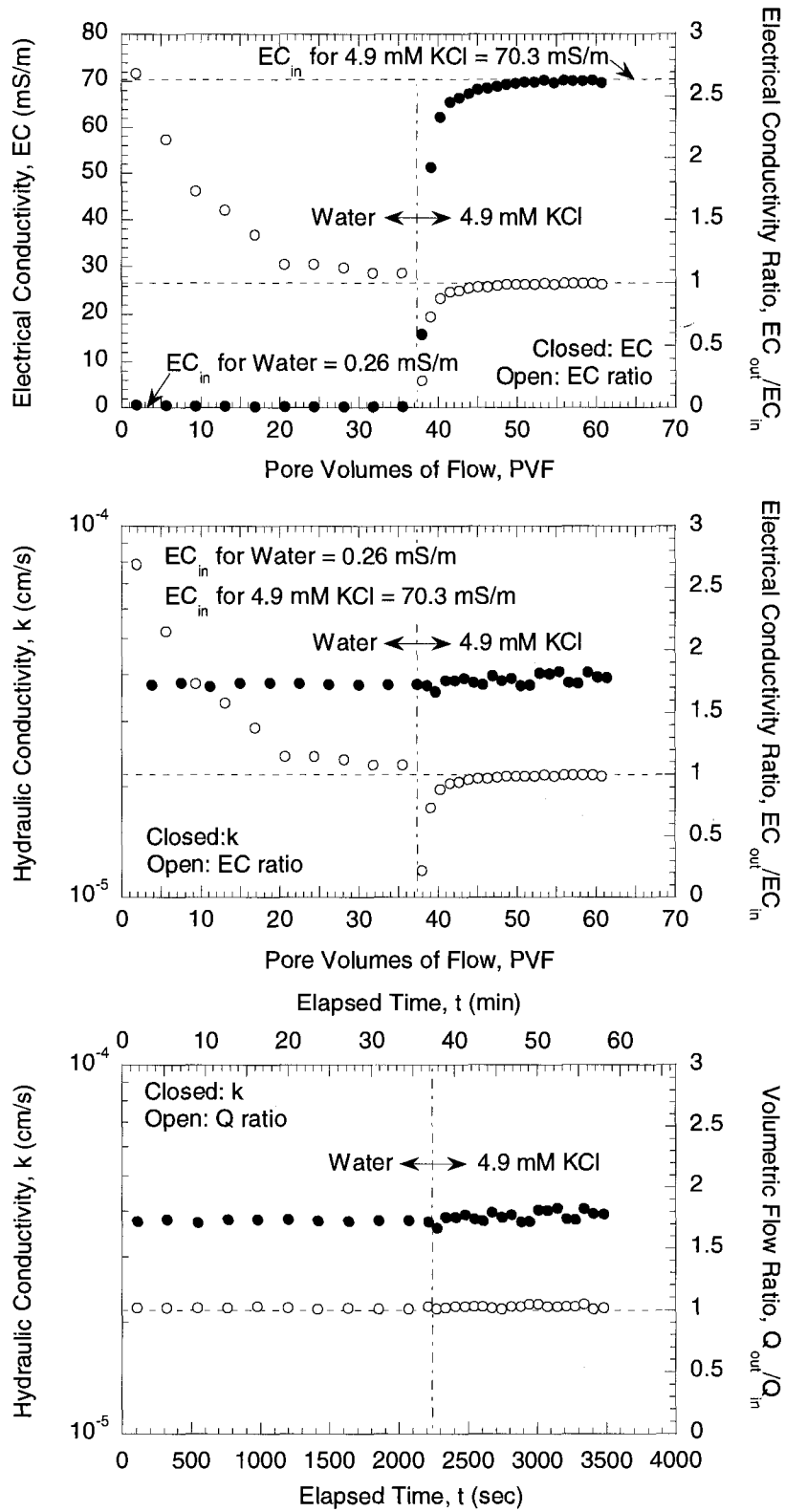


Fig. F.1 – Hydraulic conductivity due to water and KCl solution for porous stainless steel disk.